



LEHIGH
UNIVERSITY

Library &
Technology
Services

The Preserve: Lehigh Library Digital Collections

Degradation of Bioactive Peptides by Exopeptidases Influences Cell Behavior

Citation

Rozans, Samuel. *Degradation of Bioactive Peptides by Exopeptidases Influences Cell Behavior*. 2024, <https://preserve.lehigh.edu/lehigh-scholarship/graduate-publications-theses-dissertations/theses-dissertations/degradation-1>.

Find more at <https://preserve.lehigh.edu/>

This document is brought to you for free and open access by Lehigh Preserve. It has been accepted for inclusion by an authorized administrator of Lehigh Preserve. For more information, please contact preserve@lehigh.edu.

Degradation of Bioactive Peptides by Exopeptidases Influences Cell Behavior

By

Samuel Jacob Rozans

A Dissertation

Presented to the Graduate and Research Committee

Of Lehigh University

In Candidacy for the Degree of Doctor of Philosophy

in

Bioengineering

Lehigh University

August 2024

© 2024 Copyright

Samuel Jacob Rozans

Approved and Recommended for Acceptance as a dissertation in partial fulfillment of the requirements for the degree of Doctor of Philosophy

Samuel J. Rozans

Degradation of Bioactive Peptides by Exopeptidases Influences Cell Behavior

Defense Date

Approved Date

Dissertation Director

Committee Members:

E. Thomas Pashuck III

Lesley Chow

Anand Ramamurthi

Damien Thévenin

Acknowledgements

First, I would like to thank my advisor, Dr. E. Thomas Pashuck, for welcoming me into his lab with full support and confidence. I am grateful for his guidance throughout my doctoral journey. I would also like to thank my committee members Dr. Lesley Chow, Dr. Anand Ramamurthi, and Dr. Damien Thévenin for advice, support, and thoughtful discussion during our meetings.

A very special thank you goes out to the Pashuck lab members, past and present. In particular I would like to thank Abolfazl Salehi Moghaddam for his friendship, helping with this work, and assisting in creating a kind supportive environment in which to learn. Kayleigh Atanasoff for her friendship, contributions this work, and for being a huge support through a difficult time during the COVID-19 pandemic. Yingjie Wu for his friendship, contributions to this work, and a very welcome sense of humor.

I would like to thank the staff and faculty of the Bioengineering Department at Lehigh University. A very special thank you goes to Dr. Susan Perry, Rebekkah Short, Gwen Hughes, and Jarmaine Lomax. Thank you also to the staff of the Health, Science, and Technology building, past and present, especially George Yasko and Julie Shriver. Thank you for all you do behind the scenes to create a working research environment. Your efforts do not go unnoticed.

I would like to extend a special thank you to all of my mentors, past, present, and future including Sah-Bum-Nim Straga, Dr. Lin Han, Dr. Andrew Magenau, Professor Falcinelli,

and once again Dr. Pashuck. Each of you has contributed with impact to my past, present, and future.

To my grandfather, Alan E. Kligerman. Thank you so much for being a constant source of inspiration. For showing that a single innovation may have a profound impact upon the world. For the love, support, and example you set for all those around you, myself included. Lessons I learn from you have shaped who I am today, and will continue to shape who I will become tomorrow.

A profound thank you goes to my greatest support system, my family. To my parents for their unconditional love and support. To my amazing fiancé Elena Nasto, you have been my strongest source of support in all ways. All you do has not gone unnoticed. thank you for your love, support, and patience. This journey would not have been possible without you.

I dedicate this dissertation to my father Mark H. Rozans and my grandmother Elaine Budnick Kligerman. Although you are not here to see this journey to completion, I know you would be proud.

Table of Contents

Abstract	1
Chapter 1: Introduction	3
1.1 Introduction	3
1.2 Introduction to Peptide Quantification.....	5
1.3 Introduction to Synthetic Hydrogels	7
1.4 Introduction to Peptide Synthesis and Their Use in Biomaterials	9
1.5 Introduction to RGD	11
1.6 Introduction to Proteases.....	12
1.7 The Problem.....	14
Chapter 2: Developing a Method for Quantifying Peptide Degradation by Cells using LCMS.....	16
2.1 Introduction.....	16
2.2 Experimental	20
2.2.1 Peptide Synthesis	20
2.2.2 Peptide Cleavage from Solid Phase	21
2.2.3 Peptide Purification.....	22
2.2.4 Degradation of Peptides by Human Mesenchymal Stem Cells on Tissue Culture Plastic.....	22
2.2.5 Sample Treatment	23
2.2.6 Standard Selection	23
2.2.7 Injection Solvent Effects.....	24
2.2.8 Column Performance	24
2.2.9 Liquid Chromatography – Mass Spectrometry	25
2.3 Results and Discussion	26
2.3.1 Internal Standard Selection.....	26
2.3.2 Sample linearity	29
2.3.3 Effect of Acetic Acid Treatment on Reproducibility.....	30
2.3.4 Effects of Injection Solvent on LC-MS performance	32
2.3.5 Quantifying column Failure.....	36
2.4 Conclusion	39
Chapter 3: Chain End Modification Modulates Non-Specific Degradation of Peptides ..	41
3.1 Introduction.....	41

3.2	Experimental	43
3.2.1	Solid Phase Peptide Synthesis	43
3.2.2	Peptide Cleavage from Solid Phase	46
3.2.3	Peptide Purification.....	46
3.2.4	Degradation of Peptides by Human Umbilical Vein Endothelial Cells Stem Cells on Tissue Culture Plastic	47
3.2.5	Degradation of Peptides by Human Mesenchymal Stem Cells on Tissue Culture Plastic.....	48
3.2.6	Degradation of Peptides by Peripheral Blood Mononuclear Cell Derived Macrophages on Tissue Culture Plastic.....	48
3.2.7	Degradation of Peptides by THP1 Derived Macrophages on Tissue Culture Plastic	49
3.2.8	Liquid Chromatography – Mass Spectrometry.....	50
3.3	Results and Discussion	51
3.3.1	Degradation of RGEFV Peptide Libraries.....	51
3.3.2	Quantification of Biological Variance	61
3.3.3	Sequence Specific Degradation	75
3.3.4	Statistical Analysis.....	79
3.4	Conclusion	79
	Chapter 4: Other Methods of Modifying Degradation Rate	81
4.1	Introduction.....	81
4.2	Experimental	83
4.2.1	Solid Phase Peptide Synthesis	83
4.2.2	Peptide Cleavage from Solid Phase	84
4.2.3	Reagent Preparation for peptides of different concentrations.....	84
4.2.4	PEGylation of peptides	85
4.2.5	Degradation of Peptides by Human Umbilical Vein Endothelial Cells on Tissue Culture Plastic.....	85
4.2.6	Degradation of Peptides by Human Mesenchymal Stem Cells on Tissue Culture Plastic.....	86
4.2.7	Degradation of Peptides by THP-1 Derived Macrophages on Tissue Culture Plastic	87
4.2.8	Liquid Chromatography – Mass Spectrometry.....	87
4.3	Results and Discussion	88

4.3.1	Concentration effects of Peptides on Degradation.....	88
4.3.2	PEGylation/Matrix Mimicking effects on Peptide Degradation.....	93
4.4	Conclusion	95
Chapter 5: Cells in Gels influence Peptide Degradation, and Peptide Degradation influences Cells in Gels		96
5.1	Introduction.....	96
5.2	Experimental	98
5.2.1	8-Arm PEG evaluation.....	98
5.2.2	2-Azidoacetic Acid	98
5.2.3	Solid Phase Peptide Synthesis	99
5.2.4	Peptide Cyclization	99
5.2.5	Degradation of Peptides by Human Umbilical Vein Endothelial Cells in PEG hydrogels.....	100
5.2.6	Degradation of Peptides by Human Mesenchymal Stem Cells in PEG hydrogels.....	101
5.2.7	Degradation of Peptides by THP1 Derived Macrophages in PEG hydrogels	101
5.2.8	Liquid Chromatography – Mass Spectrometry	102
5.2.9	Imaging hMSCs in Gels Containing Fast and Slow Degrading Cell-Adhesion Peptides.....	102
5.2.10	Viability Assay.....	104
5.2.11	DNA Quantification Assay	104
5.3	Results and Discussions.....	106
5.3.1	Peptides degraded by cells in hydrogels.	106
5.3.2	Effects of RGD End Group Chemistry on Cell Behavior in Hydrogels	114
5.3.3	Statistical Analysis.....	115
5.4	Conclusions.....	115
Chapter 6: Overall Conclusions and Future Directions		117
6.1	Overall Conclusions.....	117
6.2	Future Directions	120
6.2.1	HPLC Column performance tracking	120
6.2.2	HPLC Column performance tracking	122
6.2.3	Expand on Non-Specific Degradation Profile of More Cell Types & Chain End Chemistries	122
6.2.4	Structure-Function Relationship of Acetylated Histidine.....	123

6.2.5 Functional investigation of Proteolytic Activity on Implanted Devices.....	123
6.2.6 Comparative Functional Proteolytic Activity in Cancer versus Healthy Cells.....	124
6.2.7 Development of Functional Intracellular Protease Activity.	124
6.2.8 How cell interaction through coculture influences proteolytic activity within biomaterials.....	125
6.2.9 In-depth Evaluation of how the Non-Specific Degradation of Adhesion Peptides Influences Cells in Gels	126
References.....	127
Appendix.....	143
7.1 RGEFV Libraries	143
7.2 LIAANK and IVKVA Peptides	206
7.3 Glycine, Azide, and PEGylated RGEFV Peptides.....	213
7.3.1 Cells in Gels: Imaging, Viability, DNA, and Live/Dead.....	226
7.3.2 Statistical Analysis.....	231
Vita	255

List of Tables

TABLE 1 – LIST OF ALL PEPTIDES USED TO DEVELOP METHOD LC-MS METHOD OF PEPTIDE QUANTIFICATION. AN NH ₂ ON THE N-TERMINUS STANDS FOR AN AMINE, BA FOR B-ALANINE, BF FOR B-PHENYLALANINE, AND X STANDS FOR EVERY CANONICAL AMINO ACID EXCEPT FOR CYSTEINE.	21
TABLE 2 – SLOPES, INTERCEPTS, AND COEFFICIENTS OF CORRELATION FOR LINEAR FIT OF PEPTIDE LIBRARIES ACBA-RGEFVX-AM (TOP), AND ACBA-XRGEFV-BA (BOTTOM).	30
TABLE 3 - LIST OF ALL PEPTIDES USED TO DEMONSTRATE HOW CHAIN END MODIFICATION MODULATES NON-SPECIFIC DEGRADATION OF PEPTIDES. ASIDES FROM PEPTIDE 3.1, FOUR N-TERMINAL MODIFICATIONS INCLUDING AN ACETYLATED B-ALANINE (ACBA), A B-ALANINE (BA), ACETYLATION (AC), AND AMINE (NH ₂). THREE C-TERMINAL MODIFICATIONS INCLUDE AMIDATION (AMIDE), A CARBOXYLIC ACID (COOH), AND A B-ALANINE (BA). FOR PEPTIDE LIBRARIES, X REPRESENTS A VARIABLE AMINO ACID WHICH INCLUDES: A, D, E, F, G, H, I, K, L, M, N, P, Q, R, S, T, V, W, AND Y.	45
TABLE 4 - CONTAINS INFORMATION ON CELL TYPE AND DONOR USED TO DEGRADE RGEFV PEPTIDE LIBRARIES.	62
TABLE 5 – RGEFV LIBRARIES WERE DEGRADED AND LOTS WERE COMPARED AFTER 48 HOURS. LOTS ARE COMPARED ALONG THE ROW, AND THE P VALUE IS THE RESULT OF AN ANNOVA FOLLOWED BY A TUKEY-KRAMER POST HOC ANALYSIS. HIGHLIGHTED ARE COMPARISONS THAT FAILED TO REJECTED THE NULL-HYPOTHESIS DEFINED AT P=0.05.	64
TABLE 6 - LIST OF ALL PEPTIDES USED TO EVALUATE OTHER METHODS OF MODIFYING DEGRADATION RATES. NOTE: N ₃ STANDS FOR AN AZIDE MOIETY, AND PEG ₁₂ STANDS FOR MONODISPERSE POLYETHYLENE GLYCOL CONTAINING 12 MONOMERS.	84
TABLE 7 - LIST OF ALL PEPTIDES USED TO DEMONSTRATE HOW CHAIN END MODIFICATION MODULATES NON-SPECIFIC DEGRADATION OF PEPTIDES. ASIDES FROM PEPTIDE 5.1, FOUR N-TERMINAL MODIFICATIONS INCLUDING AN ACETYLATED B-ALANINE (ACBA), A B-ALANINE (BA), ACETYLATION (AC), AND AMINE (NH ₂). THREE C-TERMINAL MODIFICATIONS INCLUDE AMIDATION (AM), A CARBOXYLIC ACID (COOH), AND A B-ALANINE (BA). FOR PEPTIDE LIBRARIES, X REPRESENTS A VARIABLE AMINO ACID WHICH INCLUDES: A, D, E, F, G, H, I, K, L, M, N, P, Q, R, S, T, V, W, AND Y. AN AZIDE MOIETY IS SHOWN AS N ₃	99

List of Figures

FIGURE 1 - SHOWS THE DIFFERENCE BETWEEN ARG-GLY-ASP, RGD (TOP) AND ARG-GLY-GLU, RGE (BOTTOM). NOTE THE RGE CELL-ADHESION CONTROL PEPTIDE IS ONLY DIFFERENT BY 1 CARBON AND 2 HYDROGENS.	12
FIGURE 2 - (TOP) ILLUSTRATES ENDOPEPTIDASE HYDROLYZATION OF A PEPTIDE ALONG THE INTERIOR AND (BOTTOM) EXOPEPTIDASE HYDROLYZATION OF A PEPTIDE ALONG THE N- OR C- TERMINAL END.	15
FIGURE 3 – PROPOSED EXPERIMENTAL WORKFLOW FOR LC-MS BASED QUANTIFICATION OF PEPTIDES. 1) PEPTIDES WITH UNIQUE MASSES ARE MIXED TOGETHER ALONG WITH A PROTEOLYTICALLY STABLE INTERNAL STANDARD. 2) PEPTIDES ARE INCUBATED WITH CELLS AND SUBJECTED TO CELL-SECRETED PROTEASES. 3) CONDITIONED MEDIA IS SAMPLED AND PLACED DIRECTLY INTO AN LC-MS MICROTITER PLATE. 4) GLACIAL ACETIC ACID IS ADDED TO EACH SAMPLE WELL TO A FINAL CONCENTRATION OF 10%. 5) SAMPLE IS INJECTED INTO LC-MS, QUANTIFIED, AND 6) ANALYZED AND VISUALIZED.	19
FIGURE 4 - EVALUATION OF 10 B-ALANINE BASED STANDARDS TO IDENTIFY MOLECULES WITH BOTH DESIRED RETENTION TIMES AND STABILITY DURING CULTURE. A) THE RETENTION TIME OF PEPTIDES CAN BE TUNED THROUGH N-TERMINAL MODIFICATIONS TO THE PEPTIDE SEQUENCE AND THE INCORPORATION OF HYDROPHOBIC RESIDUES. B) THE STABILITY OF PEPTIDE SEQUENCES AFTER 48 HOURS IN CULTURE WITH hMSCs WAS DEPENDENT ON PEPTIDE SEQUENCE. THOSE WITH A FRACTION REMAINING OF GREATER THAN 90% ARE SHOWN IN GREEN.	28
FIGURE 5 – A) CALIBRATION CURVES FOR LIBRARIES ACBA-RGEFV-X-AM AND B) ACBA-X-RGEFV-BA, WHERE X IS ALL CANONICAL AMINO ACIDS EXCEPT FOR CYSTEINE. SHOWN ARE REPRESENTATIVE CALIBRATION CURVES WHERE X IS K, N, I/L, AND F ALONG WITH COEFFICIENTS OF CORRELATION.....	30

FIGURE 6 - THE GRAPH SHOWS AVERAGE CONSISTENCY OF ALL PEPTIDES WITHIN THE PEPTIDE LIBRARY, WHERE THE ERROR BARS ARE THE STANDARD DEVIATION OF THE ENTIRE PEPTIDE LIBRARY CONSISTENCY. CONSISTENCY IS REPORTED FOR EACH TIMEPOINT. ACETIC ACID TREATED (T) AND UNTREATED SAMPLES (U) ARE COMPARED FOR CONSISTENCY OF MEASUREMENT. U1 IS UNTREATED SAMPLES INJECTED ON THE LC-MS IMMEDIATELY AFTER SAMPLE COLLECTION AT ANY GIVEN TIMEPOINT, U2 ARE THE SAME UNTREATED SAMPLES COLLECTED 23 DAYS LATER. T1 ARE THE TREATED SAMPLES COLLECTED IMMEDIATELY AFTER THE 48-HOUR TIMEPOINT, AND T2 ARE THE TREATED SAMPLES COLLECTED 23 DAYS LATER.....	32
FIGURE 7 - ACBA-X-RGEFV-BA LIBRARY, WHERE X IS AMINO ACID A, D, E, F, G, H, I, K, L, M, N, P, Q, R, S, T, V, W, AND Y, WAS DISSOLVED AT TOTAL CONCENTRATION OF 37uM IN A) DIFFERENT SOLVENTS. B) SHOWS AREA RATIO OF EACH PEPTIDE IN THE LIBRARY NORMALIZED TO NH ₂ -bF(BA) ₆ -NH ₂ (TOP) WITH ITS CORRESPONDING RETENTION TIME (BOTTOM).....	35
FIGURE 8 - A) SHOWS THE INTERNAL STANDARD PEAK NH ₂ -bF(BA) ₆ -NH ₂ IN WATER. THE LEFT PANE IS REPRESENTATIVE OF WHAT WAS OBSERVED IN SOLVENTS 1, 2, AND 5-12; WHILE THE RIGHT PANE DEMONSTRATES PEAK SPLITTING AND IS REPRESENTATIVE OF SOLVENT'S 2 AND 3. B) QUANTIFIES THE PROPORTION INTERNAL STANDARD (IS) AND ANALYTES THAT ARE IN THE BREAKTHROUGH PEAK AS COMPARED TO WHAT ELUTES AT THE EXPECTED RETENTION TIME.	36
FIGURE 9 - EVALUATION OF COLUMN LIFESPAN AND PERFORMANCE CAN BE SEEN. EVALUATION WOULD START WITH INJECTION OF PEPTIDE LIBRARY ACBA-X-RGEFV-BA, FOLLOWED BY FOUR INJECTIONS OF MEDIA CONTAINING 10% FBS, AND FINALLY THAT CYCLE WAS REPEATED. SO INJECTION #/4 REPRESENTS THE NUMBER OF PEPTIDE LIBRARIES THAT WERE INJECTED ONTO THE COLUMN. A) SHOWS THE AREA RATIO, WHILE C) SHOWS HOW THE RETENTION TIME OF EVERY PEPTIDE. B) CONTAINS THE LEGEND OF EVERY PEPTIDE FOR WITHIN A, B, AND C AS WELL AS THE AREA RATIO NORMALIZED TO INJECTION NUMBER 3-20 OF THE PEPTIDE LIBRARY MINUS 1. THE PANE WITHIN B CONTAINS THE SQUARE ROOT SUM OF THE NORMALIZED AREA RATIO TO QUANTIFY THE TOTAL ERROR OF EACH QUANTIFIED PEPTIDES WITHIN THE LIBRARY. D) SHOWS HOW THE PRESSURE WITHIN THE HPLC AT TIME ZERO OF THE INJECTION. THE BLACK AND RED ARROWS POINT TO WHEN THE FIRST INJECTION WAS PERFORMED AFTER AT LEAST 24 HOURS OF NON-USE. THE RED ARROW POINTS TO WHERE FAILURE OF THE COLUMN IS INITIATED.....	39
FIGURE 10 - DESIGN OF N-TERMINAL AND C-TERMINAL PEPTIDE LIBRARIES. SPLIT-AND-POOL WITH FOUR DIFFERENT N-TERMINAL MODIFICATIONS AND THREE DIFFERENT C-TERMINAL MODIFICATIONS.....	42

FIGURE 11 - DEGRADATION OF SOLUBLE PEPTIDES CULTURED WITH CELLS ON TISSUE CULTURE PLASTIC. DEGRADATION WAS QUANTIFIED AT 1 HOUR.....	53
FIGURE 12 - DEGRADATION OF SOLUBLE PEPTIDES CULTURED WITH CELLS ON TISSUE CULTURE PLASTIC. DEGRADATION WAS QUANTIFIED AT 4 HOURS.....	53
FIGURE 13 - DEGRADATION OF SOLUBLE PEPTIDES CULTURED WITH CELLS ON TISSUE CULTURE PLASTIC. DEGRADATION WAS QUANTIFIED AT 8 HOURS.....	54
FIGURE 14 - DEGRADATION OF SOLUBLE PEPTIDES CULTURED WITH CELLS ON TISSUE CULTURE PLASTIC. DEGRADATION WAS QUANTIFIED AT 24 HOURS.....	54
FIGURE 15 - DEGRADATION OF SOLUBLE PEPTIDES CULTURED WITH CELLS ON TISSUE CULTURE PLASTIC. DEGRADATION WAS QUANTIFIED AT 48 HOURS.....	55
FIGURE 16 - DEGRADATION OF SOLUBLE PEPTIDES CULTURED WITH CELLS ON TISSUE CULTURE PLASTIC. DEGRADATION WAS QUANTIFIED BY THE CHEMISTRY OF THE PEPTIDE TERMINI AC-BA.....	55
FIGURE 17 - DEGRADATION OF SOLUBLE PEPTIDES CULTURED WITH CELLS ON TISSUE CULTURE PLASTIC. DEGRADATION WAS QUANTIFIED BY THE CHEMISTRY OF THE PEPTIDE TERMINI AC.	56
FIGURE 18 - DEGRADATION OF SOLUBLE PEPTIDES CULTURED WITH CELLS ON TISSUE CULTURE PLASTIC. DEGRADATION WAS QUANTIFIED BY THE CHEMISTRY OF THE PEPTIDE TERMINI N-BA.....	56
FIGURE 19 - DEGRADATION OF SOLUBLE PEPTIDES CULTURED WITH CELLS ON TISSUE CULTURE PLASTIC. DEGRADATION WAS QUANTIFIED BY THE CHEMISTRY OF THE PEPTIDE TERMINI NH ₂	57
FIGURE 20 - DEGRADATION OF SOLUBLE PEPTIDES CULTURED WITH CELLS ON TISSUE CULTURE PLASTIC. DEGRADATION WAS QUANTIFIED BY THE CHEMISTRY OF THE PEPTIDE TERMINI C-BA.	57
FIGURE 21 - DEGRADATION OF SOLUBLE PEPTIDES CULTURED WITH CELLS ON TISSUE CULTURE PLASTIC. DEGRADATION WAS QUANTIFIED BY THE CHEMISTRY OF THE PEPTIDE TERMINI AM.	58
FIGURE 22 - DEGRADATION OF SOLUBLE PEPTIDES CULTURED WITH CELLS ON TISSUE CULTURE PLASTIC. DEGRADATION WAS QUANTIFIED BY THE CHEMISTRY OF THE PEPTIDE TERMINI COOH.....	58

FIGURE 23 - NON-SPECIFIC DEGRADATION OF PEPTIDES WITH N-TERMINAL AMINES ACROSS THREE DIFFERENT CELL TYPES. THE AMOUNT OF DEGRADATION AT DIFFERENT TIME POINTS WAS QUANTIFIED. AVERAGING OVER ALL AMINO ACIDS, QUANTIFIED THE EFFECTS OF N-TERMINAL MODIFICATIONS FOR (A) hMSCs, (B) HUVECs, AND (C) MACROPHAGES, AND C-TERMINAL MODIFICATIONS FOR (D) hMSCs, (E) HUVECs, AND (F) MACROPHAGES. ERROR BARS REPRESENT THE STANDARD DEVIATION ACROSS ALL TERMINAL AMINO ACIDS.	60
FIGURE 24 - COMPARISON OF PEPTIDE DEGRADATION BY DIFFERENT HUVEC DONORS. HUVECS WERE CULTURED WITH RGEFV LIBRARIES CONTAINING END GROUP AC-BA.	65
FIGURE 25 - COMPARISON OF PEPTIDE DEGRADATION BY DIFFERENT HUVEC DONORS. HUVECS WERE CULTURED WITH RGEFV LIBRARIES CONTAINING END GROUP AC.....	65
FIGURE 26 - COMPARISON OF PEPTIDE DEGRADATION BY DIFFERENT HUVEC DONORS. HUVECS WERE CULTURED WITH RGEFV LIBRARIES CONTAINING END GROUP N-BA.	66
FIGURE 27 - COMPARISON OF PEPTIDE DEGRADATION BY DIFFERENT HUVEC DONORS. HUVECS WERE CULTURED WITH RGEFV LIBRARIES CONTAINING END GROUP NH2.....	66
FIGURE 28 - COMPARISON OF PEPTIDE DEGRADATION BY DIFFERENT HUVEC DONORS. HUVECS WERE CULTURED WITH RGEFV LIBRARIES CONTAINING END GROUP C-BA.....	67
FIGURE 29 - COMPARISON OF PEPTIDE DEGRADATION BY DIFFERENT HUVEC DONORS. HUVECS WERE CULTURED WITH RGEFV LIBRARIES CONTAINING END GROUP AM.....	67
FIGURE 30 - COMPARISON OF PEPTIDE DEGRADATION BY DIFFERENT HUVEC DONORS. HUVECS WERE CULTURED WITH RGEFV LIBRARIES CONTAINING END GROUP COOH.	68
FIGURE 31 - COMPARISON OF PEPTIDE DEGRADATION BY DIFFERENT hMSC DONORS. hMSCs WERE CULTURED WITH RGEFV LIBRARIES CONTAINING END GROUP AC-BA.	68
FIGURE 32 - COMPARISON OF PEPTIDE DEGRADATION BY DIFFERENT hMSC DONORS. hMSCs WERE CULTURED WITH RGEFV LIBRARIES CONTAINING END GROUP AC.....	69

FIGURE 33 - COMPARISON OF PEPTIDE DEGRADATION BY DIFFERENT hMSC DONORS. hMSCs WERE CULTURED WITH RGEFV LIBRARIES CONTAINING END GROUP N-BA.....	69
FIGURE 34 - COMPARISON OF PEPTIDE DEGRADATION BY DIFFERENT hMSC DONORS. hMSCs WERE CULTURED WITH RGEFV LIBRARIES CONTAINING END GROUP NH2.....	70
FIGURE 35 - COMPARISON OF PEPTIDE DEGRADATION BY DIFFERENT hMSC DONORS. hMSCs WERE CULTURED WITH RGEFV LIBRARIES CONTAINING END GROUP C-BA.....	70
FIGURE 36 - COMPARISON OF PEPTIDE DEGRADATION BY DIFFERENT hMSC DONORS. hMSCs WERE CULTURED WITH RGEFV LIBRARIES CONTAINING END GROUP AM.....	71
FIGURE 37- COMPARISON OF PEPTIDE DEGRADATION BY DIFFERENT hMSC DONORS. hMSCs WERE CULTURED WITH RGEFV LIBRARIES CONTAINING END GROUP COOH.	71
FIGURE 38 - COMPARISON OF PEPTIDE DEGRADATION BY DIFFERENT DONORS. MACROPHAGES WERE CULTURED WITH RGEFV LIBRARIES CONTAINING END GROUP AC-BA.....	72
FIGURE 39 - COMPARISON OF PEPTIDE DEGRADATION BY DIFFERENT DONORS. MACROPHAGES WERE CULTURED WITH RGEFV LIBRARIES CONTAINING END GROUP AC.	72
FIGURE 40 - COMPARISON OF PEPTIDE DEGRADATION BY DIFFERENT DONORS. MACROPHAGES WERE CULTURED WITH RGEFV LIBRARIES CONTAINING END GROUP N-BA.....	73
FIGURE 41 - COMPARISON OF PEPTIDE DEGRADATION BY DIFFERENT DONORS. MACROPHAGES WERE CULTURED WITH RGEFV LIBRARIES CONTAINING END GROUP NH2.	73
FIGURE 42 - COMPARISON OF PEPTIDE DEGRADATION BY DIFFERENT DONORS. MACROPHAGES WERE CULTURED WITH RGEFV LIBRARIES CONTAINING END GROUP C-BA.	74
FIGURE 43 - COMPARISON OF PEPTIDE DEGRADATION BY DIFFERENT DONORS. MACROPHAGES WERE CULTURED WITH RGEFV LIBRARIES CONTAINING END GROUP AM.	74

FIGURE 44 – COMPARISON OF PEPTIDE DEGRADATION BY DIFFERENT DONORS. MACROPHAGES WERE CULTURED WITH RGEFV LIBRARIES CONTAINING END GROUP COOH.....	75
FIGURE 45 - EFFECTS OF DIFFERENT PEPTIDE SEQUENCES ON NON-SPECIFIC DEGRADATION. DEGRADATION WAS QUANTIFIED FOR CELL TYPE hMSC.	76
FIGURE 46 - EFFECTS OF DIFFERENT PEPTIDE SEQUENCES ON NON-SPECIFIC DEGRADATION. DEGRADATION WAS QUANTIFIED FOR CELL TYPE HUVEC.....	76
FIGURE 47 - EFFECTS OF DIFFERENT PEPTIDE SEQUENCES ON NON-SPECIFIC DEGRADATION. DEGRADATION WAS QUANTIFIED FOR CELL TYPE MACROPHAGE.	77
FIGURE 48 - EFFECTS OF DIFFERENT PEPTIDE SEQUENCES ON NON-SPECIFIC DEGRADATION. DEGRADATION WAS QUANTIFIED FOR PEPTIDE IVKVA.	77
FIGURE 49 - EFFECTS OF DIFFERENT PEPTIDE SEQUENCES ON NON-SPECIFIC DEGRADATION. DEGRADATION WAS QUANTIFIED FOR PEPTIDE LIAANK.....	78
FIGURE 50 – EFFECTS OF DIFFERENT PEPTIDE SEQUENCES ON NON-SPECIFIC DEGRADATION. DEGRADATION WAS QUANTIFIED FOR PEPTIDE RGEFV.....	78
FIGURE 51 - DEGRADATION OF PEPTIDES AT DIFFERENT CONCENTRATIONS. DATA WAS QUANTIFIED FOR hMSCs (A) AC-BA, (B) AC, (C) N-BA, (D) NH ₂ , (E) C-BA, (F) AM, (G) COOH.....	90
FIGURE 52 - DEGRADATION OF PEPTIDES AT DIFFERENT CONCENTRATIONS. DATA WAS QUANTIFIED FOR HUVECS (A) AC-BA, (B) AC, (C) N-BA, (D) NH ₂ , (E) C-BA, (F) AM, (G) COOH.....	91
FIGURE 53 – DEGRADATION OF PEPTIDES AT DIFFERENT CONCENTRATIONS. DATA WAS QUANTIFIED FOR MACROPHAGES (A) AC-BA, (B) AC, (C) N-BA, (D) NH ₂ , (E) C-BA, (F) AM, (G) COOH.....	92
FIGURE 54 – EXAMPLE OF RGEFV PEPTIDE WITH DIFFERENT TERMINAL CHEMISTRIES. PEPTIDES WERE SYNTHESIZED WITH AZIDES (TOP) ON EITHER THE N- OR C- TERMINUS. A PORTION WERE MODIFIED WITH A (PEG) ₁₂ -DBCO (BOTTOM). THE AMINE VERSION OF THE RGEFV PEPTIDE IS DISPLAYED.	93
FIGURE 55 – PEG CONJUGATION TO PEPTIDES SLOWS DEGRADATION ACROSS ENDGROUPS AND CELL TYPES. (A) hMSC N-TERMINAL CHEMISTRIES, (B) hMSC C- TERMINAL CHEMISTRIES, (C) HUVEC N-TERMINAL CHEMISTRIES, (D) HUVEC C-TERMINAL CHEMISTRIES, (E) MACROPHAGE N-TERMINAL CHEMISTRIES, (F) MACROPHAGE C-TERMINAL CHEMISTRIES.....	94

FIGURE 56 – SCHEMATIC OF 2-AZIDOACETIC ACID SYNTHESIS	99
FIGURE 57 - DEGRADATION OF SOLUBLE PEPTIDE LIBRARIES BY hMSCs IN PEG HYDROGELS.	108
FIGURE 58 - DEGRADATION OF SOLUBLE PEPTIDE LIBRARIES BY HUVECs IN PEG HYDROGELS.	108
FIGURE 59 - DEGRADATION OF SOLUBLE PEPTIDE LIBRARIES BY MACROPHAGES IN PEG HYDROGELS.	109
FIGURE 60 - DEGRADATION OF SOLUBLE AC-BA PEPTIDE LIBRARIES BY CELLS IN PEG HYDROGELS.	109
FIGURE 61 - DEGRADATION OF SOLUBLE AC PEPTIDE LIBRARIES BY CELLS IN PEG HYDROGELS.	110
FIGURE 62 - DEGRADATION OF SOLUBLE N-BA PEPTIDE LIBRARIES BY CELLS IN PEG HYDROGELS.	110
FIGURE 63 - DEGRADATION OF SOLUBLE NH ₂ PEPTIDE LIBRARIES BY CELLS IN PEG HYDROGELS.	111
FIGURE 64 - DEGRADATION OF SOLUBLE C-BA PEPTIDE LIBRARIES BY CELLS IN PEG HYDROGELS.	111
FIGURE 65 - DEGRADATION OF SOLUBLE AM PEPTIDE LIBRARIES BY CELLS IN PEG HYDROGELS.	112
FIGURE 66 - DEGRADATION OF SOLUBLE COOH PEPTIDE LIBRARIES BY CELLS IN PEG HYDROGELS.	112
FIGURE 67 - COMPARISON OF PEPTIDE LIBRARY DEGRADATION BY CELLS ON TISSUE CULTURE PLASTIC AND CELLS IN GELS.	113
FIGURE 68 - RGD IS REQUIRED FOR CELL SPREADING AND VIABILITY WITHIN HYDROGELS. (A) AC-BA-GRGDS, (B) NH ₂ -GRGDS, (C) CYCLIC RGDs (cRGD), AND (D) NO ADDED RGDs. (E) hMSC SPREADING WAS INCREASED IN HYDROGELS WHICH WERE FUNCTIONALIZED WITH RGD PEPTIDES. RED IS ACTIN AND BLUE IS THE NUCLEI. SCALE BAR IS 100 μ M AND * INDICATES P < 0.05, *** INDICATES P < 0.001 BY TUKEY’S POST HOC TEST.	114

APPENDIX FIGURE 1 - LCMS SPECTRA OF THE AC-X-RGEFV-BA-NH ₂ LIBRARIES, WHERE X = ALA.....	143
APPENDIX FIGURE 2 - LCMS SPECTRA OF THE AC-X-RGEFV-BA-NH ₂ LIBRARIES, WHERE X = ARG.....	143
APPENDIX FIGURE 3 - LCMS SPECTRA OF THE AC-X-RGEFV-BA-NH ₂ LIBRARIES, WHERE X = ASN.....	144
APPENDIX FIGURE 4 - LCMS SPECTRA OF THE AC-X-RGEFV-BA-NH ₂ LIBRARIES, WHERE X = ASP.	144
APPENDIX FIGURE 5 - LCMS SPECTRA OF THE AC-X-RGEFV-BA-NH ₂ LIBRARIES, WHERE X = GLN.....	145
APPENDIX FIGURE 6 - LCMS SPECTRA OF THE AC-X-RGEFV-BA-NH ₂ LIBRARIES, WHERE X = GLU.....	145
APPENDIX FIGURE 7 - LCMS SPECTRA OF THE AC-X-RGEFV-BA-NH ₂ LIBRARIES, WHERE X = GLY.....	146
APPENDIX FIGURE 8 - LCMS SPECTRA OF THE AC-X-RGEFV-BA-NH ₂ LIBRARIES, WHERE X = HIS.	146
APPENDIX FIGURE 9 - LCMS SPECTRA OF THE AC-X-RGEFV-BA-NH ₂ LIBRARIES, WHERE X = ILE/LEU.....	147
APPENDIX FIGURE 10 - LCMS SPECTRA OF THE AC-X-RGEFV-BA-NH ₂ LIBRARIES, WHERE X = LYS.	147
APPENDIX FIGURE 11 - LCMS SPECTRA OF THE AC-X-RGEFV-BA-NH ₂ LIBRARIES, WHERE X = MET.	148
APPENDIX FIGURE 12 - LCMS SPECTRA OF THE AC-X-RGEFV-BA-NH ₂ LIBRARIES, WHERE X = PHE.	148
APPENDIX FIGURE 13 - LCMS SPECTRA OF THE AC-X-RGEFV-BA-NH ₂ LIBRARIES, WHERE X = PRO.	149
APPENDIX FIGURE 14 - LCMS SPECTRA OF THE AC-X-RGEFV-BA-NH ₂ LIBRARIES, WHERE X = SER.....	149

APPENDIX FIGURE 15 - LCMS SPECTRA OF THE AC-X-RGEFV-BA-NH ₂ LIBRARIES, WHERE X = THR.	150
APPENDIX FIGURE 16 - LCMS SPECTRA OF THE AC-X-RGEFV-BA-NH ₂ LIBRARIES, WHERE X = TRP.	150
APPENDIX FIGURE 17 - LCMS SPECTRA OF THE AC-X-RGEFV-BA-NH ₂ LIBRARIES, WHERE X = TYR.	151
APPENDIX FIGURE 18 LCMS SPECTRA OF THE AC-X-RGEFV-BA-NH ₂ LIBRARIES, WHERE X = VAL.	151
APPENDIX FIGURE 19 - LCMS SPECTRA OF THE AC-BA-X-RGEFV-BA-NH ₂ LIBRARIES, WHERE X = A) ALA.	152
APPENDIX FIGURE 20 - LCMS SPECTRA OF THE AC-BA-X-RGEFV-BA-NH ₂ LIBRARIES, WHERE X = ARG.	152
APPENDIX FIGURE 21 - LCMS SPECTRA OF THE AC-BA-X-RGEFV-BA-NH ₂ LIBRARIES, WHERE X = ASN.	153
APPENDIX FIGURE 23 - LCMS SPECTRA OF THE AC-BA-X-RGEFV-BA-NH ₂ LIBRARIES, WHERE X = GLN.	154
APPENDIX FIGURE 24 - LCMS SPECTRA OF THE AC-BA-X-RGEFV-BA-NH ₂ LIBRARIES, WHERE X = GLU.	154
APPENDIX FIGURE 25 - LCMS SPECTRA OF THE AC-BA-X-RGEFV-BA-NH ₂ LIBRARIES, WHERE X = GLY.	155
APPENDIX FIGURE 26 - LCMS SPECTRA OF THE AC-BA-X-RGEFV-BA-NH ₂ LIBRARIES, WHERE X = HIS.	155
APPENDIX FIGURE 27 - LCMS SPECTRA OF THE AC-BA-X-RGEFV-BA-NH ₂ LIBRARIES, WHERE X = ILE/LEU.	156
APPENDIX FIGURE 28 - LCMS SPECTRA OF THE AC-BA-X-RGEFV-BA-NH ₂ LIBRARIES, WHERE X = LYS.	156
APPENDIX FIGURE 29 - LCMS SPECTRA OF THE AC-BA-X-RGEFV-BA-NH ₂ LIBRARIES, WHERE X = MET.	157

APPENDIX FIGURE 30 - LCMS SPECTRA OF THE AC-BA-X-RGEFV-BA-NH ₂ LIBRARIES, WHERE X = PHE.	157
APPENDIX FIGURE 31 - LCMS SPECTRA OF THE AC-BA-X-RGEFV-BA-NH ₂ LIBRARIES, WHERE X = PRO.	158
APPENDIX FIGURE 32 - LCMS SPECTRA OF THE AC-BA-X-RGEFV-BA-NH ₂ LIBRARIES, WHERE X = SER.	158
APPENDIX FIGURE 33 - LCMS SPECTRA OF THE AC-BA-X-RGEFV-BA-NH ₂ LIBRARIES, WHERE X = THR.	159
APPENDIX FIGURE 34 - LCMS SPECTRA OF THE AC-BA-X-RGEFV-BA-NH ₂ LIBRARIES, WHERE X = TRP.	159
APPENDIX FIGURE 35 - LCMS SPECTRA OF THE AC-BA-X-RGEFV-BA-NH ₂ LIBRARIES, WHERE X = TYR.	160
APPENDIX FIGURE 36 LCMS SPECTRA OF THE AC-BA-X-RGEFV-BA-NH ₂ LIBRARIES, WHERE X = VAL.	160
APPENDIX FIGURE 37 - LCMS SPECTRA OF THE AC-BA-RGEFV-X-NH ₂ LIBRARIES, WHERE X = ALA.	161
APPENDIX FIGURE 38 - LCMS SPECTRA OF THE AC-BA-RGEFV-X-NH ₂ LIBRARIES, WHERE X = ARG.	161
APPENDIX FIGURE 39 - LCMS SPECTRA OF THE AC-BA-RGEFV-X-NH ₂ LIBRARIES, WHERE X = ASN.	162
APPENDIX FIGURE 40 - LCMS SPECTRA OF THE AC-BA-RGEFV-X-NH ₂ LIBRARIES, WHERE X = ASP.	162
APPENDIX FIGURE 41 - LCMS SPECTRA OF THE AC-BA-RGEFV-X-NH ₂ LIBRARIES, WHERE X = GLN.	163
APPENDIX FIGURE 42 - LCMS SPECTRA OF THE AC-BA-RGEFV-X-NH ₂ LIBRARIES, WHERE X = GLU.	163
APPENDIX FIGURE 43 - LCMS SPECTRA OF THE AC-BA-RGEFV-X-NH ₂ LIBRARIES, WHERE X = GLY.	164

APPENDIX FIGURE 44 - LCMS SPECTRA OF THE AC-BA-RGEFV-X-NH ₂ LIBRARIES, WHERE X = HIS.	164
APPENDIX FIGURE 45 - LCMS SPECTRA OF THE AC-BA-RGEFV-X-NH ₂ LIBRARIES, WHERE X = ILE/LEU.	165
APPENDIX FIGURE 46 - LCMS SPECTRA OF THE AC-BA-RGEFV-X-NH ₂ LIBRARIES, WHERE X = LYS.	165
APPENDIX FIGURE 47 - LCMS SPECTRA OF THE AC-BA-RGEFV-X-NH ₂ LIBRARIES, WHERE X = MET.	166
APPENDIX FIGURE 48 - LCMS SPECTRA OF THE AC-BA-RGEFV-X-NH ₂ LIBRARIES, WHERE X = PHE.	166
APPENDIX FIGURE 49 - LCMS SPECTRA OF THE AC-BA-RGEFV-X-NH ₂ LIBRARIES, WHERE X = PRO.	167
APPENDIX FIGURE 50 - LCMS SPECTRA OF THE AC-BA-RGEFV-X-NH ₂ LIBRARIES, WHERE X = SER.	167
APPENDIX FIGURE 51 - LCMS SPECTRA OF THE AC-BA-RGEFV-X-NH ₂ LIBRARIES, WHERE X = THR.	168
APPENDIX FIGURE 52 - LCMS SPECTRA OF THE AC-BA-RGEFV-X-NH ₂ LIBRARIES, WHERE X = TRP.	168
APPENDIX FIGURE 53 - LCMS SPECTRA OF THE AC-BA-RGEFV-X-NH ₂ LIBRARIES, WHERE X = TYR.	169
APPENDIX FIGURE 54 - LCMS SPECTRA OF THE AC-BA-RGEFV-X-NH ₂ LIBRARIES, WHERE X = VAL.	169
APPENDIX FIGURE 55 - LCMS SPECTRA OF THE AC-BA-RGEFV-X-BA-NH ₂ LIBRARIES, WHERE X = ALA.	170
APPENDIX FIGURE 56 - LCMS SPECTRA OF THE AC-BA-RGEFV-X-BA-NH ₂ LIBRARIES, WHERE X = ARG.	170
APPENDIX FIGURE 57 - LCMS SPECTRA OF THE AC-BA-RGEFV-X-BA-NH ₂ LIBRARIES, WHERE X = ASN.	171

APPENDIX FIGURE 58 - LCMS SPECTRA OF THE AC-BA-RGEFV-X-BA-NH ₂ LIBRARIES, WHERE X = ASP.	171
APPENDIX FIGURE 59 - LCMS SPECTRA OF THE AC-BA-RGEFV-X-BA-NH ₂ LIBRARIES, WHERE X = GLN.....	172
APPENDIX FIGURE 60 - LCMS SPECTRA OF THE AC-BA-RGEFV-X-BA-NH ₂ LIBRARIES, WHERE X = GLU.....	172
APPENDIX FIGURE 61 - LCMS SPECTRA OF THE AC-BA-RGEFV-X-BA-NH ₂ LIBRARIES, WHERE X = GLY.....	173
APPENDIX FIGURE 62 - LCMS SPECTRA OF THE AC-BA-RGEFV-X-BA-NH ₂ LIBRARIES, WHERE X = HIS.	173
APPENDIX FIGURE 63 - LCMS SPECTRA OF THE AC-BA-RGEFV-X-BA-NH ₂ LIBRARIES, WHERE X = ILE/LEU.....	174
APPENDIX FIGURE 64 - LCMS SPECTRA OF THE AC-BA-RGEFV-X-BA-NH ₂ LIBRARIES, WHERE X = LYS.	174
APPENDIX FIGURE 65 - LCMS SPECTRA OF THE AC-BA-RGEFV-X-BA-NH ₂ LIBRARIES, WHERE X = MET.	175
APPENDIX FIGURE 66 - LCMS SPECTRA OF THE AC-BA-RGEFV-X-BA-NH ₂ LIBRARIES, WHERE X = PHE.	175
APPENDIX FIGURE 67 - LCMS SPECTRA OF THE AC-BA-RGEFV-X-BA-NH ₂ LIBRARIES, WHERE X = PRO.	176
APPENDIX FIGURE 68 - LCMS SPECTRA OF THE AC-BA-RGEFV-X-BA-NH ₂ LIBRARIES, WHERE X = SER.	176
APPENDIX FIGURE 69 - LCMS SPECTRA OF THE AC-BA-RGEFV-X-BA-NH ₂ LIBRARIES, WHERE X = THR.	177
APPENDIX FIGURE 70 - LCMS SPECTRA OF THE AC-BA-RGEFV-X-BA-NH ₂ LIBRARIES, WHERE X = TRP.	177
APPENDIX FIGURE 71 - LCMS SPECTRA OF THE AC-BA-RGEFV-X-BA-NH ₂ LIBRARIES, WHERE X = TYR.	178

APPENDIX FIGURE 72 - LCMS SPECTRA OF THE AC-BA-RGEFV-X-BA-NH ₂ LIBRARIES, WHERE X = VAL.....	178
APPENDIX FIGURE 73 - LCMS SPECTRA OF THE AC-BA-RGEFV-X-COOH LIBRARIES, WHERE X = ALA.....	179
APPENDIX FIGURE 74 - LCMS SPECTRA OF THE AC-BA-RGEFV-X-COOH LIBRARIES, WHERE X = ARG.	179
APPENDIX FIGURE 75 - LCMS SPECTRA OF THE AC-BA-RGEFV-X-COOH LIBRARIES, WHERE X = ASN.....	180
APPENDIX FIGURE 76 - LCMS SPECTRA OF THE AC-BA-RGEFV-X-COOH LIBRARIES, WHERE X = ASP.	180
APPENDIX FIGURE 77 - LCMS SPECTRA OF THE AC-BA-RGEFV-X-COOH LIBRARIES, WHERE X = GLN.....	181
APPENDIX FIGURE 78 - LCMS SPECTRA OF THE AC-BA-RGEFV-X-COOH LIBRARIES, WHERE X = GLU.....	181
APPENDIX FIGURE 79 - LCMS SPECTRA OF THE AC-BA-RGEFV-X-COOH LIBRARIES, WHERE X = GLY.....	182
APPENDIX FIGURE 80 - LCMS SPECTRA OF THE AC-BA-RGEFV-X-COOH LIBRARIES, WHERE X = HIS.	182
APPENDIX FIGURE 81 - LCMS SPECTRA OF THE AC-BA-RGEFV-X-COOH LIBRARIES, WHERE X = ILE/LEU.....	183
APPENDIX FIGURE 82 - LCMS SPECTRA OF THE AC-BA-RGEFV-X-COOH LIBRARIES, WHERE X = LYS.	183
APPENDIX FIGURE 83 - LCMS SPECTRA OF THE AC-BA-RGEFV-X-COOH LIBRARIES, WHERE X = MET.	184
APPENDIX FIGURE 84 - LCMS SPECTRA OF THE AC-BA-RGEFV-X-COOH LIBRARIES, WHERE X = PHE.	184
APPENDIX FIGURE 85 - LCMS SPECTRA OF THE AC-BA-RGEFV-X-COOH LIBRARIES, WHERE X = PRO.	185

APPENDIX FIGURE 86 - LCMS SPECTRA OF THE AC-BA-RGEFV-X-COOH LIBRARIES, WHERE X = SER.	185
APPENDIX FIGURE 87 - LCMS SPECTRA OF THE AC-BA-RGEFV-X-COOH LIBRARIES, WHERE X = THR.	186
APPENDIX FIGURE 88 - LCMS SPECTRA OF THE AC-BA-RGEFV-X-COOH LIBRARIES, WHERE X = TRP.	186
APPENDIX FIGURE 89- LCMS SPECTRA OF THE AC-BA-RGEFV-X-COOH LIBRARIES, WHERE X = TYR.	187
APPENDIX FIGURE 90 - LCMS SPECTRA OF THE AC-BA-RGEFV-X-COOH LIBRARIES, WHERE X = VAL.....	187
APPENDIX FIGURE 91 - LCMS SPECTRA OF THE NH ₂ -BA-X-RGEFV-BA-NH ₂ LIBRARIES, WHERE X = ALA.....	188
APPENDIX FIGURE 92 - LCMS SPECTRA OF THE NH ₂ -BA-X-RGEFV-BA-NH ₂ LIBRARIES, WHERE X = ARG.	188
APPENDIX FIGURE 93 - LCMS SPECTRA OF THE NH ₂ -BA-X-RGEFV-BA-NH ₂ LIBRARIES, WHERE X = ASN.....	189
APPENDIX FIGURE 94 - LCMS SPECTRA OF THE NH ₂ -BA-X-RGEFV-BA-NH ₂ LIBRARIES, WHERE X = ASP.	189
APPENDIX FIGURE 95 - LCMS SPECTRA OF THE NH ₂ -BA-X-RGEFV-BA-NH ₂ LIBRARIES, WHERE X = GLN.....	190
APPENDIX FIGURE 96 - LCMS SPECTRA OF THE NH ₂ -BA-X-RGEFV-BA-NH ₂ LIBRARIES, WHERE X = GLU.....	190
APPENDIX FIGURE 97 - LCMS SPECTRA OF THE NH ₂ -BA-X-RGEFV-BA-NH ₂ LIBRARIES, WHERE X = GLY.....	191
APPENDIX FIGURE 98 - LCMS SPECTRA OF THE NH ₂ -BA-X-RGEFV-BA-NH ₂ LIBRARIES, WHERE X = HIS.	191
APPENDIX FIGURE 99 - LCMS SPECTRA OF THE NH ₂ -BA-X-RGEFV-BA-NH ₂ LIBRARIES, WHERE X = ILE/LEU.....	192

APPENDIX FIGURE 100 - LCMS SPECTRA OF THE NH ₂ -BA-X-RGEFV-BA-NH ₂ LIBRARIES, WHERE X = LYS.	192
APPENDIX FIGURE 101 - LCMS SPECTRA OF THE NH ₂ -BA-X-RGEFV-BA-NH ₂ LIBRARIES, WHERE X = MET.	193
APPENDIX FIGURE 102 - LCMS SPECTRA OF THE NH ₂ -BA-X-RGEFV-BA-NH ₂ LIBRARIES, WHERE X = PHE.	193
APPENDIX FIGURE 103 - LCMS SPECTRA OF THE NH ₂ -BA-X-RGEFV-BA-NH ₂ LIBRARIES, WHERE X = PRO.	194
APPENDIX FIGURE 104 - LCMS SPECTRA OF THE NH ₂ -BA-X-RGEFV-BA-NH ₂ LIBRARIES, WHERE X = SER.	194
APPENDIX FIGURE 105 - LCMS SPECTRA OF THE NH ₂ -BA-X-RGEFV-BA-NH ₂ LIBRARIES, WHERE X = THR.	195
APPENDIX FIGURE 106 - LCMS SPECTRA OF THE NH ₂ -BA-X-RGEFV-BA-NH ₂ LIBRARIES, WHERE X = TRP.	195
APPENDIX FIGURE 107 - LCMS SPECTRA OF THE NH ₂ -BA-X-RGEFV-BA-NH ₂ LIBRARIES, WHERE X = Q) TYR.	196
APPENDIX FIGURE 108 - LCMS SPECTRA OF THE NH ₂ -BA-X-RGEFV-BA-NH ₂ LIBRARIES, WHERE X = VAL.	196
APPENDIX FIGURE 109 - LCMS SPECTRA OF THE NH ₂ -X-RGEFV-BA-NH ₂ LIBRARIES, WHERE X = ALA.	197
APPENDIX FIGURE 110 - LCMS SPECTRA OF THE NH ₂ -X-RGEFV-BA-NH ₂ LIBRARIES, WHERE X = ARG.	197
APPENDIX FIGURE 111 - LCMS SPECTRA OF THE NH ₂ -X-RGEFV-BA-NH ₂ LIBRARIES, WHERE X = ASN.	198
APPENDIX FIGURE 112 - LCMS SPECTRA OF THE NH ₂ -X-RGEFV-BA-NH ₂ LIBRARIES, WHERE X = ASP.	198
APPENDIX FIGURE 113 - LCMS SPECTRA OF THE NH ₂ -X-RGEFV-BA-NH ₂ LIBRARIES, WHERE X = GLN.	199

APPENDIX FIGURE 114 - LCMS SPECTRA OF THE NH ₂ -X-RGEFV-BA-NH ₂ LIBRARIES, WHERE X = GLU.....	199
APPENDIX FIGURE 115 - LCMS SPECTRA OF THE NH ₂ -X-RGEFV-BA-NH ₂ LIBRARIES, WHERE X = GLY.....	200
APPENDIX FIGURE 116 - LCMS SPECTRA OF THE NH ₂ -X-RGEFV-BA-NH ₂ LIBRARIES, WHERE X = HIS.	200
APPENDIX FIGURE 117 - LCMS SPECTRA OF THE NH ₂ -X-RGEFV-BA-NH ₂ LIBRARIES, WHERE X = ILE/LEU.....	201
APPENDIX FIGURE 118 - LCMS SPECTRA OF THE NH ₂ -X-RGEFV-BA-NH ₂ LIBRARIES, WHERE X = LYS.	201
APPENDIX FIGURE 119 - LCMS SPECTRA OF THE NH ₂ -X-RGEFV-BA-NH ₂ LIBRARIES, WHERE X = MET.	202
APPENDIX FIGURE 120 - LCMS SPECTRA OF THE NH ₂ -X-RGEFV-BA-NH ₂ LIBRARIES, WHERE X = PHE.	202
APPENDIX FIGURE 121 - LCMS SPECTRA OF THE NH ₂ -X-RGEFV-BA-NH ₂ LIBRARIES, WHERE X = PRO.	203
APPENDIX FIGURE 122 - LCMS SPECTRA OF THE NH ₂ -X-RGEFV-BA-NH ₂ LIBRARIES, WHERE X = SER.	203
APPENDIX FIGURE 123 - LCMS SPECTRA OF THE NH ₂ -X-RGEFV-BA-NH ₂ LIBRARIES, WHERE X = THR.....	204
APPENDIX FIGURE 124 - LCMS SPECTRA OF THE NH ₂ -X-RGEFV-BA-NH ₂ LIBRARIES, WHERE X = TRP.	204
APPENDIX FIGURE 125 - LCMS SPECTRA OF THE NH ₂ -X-RGEFV-BA-NH ₂ LIBRARIES, WHERE X = TYR.....	205
APPENDIX FIGURE 126 - LCMS SPECTRA OF THE NH ₂ -X-RGEFV-BA-NH ₂ LIBRARIES, WHERE X = VAL.....	205
APPENDIX FIGURE 127 - LCMS SPECTRA OF THE LIAANK PEPTIDE IN WHICH A GLYCINE WAS PLACED IMMEDIATELY ADJACENT TO AN N-TERMINAL AC-BA.	206

APPENDIX FIGURE 128 - LCMS SPECTRA OF THE LIAANK PEPTIDE IN WHICH A GLYCINE WAS PLACED IMMEDIATELY ADJACENT TO AN N-TERMINAL AC.....	206
APPENDIX FIGURE 129 - LCMS SPECTRA OF THE LIAANK PEPTIDE IN WHICH A GLYCINE WAS PLACED IMMEDIATELY ADJACENT TO AN N-TERMINAL BA.....	207
APPENDIX FIGURE 130 - LCMS SPECTRA OF THE LIAANK PEPTIDE IN WHICH A GLYCINE WAS PLACED IMMEDIATELY ADJACENT TO AN N-TERMINAL NH ₂	207
APPENDIX FIGURE 131 - LCMS SPECTRA OF THE LIAANK PEPTIDE IN WHICH A GLYCINE WAS PLACED IMMEDIATELY ADJACENT TO A C-TERMINAL BA.	208
APPENDIX FIGURE 132 - LCMS SPECTRA OF THE LIAANK PEPTIDE IN WHICH A GLYCINE WAS PLACED IMMEDIATELY ADJACENT TO A C-TERMINAL AM.	208
APPENDIX FIGURE 133 - LCMS SPECTRA OF THE LIAANK PEPTIDE IN WHICH A GLYCINE WAS PLACED IMMEDIATELY ADJACENT TO A C-TERMINAL COOH.....	209
APPENDIX FIGURE 134 - LCMS SPECTRA OF THE IVKVA PEPTIDE IN WHICH A GLYCINE WAS PLACED IMMEDIATELY ADJACENT TO AN N-TERMINAL AC-BA.	209
APPENDIX FIGURE 135 - LCMS SPECTRA OF THE IVKVA PEPTIDE IN WHICH A GLYCINE WAS PLACED IMMEDIATELY ADJACENT TO AN N-TERMINAL AC.....	210
APPENDIX FIGURE 136 - LCMS SPECTRA OF THE IVKVA PEPTIDE IN WHICH A GLYCINE WAS PLACED IMMEDIATELY ADJACENT TO AN N-TERMINAL BA.....	210
APPENDIX FIGURE 137 - LCMS SPECTRA OF THE IVKVA PEPTIDE IN WHICH A GLYCINE WAS PLACED IMMEDIATELY ADJACENT TO AN N-TERMINAL NH ₂	211
APPENDIX FIGURE 138 - LCMS SPECTRA OF THE IVKVA PEPTIDE IN WHICH A GLYCINE WAS PLACED IMMEDIATELY ADJACENT TO A C-TERMINAL BA.	211
APPENDIX FIGURE 139 - LCMS SPECTRA OF THE IVKVA PEPTIDE IN WHICH A GLYCINE WAS PLACED IMMEDIATELY ADJACENT TO A C-TERMINAL AM.	212
APPENDIX FIGURE 140 - LCMS SPECTRA OF THE IVKVA PEPTIDE IN WHICH A GLYCINE WAS PLACED IMMEDIATELY ADJACENT TO A C-TERMINAL COOH.....	212
APPENDIX FIGURE 141 - LCMS SPECTRA OF THE PEPTIDE USED FOR THE CONCENTRATION STUDIES IN WHICH A GLYCINE WAS PLACED IMMEDIATELY ADJACENT TO AN N-TERMINAL AC-BA.	213

APPENDIX FIGURE 142 - LCMS SPECTRA OF THE PEPTIDE USED FOR THE CONCENTRATION STUDIES IN WHICH A GLYCINE WAS PLACED IMMEDIATELY ADJACENT TO AN N-TERMINAL AC.	213
APPENDIX FIGURE 143 - LCMS SPECTRA OF THE PEPTIDE USED FOR THE CONCENTRATION STUDIES IN WHICH A GLYCINE WAS PLACED IMMEDIATELY ADJACENT TO AN N-TERMINAL BA.	214
APPENDIX FIGURE 144 - LCMS SPECTRA OF THE PEPTIDE USED FOR THE CONCENTRATION STUDIES IN WHICH A GLYCINE WAS PLACED IMMEDIATELY ADJACENT TO AN N-TERMINAL NH ₂	214
APPENDIX FIGURE 145 - LCMS SPECTRA OF THE PEPTIDE USED FOR THE CONCENTRATION STUDIES IN WHICH A GLYCINE WAS PLACED IMMEDIATELY ADJACENT TO A C-TERMINAL BA.	215
APPENDIX FIGURE 146 - LCMS SPECTRA OF THE PEPTIDE USED FOR THE CONCENTRATION STUDIES IN WHICH A GLYCINE WAS PLACED IMMEDIATELY ADJACENT TO A C-TERMINAL AM.	215
APPENDIX FIGURE 147 - LCMS SPECTRA OF THE PEPTIDE USED FOR THE CONCENTRATION STUDIES IN WHICH A GLYCINE WAS PLACED IMMEDIATELY ADJACENT TO A C-TERMINAL COOH.	216
APPENDIX FIGURE 148 - THE STRUCTURE OF AZIDE AND PEG RGEFV PEPTIDE. SHOWN, THE STRUCTURES ARE IMMEDIATELY ADJACENT TO AN AMINE TERMINATED RGEFV PEPTIDE.	216
APPENDIX FIGURE 149 - LCMS SPECTRA OF THE AZIDE MODIFIED AC-BA PEPTIDE IN WHICH A GLYCINE WAS PLACED ON THE N-TERMINUS.	217
APPENDIX FIGURE 150 - LCMS SPECTRA OF THE AZIDE MODIFIED AC PEPTIDE IN WHICH A GLYCINE WAS PLACED ON THE N-TERMINUS.	217
APPENDIX FIGURE 151 - LCMS SPECTRA OF THE AZIDE MODIFIED N-BA PEPTIDE IN WHICH A GLYCINE WAS PLACED ON THE N-TERMINUS.	218
APPENDIX FIGURE 152 - LCMS SPECTRA OF THE AZIDE MODIFIED NH ₂ PEPTIDE IN WHICH A GLYCINE WAS PLACED ON THE N-TERMINUS. F) C-BA, g) AM, h) COOH. THE PEG-MODIFIED PEPTIDES CONTAINED THE FOLLOWING FUNCTIONALIZATION'S: i) AC-BA, j) AC, k) N-BA, l) NH ₂ , m) C-BA, n) AM, o) COOH.	218

APPENDIX FIGURE 153 - LCMS SPECTRA OF THE AZIDE MODIFIED C-BA PEPTIDE IN WHICH A GLYCINE WAS PLACED ON THE C-TERMINUS.	219
APPENDIX FIGURE 154 - LCMS SPECTRA OF THE AZIDE MODIFIED AM PEPTIDE IN WHICH A GLYCINE WAS PLACED ON THE C-TERMINUS.	219
APPENDIX FIGURE 155 - LCMS SPECTRA OF THE AZIDE MODIFIED COOH PEPTIDE IN WHICH A GLYCINE WAS PLACED ON THE C-TERMINUS.	220
APPENDIX FIGURE 156 - LCMS SPECTRA OF THE PEG MODIFIED AC-BA PEPTIDE IN WHICH A GLYCINE WAS PLACED ON THE N-TERMINUS.	220
APPENDIX FIGURE 157 - LCMS SPECTRA OF THE PEG MODIFIED AC PEPTIDE IN WHICH A GLYCINE WAS PLACED ON THE N-TERMINUS.	221
APPENDIX FIGURE 158 - LCMS SPECTRA OF THE PEG MODIFIED N-BA PEPTIDE IN WHICH A GLYCINE WAS PLACED ON THE N-TERMINUS.	221
APPENDIX FIGURE 159 - LCMS SPECTRA OF THE PEG MODIFIED NH ₂ PEPTIDE IN WHICH A GLYCINE WAS PLACED ON THE N-TERMINUS.	222
APPENDIX FIGURE 160 - LCMS SPECTRA OF THE PEG MODIFIED C-BA PEPTIDE IN WHICH A GLYCINE WAS PLACED ON THE C-TERMINUS.	222
APPENDIX FIGURE 161 - LCMS SPECTRA OF THE PEG MODIFIED AM PEPTIDE IN WHICH A GLYCINE WAS PLACED ON THE C-TERMINUS.	223
APPENDIX FIGURE 162 - LCMS SPECTRA OF THE PEG MODIFIED COOH PEPTIDE IN WHICH A GLYCINE WAS PLACED ON THE C-TERMINUS.	223
APPENDIX FIGURE 163 - LCMS SPECTRA OF THE PEPTIDES USED FOR CELL CULTURE: N ₃ -KGPQGIWGQKLys(N ₃)-NH ₂ . NOTE THAT THE N-TERMINUS OF THE PEPTIDE CONTAINED AN AZIDE-ACETIC ACID MOIETY.	224
APPENDIX FIGURE 164 - LCMS SPECTRA OF THE PEPTIDES USED FOR CELL CULTURE: NH ₂ -GRGDS-Lys(N ₃)-NH ₂	224
APPENDIX FIGURE 165 - LCMS SPECTRA OF THE PEPTIDES USED FOR CELL CULTURE: AC-BA-GRGDS-Lys(N ₃)-NH ₂	225
APPENDIX FIGURE 166 - LCMS SPECTRA OF THE PEPTIDES USED FOR CELL CULTURE: CYCLIC GRGDS-Lys(N ₃).	225

APPENDIX FIGURE 167 - LCMS SPECTRA OF THE PEPTIDES USED FOR CELL CULTURE: THE NON-PROTEOLYTICALLY DEGRADABLE NH ₂ -bFbABABABABA-NH ₂ INTERNAL STANDARD.	226
APPENDIX FIGURE 168 - CELLS GROWING IN GELS WITH DIFFERENT RGD PRESENTATIONS. HUVECS GROWING IN GELS WITH (A) CYCLIC RGDS, (B) AC-BA-GRGDS, (C) NH ₂ -GRGDS, AND (D) NO ADDED RGDS. MACROPHAGES GROWING IN GELS WITH (E) CYCLIC RGDS, (F) AC-BA-GRGDS, (G) NH ₂ -GRGDS, AND (H) NO ADDED RGDS. IT SHOULD BE NOTED THAT THE VIABILITY ASSAY (FIG. S9) INDICATES NEGLIGIBLE OF METABOLIC ACTIVITY WITHIN HUVEC GELS LACKING RGD SEQUENCES. SCALE BAR IS 100 μ M, AND RED IS ACTIN AND BLUE IS THE CELL NUCLEI.....	226
APPENDIX FIGURE 169 - QUANTIFICATION OF VIABILITY AND PROLIFERATION IN HYDROGELS CONTAINING DIFFERENT RGD SEQUENCES. AN ALAMARBLUE METABOLIC ACTIVITY ASSAYS WAS PERFORMED ON (A) hMSCs, (B) HUVECs, AND (C) MACROPHAGES AND A DNA QUANTIFICATION ASSAY WAS PERFORMED ON (D) hMSCs, (E) HUVECs, AND (F) MACROPHAGES. * INDICATES P < 0.05, ** INDICATES P < 0.01, *** INDICATES P < 0.0001 BY TUKEY'S POST HOC TEST.	227
APPENDIX FIGURE 170 - LIVE/DEAD STAINING OF hMSCs IN GELS WITH DIFFERENT RGD CONDITIONS. hMSCs WERE STAINED AT DAY 1 IN GELS WITH (A) NO RGD, (B) NH ₂ -GRGDS, (C) AC-BA-GRGDS, AND (D) CYCLIC GRGDS. hMSCs WERE STAINED AT DAY 3 IN GELS WITH (E) NO RGD, (F) NH ₂ -GRGDS, (G) AC-BA-GRGDS, AND (H) CYCLIC GRGDS. hMSCs WERE STAINED AT DAY 7 IN GELS WITH (I) NO RGD, (J) NH ₂ -GRGDS, (K) AC-BA-GRGDS, AND (L) CYCLIC GRGDS. SCALE BAR IS 500 μ M.....	228
APPENDIX FIGURE 171 - LIVE/DEAD STAINING OF HUVECs IN GELS WITH DIFFERENT RGD CONDITIONS. HUVECs WERE STAINED AT DAY 1 IN GELS WITH (A) NO RGD, (B) NH ₂ -GRGDS, (C) AC-BA-GRGDS, AND (D) CYCLIC GRGDS. HUVECs WERE STAINED AT DAY 3 IN GELS WITH (E) NO RGD, (F) NH ₂ -GRGDS, (G) AC-BA-GRGDS, AND (H) CYCLIC GRGDS. HUVECs WERE STAINED AT DAY 7 IN GELS WITH (I) NO RGD, (J) NH ₂ -GRGDS, (K) AC-BA-GRGDS, AND (L) CYCLIC GRGDS. SCALE BAR IS 500 μ M.	229

APPENDIX FIGURE 172 - LIVE/DEAD STAINING OF MACROPHAGES IN GELS WITH DIFFERENT RGD CONDITIONS. MACROPHAGES WERE STAINED AT DAY 1 IN GELS WITH (A) NO RGD, (B) NH ₂ -GRGDS, (C) AC-BA-GRGDS, AND (D) CYCLIC GRGDS. MACROPHAGES WERE STAINED AT DAY 3 IN GELS WITH (E) NO RGD, (F) NH ₂ -GRGDS, (G) AC-BA-GRGDS, AND (H) CYCLIC GRGDS. MACROPHAGES WERE STAINED AT DAY 7 IN GELS WITH (I) NO RGD, (J) NH ₂ -GRGDS, (K) AC-BA-GRGDS, AND (L) CYCLIC GRGDS. SCALE BAR IS 500 μ M.	230
APPENDIX FIGURE 173 - STATISTICAL ANALYSES USING MULTI-WAY ANOVAS WITH A TURKEY POST-HOC TEST. THREE TECHNICAL REPLICATES WERE AVERAGED TO A SINGLE VALUES, AND STATISTICS WERE DONE ON EXPERIMENTAL/BIOLOGICAL REPLICATES. STATISTICAL ANALYSIS ON A) SOLUBLE PEPTIDES CULTURED WITH CELLS ON TISSUE CULTURE PLASTIC, ALL TIME POINTS B) SOLUBLE PEPTIDES CULTURED WITH CELLS ON TISSUE CULTURE PLASTIC AT 48 HOURS, C) LIAANK PEPTIDES AT 48 HOURS, D) IVKVA PEPTIDES AT 48 HOURS E) CONCENTRATION STUDY PEPTIDES AT 48 HOURS F) AZIDE/PEG FUNCTIONALIZED PEPTIDES CULTURED WITH CELLS AT 48 HOURS G) SOLUBLE PEPTIDES CULTURED WITH CELLS IN PEG HYDROGELS AT 48 HOURS.	254

Abstract

Biomaterials act at the interface of biology to enhance, impart, or recapitulate function to biologic systems. Incorporation of bioactive peptides within these materials is often necessary to improve function, however, the stability of these peptides is often unclear. Current methods of peptide quantification are laborious, and are mostly designed to test one substrate, or one protease at a time. A more functional assay capable of quantifying peptide stability in the presence of cells, with all the proteases and inhibitors that cells produce is needed to better understand cell-material interactions. Presented in this thesis is a novel liquid chromatography – mass spectrometry (LC-MS) based assay capable of multiplex quantification of peptides in the presence of cells and all the proteases they excrete. Medium is sampled and directly injected into the LC-MS to maintain sample integrity, at the cost of chromatography column lifespan. This method was used show simple chain-end modifications to peptides provides the most control over non-specific degradation of those peptides. Also, a novel N-terminal acetylated β -alanine was shown to impart the most protection against non-specific aminopeptidases. Additionally, data to support the theory that non-specific degradation of peptides tethered to biomaterials influence cell behavior

This work 1) develops new LC-MS based analytical techniques quantification of peptide stability in the presence of cells, 2) using RGEFV as a model peptide, demonstrate the importance of chain-end chemistry on peptide fidelity, and 3) demonstrate that non-specific degradation of peptides incorporated into hydrogels influences biological performance. Our results show that N-terminal amines were almost completely degraded in the presence

of hMSCs, hUVECs, and Macrophages by 48 hours of culture independent of the terminal amino acid. Peptides with C-terminal carboxylic acids were also mostly degraded independent of terminal amino acid. However, simple chain-end modifications may prevent non-specific degradation of peptides, preserving function.

Chapter 1: Introduction

1.1 Introduction

Biomaterials act at the interface of materials and biology to impart, enhance, or recapitulate function. For example, composite hydrogels combining natural and synthetic materials demonstrated wound healing was accelerated when the combination materials was used as opposed to any one material¹. Drug delivery may be achieved by physically and chemically linking them to a hydrogel via hydrostatic and physical peptide conjugation techniques². Upon enzymatic cleavage these drugs are then delivered to the site of interest². Biomaterials are also used study cells in three-dimensional tissue culture using a variety of different techniques. Camacho and colleges are able to print three-dimensional scaffolds with high resolution polycaprolactone inks, capable of printing multiple bioactive cues into scaffolds with a high degree of spatial organization³. Hydrogels are often used for such applications because they are soft, mostly water, and resembling much of physical characteristics of our own human tissues⁴. The study of biomaterials may be performed from two directions: 1) new biomaterials may be developed and cell behavior observed, or 2) cell-behavior is observed and biomaterials are designed based on that observation. This thesis develops a novel liquid chromatography – mass spectrometry (LC-MS) technique for multiplex quantification of peptides. Findings were then utilized to inform design parameters for the incorporation of peptides into hydrogels containing human mesenchymal stem cells (hMSCs), human umbilical vein endothelial cells (hUVECs), or macrophages in order to optimize peptide stability when desired.

The extracellular matrix (ECM) is a complex network of biomolecules that provides structural and biochemical support to surrounding cells in tissues⁵. Common components of the ECM include collagens, glycosaminoglycans, proteoglycans, fibronectin, elastins, and other proteins^{6,7}, each have unique structures and functions that support normal physiological function. Tissue development, regeneration, and homeostasis involves constant feedback between cells and the ECM, in which the ECM signals cells, and cells both producing and degrading the ECM⁸. Cell-ECM interactions are important for most physiological processes, including proliferation, differentiation, and cell survival⁹. A key feature of the ECM is that cells are able to directly bind the matrix using cell surface proteins. Many ECM proteins, such as collagens and fibronectin, have adhesion domains containing peptide sequences like RGD which enable the physical coupling of the cell to the local matrix. Cells can modulate and regulate the local ECM is via four main processes: 1) Force mediated remodeling, 2) ECM deposition, 3) post-translational chemical remodeling of the ECM, and 4) proteolytic degradation through secretion of proteases¹⁰. Proteolytic degradation of the ECM is known to releases bioactive factors, enables cell migration through a covalently matrix¹⁰, and degrade ECM bound components¹¹. One overarching themes of biomaterials research is to utilize native signaling strategies to elicited a desired result¹². This may be done by modulating ECM signaling molecules, proteolytic modification of the extracellular matrix, and changing the cell-matrix interactions¹². Proteolytic degradation offers a promising strategy for cell responsive materials because proteases are diverse in structure and function. Some are attached to the cell membrane¹³ are hypothesized to act within nanometers of the cell causing a highly

localized biomaterials response, and may induce cell signaling once activated¹³. Others are secreted and capable of action hundreds of microns away from the cell¹⁴ capable of causing bulk changes in the biomaterial¹⁵.

Extracellular matrix proteins are regularly used as a source of inspiration for smaller peptide design. Where a protein may have many ECM and cell regulating functions¹⁶, one small section of a protein, known as a peptide, may induce a more specified function to a cell¹⁷. For example, within the fibronectin amino acid sequence¹⁸ is the commonly utilized cell adhesion peptide RGD which was first recognized as the smallest peptide unit within the fibronectin protein that would induce cell adhesion¹⁷. Peptides are numerous in structure and function: While some promote adhesion, others are proteolytically cleavable¹⁹. Others will influence cell fate inducing osteogenic differentiation in stem cells²⁰. There are many more peptides that induce a variety of different functions in cells²¹. While many scientists and engineers will incorporate peptides into biomaterials to impart function, quantification of those peptides incorporated into biomaterials in the presence of cells is often not reported and remains technologically challenging. While some peptides are designed to degrade, others are designed to impart function and, degradation of that peptide will likely have a negative impact on bioactivity.

1.2 Introduction to Peptide Quantification

Current methods for quantifying the degradation of proteins and peptides include zymography²², fluorogenic assays, and LC-MS using the UV trace. Fluorogenic assays have been developed such as one that utilizes 7-Amino-4-methylcoumarin (AMC)²³. As a

protease cleaves the peptide, the AMC will fluoresce²³. This fluorescence may be measured and quantified²³. The advantage is this technique may be done in liquid, in the presence of cells, is rapid, and may be measured using a plate reader²³. The main disadvantage of this technique is only one protease substrate may be measured at a time. One other technique worth mentioning is the use of the UV-detector from LC-MS²⁴. Zymography involves isolating proteases, loading them into an electrophoretic gel which is comprised of a protease substrate, typically gelatin²². The proteases are then separated based on size, and buffer is exchanged allowing activation of those proteases²². After incubation overnight, the gel is stained for protein, and lack of stain will appear as a band indicating proteolytic activity²². That band may then be quantified²². Modifications to this technique have been made by the Leight lab wherein the gelatin was substituted with polyacrylamide containing a peptide containing a fluorescent molecule on the N-terminal end, and a quencher molecule on the C-terminal end²⁵. Upon proteolytic cleavage, the quencher molecule be released from the gel, and a fluorescent band will become visible when imaged. This band may then be quantified and degradation kinetics may be quantified²⁵. Disadvantages include only being able to test one substrate at a time, lengthy protocol requiring at least 24 hours, and is designed to visualize one-substrate at a time without the presence of cells. The technique will also separate regulating molecules that may naturally inhibit proteolytic behavior, so observed characteristics may not be representative of *invitro* or *in vivo* activity. This protocol incubated peptides with blood isolated immediately prior to incubation where degradation occurred²⁴. These analytes were separated using liquid chromatography, analytes were identified using mass spectrometry, and quantified using the peaks from the

UV detector (absorbance 214 nm)²⁴. The advantages of this technique are being able to measure proteolytic degradation within a complex fluid, the ability to observe metabolic products from the parent peptide, and the ability to identify each analyte. A major disadvantage is peptides that co-elute from the liquid chromatography system will be convoluted.

Quantification of peptides and proteolytic activity remains challenging. Especially if more than one protease or substrate needs to be quantified. LC-MS is a powerful technique for quantifying peptide amount due to its combination of separation by high pressure liquid chromatography and analyte identification/quantification by mass spectrometry. This technique has a major advantage that an aliquot from cell culture medium can be injected directly onto the LC-MS, separated, and quantified. This thesis shows that multiplex quantification of peptides is possible using optimized internal standards, sample preparation and storage, and careful experimental design²⁶.

1.3 Introduction to Synthetic Hydrogels

The extracellular matrix that surrounds cells is a hydrogel, and significant efforts have been made to recapitulate the important properties of the ECM within engineered systems²⁷. There are two common routes to forming hydrogels for cell culture: using biologically-derived materials and using synthetic materials.²⁸ The ECM is incredibly complex, containing dozens or more different proteins, each of which can have numerous signaling functions or have bound signaling molecules. A distinct advantage of biologically derived materials is that they often contain much of this signaling complexity²⁹. Matrigel is an

example of a biologically-derived cell culture matrix that is widely-used in research labs³⁰. Matrigel is made from the matrix produced by Engelbreth-Holm-Swarm mouse tumors, and contains many desirable bioactive components such as collagens, laminins³¹. While Matrigel is an excellent material for mimicking the native extracellular matrix, it suffers from batch-to-batch variation³¹, and empirically driven results are not reliably representative of physiological/pathological processes that occur in humans³². Matrigel has been described as a “black box,” due to its complexity, limited tunability³³, and production of hard to explain results³⁴. Another issue with biologically derived materials, and specifically reconstituted ECMs, is that they typically form weak gels whose mechanical properties are below that of most human tissues. Furthermore, modulating the mechanical properties without significantly reducing the bioactivity is often not possible.

Another approach to designing hydrogels is to use synthetic materials that have a high degree of tunability and reproducibility. These materials often have minimal interaction with the surrounding cells/tissue, and need to be modified with bioactive groups to enable many crucial physiological processes, such as cell adhesion and spreading²⁸. Polyethylene glycol (PEG), also known as polyethylene oxide (PEO), is a bioinert molecule³⁵ that resists protein adsorption and is readily modifiable^{36,37}. PEG is commonly used in biomaterials research^{38–40} because it offers diverse control in terms of molecular weight, structure, and functionality³⁶. This allows for targeted, reliable, and repeatable design of structure, which ultimately translates to function.

PEG is synthesized as a polymer with terminal hydroxyl groups,³⁶ which can be readily functionalized into a variety of different chemistries including: chloro⁴¹, amine³⁶,

dibenzoazacyclo-octyne⁴² and more^{36,41,42}. Importantly, PEG molecules in a variety of architectures, molecular weights, and functionalities can be readily purchased commercially.

PEG hydrogels are also convenient for engineered uses due to their tunable physical properties and their ability to modulate cell behavior. The mechanical properties of PEG hydrogels can be finely tuned through molecular weight, concentration and structure of the PEG polymer used⁴³. The crosslinking density can also be used to tune the mechanical properties, however it is also coupled with the diffusivity of solute molecules within the PEG network^{44,45}. Tuning the mechanical properties of PEG hydrogels has been shown to influence the rate of cell migration, with stiffer gels producing a slower migration rate⁴⁶. In total, PEG based biomaterials are highly versatile platforms that can be readily tuned by biomaterials laboratories for a range of different biomedical applications.

1.4 Introduction to Peptide Synthesis and Their Use in Biomaterials

Peptides are short protein fragments that are comprised of amino acids and have been widely used within biomaterials research^{21,47-49}. Peptides are easy to synthesize, can be modified with a variety of functional groups for biomaterial conjugation, and can be utilized for diverse range of bioactive functions. Peptides synthesis was revolutionized in 1963 by Bruce Merrifield when he published his work on Solid Phase Peptide Synthesis (SPPS)⁵⁰, allowing for the synthesis of peptides on a solid support. This approach vastly simplified the separation of desired products, which are attached to the solid support, from the soluble chemical byproducts. Since then peptide synthesis has been advanced through

the development of the 9-fluorenylmethoxycarbonyl (Fmoc) protected amino acids⁵¹, the development of new solid-support linkers and resins^{52–56}, and the development advancement of automated peptide synthesizers⁵⁷. The importance of SPPS was noted when Bruce Merrifield, who designed both solid phase peptide synthesis and the first automated peptide synthesizer, won the Nobel Prize in chemistry in 1984 for his “development of methodology for chemical synthesis on a solid matrix”⁵⁸.

Peptides are routinely conjugated into biomaterials to selectively impart bioactive functions^{59,60}. These functions include cell adhesion peptides that enable cell mobility and spreading^{61–63}, which may be attached to biomaterials through either the N-terminus, the C- terminus, or through an amino acid side chain. Another common method to conjugate peptides into network is by the N- and C- termini simultaneously to crosslink polymer chains and induce hydrogel formation⁶². Peptides attached in this manor are generally designed to be cleavable by endopeptidases secreted by cells, which enables spreading and migration throughout the hydrogel⁶². A variety of approaches have been used to attach peptides to biomaterials, including covalent conjugation, photoinitiated reactions, enzymatic coupling and non-covalent interactions⁶⁴. Canonical peptides contain multiple functional groups which are amenable to bioconjugation, including amines, carboxylic acids, and thiols,⁶⁴ which can be found on the side chains of lysine, glutamic & aspartic acid, and cysteine respectively. It is often desirable to have peptides and other molecules undergo reactions in the presence of cells, which is a challenge because of problems with unwanted cross reactivity with biomolecules present in the local environment. A class of biologically orthogonal “click” reactions have been developed to circumvent these issues.

This is most commonly done using cycloaddition between an azide and alkyne,⁶⁴ although this technique suffers from a significant drawback that it typically requires the presence of Cu(I), which is cytotoxic²⁶. A strained alkyne, such as cyclooctyne, dibenzocyclooctyne (DBCO) or bicyclo[6.1.0]non-4-yne (BCN), will enable the reaction of azide functionalized molecules with alkynes to form a triazole linker under physiological conditions without needing a catalyst⁶⁵. Attaching peptides to PEG is a powerful method for imparting engineered function to a synthetic biomaterial to improve bioactivity, including signaling, cell adhesion, and synthetic matrix modification²¹. This is most frequently done using the cell adhesion peptide RGD, which dramatically improves cell spreading and migration when covalently bonded to a synthetic PEG matrix facilitates.

1.5 Introduction to RGD

The extracellular matrix (ECM) is a rich source of inspiration for biomaterials design⁶⁶. Fibronectin was first described by Vaheri and Rouslahti as a “specific surface glycoprotein (SF)” in 1974⁶⁷, and independently by Hynes and Bye who described it as “a large, external, transformation-sensitive (LETS) glycoprotein” also in 1974⁶⁸. Four years later Hynes and Destree noted fibroblast spreading occurred when cultured on the “LETS” [fibronectin] protein⁶⁹. This was the first major clue that fibronectin plays an important role in cell adhesion, integrins, and that ECM components may induce cell spreading. From here, Pierschbacher first describes the fibronectin derived amino acid sequence RGD, as the smallest peptide unit that will enable cell attachment¹⁷. The RGD cell adhesion motif was

subsequently found to be conserved in ECM proteins vitronectin, von Willebrand factor, fibrinogen, osteopontin, and thrombospondin⁷⁰. Cell adhesion proteins such as RGD enable cell-spreading and motility through temporary binding to transmembrane proteins known as integrins⁷⁰. RGD plays a vital role in cell-matrix interactions in vivo, and as a tri-peptide it can be easily integrated into biomaterials to improve cell adhesion. As a result, peptides containing the RGD sequence have been the subject of intense study has resulted in much

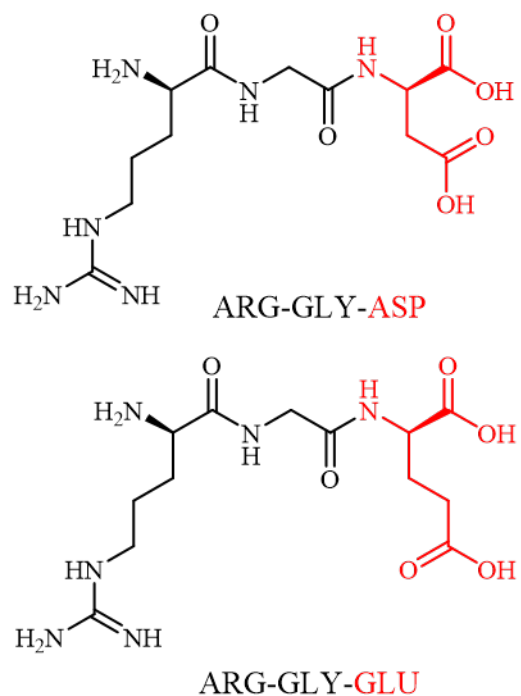


Figure 1 - Shows the difference between ARG-GLY-ASP, RGD (top) and ARG-GLY-GLU, RGE (bottom). Note the RGE cell-adhesion control peptide is only different by 1 carbon and 2 hydrogens.

research⁷¹. While the RGD tripeptide can facilitate cell adhesion, addition of amino acids to the sequence will modulate how cells interact with the peptide. A variety of RGDs, GRGDSP, GRGDNP, cyclic GPenGRGDSPCA have been used^{72,73}. Changing RGD sequence can tune which integrin a cell uses for adhesion and mobility⁷³. Interestingly, replacing the aspartate in RGD with a glutamate creates the cell adhesion control peptide RGE (Figure 1), in which cell-adhesion does not occur⁷⁴, and is a major inspiration for experimental design within this thesis.

1.6 Introduction to Proteases

Enzymes provide function in all essential processes including cell migration, differentiation, gene expression, immune function, and others⁷⁵. With more than 3,500

enzymes reported in the human proteome⁷⁶, enzymes are categorized into seven enzyme classes according to the reactions they catalyze. These classes consisting of: 1) oxidoreductases, 2) transferases, 3) hydrolases, 4) lyases, 5) isomerases, 6) ligases, and 7) translocases labeled EC 1 – EC 7 respectively⁷⁵. There are about 600 known proteases in the human body⁷⁶ which fall under the hydrolytic enzyme class (EC 3) and cleave amide bonds⁷⁵. Proteases may be broken down into two general categories, endopeptidases or exopeptidases^{75,77}. Endopeptidases cleave proteins/peptides in the middle of a protein/peptide chain⁷⁷. Exopeptidases cleave peptides/proteins at either the N or C terminus of a peptide, and may cleave anywhere from one-to-three amino acid residues⁷⁷. Exopeptidases that cleave peptides at the N-terminus are known as aminopeptidases⁷⁸. Exopeptidases that cleave peptides at the C-terminus are known as carboxypeptidases⁷⁸. Exopeptidases may be found within different organelles throughout the cell including cytoplasm, lysosomes and membranes or excreted into the extracellular matrix⁷⁸. They are coordinated with other proteases for diverse functions including amino acid retrieval from proteins consumed by an organism, endogenous protein turnover, protein maturation, and have a role in controlling the cell-cycle⁷⁸. Most scientists and engineers design protease sensitive peptides to be degraded by endopeptidases, however as long as cells are present exopeptidase are likely present as well within these engineered systems and should be considered anytime there is an N- or C- terminus of a peptide.

One such subclass of endopeptidases are metalloproteinases (MMPs)⁷⁵, which can be further broken down into a matrix metalloproteinase subclass⁷⁹ commonly utilized by scientists and engineers in biomaterials design^{80–83}. As a quick note, protease refer to endo-

and exo-peptidases, while proteinases are specific to endopeptidases⁷⁸. It is common for scientists and engineers to incorporate protease sensitive peptides into biomaterials design⁸⁰⁻⁸³ to increase crosslinks⁸⁴, degrade crosslinks⁸⁵, and dynamically change materials over time⁸⁶. This may be designed in support of drug delivery purposes, wherein cleavage of a drug conjugated to a hydrogel will allow it to diffuse out of that hydrogel². They are used for proteolytic remodeling of engineered scaffolds⁸³, and have been shown to be decrease crosslink density, facilitating cell migration⁸⁷. One peptide crosslinker is GPQGIWGQ, which has been demonstrated to mimic MMP-mediated cell invasion engineered matrix scaffolds.⁸⁷. By introducing peptide-based crosslinkers that are proteolytically degradable, scientists and engineers are able to impart desired functions such as release of a bioactive model, or planned matrix remodeling into an engineered construct. This is in stark contrast to other function-imparting peptides, like RGD, where long-lasting function is desired.

1.7 The Problem

While peptides such as RGD are routinely used in biomaterials to impart function, the long-term stability of these function peptides are generally unknown, but are assumed to be stable throughout the length of the study⁸⁸. This surprising, since the proteolytic remodeling of matrices with peptide crosslinks often utilized by scientists and engineers to achieved planned changes in mechanical properties⁸⁹ and/or achieve cellular migration⁸⁴. Peptides are degraded by two distinct classes of protease: 1) endopeptidases and 2) exopeptidases. Endopeptidases hydrolyze amide bonds in the center of peptides, whereas exopeptidases hydrolyze amide bonds at either the N or C terminus of a peptide (Figure 2)

and are generally considered non-specific in nature⁹⁰. In addition, it is known that peptide-

based therapeutics

are susceptible to

non-specific

proteolytic

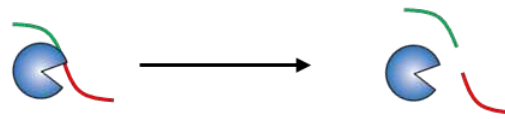
degradation and

remains one of the

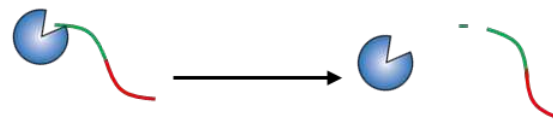
largest barriers to

efficacy⁹¹⁻⁹³. The

Endopeptidases – Hydrolyze Peptides in the Center



Exopeptidases – Hydrolyze Peptides at their Termini



Legend



Protease



Peptide

Figure 2 - (top) Illustrates endopeptidase hydrolyzation of a peptide along the interior and (bottom) exopeptidase hydrolyzation of a peptide along the N- or C-terminal end.

half-life of most peptides based therapeutics being less than 5 hours⁹¹. Peptide stability

with biomaterials is not commonly reported. **Highlighted is a fundamental knowledge**

gap regarding the stability of peptides within biomaterials, in the presence of cells,

and the influence this has on cell behavior. This thesis introduces technology

development in the area of LC-MS based quantification of peptides, and applies that

development to gather data to support the theory that exopeptidase degradation of bioactive

peptides in biomaterials influences cellular behavior.

Chapter 2: Developing a Method for Quantifying Peptide Degradation by Cells using LCMS

2.1 Introduction

Peptides are often incorporated into bioengineered systems due to their ease of synthesis, diversity of structure/function, and ability to directly and predictably modify the local or bulk environment. For example, some peptide have the ability to modify crosslinking density⁸⁴⁻⁸⁶, others allow motility and spreading of cells^{61,94}, and influence cell differentiation⁹⁵⁻⁹⁷ and more. However, cells produce many more proteases than the ones engineers typically design systems for, and without characterization of how the total proteolytic activity of cells degrade peptide sequences there is a significant chance that peptides will undergo unwanted degradation. As a result, there is a need to quickly and accurately quantify peptides amount as peptide stability directly influences function.

There are numerous methods of quantifying peptide degradation. Zymography-based techniques incorporate a proteolytic substrate, typically gelatin, into the gels typically used for electrophoresis⁹⁸. Non-heat deactivated samples are loaded into the gel, and after electrophoresis active proteases reform proteins are stained⁹⁸⁻¹⁰⁰. Lack of protein staining is indicative of gelatin degradation from proteolytic activity, which can then be quantified⁹⁸⁻¹⁰⁰. The Leight Lab has performed fluorogenic modifications to zymography by attaching a fluorescent and quenching molecule to the N- and C- terminal end of a protease substrate respectively²⁵. Upon proteolytic cleavage of that substrate, the quenching molecule is released from the matrix, producing a fluorescent band which can

be measured and quantified²⁵. Although a sensitive technique, the sample preparation is time consuming, and assay length takes at least a day for data acquisition, and the technique is ill-suited to examination of multiple substrates at once.

Others quantify protease degradation using fluorogenic assays in solution²³. One such example is illustrated by Ihssen and colleagues, wherein aminomethyl coumarin is attached on the c-terminus of a protease substrate of interest and, when proteolytically cleaved from the substrate produces fluorescence that may be measured²³. However, this technique is typically limited to assessing the degradation of a single peptide per sample. Another method quantifying degradation of peptides is by using HPLC, and LC-MS comparing the area under the curve of the UV (absorbance 214 nm) trace and normalizing that to a time zero trace,²⁴ with the mass spectrometer only being used to identify the species being quantified²⁴. While this method is suitable for one, or even multiple peptides that elute at different times, it is ill-suited at quantifying co-eluting peptides.

LC-MS quantification of peptides and proteins in the literature is mostly focused on quantifying a specific analyte of interest, such as a therapeutic peptide. This is typically quantified using LC-MS-MS, in which a complex mixture is separated using LC, the mass of interest is identified in the first MS and then a second round of mass spectrometry is performed after the mass of interest has been fragmented. LC-MS-MS gives information on both the parent mass, and the fragmented masses, which can be needed to validate that the identified molecule in highly complex biological samples where many masses may overlap ¹⁰¹. Internal standards are commonly applied as a calibration technique for

correcting errors associated with experiential procedure to improve reliability of quantitative techniques¹⁰²⁻¹⁰⁴.

Internal standards correct for volumetric changes throughout an experiment caused by sample preparation, evaporation, or instrumentation sampling errors^{103,104}. Wieling describes four classes of LC-MS internal standards: 1) no internal standard, 2) A structurally related compound, 3) a structurally similar compound, or 4) a stable isotope labelled (SIL) compound¹⁰⁴. A structurally similar compound contains the same mass, same chemical formula, however contains a different elution time due to structural dissimilarities¹⁰⁴. A structurally related compound is contains a similar structure with the same functional groups, with a different mass, and perhaps a different elution time¹⁰⁴. Finally SIL peptides contain ²H, ¹³C, and/or ¹⁵O isotopes integrated into their structure to allow for chemical, structural, and elution time similarities¹⁰⁴. However, in the context of small peptide quantification in which the starting amount is known, a stable peptide-based standard should be sufficient for quantification.

In addition, LC-MS quantification of analytes with complex sample preparation is subject to sample preparation bias^{105,106} and requires careful consideration. This sample bias may selectively screen for or deplete analytes of interest, affect reproducibility, or skew results in a non-representative way^{105,106}. However, quantification of peptides directly from a crude sample matrix will limit sample losses and variance from preparation. Using a peptide-based internal standard that is proteolytically stable is a believed to be a sufficient and cost-effective solution to track the stability of multiple peptide-based targets.

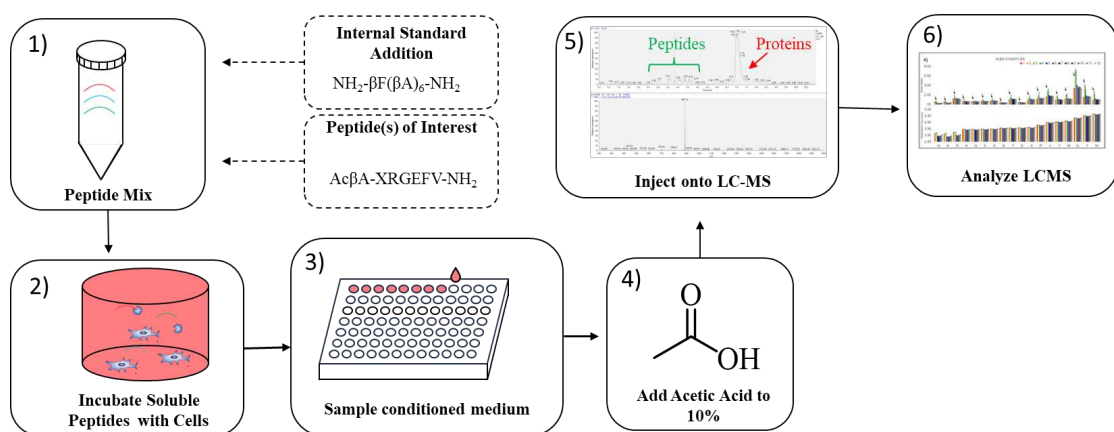


Figure 3 – Proposed experimental workflow for LC-MS based quantification of peptides. 1) Peptides with unique masses are mixed together along with a proteolytically stable internal standard. 2) Peptides are incubated with cells and subjected to cell-secreted proteases. 3) Conditioned media is sampled and placed directly into an LC-MS microtiter plate. 4) Glacial acetic acid is added to each sample well to a final concentration of 10%. 5) Sample is injected into LC-MS, quantified, and 6) analyzed and visualized.

In this Chapter we developed a convenient strategy for assessing peptide stability in the presence of cells using LC-MS (Figure 3). In our approach peptide libraries are added to cell culture media and incubated with cells. The conditioned medium is injected directly onto the LC-MS, limiting losses or modifications of analytes from the sample matrix, as well as enhancing separation of endogenous proteins from the peptides being studied. A drawback of this methodology is that several classes of molecules present in conditioned cell culture media, including proteins and lipids, can permanently damage chromatography columns which will eventually reduce the ability of peptides to be quantified using LC-MS. To validate this protocol, we characterized multiple variables involved in sample collection and LC-MS analysis, including internal standard selection, the influence of injection conditions on separation, quantifying chromatography column failure, and sample preservation. This method may be generally applicable for the quantitative characterization of peptide stability within a complex solution using LCMS.

2.2 Experimental

2.2.1 Peptide Synthesis

Peptides were synthesized using standard solid phase peptide synthesis (SPPS) protocols using either manual synthesis or an automated peptide synthesizer (CEM Liberty Blue) using standard Fmoc-protected amino acids (Chemscene) on a Rink amide resin (Supra Sciences) unless a C-terminal carboxylic acid was desired, in which case 2-chlorotrityl resin was used. All amide couplings were done using O-(6-chlorobenzotriazol-1-yl)-N,N,N',N'-tetramethyluronium hexafluorophosphate (HCTU) in DMF unless otherwise noted. For each coupling the amino acid, HCTU, and DIPEA were added in a 4:4:6 molar ratio to the peptide. During peptide synthesis a ninhydrin test was performed after every addition to test for the presence of free amines. Upon a positive test, the coupling was replicated until the test was negative. A capping step was then performed with acetic anhydride (Sigma-Aldrich) in a 10:5:100 acetic anhydride:DIPEA:DMF solution twice for 5 min, and then a ninhydrin test was performed to check for complete capping of the free amines. After successful coupling, the Fmoc group was removed, washing the resin with 20% piperidine in DMF twice for 5 min. A ninhydrin test was performed to check for a positive result.

Split-and-pool methods¹⁰⁷ were used to rapidly create peptide libraries. For the split and pool steps, the resin was washed 3× with DMF and then the entire amount of resin was weighed on a scale. This number was divided by approximately 22 and this was split 19 ways into 19 separate tubes, with some excess to account for resin loss during transport and weighing. The reactions were performed in 15 mL tubes and upon successful coupling

of all 19 amino acids all 19 fractions of resin were re-combined. Peptide libraries attached to the C-terminal end were completed in one vessel.

Table 1 – List of all peptides used to develop method LC-MS method of peptide quantification. An NH₂ on the N-terminus stands for an amine, βA for β-Alanine, βF for β-phenylalanine, and X stands for every canonical amino acid except for cysteine.

Peptide	Amino Acid Sequence		Peptide	Amino Acid Sequence
2.1	NH ₂ -βA6-Amide		2.2	Ac-βA6-Amide
2.3	NH ₂ -βA3FβA3-NH ₂		2.4	Ac-βA3FβA3-Amide
2.5	NH ₂ -βA3βFβA3-NH ₂		2.6	Ac-βA3βFβA3-Amide
2.7	NH ₂ -FβA6-NH ₂		2.8	Ac-FβA6-Amide
2.9	NH ₂ -βFβA6-NH ₂		2.10	Ac-βFβA6-Amide
2.11	AcβA-XRGEFV-βA		2.12	AcβA-RGEFVX-Amide

2.2.2 Peptide Cleavage from Solid Phase

Peptides libraries and all peptides containing tryptophan were cleaved using 92.5% trifluoroacetic acid (TFA), 2.5% H₂O, 2.5% triisopropylsilane (TIPS), and 2.5% dithiothreitol (DTT). Peptides which lacked a tryptophan were cleaved without DTT. Peptides were typically cleaved for 2-3 hours at room temperature using approximately 25 mL of cleavage solution per mM of peptide. However, peptides containing azides were cleaved for 30 minutes to prevent degradation of the azide group. Peptide mass was checked using electrospray ionization and if protecting groups remained the peptide was re-cleaved for 30 minutes. The masses of the peptide libraries were checked using liquid chromatography mass spectrometry (LCMS) and if protecting groups remained the peptides were re-cleaved for 30 minutes. At the end of the cleavage the peptides were precipitated in diethyl ether. These were then centrifuged for 5 minutes at 4,000 rpm, and

the supernatant was discarded. The peptide pellet was washed with diethyl ether, and centrifuged, and this was repeated twice. The peptide pellet was allowed to dry, and then dissolved in water and neutralized with ammonium hydroxide prior to purification.

2.2.3 Peptide Purification

All peptides were purified using HPLC using a Phenomenex Gemini 5 μm NX-C18 110 Å LC Column 150 \times 21.2 mm. Gradients were run from 95% Mobile Phase A (water with 0.1% TFA) and 5% Mobile Phase B (acetonitrile with 0.1% TFA) to 100% Mobile Phase B. A typical HPLC run featured a two-minute equilibration step, followed by a 10-minute ramp from 95% Mobile Phase A to 100% Mobile Phase B, and then two minutes of equilibration at 100% Mobile Phase B, before ramping back down to the starting conditions. Notably, the split-and-pool libraries were ramped up to 100% Mobile Phase B over two minutes, since these libraries consisted of approximately 19 different peptides which weren't intended to be separated from each other. The protected cyclic RGD peptides was purified using a gradient that ramped from 30% Mobile Phase B to 100% Mobile Phase B. After purification all peptides evaluated for purity using LC-MS. If unpure peptides were repurified via preparative HPLC). were lyophilized and were ready to use.

2.2.4 Degradation of Peptides by Human Mesenchymal Stem Cells on Tissue Culture Plastic

Human mesenchymal stem cells (hMSCs) (Rooster Bio) at passage 3 were seeded into 24 well plates at a seeding density of 75,000 cells per well in 1ml of RoosterBasal™-MSC-CC (RoosterBio, SU-022) containing RoosterBooster™-MSC (RoosterBio SU-003). After 24 hour the media was changed. 24 hours later and peptides of interest were added to the

cell media for a final concentration of 37 μ M per peptide. Each peptide was tested with three experimental replicates each with three technical replicates for a total of 9 wells. 40 μ l samples were collected from the media at hours 0, 1, 4, 8, 24, and 48. Studies were performed using Lot 310268 a 19-year-old Eritrean/east african female.

2.2.5 Sample Treatment

Human mesenchymal stem cells (hMSCs) (Rooster Bio, LOT 310368) at passage 3 were seeded into 24 well plates at a seeding density of 75,000 cells per well in 1ml of RoosterBasal™-MSC-CC (RoosterBio, SU-022) containing RoosterBooster™-MSC (RoosterBio SU-003). After 24 hour the media was changed, and peptide library Ac β A-RGEFV-X-NH₂ was added to the cell media for a final concentration of 37 μ M per peptide. Each Library was tested with three experimental, each in triplicate for a total of 9 wells. 40 μ l samples were collected from the media at hours 0, 1, 4, 8, 24, and 48 in duplicate.

In-between timepoints, one set of samples was loaded directly within the LC-MS and measured as soon as possible, then stored at 4°C. The second set of samples was immediately frozen at -80°C. After 48 hours, samples were kept frozen and thawed just prior to LC-MS, and 4 μ l of acetic acid was added to each well. After three weeks the samples were tested again.

2.2.6 Standard Selection

hMSCs (Rooster Bio, LOT 310368) at passage 3 were seeded into 24 well plates as described above. After 24 hour the media was changed, and Standard peptides (Table 1, peptides 2.1-2.10) was added to the cell media for a final concentration of 37 μ M per

peptide. The library was tested in three times, each in triplicate with three technical repeats for a total of 9 wells. 40 μ l samples were collected from the media at hours 0, 1, 4, 8, 24, and 48 in duplicate. After 48 hours, samples were kept frozen and only thawed immediately prior to LC-MS, and 4 μ l of acetic acid was added to each well and analyzed via LC-MS.

2.2.7 Injection Solvent Effects

Peptide Library Ac β A-X-RGEFV- β A was added to solvents: Water, 50% Acetonitrile in Water, PBS, RoosterBasalTM-MSC-CC (RoosterBio, SU-022) containing RoosterBoosterTM-MSC (RoosterBio SU-003), Vasculife Basal Media (Lifeline Cell TechnologyTM, LM-0002), and macrophage serum free media with L-Glutamine (Gibco 12065-074) with 1% antibiotic-antimycotic (Gibco, 15240-062) at a concentration of 37 μ M per peptide. This was also repeated with each solvent containing 10% acetic acid at a concentration of 37 μ M for a total of 12 different solvents tested. The library within any given solvent was tested three times, each in triplicate with three technical repeats for a total of 9 wells. Samples were immediately loaded into the LC-MS for data collection.

2.2.8 Column Performance

A new column (ProntoSIL C18 AQ, 120 \AA , 3 μ m, 2.0x50 mm HPLC column, PN 0502F184PS030) was first primed by flushing 0.1% acetic acid in ultrapure water, followed by 0.1% acetic acid in acetonitrile, and last with 0.1% acetic acid in ultrapure water all at a volumetric flow rate of 300 μ l/min for 20 minutes. Peptide Library Ac β A-X-RGEFV- β A was dissolved in ultrapure water containing 10% acetic acid and was used to track performance of the HPLC column. Conditioned media containing 10% fetal bovine serum (FBS) was used as a fouling agent. After every injection of the peptide library into

the HPLC, the fouling agent was injected four times. This was continued until column failure was observed via LC-MS.

2.2.9 Liquid Chromatography – Mass Spectrometry

Immediately after the 96-well sample plate were removed from the -80°C freezer, 4 µL of neat acetic acid was added to each well to acidify the media and prevent further peptide degradation by proteases, except for the solvent study and sample treatment study. From each sample, 10 µL of sample solution was introduced by the LC-MS through an Thermo Scientific Vanquish LC System (Thermo Fisher Scientific) and then to a Thermo Scientific LTQ XL Linear Ion Trap Mass Spectrometer (Thermo Fisher Scientific). The sampled mixture was trapped on a column (ProntoSIL C18 AQ, 120 Å, 3 µm, 2.0 x 50 mm HPLC Column, PN 0502F184PS030, MAC-MOD Analytical Inc.). The samples were loaded onto the column with a solvent containing acetonitrile/water, 5:95 (v/v) containing 1% acetic acid at a flow rate of 300 µL/min and held for one minute. The sample was then eluted from the column with a linear gradient of 5-40% Solvent B (1% acetic acid in acetonitrile) at the same flow rate for five minutes. This was followed by a 1 min ramp up to 100% Solvent B, where it was re-equilibrated with Solvent A (1% acetic acid) to 5% solvent B over the course of 1 min and held there for 2 min. The column temperature was a constant 29 °C. The mass spectrometer was operated in positive ion mode. Using a heated ESI, the source voltage was set to 4.1 kV, and the capillary temperature was 350 °C.

Data analysis was performed on Xcalibur Software (Thermo Scientific). Peptides were identified automatically using the Thermo Xcalibur Processing Setup window where the mass (m/z) ± 0.5 atomic mass units and expected retention times for each quantified peptide

were inputted. This was later used to isolate individual peptide species from the total ion count (TIC) trace using the Thermo Xcalibur Quan Setup window, where the area under the curve was calculated and visually inspected for accuracy. All peptides were normalized to a non-degradable internal standard, NH₂-βFβA6-Amide, where βA is a β-alanine and βF is β-homophenylalanine. The integrated peak area of the peptide of interest was divided by the NH₂-βFβA6-amide internal standard to create an area ratio. Relative amounts of a peptide of peptide were then calculated by normalized all values to their corresponding time zero area ratio. Calculated data was visualized using RStudio.

2.3 Results and Discussion

2.3.1 Internal Standard Selection

The degradation of peptides was determined by quantifying the amount of peptides present a given time points and normalizing it to the initial amount present. This was done by injecting a specified sample volume of sample onto the LC-MS column for each run. However, a variety of factors can influence the concentration of peptide that is present within the samples independently of the peptide degradation, including sample evaporation, dilution, or errors in the amount of peptide injected due to factors such as air bubbles. Furthermore, the amount of peptide that is measured on the MS can vary due to changes in instrument parameters over time.¹⁰⁸ To compensate for this variability, quantitative studies in LC-MS typically use stable internal standards in each run to benchmark each of the analytes to in order to compensate for sources of error. Internal standard selection is important to ensure accurate and reliable analysis of LC-MS based quantification of peptide based systems to compensate for variability in external factors on

the LC-MS^{109,110}. The complexity of biological systems necessitates careful internal standard selection, as these standards are subject variation in technique, processing, biologic interaction, and the sample matrix¹¹⁰. To that end, a systematic approach was taken to choosing and assessing the appropriateness of the standard based on need.

It is typically desired to have an internal standard that is chemically similar to the analyte of interest in order to best mimic losses and modifications due to processing steps and better track LC-MS based variations in ionization efficiency¹¹⁰. The processing steps in the proposed workflow are limited to sample collection, the opportunities for sample loss are limited to interactions between sample and micropipette tip and LCMS microtiter plate. The major concern is that the internal standard needs to be stable through cell-culture and compensate variances within the LC-MS. A polypeptide would make an ideal internal standard for peptide degradation studies as long as it tracks the analyte of interest during LC-MS. That said, the ability of enzymes to degrade peptides is a challenge for using polypeptides. Non-canonical amino acids, including β -amino acids which have two carbons between amide bonds instead of one, have been shown to be particularly resistant to most proteolytic degradation^{111–113}. We designed a series of 10 different β -alanine based peptides as candidate internal standards. These peptides were incubated with hMSCs for 48h and evaluated for signal intensity, retention time, and peptide stability.

NH₂- β A₆-Amide, where the N-terminal NH₂ is an amine, shows poor affinity to the LC-MS column, eluting before the chromatography gradient begins (Figure 4.A). This is a problem because salts from cell culture media elute before the gradient begins, and salts influence the ionization process, and are non-volatile molecules that can damage or dirty

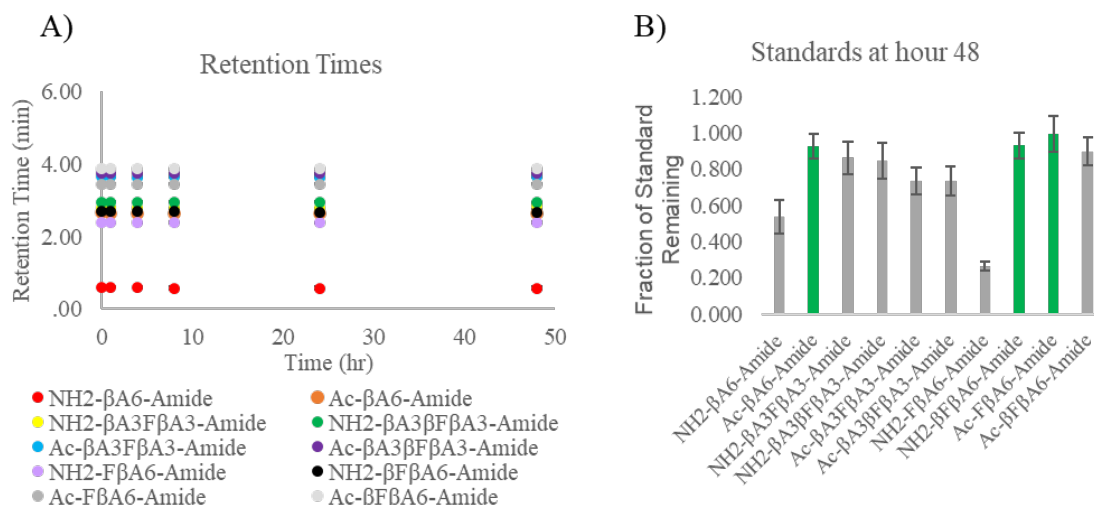


Figure 4 - Evaluation of 10 β -alanine based standards to identify molecules with both desired retention times and stability during culture. A) The retention time of peptides can be tuned through N-terminal modifications to the peptide sequence and the incorporation of hydrophobic residues. B) The stability of peptide sequences after 48 hours in culture with hMSCs was dependent on peptide sequence. Those with a fraction remaining of greater than 90% are shown in green.

the mass spectrometer. To account for this, the first 60 seconds of the mobile phase is sent to waste prior to ionization to prevent salts from entering the mass spectrometer and peptides and internal standards which elute before the gradient begins will not enter the mass spectrometer for quantification. N-terminal acetylation, the addition of a phenylalanine, or β -phenylalanine improves retention time by increasing the hydrophobicity of the polypeptide and increases the affinity to the column (Figure 4.A). After 48 hours of degradation, three internal standards candidates appeared viable with the fraction of peptides remaining measuring over 90% (Figure 4.B, green), 1) Ac- β A₆-NH₂, where the N-terminal Ac is acetyl group; 2) NH₂- β F β A₆-amide; and 3) Ac-F β A₆-amide. Ac- β A₆-amide was ruled out due to weak signal intensity of the LC-MS (not shown), due to lack of charge. NH₂- β F β A₆-amide was chosen for its highly repeatable peptide elution time of 2.68 minutes, its repeatability in measurement within 48 hours of incubation with

within the sample matrix, and its net charge of +1 under the acidic conditions of the LC-MS mobile phase.

2.3.2 Sample linearity

Sample linearity must be assessed to ensure the experimental range can produce quantifiable results by LCMS. A linear correlation is important because they experimentally confirm that results may be obtained in an accurate and precise manner¹¹⁴.

The accuracy of peptide quantification by LC-MS is heavily dependent on the choice of internal standard, as well as the sample preparation protocol¹¹⁵. In this workflow, peptides are incubated with cells, and timepoints are sampled from the same well. Sample preparation focused on collecting and treating samples with acetic acid to prevent proteolytic activity, ensuring the internal standard remains constant across all paired samples. The internal standard NH₂-βFβA₆-amide was used as an internal calibrant, and the linearity of the sample within the sample matrix was assessed by incubating peptide libraries AcβA-RGEFV-X-βA and AcβA-X-RGEFV-βA within RoosterBasal media. By keeping the internal standard constant and varying the level of analyte (Figure 5) linearity was observed, quantified, and can be seen in four representative samples where K, N, I/L, and F occupies the X position in the peptide libraries. The rest of the libraries are quantified in Table 2. Note: 100% is indicative of a peptide concentration of a 37 μM in the cell culture media, followed by an injection of 10 μL of sample onto the LC-MS. We observed a high degree of sample linearity across all peptides, with R² values typically above 0.97.

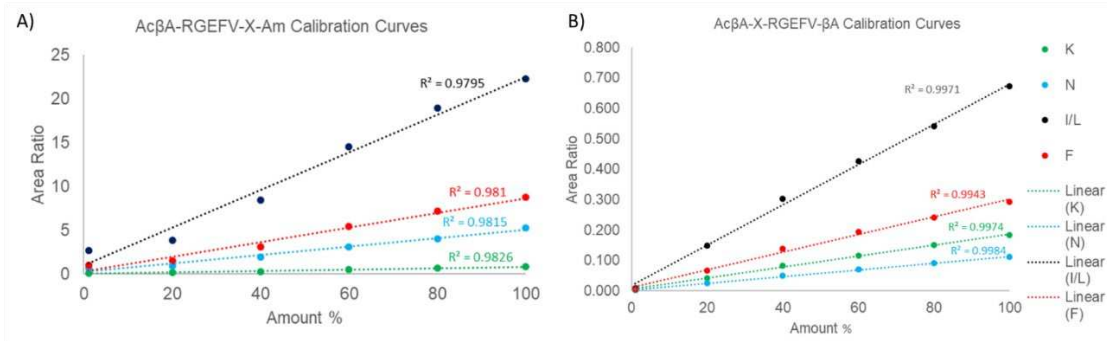


Figure 5 – A) Calibration curves for libraries AcβA-RGEFV-X-Am and B) AcβA-X-RGEFV-βA, where X is all canonical amino acids except for cysteine. Shown are representative calibration curves where X is K, N, I/L, and F along with coefficients of correlation.

Table 2 – Slopes, Intercepts, and coefficients of correlation for linear fit of peptide libraries AcβA-RGEFVX-Am (top), and AcβA-XRGEFV-βA (bottom).

AcβA-RGEFV-X-Am									
	K	H	R	N	S	E	Q	G	D
SLOPE	0.008	0.004	0.009	0.048	0.055	0.048	0.045	0.079	0.053
INTERCEP	0.040	0.016	0.019	0.267	0.311	0.158	0.238	0.334	0.147
R ²	0.983	0.975	0.973	0.981	0.982	0.979	0.982	0.977	0.975
	A	T	P	Y	V	M	I/L	F	W
SLOPE	0.077	0.050	0.091	0.053	0.048	0.076	0.215	0.084	0.044
INTERCEP	0.248	0.240	0.308	0.237	0.180	0.257	0.988	0.292	0.161
R ²	0.981	0.982	0.978	0.983	0.978	0.977	0.979	0.981	0.963
AcβA-X-RGEFV-βA									
	K	H	R	N	S	E	Q	G	D
SLOPE	0.002	1.110	1.820	0.300	1.092	0.675	1.381	1.204	0.565
INTERCEP	0.005	0.001	-0.003	0.000	0.000	0.000	-0.002	0.001	0.001
R ²	0.997	1.000	1.000	1.000	1.000	0.999	0.998	1.000	0.998
	A	T	P	Y	V	M	I/L	F	W
SLOPE	2.421	0.836	1.523	0.789	1.702	0.698	2.989	0.439	0.641
INTERCEP	-0.004	0.001	0.000	0.001	-0.003	0.000	0.003	0.002	-0.002
R ²	0.998	1.000	1.000	0.999	1.000	1.000	1.000	0.999	0.999

2.3.3 Effect of Acetic Acid Treatment on Reproducibility

In most of our studies peptide libraries were incubated with hMSCs for 48 hours, after which the extent of peptide degradation was quantified using LC-MS. However, LC-MS is not typically done immediately after culture, and in most cases the samples are stored in a -80°C freezer prior to analysis. Since the collected cell culture media contains proteases, including MMPs⁸⁷ and other cell-secreted proteases, these enzymes have the potential to further degrade peptide libraries after the sample time point, which is undesirable.

To study the influence that sample processing can have on peptide degradation, the peptide library Ac β A-RGEFV-X- β A was selected because it was previously shown to degrade in the presence of hMSCs within a 48 hour period²⁶ and shown in Chapter 3 Figure 22. The goal of this study was to obtain conditions under which LC-MS based quantification could be obtained in a consistent manner over a three-week period. Untreated samples are defined as samples that were collected, placed in an LC-MS 96 well microtiter plate, and injected as is. 40 μ L of untreated samples were collected and immediately the amount of peptide present in the samples was immediately quantified. These plates were then placed in fridge at 4°C for storage. Treated samples were frozen at -80°C until after the 48-hour timepoint, where they were treated with 4 μ L of acetic acid, injected onto the LC-MS, and then stored again at -80°C. Note, that the all samples were taken from the same well and are therefore paired. After 23 days the samples were injected again onto the LC-MS and it was seen that the acetic acid treated samples had minimal additional degradation, whereas untreated samples showed significant degradation after 24 hours (Figure 6.A). The area ratio was used to quantify observations and is defined by normalizing the raw measurement to that of the internal standard. That was then normalized a second time to the time zero area ratio to quantify if the measurement was consistent 23 days after sample collection. Acetic acid treatment was not observed to alter the LC-MS area ratio measurement as compared to the untreated samples (Figure 6 – Green). After 23 days the treatment was observed to yield consistent results (Figure 6 – Red).

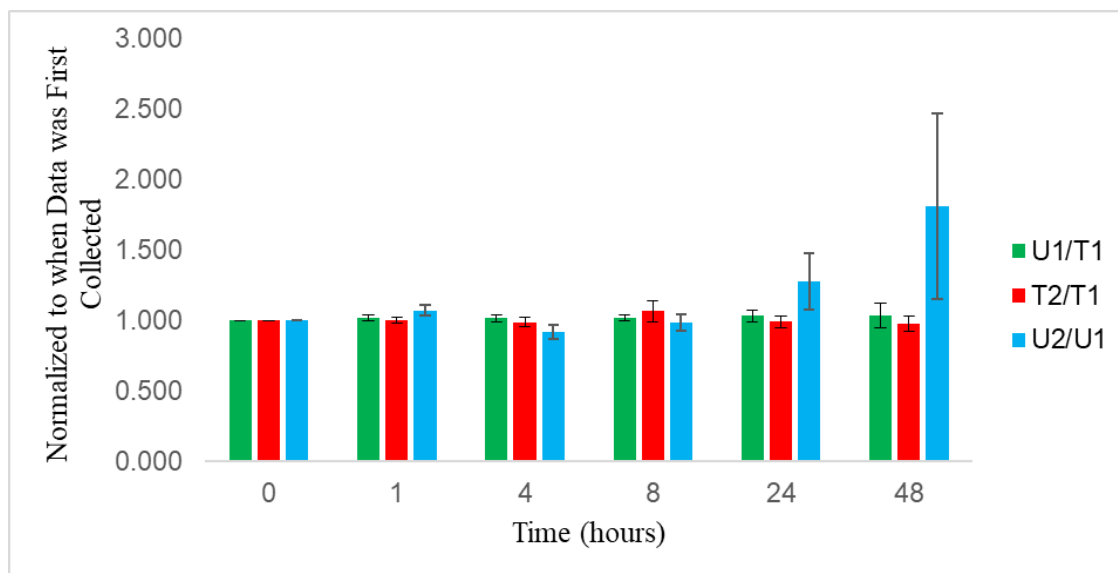


Figure 6 - The graph shows average consistency of all peptides within the peptide library, where the error bars are the standard deviation of the entire peptide library consistency. Consistency is reported for each timepoint. Acetic acid Treated (T) and Untreated samples (U) are compared for consistency of measurement. U1 is untreated samples injected on the LC-MS immediately after sample collection at any given timepoint, U2 are the same untreated samples collected 23 days later. T1 are the treated samples collected immediately after the 48-hour timepoint, and T2 are the treated samples collected 23 days later.

2.3.4 Effects of Injection Solvent on LC-MS performance

Reverse-phased chromatography is a highly effective technique for separating peptides¹¹⁶.

The use of a hydrophobic sorbent as the stationary phase results in affinity-based partitions, determined by the interactions of the solute with the mobile phase and the stationary phase¹¹⁶. Convenient parameters that can be optimized include solvent, temperature of the column, alkyl tail length of the stationary phase, choice of ion pairing reagent. The stationary phase (C18 alkyl tails), solvent composition (water and acetonitrile), and ion pair reagent (acetic acid) were held constant. Investigation of initial, common solvents peptides were dissolved in was performed.

To study effects of peptide solvent on column performance we used the peptide library Ac β A-X-RGEFV- β A, where X is each of the canonical amino acids except cysteine.

Previous work has shown that chemistry of peptide termini is the most effective means by which non-specific degradation of peptides may be controlled as compared to concentration or even PEGylation²⁶. The acetylated- β -alanine was shown to be the most proteolytically resistant to degradation within a 48 hour period when incubated with hMSCs, hUVECs, and pro inflammatory macrophages²⁶. This resistance to proteolytic degradation makes the Ac β A-X-RGEFV- β A library a good model system to study the effects of the sample matrix on peptide affinity to the stationary phase of the LC-MS, as well as performance on the mass spectrometer.

The Ac β A-X-RGEFV- β A library was dissolved in 12 solvents commonly found in a biomaterials lab, and immediately injected into the LC-MS for analysis (Figure 8.A). Solvents were chosen based on utility and include three different mediums, PBS, water, and acetonitrile which conveniently helps to dissolve more hydrophobic peptides. In all cases, peptide libraries were dissolved in any given solvent in triplicate, with three technical repeats, for a total of 9 wells per solvent. In most cases, the presence of salt (solvents 5-12) does not appear to affect the area ratio to an appreciable degree (Figure 8.B– top), but does effect the retention time of the stationary phase (Figure 8.B– bottom, solvents 5-12), especially noticeable on peptides where the variable X position contains positively charged residues H, K, and R. The presence of salts decreased the retention time of those positively charged residues, but this effect largely dissipates by the time Ac β A-NRGEFV- β A elutes from the column. Salt has a known effect of altering relative separation and retention times of species within the sample matrix due to changes in adsorption due to the electrical double layer repulsion¹¹⁷.

Organic solvents have a profound effect on LC-MS performance. Although sometimes necessary for peptide dissolution, adding 50% acetonitrile in water has significant detrimental effects on chromatographic performance (Figure 8.B, solvents 3 - 4). The presence of significant amounts of acetonitrile caused peak splitting in the internal standard (Figure 8.A – Right) such that much of it elutes from the column prior to gradient initiation. This is a problem for quantification because when collecting data from biological samples the mobile phase prior to the start of the gradient is typically sent to the waste, so peptides in these breakthrough peaks will not be quantified by the LC-MS. The observed area ratio (Figure 8.B) was correlated to an artificial increase in area ratio (Figure 8.B top) as the difference between the breakthrough peak of the analyte and the internal standard stop tracking with each other (Figure 8.B). The increased acid within the sample appears to increase column performance after the more hydrophilic residues as seen in solvent 4, in which 10% acetic acid is present within the sample.

A)

#	Solvent	#	Solvent
1	Deionized water	2	Solvent 1 with 10% Acetic Acid
3	50% acetonitrile in deionized water	4	Solvent 3 with 10% Acetic Acid
5	RPMI Media (Cytiva)	6	Solvent 5 with 10% Acetic Acid
7	Phosphate Buffered Saline	8	Solvent 7 with 10% Acetic Acid
9	Rooster Bio-MS-C-CC Media (RoosterBio)	10	Solvent 9 with 10% Acetic Acid
11	Basal Media (Lifeline)	12	Solvent 11 with 10% Acetic Acid

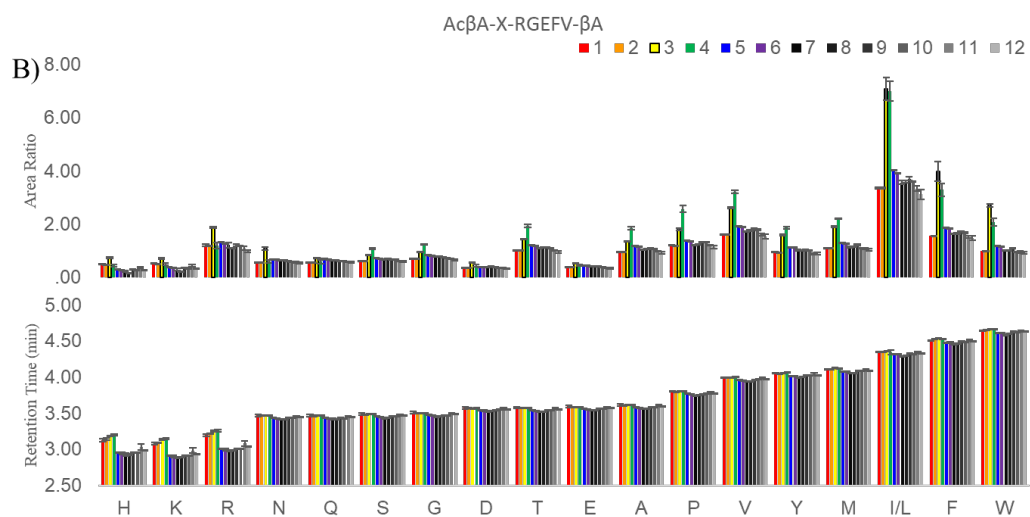


Figure 7 - AcβA-X-RGEFV-βA library, where X is amino acid A, D, E, F, G, H, I, K, L, M, N, P, Q, R, S, T, V, W, and Y, was dissolved at total concentration of 37uM in A) different solvents. B) Shows area ratio of each peptide in the library normalized to NH₂-βF(βA)₆-NH₂ (top) with its corresponding retention time (bottom).

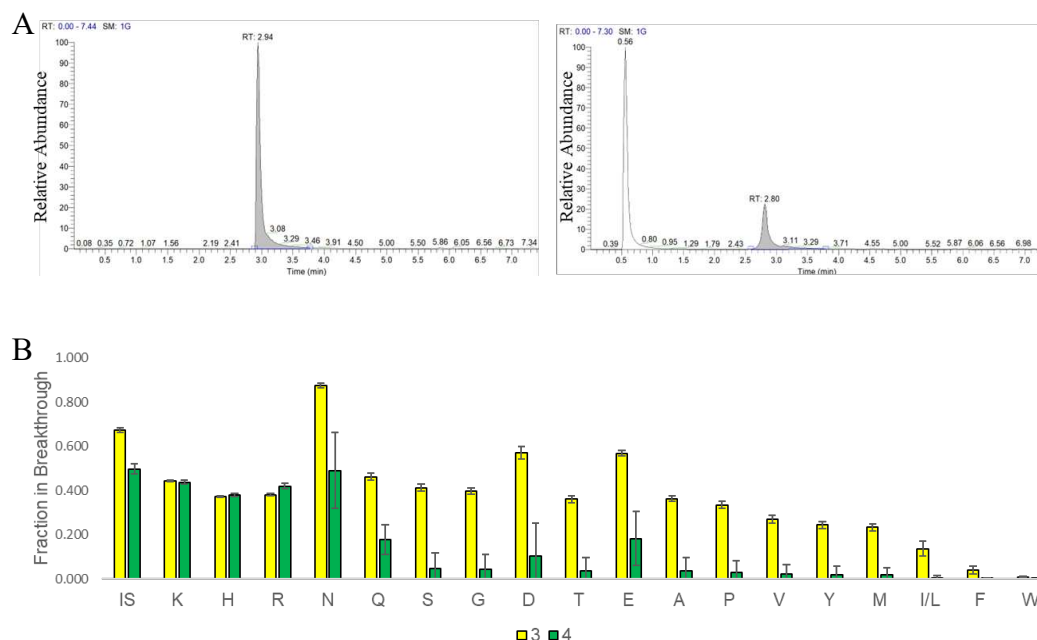


Figure 8 - A) Shows the internal standard peak $\text{NH}_2\text{-}\beta\text{F}(\beta\text{A})_6\text{-NH}_2$ in water. The left pane is representative of what was observed in solvents 1, 2, and 5-12; while the right pane demonstrates peak splitting and is representative of solvent's 2 and 3. B) Quantifies the proportion internal standard (IS) and analytes that are in the breakthrough peak as compared to what elutes at the expected retention time.

2.3.5 Quantifying column Failure

Proteins and lipids are present in most cell culture conditioned media in substantial concentrations. These biomolecules can frequently become irreversibly bound to the matrix within an HPLC column which will degrade performance and reliability. It is typically recommended that proteins and lipids are removed from each of the samples prior to LCMS analysis, and a variety of products are available to separate analytes from fouling agents, such as solid phase extraction (SPE) plates. However, these sample purification methods have three significant drawbacks. The first is that a single use 96-well SPE plate costs approximately \$375, which is 50% more than an LC-MS column. The second is that processing hundreds of samples via solid phase extraction can take ten hours or more of

lab time. Finally, sample purification protocols are typically optimized for a single analyte of interest to ensure that there is minimal sample loss during each of the steps. Our studies involve libraries of peptides having a range of physiochemical properties, and sample purification techniques have previously shown lack of consistency, and high variance of sample measurements by LC-MS (data not shown) compared to when samples were directly injected onto the column. By injecting crude material onto the LC-MS, losses from purification and processing steps are mitigated, at the cost of column lifespan.

We quantified the effects of repeatedly injecting cell culture samples that contain proteins, such as 10% fetal bovine serum (FBS), and lipids on column lifetime and consistency in data collection. We used the Ac β A-X-RGEFV- β A peptide library as a control and injected it onto the column every fifth injection after four injections of cell culture samples that contained 10% FBS. This was repeated until column failure was observed (Figure 9) and allowed us to quantify how column degradation influenced parameters such as retention time, peak area, and peak splitting on peptides with a range of physiochemical properties. The area ratio appears to remain relatively constant (Figure 9.A) over time. It is important to note that an individual set of runs will typically consist of dozens of injections in series, however our data shows that the first two or three injections of a run (Figure 9, all arrows) can have substantially altered chromatographic characteristics from the other injections, and that this is independent of column health. Pressure at the beginning of an injection can be observed to increase by ~100 bar when failure started to occur (Figure 9.D), however, the pressure differential is not an effective metric to quantify failure. This is evident because column failure was only observed in the hydrophobic residuals, that elute from the

column after 3 minutes and twenty-four seconds are still viable for quantification. Failure only started to appear after 348 injections of the media containing 10% FBS and 87 injections of the library (Figure 9.B). At this point failure becomes more visible and was analyzed further. First area ratio measurement numbers 3 - 23 were averaged. The first 2 data points were avoided as the data showed irregularities at the start of a set of measurements. Next all data-points were normalized to that average value. The number 1 was subtracted by that normalized value such that any value below zero represented a lower area ratio measured than the average of area ratios 3 – 23, and values above zero represent a higher area ratio measured than the average of area ratios 3 – 23. This value, which can be thought of as an error or deviation from when the column was new from the factory, was then propagated by taking the square root sum (Figure 9.B – inset pane) where it can be seen that peptides with the hydrophobic residuals are seen to increase higher than the rest, shown in red) by injection 124. After 348 injections of media with 10% FBS. The increase in column pressure and decrease in column performance is attributed to protein precipitation and lipid accumulation, some of which is irreversible on the column, introducing a less predictable stationary phase of the HPLC system with the LC-MS. This suggests that the useful lifetime of a column not only depends on the column, but also the characteristics of the analyte and internal standard. Fetal bovine serum from 3 lots was tested and shown to contain 32 - 42 mg/mL of total proteins¹¹⁸. Since each injection was 10 μ L, failure started to occur after at least 111 – 146 μ g of peptide was injected onto the column. In previous studies it was seen that using cell culture conditions that featured low serum or serum-free media generally extended the lifespan of the LC columns.

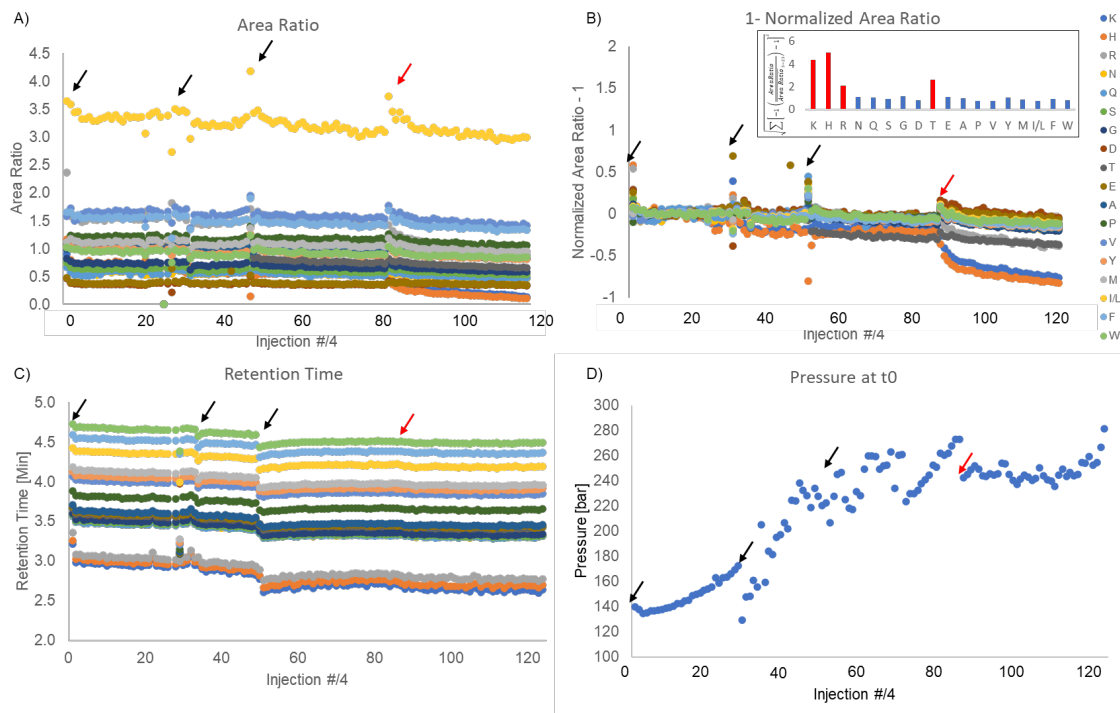


Figure 9 - Evaluation of column lifespan and performance can be seen. Evaluation would start with injection of peptide library Ac β A-X-RGEFV- β A, followed by four injections of media containing 10% FBS, and finally that cycle was repeated. So injection #/4 represents the number of peptide libraries that were injected onto the column. A) Shows the Area ratio, while C) shows how the retention time of every peptide. B) contains the legend of every peptide for within A, B, and C as well as the area ratio normalized to injection number 3-20 of the peptide library minus 1. The pane within B contains the square root sum of the normalized area ratio to quantify the total error of each quantified peptides within the library. D) shows how the pressure within the HPLC at time zero of the injection. The black and red arrows point to when the first injection was performed after at least 24 hours of non-use. The red arrow points to where failure of the column is initiated.

2.4 Conclusion

Here, a new LC-MS based method of quantifying peptide is introduced. A series of β -amino acid based internal standard were identified with two peptides were shown be capable of withstanding proteolytic degradation within a 48-hour period. Excellent linearity was demonstrated between the two peptide libraries that were tested, within the concentration range tested. An appropriate sample treatment was shown to be effective in inhibiting proteolytic degradation while also maintaining consistent results via LC-MS.

Injection solvent was demonstrated to potentially negatively impact LC-MS results, however, an injection solvent of PBS or media showed consistent characteristics, indicating that media could be used as an injection solvent. Finally, the use of a crude sample, with minimal processing, negating the need for an expensive SIL peptide comes at the cost of a chromatography column, which has been shown to last about 400 LC-MS injections. Demonstrated is a novel LC-MS based method for multiplex quantitative analysis of peptides degraded by cells.

Chapter 3: Chain End Modification Modulates Non-Specific Degradation of Peptides

3.1 Introduction

This chapter has been adapted from work previously published. Reprinted with permission from *ACS Biomater. Sci. Eng.* 2024, XXXX, XXX, XXX-XXX. Publication Date: July 5, 2024. <https://doi.org/10.1021/acsbiomaterials.4c00736>. Copyright 2024 American Chemical Society.

It is well-understood that non-specific degradation of therapeutic peptide drugs significantly limits their clinical potential⁹². However, bioactive peptides are frequently incorporated into biomaterials to better mimic native ECMs^{119–121} but typically without any characterization of their stability during culture. This includes the canonical RGD cell adhesion peptide⁷² and also signaling peptides which mimic growth factors, among other sequences^{122,123}. These peptides are generally intended to be present throughout the lifetime of the material and any degradation is undesirable and could reduce the efficacy of the biomaterial system. Cell-secreted proteases, such as MMPs⁸⁷ or cathepsins¹²⁴, are often used as stimuli to modify biomaterials⁷⁶. However, MMPs and cathepsins are only a fraction of the total number of proteases expressed by cells¹¹⁹.

The enzymes harnessed within bioengineered systems, including MMPs and cathepsins, are almost exclusively endopeptidases^{76,125} which cleave interior of peptides and protein sequences. Exopeptidases, another class of proteases which cleave amino acids at the termini of peptides and proteins, are ubiquitously expressed in human tissues¹¹⁹ and have

been used to tailor the adhesion environment within biomaterials¹²⁶. Notably, exopeptidases are believed to be largely responsible for the rapid degradation of peptide drugs^{127,128}, and modifications to the N-terminus of peptides can slow non-specific degradation^{127,129}. Modification of the N-terminus of proteins is

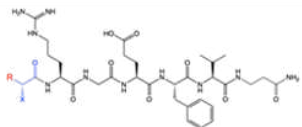
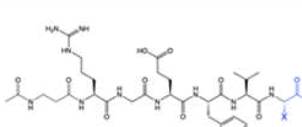
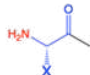
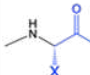
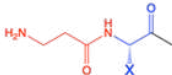
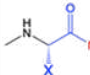
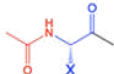
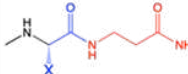
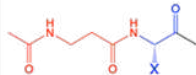
N-terminal modifications		C-terminal modifications	
			
Amine (NH ₂)		Carboxylic acid (COOH)	
N-terminal β-alanine (N-βA)		Amide (Am)	
Acetyl (Ac)		C-terminal β-alanine (C-βA)	
Acetylated β-alanine (Ac-βA)			

Figure 10 - Design of N-terminal and C-terminal peptide libraries. Split-and-pool with four different N-terminal modifications and three different C-terminal modifications.

widespread, and more than 80% of human proteins have acetylated N-termini¹³⁰. The exopeptidase family of proteases includes both aminopeptidases that are active against the N-terminus of peptides and carboxypeptidases that are active against the C-terminus, and the extent to which these classes of proteases degrade peptides is known to be heavily dependent upon the chemistry of the termini¹³¹.

In this chapter we synthesized a series of peptide libraries to better understand how cell-secreted proteases degrade bioactive peptides (Table 3). Peptide libraries were synthesized with a range of N- and C- terminal modifications to all canonical amino acids except cysteine (Table 1). Peptides with N-terminal amines were rapidly degraded by human mesenchymal stem/stromal cells (hMSCs), human umbilical vein endothelial cells (hUVECs), and pro-inflammatory macrophages across almost all terminal amino acids.

However, simple modifications could significantly reduce this non-specific degradation across most cell types. These results offer generalized design rules to improve the design and bioactivity of peptide-functionalized hydrogels

3.2 Experimental

3.2.1 Solid Phase Peptide Synthesis

Peptides were synthesized using standard solid phase peptide synthesis (SPPS) protocols using either manual synthesis or an automated peptide synthesizer (CEM Liberty Blue) using standard Fmoc-protected amino acids (Chemscene) on a Rink amide resin (Supra Sciences) unless a C-terminal carboxylic acid was desired, in which case 2-chlorotrityl resin was used. All amide couplings were done using O-(6-chlorobenzotriazol-1-yl)-N,N,N',N'-tetramethyluronium hexafluorophosphate (HCTU) in DMF unless otherwise noted. For each coupling the amino acid, HCTU, and DIPEA were added in a 4:4:6 molar ratio to the peptide. During peptide synthesis a ninhydrin test was performed after every addition to test for the presence of free amines. Upon a positive test, the coupling was replicated until the test was negative. A capping step was then performed with acetic anhydride (Sigma-Aldrich) in a 10:5:100 acetic anhydride:DIPEA:DMF solution twice for 5 min, and then a ninhydrin test was performed to check for complete capping of the free amines. After successful coupling, the Fmoc group was removed, washing the resin with 20% piperidine in DMF twice for 5 min. A ninhydrin test was performed to check for a positive result.

Loading the first amino acid on the 2-chlorotrityl resin was performed by swelling the resin in DCM for 10 minutes. While the resin was swelling, first amino acid was dissolved in dichloromethane, at a molar ratio of 1:1 per chain amino acid chain on resin, and mixed with the resin. If amino acid did not dissolve, DMF was added dropwise until amino acid dissolved prior to mixing with the resin. Next five molar equivalents of DIPEA was added to the synthesis vessel, which was placed on a wrist-action shaker for 5 minutes. After 5 minutes another 1.5 molar equivalents of DIPEA were added, and the synthesis vessel was allowed to shake for 1 hour. After 1 hour, the synthesis vessel was drained and an excess of methanol was added to the vessel with another 5 equivalents of DIPEA. After 30 minutes the resin was washed with DCM and DMF, and deprotected with Piperidine. At this point, presence of a positive ninhydrin test indicated successful coupling of the first amino acid, and the rest of the amino acids were performed using standard Fmoc SPPS techniques.

Split-and-pool methods¹⁰⁷ were used to rapidly create peptide libraries. For the split and pool steps, the resin was washed 3× with DMF and then the entire amount of resin was weighed on a scale. This number was divided by approximately 22 and this was split 19 ways into 19 separate tubes, with some excess to account for resin loss during transport and weighing. The reactions were performed in 15 mL tubes and upon successful coupling of all 19 amino acids all 19 fractions of resin were re-combined. Peptide libraries attached to the C-terminal end were completed in one vessel. Peptide libraries attached to the N-terminal end were washed with DMF 3×, weighed and split four ways followed by adding the desired chain-end chemistry. Once the N-terminal libraries were split four ways, they were not recombined again. Peptides with C-terminal carboxylic acids were synthesized

using 2-chlorotrityl chloride resin. For the COOH library 2 mmol of resin was weight out and 52.6 μmol of each amino acid (1 mmol total synthesis scale) was added into a single 50 mL tube. 25 mL of DCM was added and then DMF was added dropwise until all of the amino acids went fully into solution. The 2-chlorotrityl chloride resin was washed with DCM for five minutes to swell the resin, at which time the DCM was drained and the amino acid solution was added with 5 equivalents of DIPEA. After 30 minutes another 1.5 equivalents of DIPEA were added. After another 30 minutes 5 mL of methanol was added to cap the resin, at which time the Fmoc groups were deprotected and the peptides were synthesized using standard Fmoc-peptide synthesis procedures. All peptides used in in this chapter can be found in below and validated via LC-MS (Appendix Figure 1– 140).

Table 3 - List of all peptides used to demonstrate how chain end modification modulates non-specific degradation of peptides. Asides from peptide 3.1, four N-terminal modifications including an acetylated β -Alanine (Ac β A), a β -Alanine (β A), Acetylation (Ac), and amine (NH_2). Three C-terminal modifications include amidation (Amide), a carboxylic acid (COOH), and a β -Alanine (β A). For peptide libraries, X represents a variable amino acid which includes: A, D, E, F, G, H, I, K, L, M, N, P, Q, R, S, T, V, W, and Y.

Peptide/Library #	Amino Acid Sequence		Peptide/Library #	
3.1	NH_2 - β F β A6-Amide		3.2	Ac β A-X-RGEFV- β A
3.3	Ac-X-RGEFV- β A		3.4	β A-X-RGEFV- β A
3.5	NH_2 -X-RGEFV- β A		3.6	Ac β A-RGEFV-X-Amide
3.7	Ac β A-RGEFV-X-COOH		3.8	Ac β A-RGEFV-X- β A
3.9	Ac β A-GLIAANK- β A		3.10	Ac-GLIAANK- β A
3.11	β A-GLIAANK- β A		3.12	NH_2 -GLIAANK- β A
3.13	Ac β A-LIAANKG-Am		3.14	Ac β A-LIAANKG-COOH
3.15	Ac β A-LIAANKG- β A		3.16	Ac β A-GIVKVA- β A
3.17	Ac-GIVKVA- β A		3.18	β A-GIVKVA- β A
3.19	NH_2 -GIVKVA- β A		3.20	Ac β A-IVKVAG-Am
3.21	Ac β A-IVKVAG-COOH		3.22	Ac β A-IVKVAG- β A

3.2.2 Peptide Cleavage from Solid Phase

Peptides libraries and all peptides containing tryptophan were cleaved using 92.5% trifluoroacetic acid (TFA), 2.5% H₂O, 2.5% triisopropylsilane (TIPS), and 2.5% dithiothreitol (DTT). Peptides which lacked a tryptophan were cleaved without DTT. Peptides were typically cleaved for 2-3 hours at room temperature using approximately 25 mL of cleavage solution per mM of peptide. However, peptides containing azides were cleaved for 30 minutes to prevent degradation of the azide group. Peptide mass was checked using electrospray ionization and if protecting groups remained the peptide was re-cleaved for 30 minutes. The masses of the peptide libraries were checked using liquid chromatography mass spectrometry (LCMS) and if protecting groups remained the peptides were re-cleaved for 30 minutes. At the end of the cleavage the peptides were precipitated in diethyl ether. These were then centrifuged for 5 minutes at 4,000 rpm, and the supernatant was discarded. The peptide pellet was washed with diethyl ether, and centrifuged, and this was repeated twice. The peptide pellet was allowed to dry, and then dissolved in water and neutralized with ammonium hydroxide prior to purification.

3.2.3 Peptide Purification

All peptides were purified using HPLC using a Phenomenex Gemini 5 μ m NX-C18 110 Å LC Column 150 \times 21.2 mm. Gradients were run from 95% Mobile Phase A (water with 0.1% TFA) and 5% Mobile Phase B (acetonitrile with 0.1% TFA) to 100% Mobile Phase B. A typical HPLC run featured a two-minute equilibration step, followed by a 10-minute ramp from 95% Mobile Phase A to 100% Mobile Phase B, and then two minutes of equilibration at 100% Mobile Phase B, before ramping back down to the starting

conditions. Notably, the split-and-pool libraries were ramped up to 100% Mobile Phase B over two minutes, since these libraries consisted of approximately 19 different peptides which weren't intended to be separated from each other. The protected cyclic RGD peptides was purified using a gradient that ramped from 30% Mobile Phase B to 100% Mobile Phase B. After purification all peptides evaluated for purity using LC-MS. If unpure peptides were repurified via preparative HPLC). were lyophilized and were ready to use.

3.2.4 Degradation of Peptides by Human Umbilical Vein Endothelial Cells Stem Cells on Tissue Culture Plastic

Human umbilical vein endothelial cells (hUVECs) (Lifecell Technology) at passage 2 were seeded into 24 well plates at a seeding density of 150,000 cells per well in 1ml of Basal media (Lifeline Cell Technology, LM-0002) containing ascorbic acid, hydrocortisone, FBS, L-Glutamine, rh-EGF, heparin, and EnGS-US (All supplements LifeFactors, LS-1122). After 24 hour the media was changed. Peptide libraries, each containing 19 peptides and the non-proteolytically degradable β F β A β A β A β A-NH₂ internal standard, were added to the cell media for a final concentration of 37 μ M per peptide. Each library was tested in triplicate per cell type per study. 40 μ l samples were collected from the media at hours 0, 1, 4, 8, 24, and 48. In-between timepoints samples were frozen -80°C. After 48 hours, samples were kept frozen and thawed just prior to LCMS. The following donors were used for these studies: Lot 08119 from a Caucasian male, Lot 08478 from a Caucasian/African American female, and Lot 04608 from an African American male. Initial degradation studies with cells on tissue culture plastic were done using all three donors, sequence specific degradation studies were done using Lot 04608.

3.2.5 Degradation of Peptides by Human Mesenchymal Stem Cells on Tissue Culture Plastic

Human mesenchymal stem cells (hMSCs) (Rooster Bio) at passage 3 were seeded into 24 well plates at a seeding density of 75,000 cells per well in 1ml of RoosterBasal™-MSC-CC (RoosterBio, SU-022) containing RoosterBooster™-MSC (RoosterBio SU-003). After 24 hour the media was changed and peptide libraries were added to the cell media for a final concentration of 37 μ M per peptide. Each library was tested simultaneously, in triplicate per cell lot for a total of 63 wells. 40 μ l samples were collected from the media at hours 0, 1, 4, 8, 24, and 48. In-between timepoints samples were frozen -80°C. After 48 hours, samples were kept frozen and thawed just prior to LCMS. The following donors were used for these studies: Lot 310264 a 20-year-old African-american male, Lot 310268 a 19 year old Eritrean/east African female, and Lot 210280 a 26 year old Asian male. Initial degradation studies with cells on tissue culture plastic were done using all three donors, sequence specific degradation studies were done using Lot 310268.

3.2.6 Degradation of Peptides by Peripheral Blood Mononuclear Cell Derived Macrophages on Tissue Culture Plastic

Peripheral blood mononuclear cells (PBMCs) were purchased from Allcells placed in a 24 well plate with a seeding density of one million cells per well using RPMI (Cytiva, SJ30027.1) containing 10% FBS (Foundation Fetal Bovine Serum, Gemini Bioproducts) and 1% antibiotic-antimycotic (Gibco, 15240-062). Human M-CSF (Peprotech, 300-25-50UG) was immediately added at a concentration of 20ng/ml for five days to induce differentiation to M0 macrophages. After day 5 the media was changed to RPMI containing

interferon gamma (IFN- γ) (Peprotech, 300-02-20UG), and 100 ng/ml Lipopolysaccharide (LPS) (Sigma L4391-1MG) and allowed to polarize for three days (Day 8 of culture). On Day 9, the media was changed to macrophage serum free media with L-Glutamine (Gibco 12065-074). Peptide libraries were added 24 hours later to the cell media for a final concentration of 37 μ M per peptide. Each library was tested simultaneously, in triplicate per cell lot for a total of 63 wells. 40 μ l samples were collected from the media at 0, 1, 4, 8, 24, and 48 hours. In-between timepoints samples were frozen -80°C. After 48 hours, samples were kept frozen and thawed just prior to LCMS. Three donors and one cell line was used for these studies. The donors came from Lot 3087423 a 26-year-old Asian male, Lot 3088202 a 52-year-old White male, and Lot 3091412 a 21-year old African-american Female. The primary PBMC-derived macrophages were used for initial studies on tissue culture plastic, THP-1-derived macrophages were used for sequence specific degradation studies.

3.2.7 Degradation of Peptides by THP1 Derived Macrophages on Tissue Culture Plastic

THP-1 cells were placed into a 24 well plate with a seeding density of one million cells per well using RPMI (Cytiva, SJ30027.1) containing 10% FBS and 1% anti-anti, with PMA at a concentration of 100ng/ml for two days. After day 2 the media was changed to RPMI containing IFN- γ , 20 ng/ml MCSF, and 100 ng/ml LPS and allowed to polarize for three days (Day 5 of culture). After six days the media was changed to macrophage serum free media with L-Glutamine (Gibco 12065-074) Peptide libraries were added 24 hours later to the cell media for a final concentration of 37 μ M per peptide. Each library was tested

simultaneously, in triplicate for a total of 21 wells. 40 μ l samples were collected from the media at hours 0, 1, 4, 8, 24, and 48. In-between timepoints samples were frozen -80°C. After 48 hours, samples were kept frozen and thawed just prior to LCMS. The THP-1 cell line was used for initial degradation experiments on tissue culture plastic and all other cell studies.

3.2.8 Liquid Chromatography – Mass Spectrometry

Immediately after the 96-well sample plate were removed from the -80°C freezer, 4 μ L of neat acetic acid was added to each well to acidify the media and prevent further peptide degradation by proteases. From each sample, 10 μ L of crude solution was introduced by the LC-MS through an Thermo Scientific Vanquish LC System (Thermo Fisher Scientific) which outputted to a Thermo Scientific LTQ XL Linear Ion Trap Mass Spectrometer (Thermo Fisher Scientific). The sampled mixture was trapped on a column (ProntoSIL C18 AQ, 120 Å, 3 μ m, 2.0 x 50 mm HPLC Column, PN 0502F184PS030, MAC-MOD Analytical Inc.). The samples were loaded onto the column with a solvent containing acetonitrile/water, 5:95 (v/v) containing 1% acetic acid at a flow rate of 300 μ L/min and held for one minute. The sample was then eluted from the column with a linear gradient of 5-40% Solvent B (1% acetic acid in acetonitrile) at the same flow rate for five minutes. This was followed by a 1 min ramp up to 100% Solvent B, where it was re-equilibrated with Solvent A (1% acetic acid) to 5% solvent B over the course of 1 min and held there for 2 min. The column temperature was a constant 29 °C. The mass spectrometer was operated in positive ion mode. Using a heated ESI, the source voltage was set to 4.1 kV, and the capillary temperature was 350 °C.

Data analysis was performed on Xcalibur Software (Thermo Scientific). Peptides were identified automatically using the Thermo Xcalibur Processing Setup window where the mass (m/z) ± 0.5 atomic mass units and expected retention times for each quantified peptide were inputted. This was later used to isolate individual peptide species from the total ion count (TIC) trace using the Thermo Xcalibur Quan Setup window, where the area under the curve was calculated and visually inspected for accuracy. All peptides were normalized to a non-changing internal standard, $\text{NH}_2\text{-}\beta\text{F}\beta\text{A6-Am}$, where βA is a β -alanine and βF is β -homophenylalanine. The integrated peak area of the peptide of interest was divided by the $\text{NH}_2\text{-}\beta\text{F}\beta\text{A6-Am}$ internal standard to create an area ratio. Relative amounts of a peptide of peptide were then calculated by normalized all values to their corresponding time zero area ratio. Calculated data was visualized using RStudio.

3.3 Results and Discussion

3.3.1 Degradation of RGEFV Peptide Libraries

There are dozens of human exopeptidases^{132,133} and the activity of each protease is typically dependent on the amino acid at the termini of the peptide⁷⁸. Significant effort has gone into preventing degradation of therapeutic proteins, and its modification of the N-terminal amine or C-terminal carboxylic acid or the inclusion of β -amino acids frequently reduces non-specific peptide degradation^{112,129,134}. While most work assessing proteolytic degradation of peptides has focused on the substrate preferences for individual proteases¹³⁵, or degradation of specific peptides²⁴, we set out to better understand peptide degradation due to the total protease expression of entire cell types across a range of terminal chemistries. In order to characterize the effects of non-specific proteolytic degradation as a function of

end group, we designed a series of RGEFV peptide libraries based upon the widely-used RGD peptide. Seven peptide libraries were synthesized, each having a different terminal chemistry and containing 19 of the 20 canonical amino acids (excluding cysteine) to quantify peptide degradation by cell type (Table 3. Entries 3.2 - 3.8). The aspartic acid (D) on the RGD was mutated to glutamic acid (E) to prevent the peptides from binding cell-surface integrins while retaining their physiochemical properties¹³⁶, and also included a hydrophobic Phe-Val utilized in the RGDFV adhesion peptide¹³⁷ to improve chromatographic retention during analysis.

Each of the seven peptide libraries (Appendix Figure 1-126) was added to the cell culture media of three cell types commonly used in biomedical research: human mesenchymal stem/stromal cells (hMSCs), human umbilical vein endothelial cells (hUVECs), and classically polarized macrophages (Macrophages) cultured on tissue culture plastic. Samples of each peptide library were taken in cell culture media at 0, 1, 4, 8, 24, and 48h, acidified with acetic acid to prevent further enzymatic degradation, and quantified using LCMS. The extent of degradation was determined by calculating the ratio of peptide found at later time points to the zero-hour time point. While peptides with 19 different terminal amino acids were present in every library, isoleucine and leucine have identical masses, elute from the LC-MS column at approximately the same time, and were combined for analysis. It should be noted that any chemical modification to the peptide that changes the mass of the peptide will reduce the intensity of the peptide peak in mass spectrometry (Figure 22 -Figure 22) which is visualized in two different ways: 1) grouped by time (Figure 22 - Figure 15) and grouped by end group chemistry 1) grouped by end group

chemistry (Figure 16 - Figure 22). While our data suggest that a significant fraction of degradation is due to exopeptidase activity, it is possible and even likely that endopeptidases or other enzymes are also degrading these peptides.

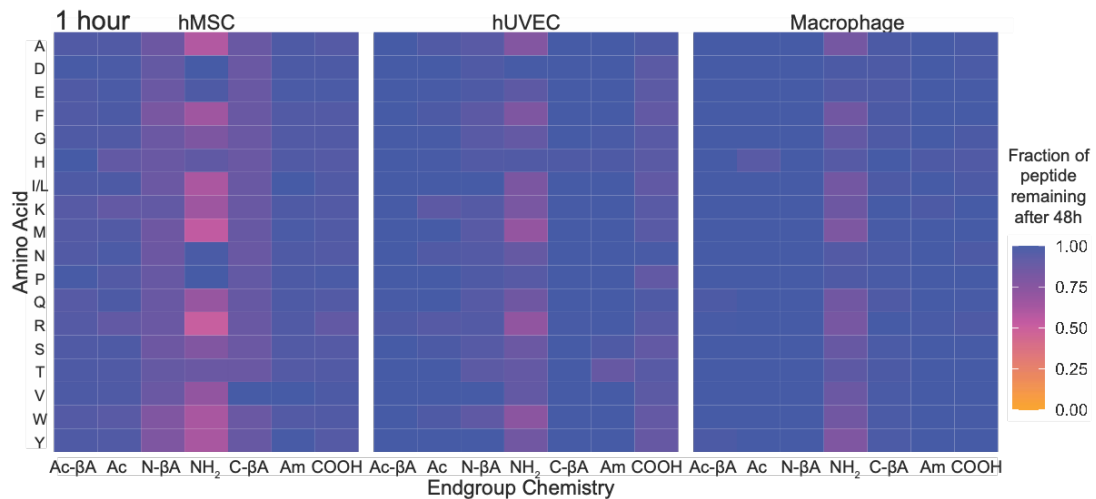


Figure 11 - Degradation of soluble peptides cultured with cells on tissue culture plastic. Degradation was quantified at 1 hour.

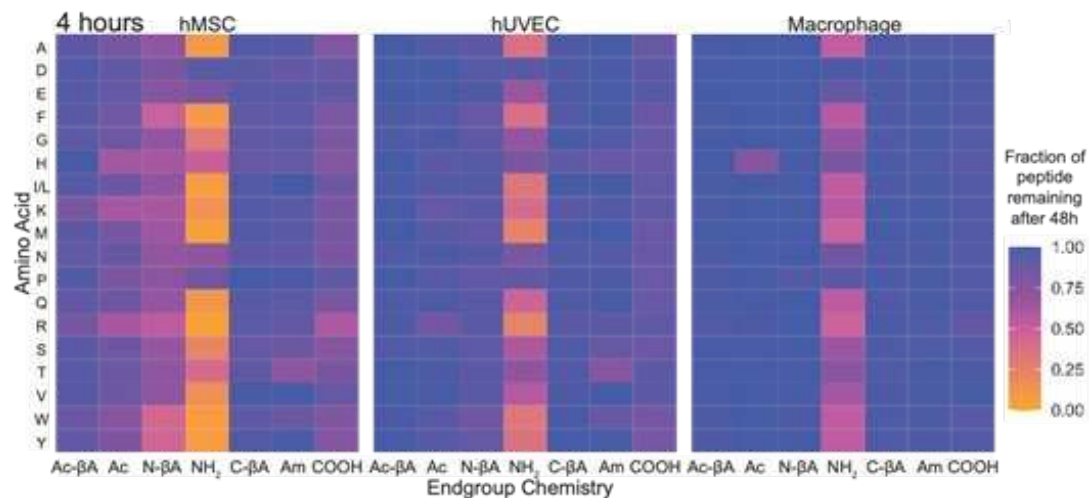


Figure 12 - Degradation of soluble peptides cultured with cells on tissue culture plastic. Degradation was quantified at 4 hours.

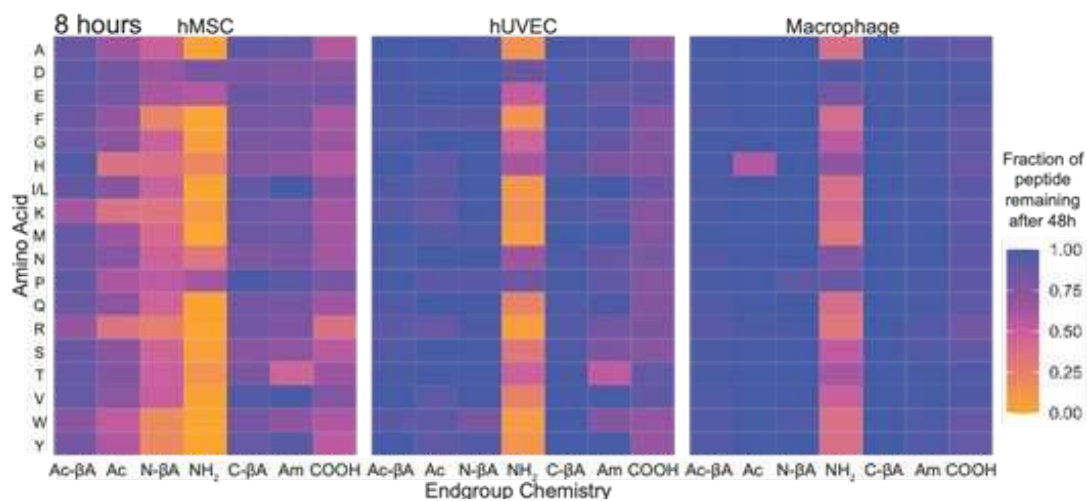


Figure 13 - Degradation of soluble peptides cultured with cells on tissue culture plastic. Degradation was quantified at 8 hours.

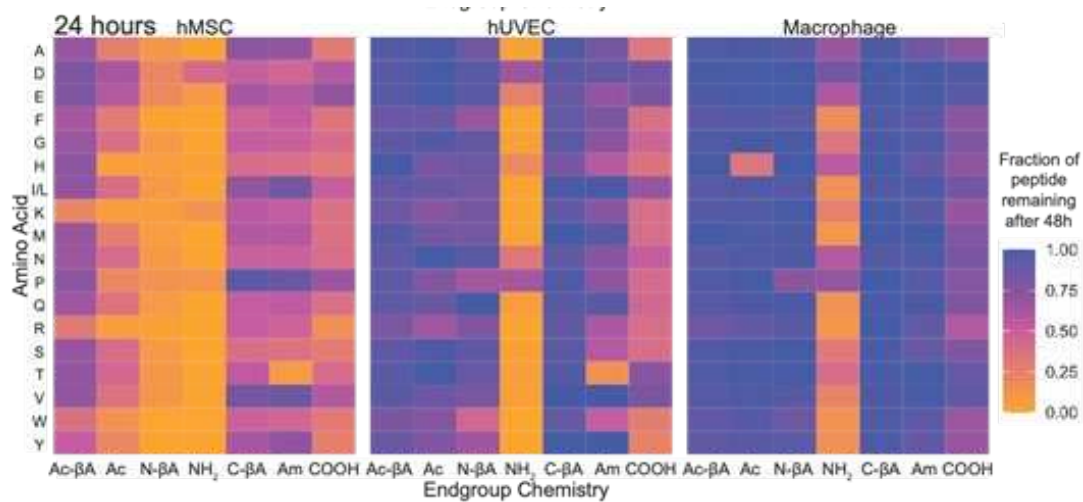


Figure 14 - Degradation of soluble peptides cultured with cells on tissue culture plastic. Degradation was quantified at 24 hours.

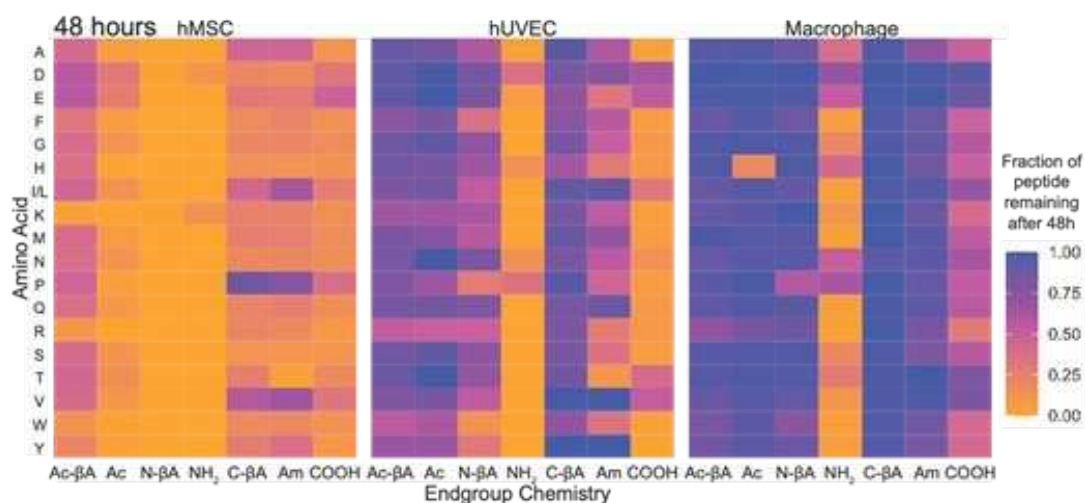


Figure 15 - Degradation of soluble peptides cultured with cells on tissue culture plastic. Degradation was quantified at 48 hours.

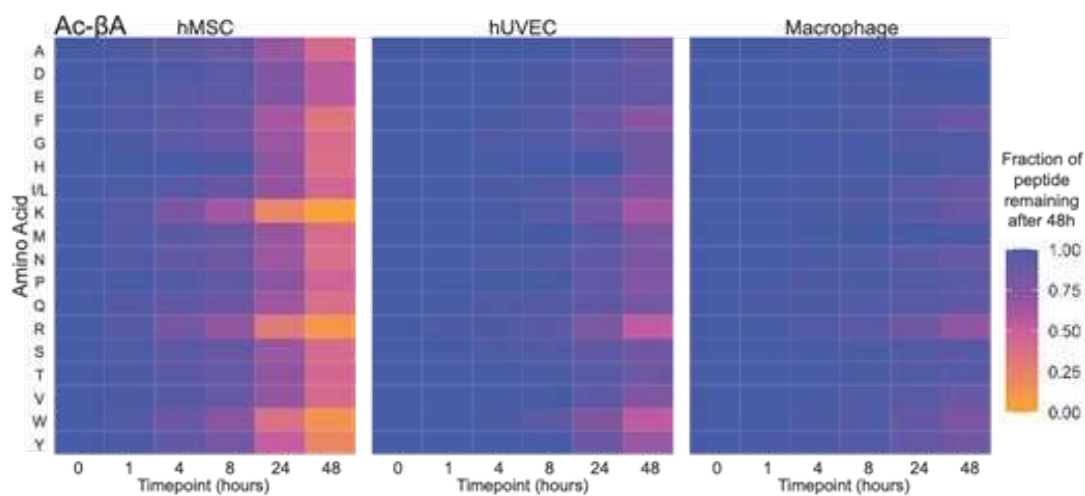


Figure 16 - Degradation of soluble peptides cultured with cells on tissue culture plastic. Degradation was quantified by the chemistry of the peptide termini Ac-βA.

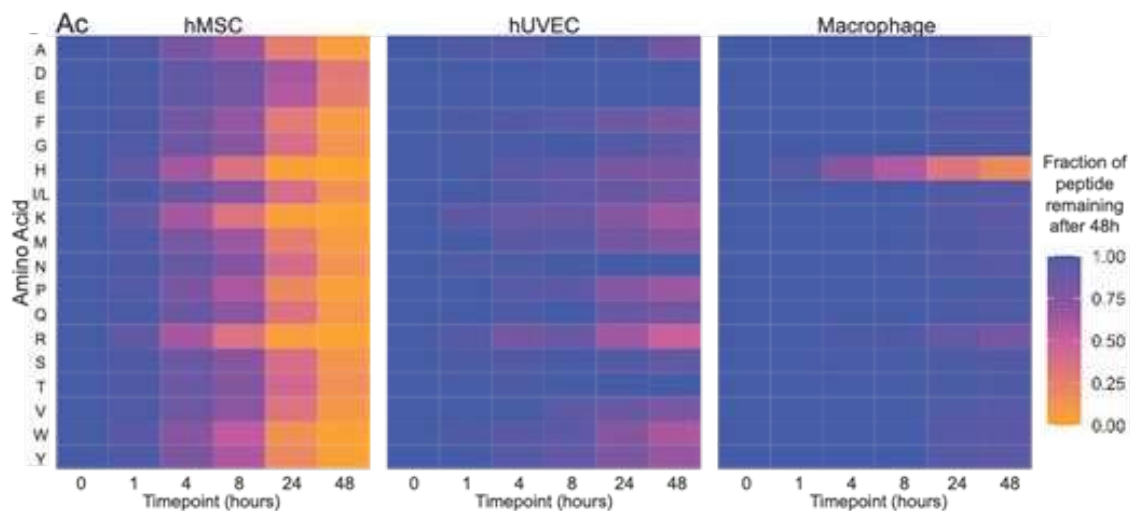


Figure 17 - Degradation of soluble peptides cultured with cells on tissue culture plastic. Degradation was quantified by the chemistry of the peptide termini Ac.

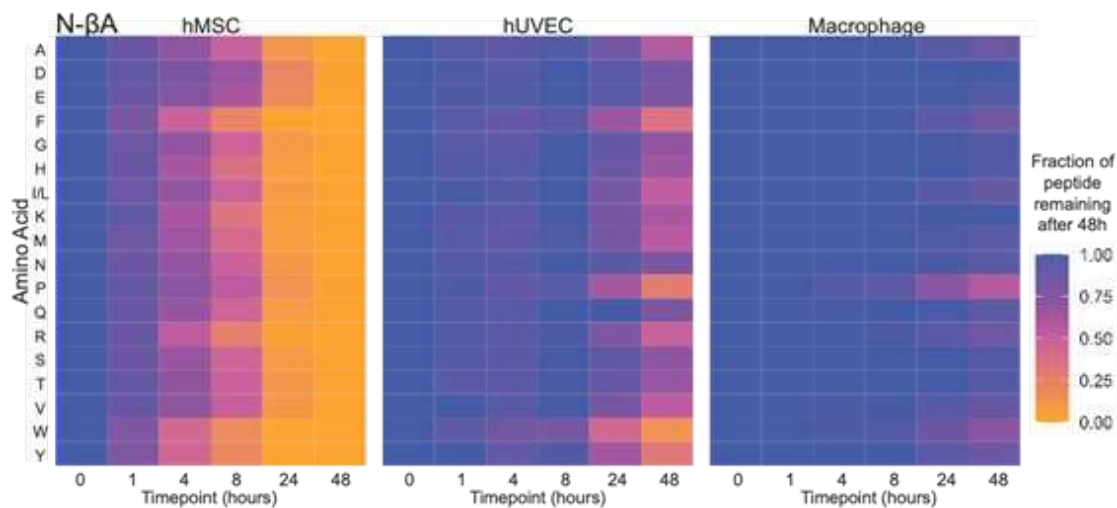


Figure 18 - Degradation of soluble peptides cultured with cells on tissue culture plastic. Degradation was quantified by the chemistry of the peptide termini N-βA.

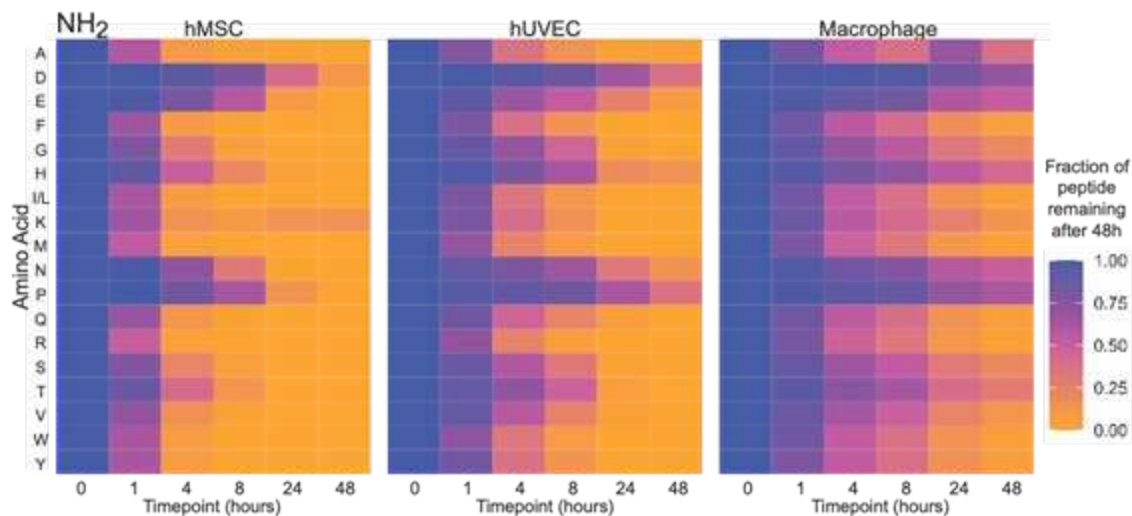


Figure 19 - Degradation of soluble peptides cultured with cells on tissue culture plastic. Degradation was quantified by the chemistry of the peptide termini NH₂.

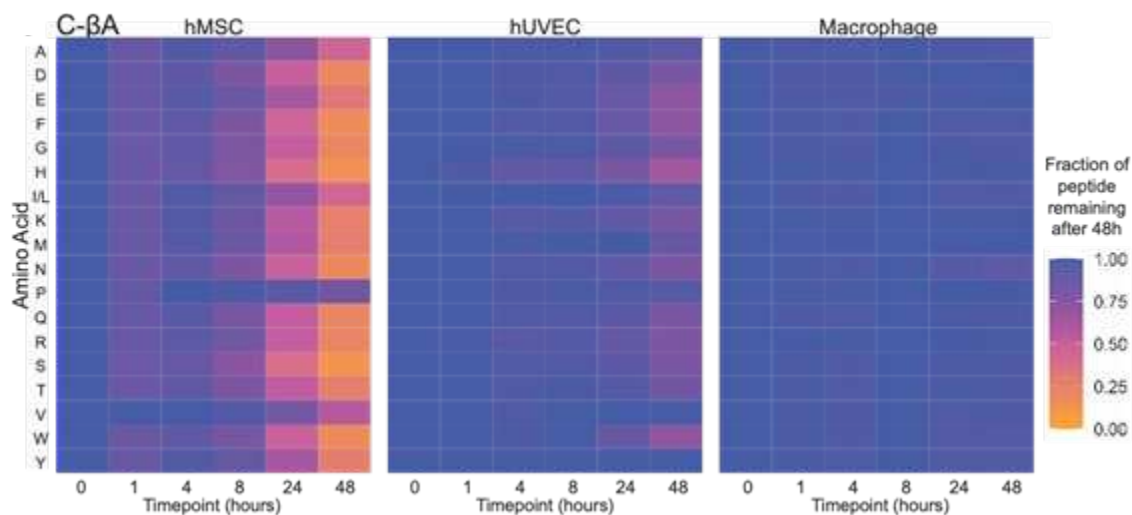


Figure 20 - Degradation of soluble peptides cultured with cells on tissue culture plastic. Degradation was quantified by the chemistry of the peptide termini C-βA.

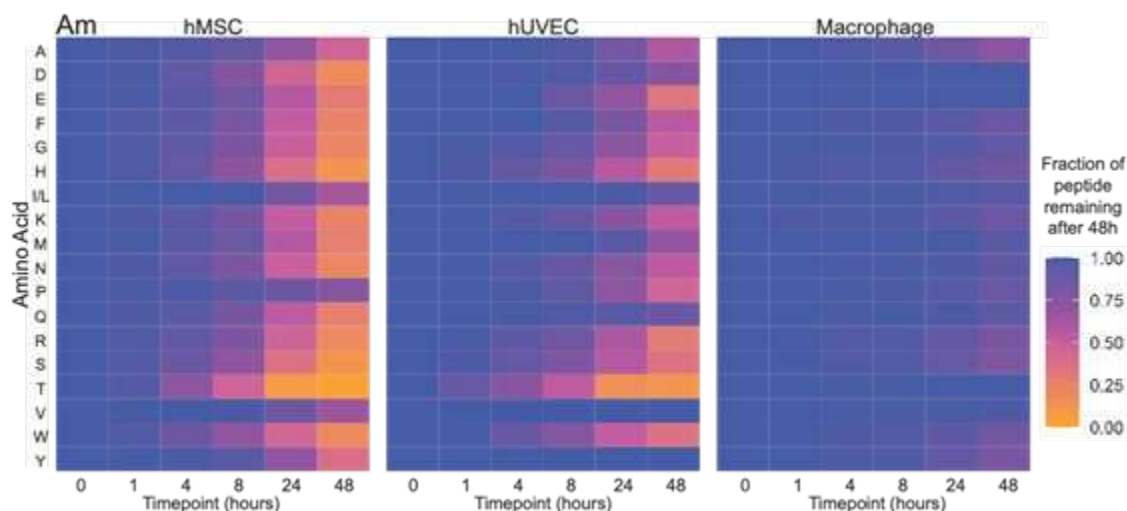


Figure 21 - Degradation of soluble peptides cultured with cells on tissue culture plastic. Degradation was quantified by the chemistry of the peptide termini Am.

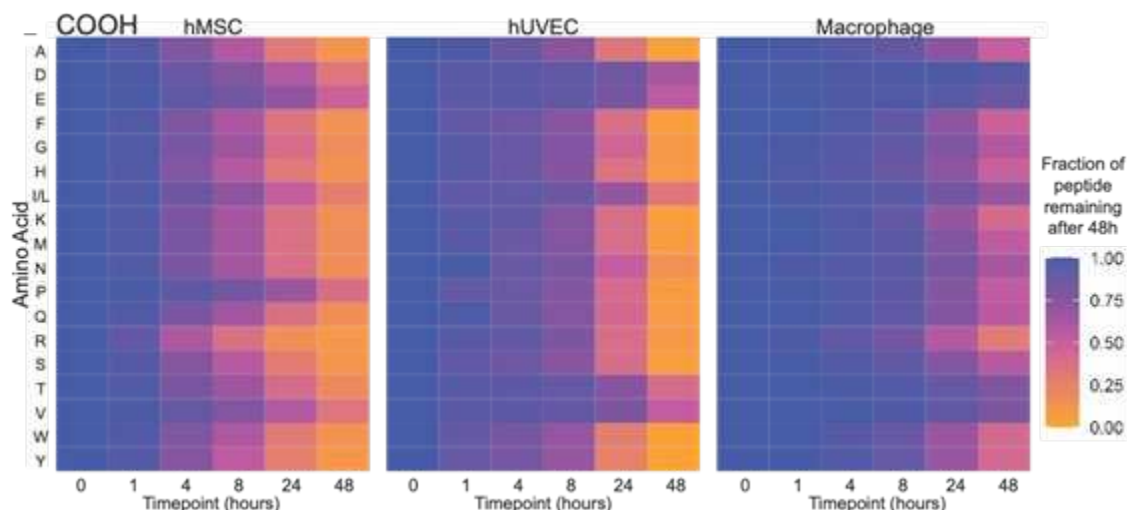


Figure 22 - Degradation of soluble peptides cultured with cells on tissue culture plastic. Degradation was quantified by the chemistry of the peptide termini COOH.

Results show that non-specific degradation is controlled by the chemistry of the peptide termini, and that simple modifications can drastically reduce peptide degradation (Figure 22 - Figure 22). The amino acids present at the termini influenced how quickly a peptide was degraded, but the difference between amino acids was much smaller than terminal chemistries. Peptides with N-terminal amines were rapidly degraded for almost every

amino acid by all three cell types. In hMSCs after eight hours in culture 15 of the 18 peptides with N-terminal amines (NH₂) had less than 50% of the peptide remaining, 13 peptides had less than 25% remaining, and 9 peptides had less than 5% of the original peptide remaining. hUVECs demonstrated less degradation of NH₂ peptides, but 13 peptides had less than 50% remaining after 8 hours, and 9 peptides had less than 25% remaining. Macrophages had the least degradation, but nine of the 18 peptides had less than 50% remaining after 8 hours in culture. For all cell types, modifications of the N-terminus reduced peptide degradation, although they different levels of efficacy in preventing degradation. While peptides with N-terminal β -alanines (N- β A) were completely degraded by 48 hours when cultured with hMSCs, 42% of N- β A peptides remained after eight hours versus 17% for peptides with N-terminal amines, suggesting that the N- β A does slow down degradation in hMSCs. The N- β A modification was more effective at inhibiting peptide degradation in hUVECs, which increased the fraction of peptides remaining after 48 hours from 7% in NH₂ to 58% in N- β A, and macrophages, which went from 25% remaining for NH₂ to over 90% for N- β A. Described are findings from Figure 22 - Figure 22 which are summarized in Figure 23 where the error bars represent the standard deviation of all peptides within the library.

The positive charge of the N-terminal amine can play a role in aminopeptidase recognition of the peptide substrate¹³⁸. Both the NH₂ and N- β A termini are positively charged, and the uncharged acetylation (Ac) and acetylated β -alanines (Ac- β A) were both more effective at preventing degradation. While there was essentially complete degradation of all peptides with N-terminal amines or N-terminal β -alanines when cultured with hMSCs on tissue

culture plastic, 10% of acetylated peptides remained, and 37% of Ac- β A peptides. For hUVECs, 82% of acetylated peptides remained, and 78% of peptides with acetylated β -alanines, and for macrophages approximately 91% of peptides remained for both Ac and Ac- β A.

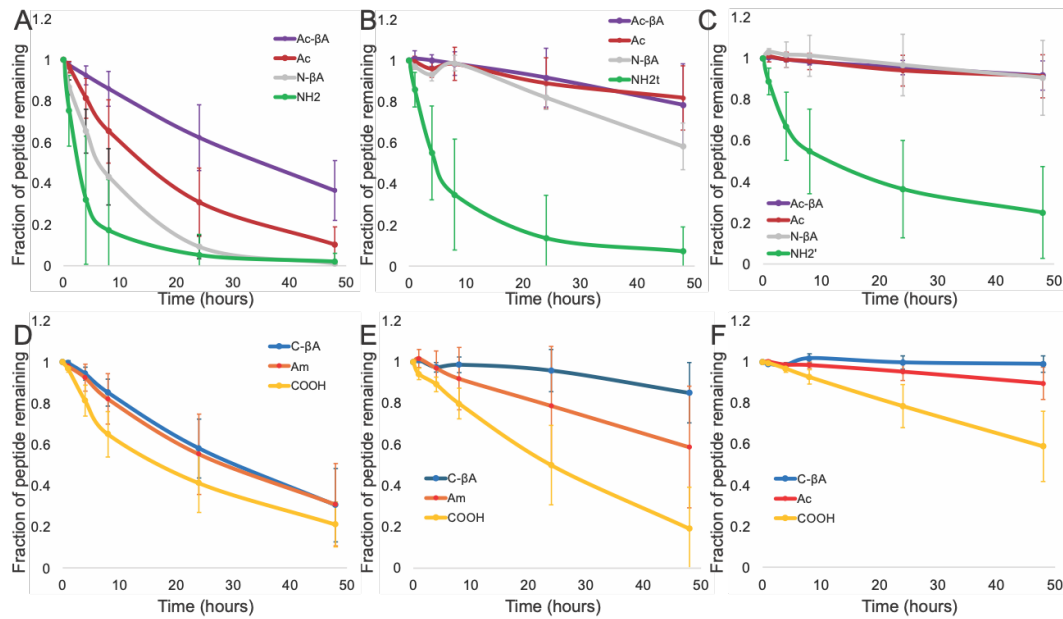


Figure 23 - Non-specific degradation of peptides with N-terminal amines across three different cell types. The amount of degradation at different time points was quantified. Averaging over all amino acids, quantified the effects of N-terminal modifications for (A) hMSCs, (B) hUVECs, and (C) macrophages, and C-terminal modifications for (D) hMSCs, (E) hUVECs, and (F) macrophages. Error bars represent the standard deviation across all terminal amino acids.

The chemistry of the C-terminus also had a significant effect on peptide degradation, although to a lesser extent than the chemistry of the N-terminus. Peptides with C-terminal carboxylic acids typically had the most degradation, with hUVECs having the most degradation, with 19% remaining, followed by hMSCs (21%) and macrophages (59%). Modification of the C-terminus reduced degradation for all cell types. C-terminal amidation and an amidated C-terminal β -alanine both had 31% of peptide remaining after 48 hours for hMSCs. However, the C- β A modification was superior to C-terminal

amidation in preventing peptide degradation hUVECs (85% remaining in C- β A versus 59% in Am) and macrophages (99% remaining in C- β A versus 90% for Am) than peptides which had C-terminal amides, and those with C-terminal β -alanines had the least. Current strategies to prevent exopeptidase degradation of peptides are largely focused on non-natural amino acids or acetylation of the N-terminus. Peptides with N-terminal acetylated β -alanines and C-terminal amidated β -alanines would largely have reduced degradation over existing strategies for all cell types. Acetylated N-terminal β -alanines result in reduced degradation compared to standard acetylation for hMSCs, and amidated C-terminal β -alanines have significantly reduced degradation for hUVECs and macrophages. Globally peptide degradation varied by cell type, and across all peptides hMSCs had more degradation than hUVECs, which had more degradation than the macrophages for every end group at 24 and 48 hours, with the exception of the C-terminal carboxylic acid, which was more degraded at 48 hours by hUVECs than hMSCs.

3.3.2 Quantification of Biological Variance

Primary cells are widely used in biomedical research because they typically have more physiological relevance than transformed cell lines which will proliferate indefinitely. However, a challenge when drawing conclusions from studies using primary cells are that there are genetic differences between donors, and it is important to ensure that results are broadly applicable across the entire population. Furthermore, quantifying biological variance can help isolate sources of variance when making conclusions¹³⁹. To ensure that our results are robust and not specific to a single donor, all degradation studies performed on RGEFV peptide libraries within this chapter were performed using at least three primary

biologic replicates, including donors from both sexes and multiple ethnicities. Degradation of peptide libraries by macrophages also included the commonly used THP-1 cell line as a fourth biologic replicate. Each peptide library was degraded in three independent experimental replicates for each biologic replicate. Each degradation study contained three technical repeats for a total of 27 wells for every peptide library. This experimental design was applied to three commonly studied cell-types: hUVECs, hMSCs, and Macrophages with vendor and donor information found in Table 4.

Table 4 - Contains information on cell type and donor used to degrade RGEFV peptide libraries.

Cell Type	Vendor	Lot #	Gender	Ethnicity	Age
hUVEC	Lifeline Cell Technology	08119	Male	Caucasian	Neonate
hUVEC	Lifeline Cell Technology	08478	Female	Caucasian/African American	Neonate
hUVEC	Lifeline Cell Technology	04608	Male	African American	Neonate
hMSC	RoosterBio	310264	Male	African American	20
hMSC	Rooste Bio	310268	Female	Eritrean/east African	19
hMSC	RoosterBio	310280	Male	Asian	26
PBMC	ALLCELLS	3087423	Male	Asian	26
PBMC	ALLCELLS	3088202	Male	White	52
PBMC	ALLCELLS	3091412	Female	Black or African American	21
THP1			Male	Japanese	Young

RGEFV peptide libraries were separated by donor and visualized in Figure 44. Each of the peptide libraries which underwent degradation followed the same trends, irrespective of donor. The 48-hour timepoints from Figure 44 were compared using an ANOVA followed by a Tukey-Kramer post hoc test (Appendix Figure 173.A) and summarized in Table 5. The macrophage donors that failed to reject the null hypothesis were dissimilar in age, sex, and race. hMSC donors that failed to reject the null hypothesis were similar in age and race, but not sex. hUVEC donors that failed to reject the null hypothesis in age and race, but not in sex. Although donors tested as statistically significant, except for hUVECs, their degradation trends typically varied by less than 10%.

Table 5 – RGEFV libraries were degraded and lots were compared after 48 hours. Lots are compared along the row, and the P value is the result of an ANNOVA followed by a Tukey-Kramer post hoc analysis. Highlighted are comparisons that failed to rejected the null-hypothesis defined at P=0.05.

Cell Type	Lot	Age	Sex	Race	Lot	Age	Sex	Race	P
Macrophage	3088202	52	M	White	3087423	26	F	Asian	0.87
	3091412	21	F	African American	3087423	26	F	Asian	0.00
	3091412	21	F	African American	3088202	52	M	White	0.00
	THP1	Young	M	Asian	3087423	26	F	Asian	0.00
	THP1	Young	M	Asian	3088202	52	M	White	0.00
	3091412	21	F	African American	THP1	Young	M	Asian	
hMSC	310264	20	M	African Amerin	310268	19	F	African	0.98
	310264	20	M	African America	310280	26	M	Asian	0.00
	310268	19	F	African	310280	26	M	Asian	0.00
hUVEC	04608	neonate	M	African American	08119	Neonate	M	White	0.04
	08478	neonate	F	White / African American	08119	Neonate	M	White	0.99
	08478	neonate	F	White / African American	04608	neonate	M	African American	0.33

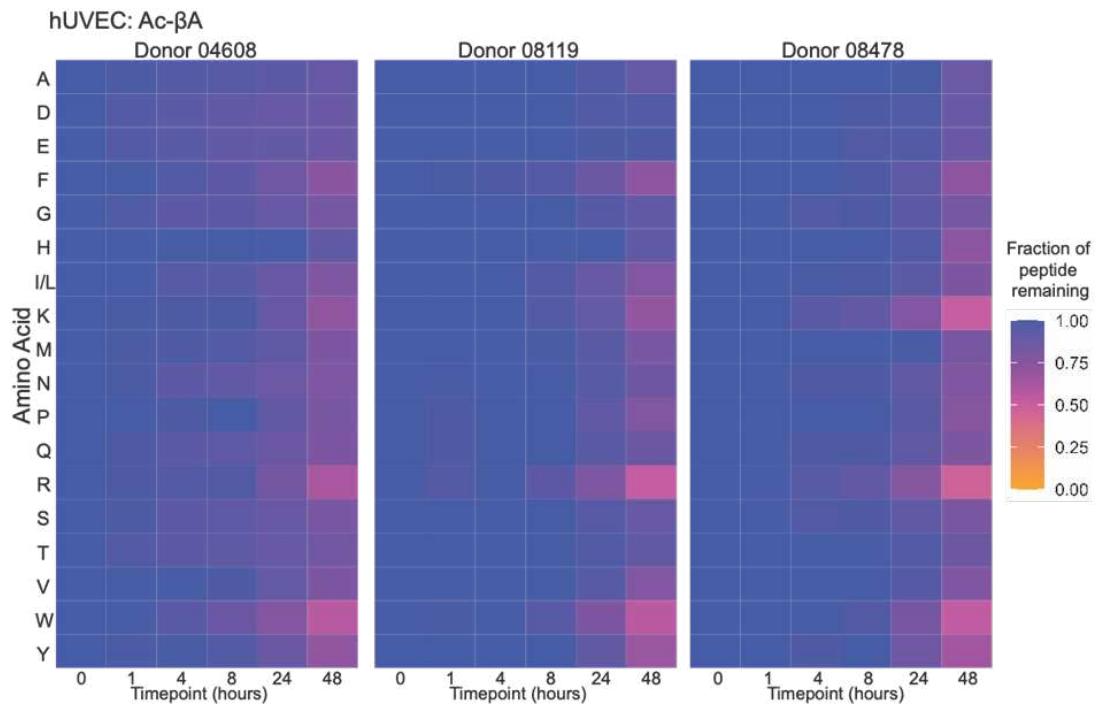


Figure 24 - Comparison of peptide degradation by different hUVEC donors. hUVECs were cultured with RGEFV libraries containing end group Ac-βA.

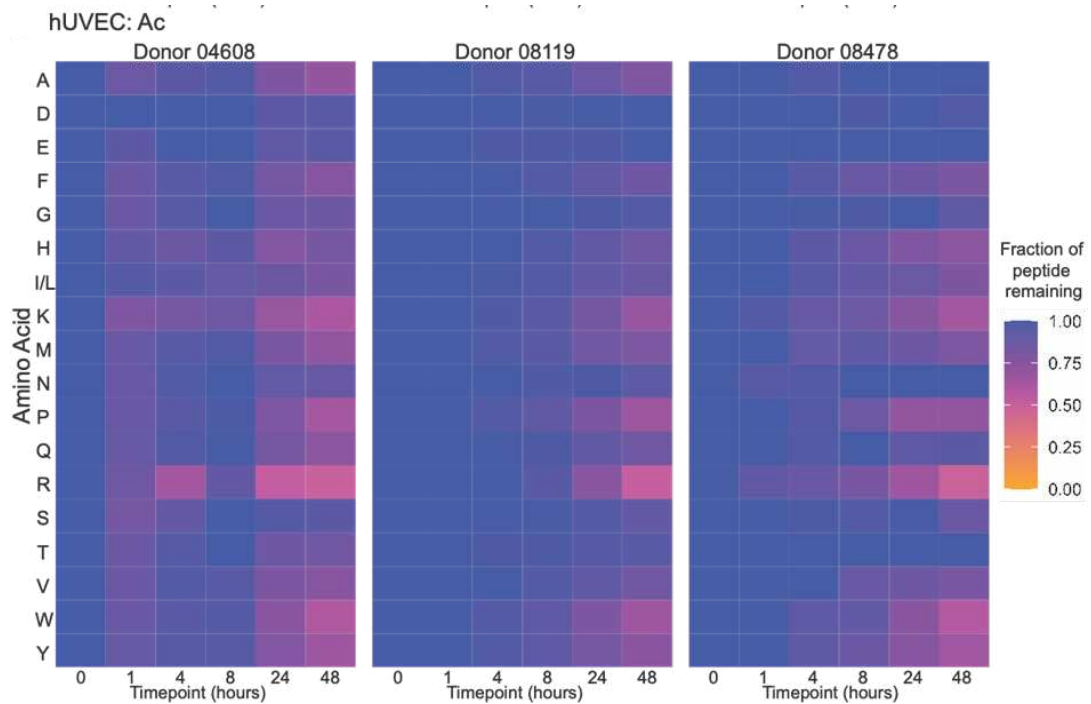


Figure 25 - Comparison of peptide degradation by different hUVEC donors. hUVECs were cultured with RGEFV libraries containing end group Ac.

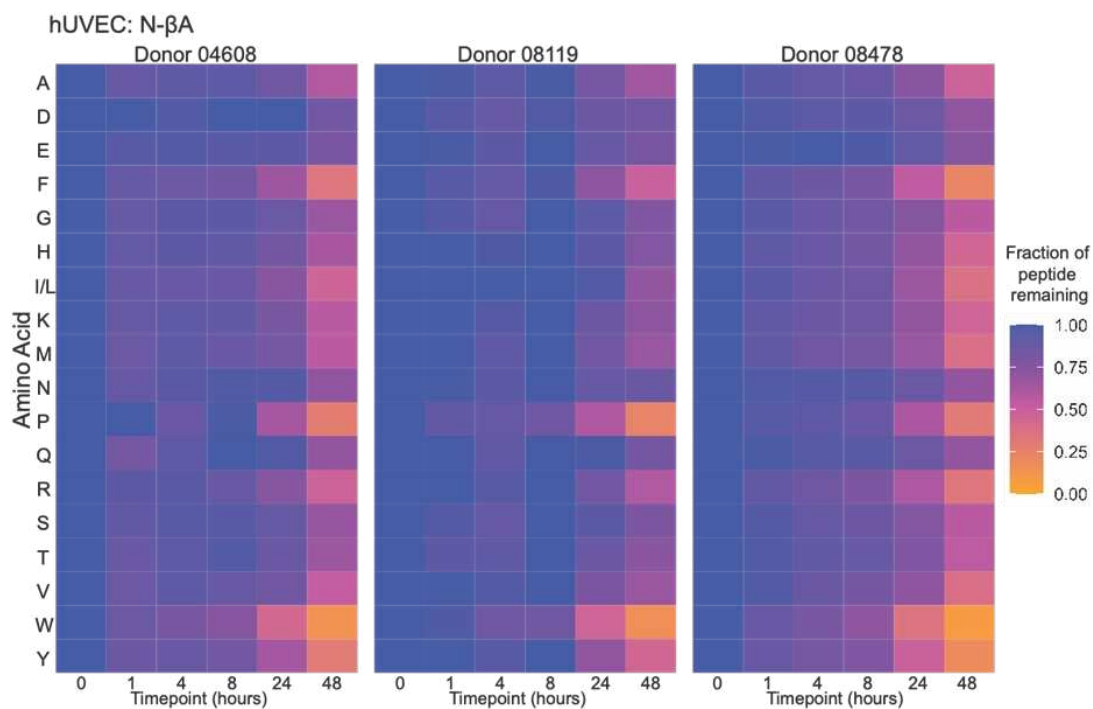


Figure 26 - Comparison of peptide degradation by different hUVEC donors. hUVECs were cultured with RGEFV libraries containing end group N-βA.

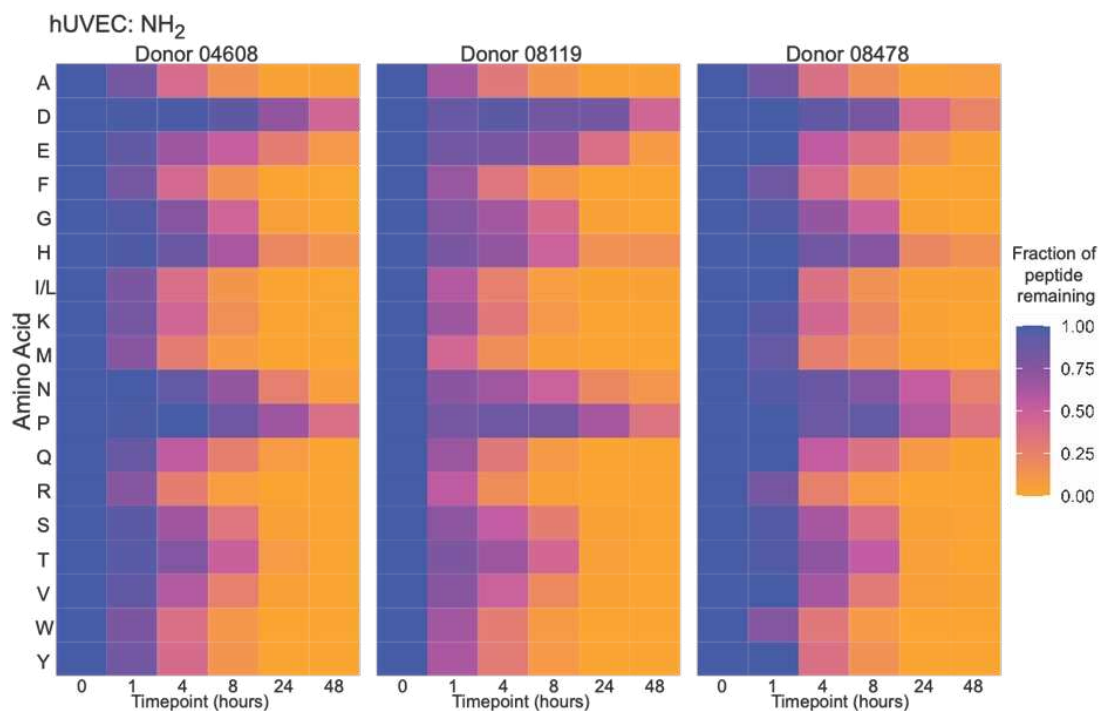


Figure 27 - Comparison of peptide degradation by different hUVEC donors. hUVECs were cultured with RGEFV libraries containing end group NH₂.

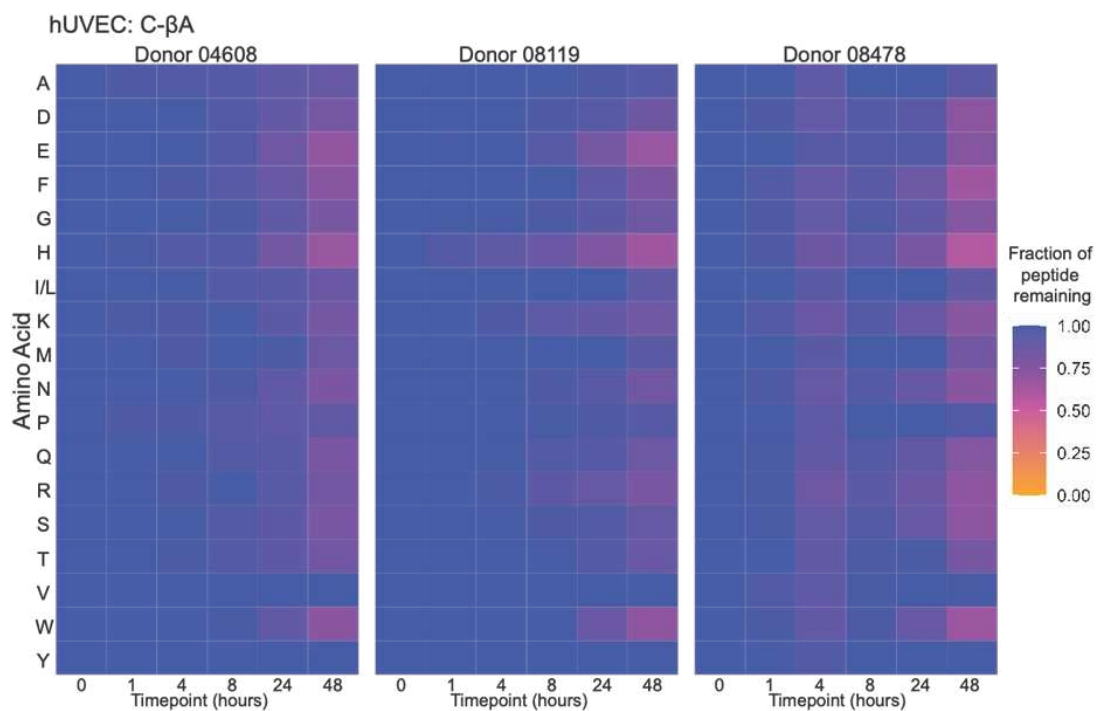


Figure 28 - Comparison of peptide degradation by different hUVEC donors. hUVECs were cultured with RGEFV libraries containing end group C-βA.

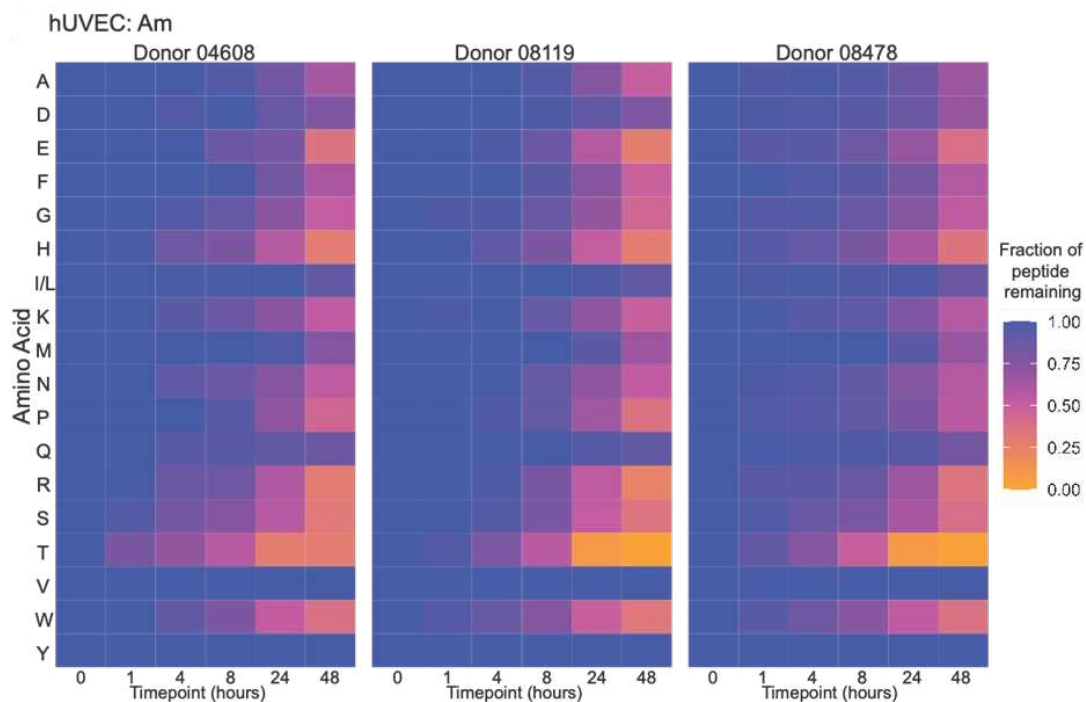


Figure 29 - Comparison of peptide degradation by different hUVEC donors. hUVECs were cultured with RGEFV libraries containing end group Am.

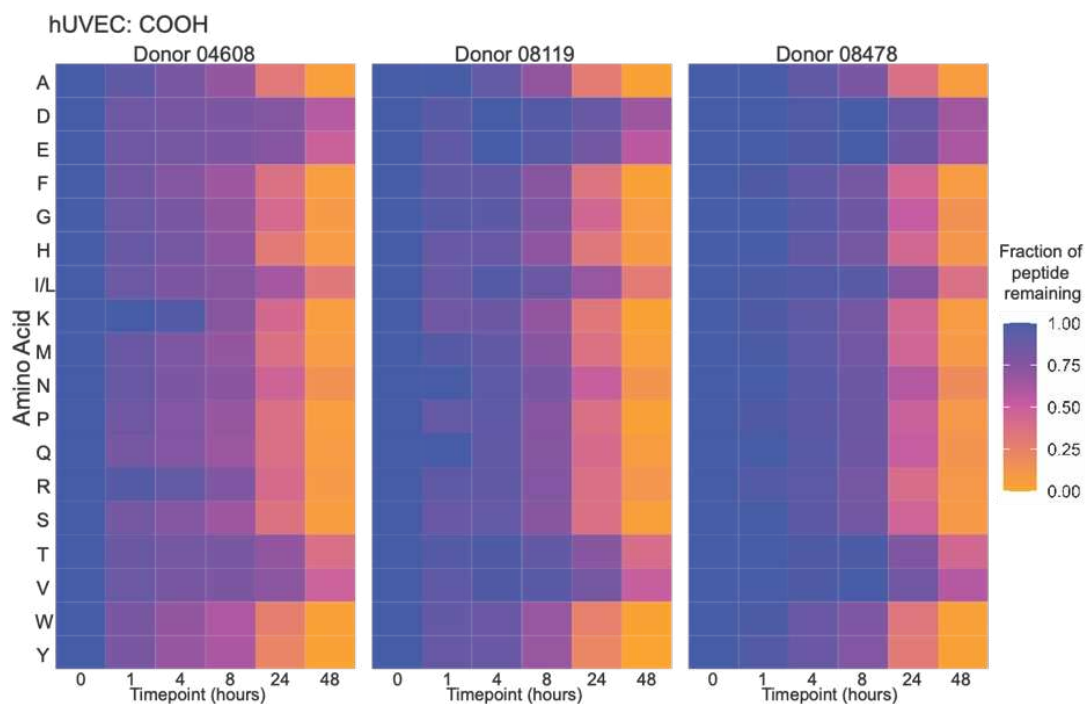


Figure 30 - Comparison of peptide degradation by different hUVEC donors. hUVECs were cultured with RGEFV libraries containing end group COOH.

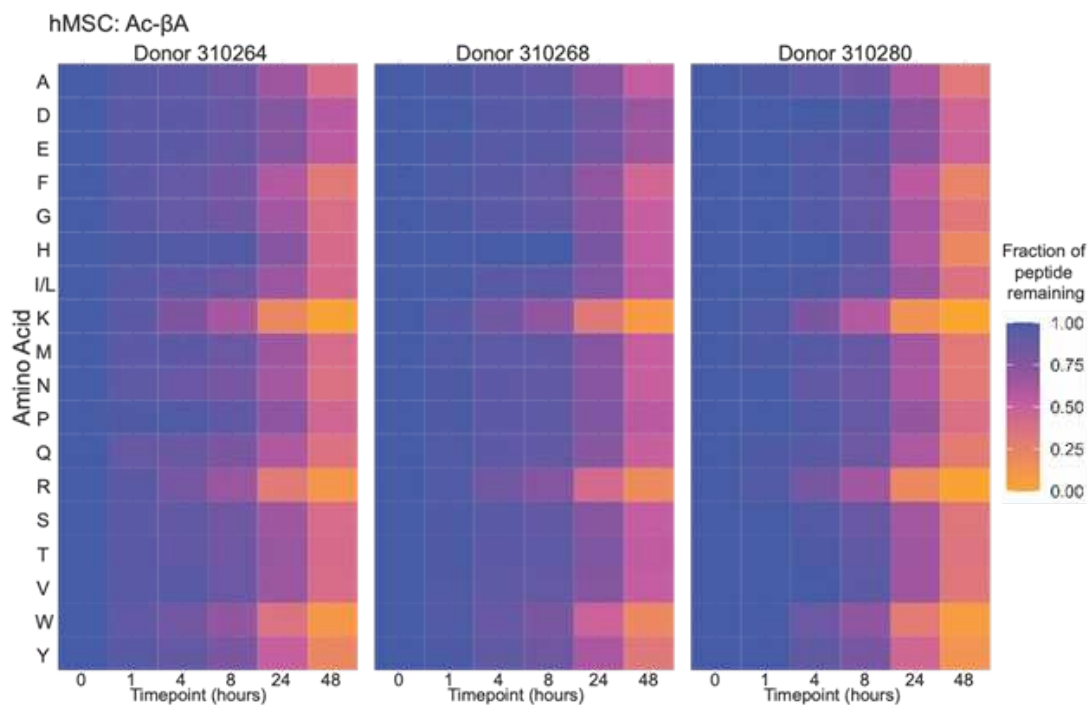


Figure 31 - Comparison of peptide degradation by different hMSC donors. hMSCs were cultured with RGEFV libraries containing end group Ac-βA.

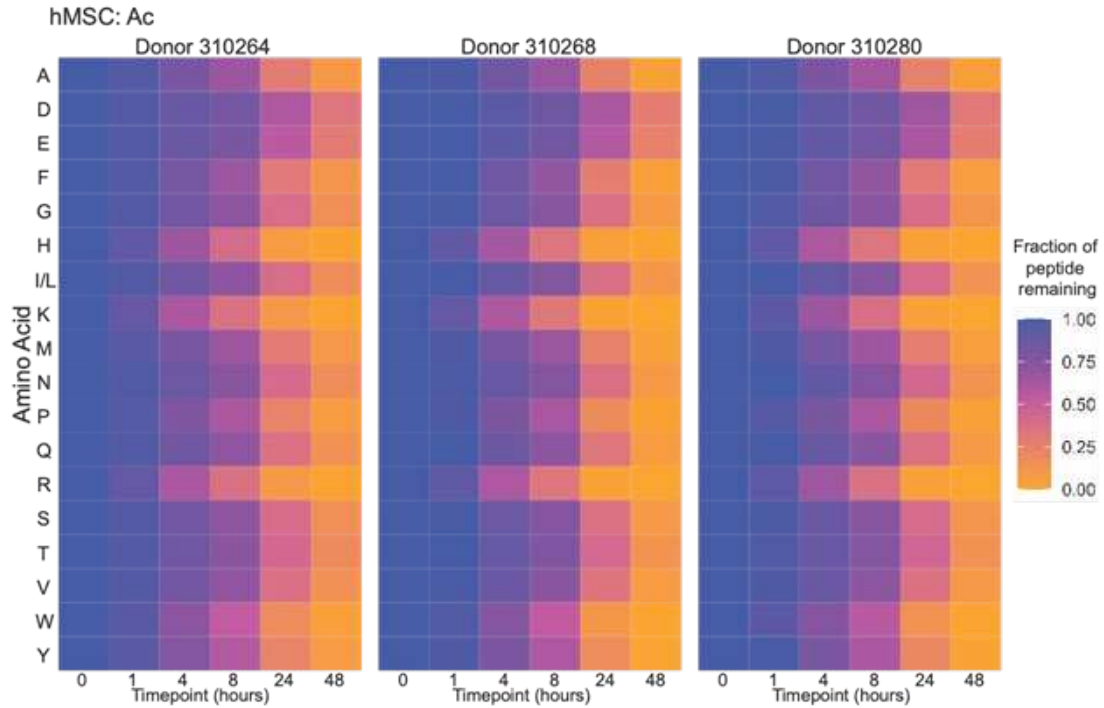


Figure 32 - Comparison of peptide degradation by different hMSC donors. hMSCs were cultured with RGEFV libraries containing end group Ac.

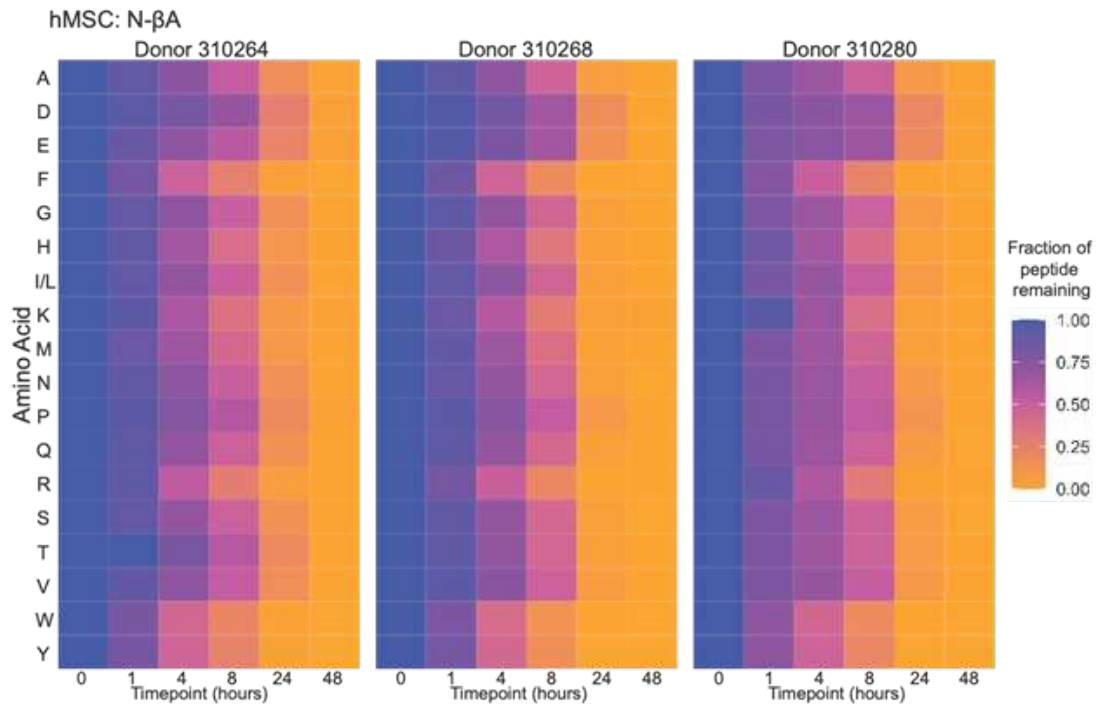


Figure 33 - Comparison of peptide degradation by different hMSC donors. hMSCs were cultured with RGEFV libraries containing end group N-βA.

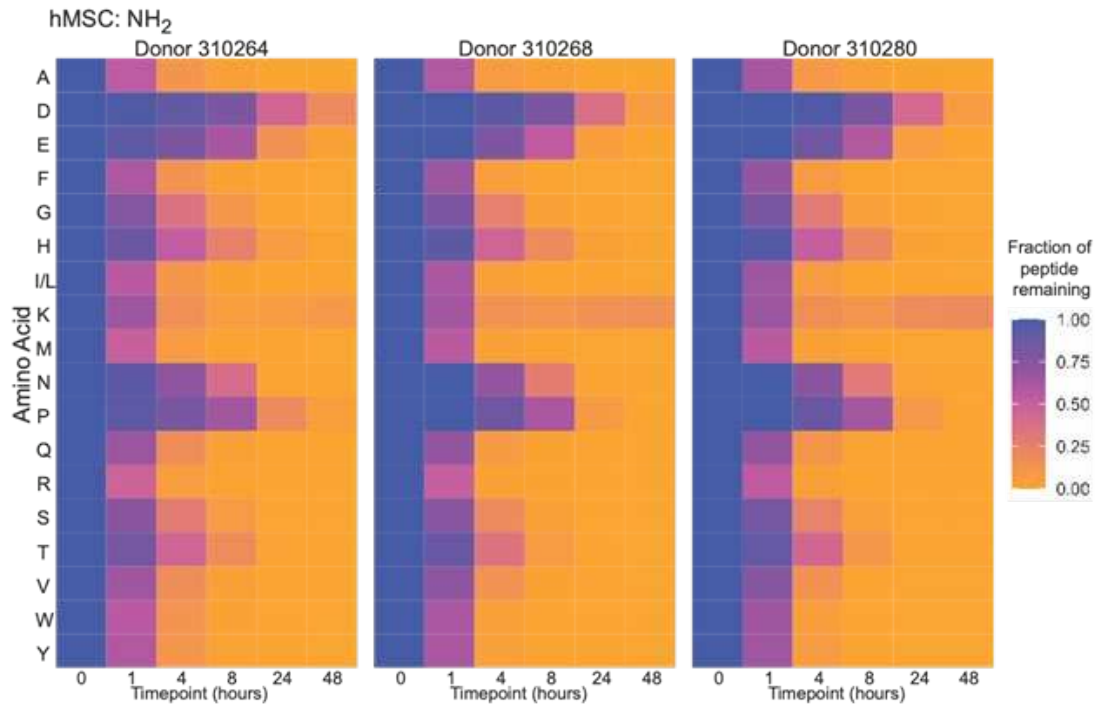


Figure 34 - Comparison of peptide degradation by different hMSC donors. hMSCs were cultured with RGEFV libraries containing end group NH₂.

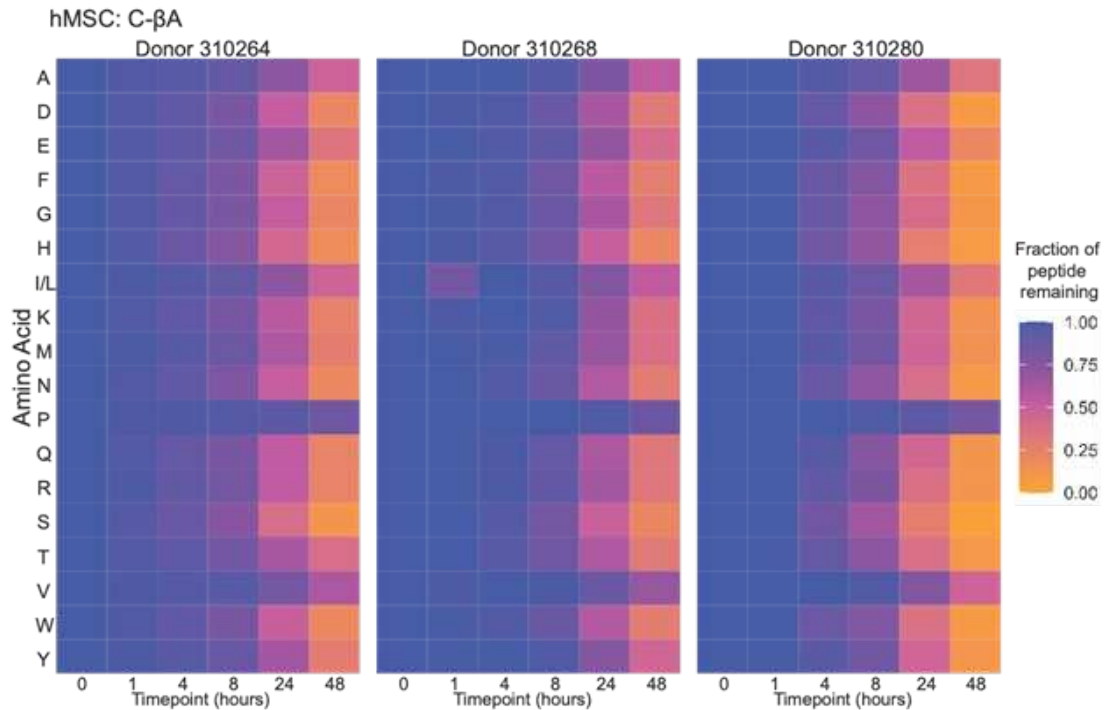


Figure 35 - Comparison of peptide degradation by different hMSC donors. hMSCs were cultured with RGEFV libraries containing end group C-βA.

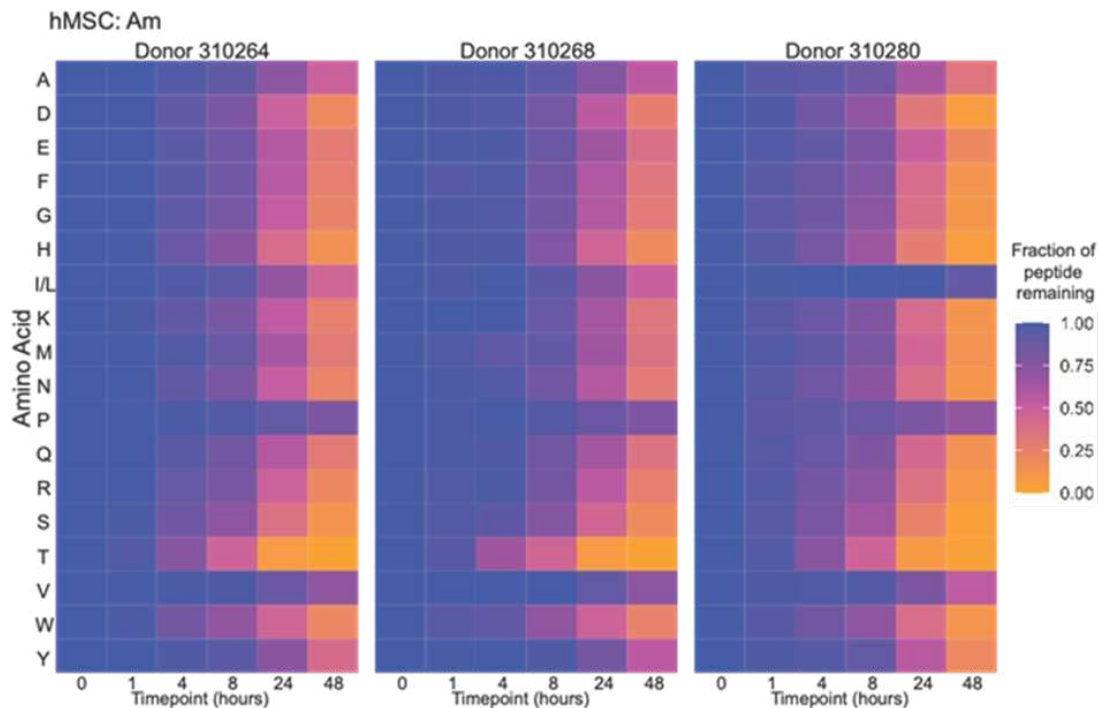


Figure 36 - Comparison of peptide degradation by different hMSC donors. hMSCs were cultured with RGEFV libraries containing end group Am.

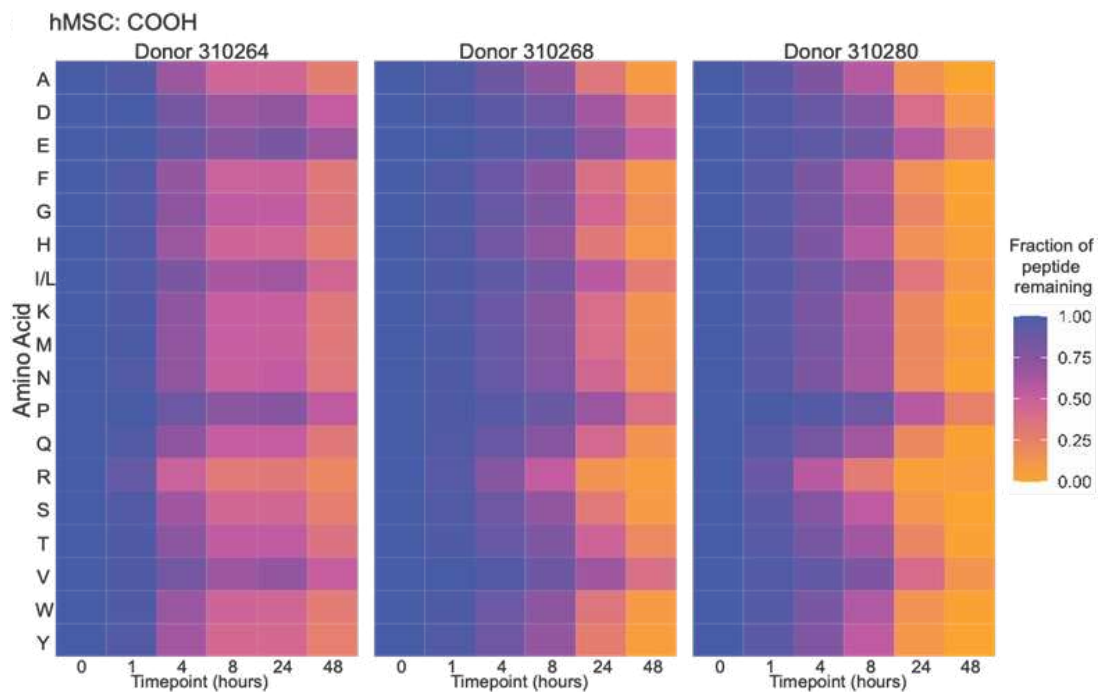


Figure 37- Comparison of peptide degradation by different hMSC donors. hMSCs were cultured with RGEFV libraries containing end group COOH.

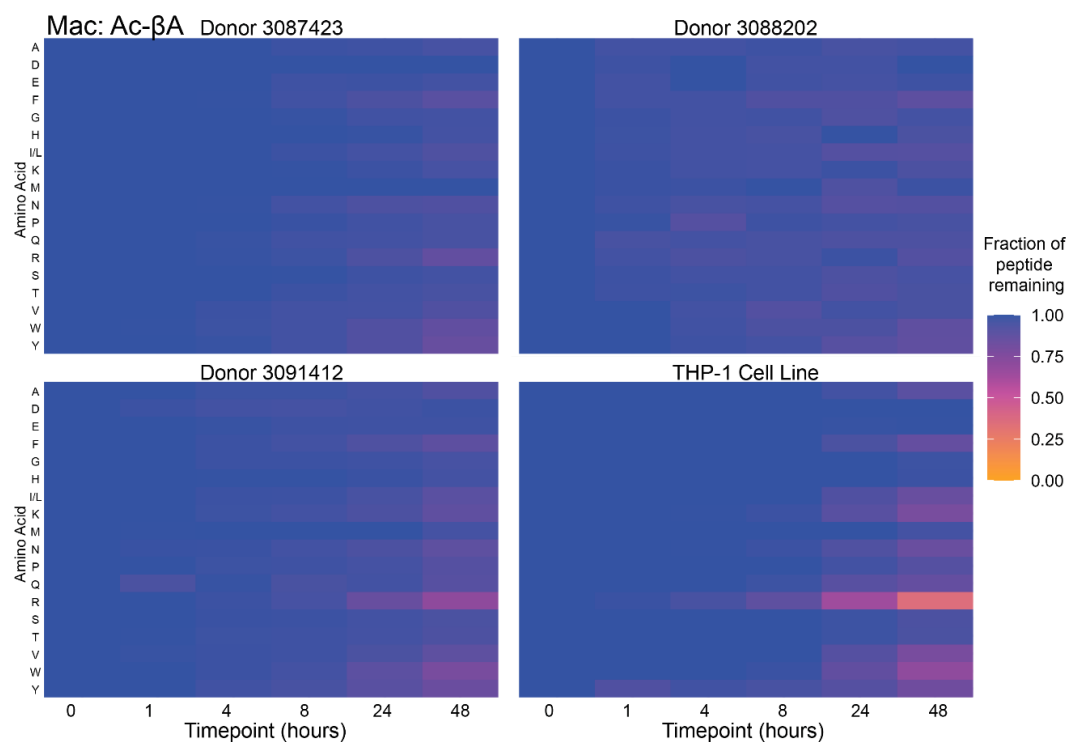


Figure 38 - Comparison of peptide degradation by different donors. Macrophages were cultured with RGEFV libraries containing end group Ac-βA.

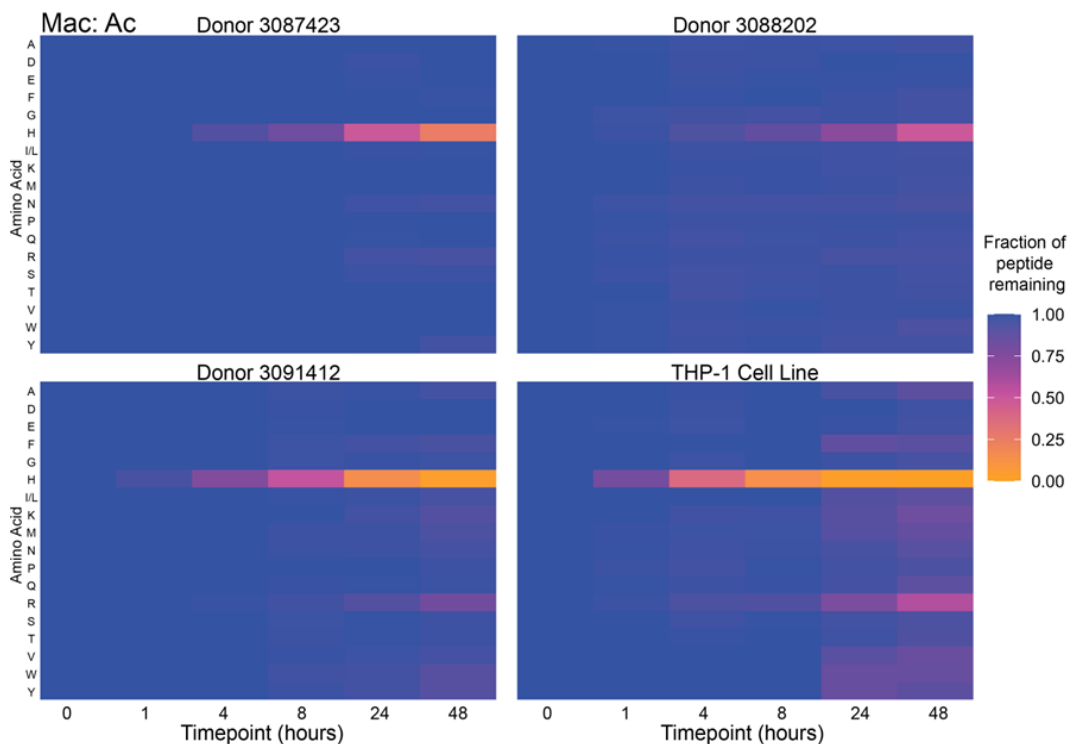


Figure 39 - Comparison of peptide degradation by different donors. Macrophages were cultured with RGEFV libraries containing end group Ac.

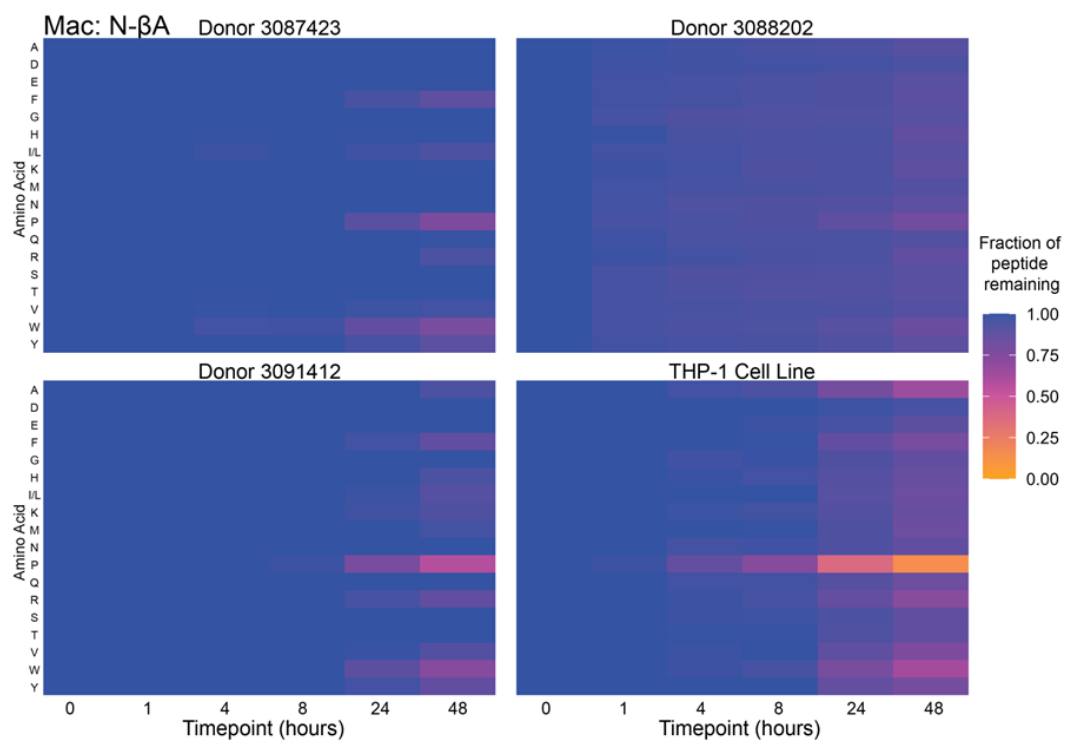


Figure 40 - Comparison of peptide degradation by different donors. Macrophages were cultured with RGEFV libraries containing end group N-βA.

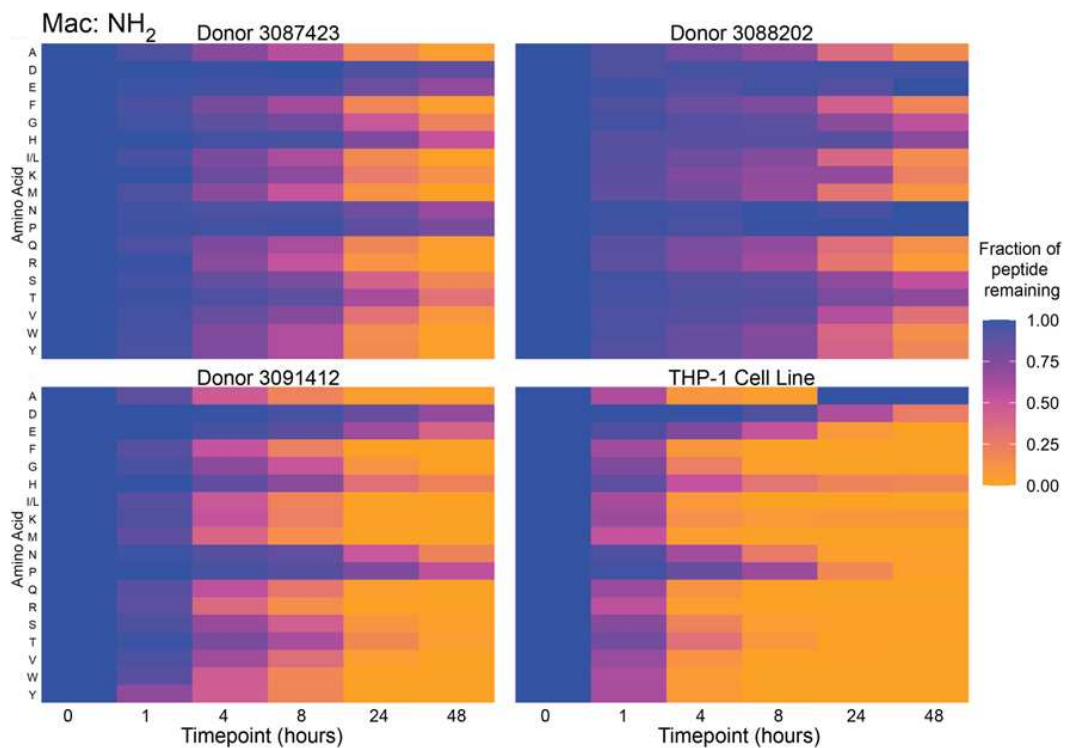


Figure 41 - Comparison of peptide degradation by different donors. Macrophages were cultured with RGEFV libraries containing end group NH₂.

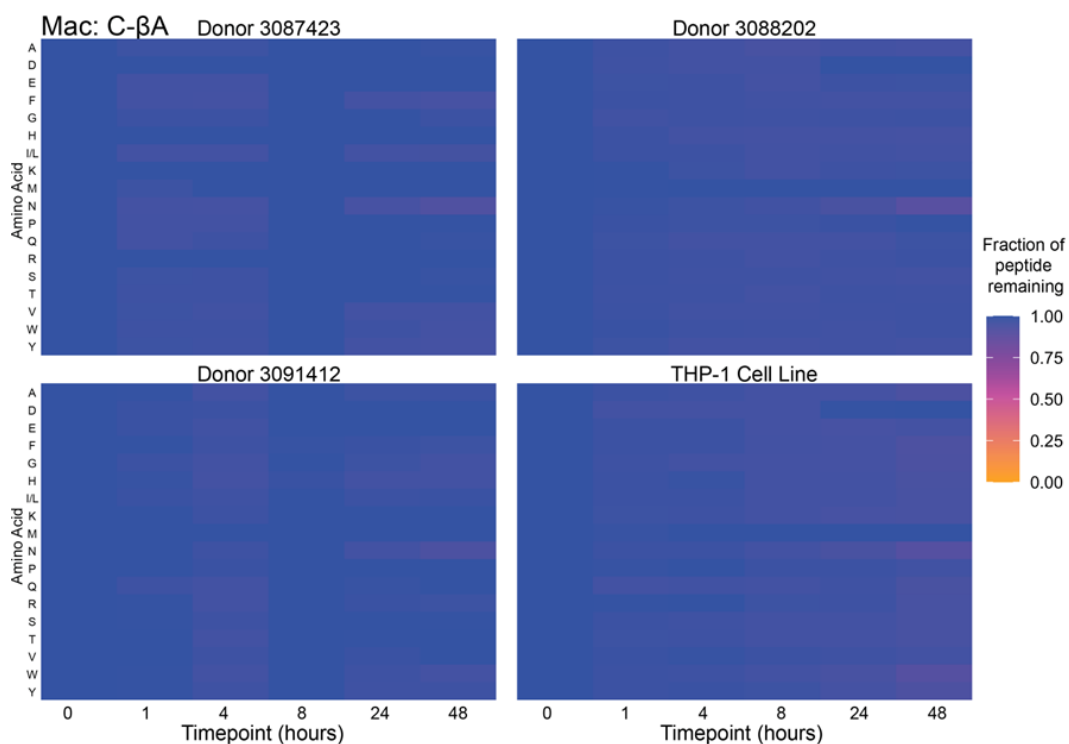


Figure 42 - Comparison of peptide degradation by different donors. Macrophages were cultured with RGEFV libraries containing end group C-βA.

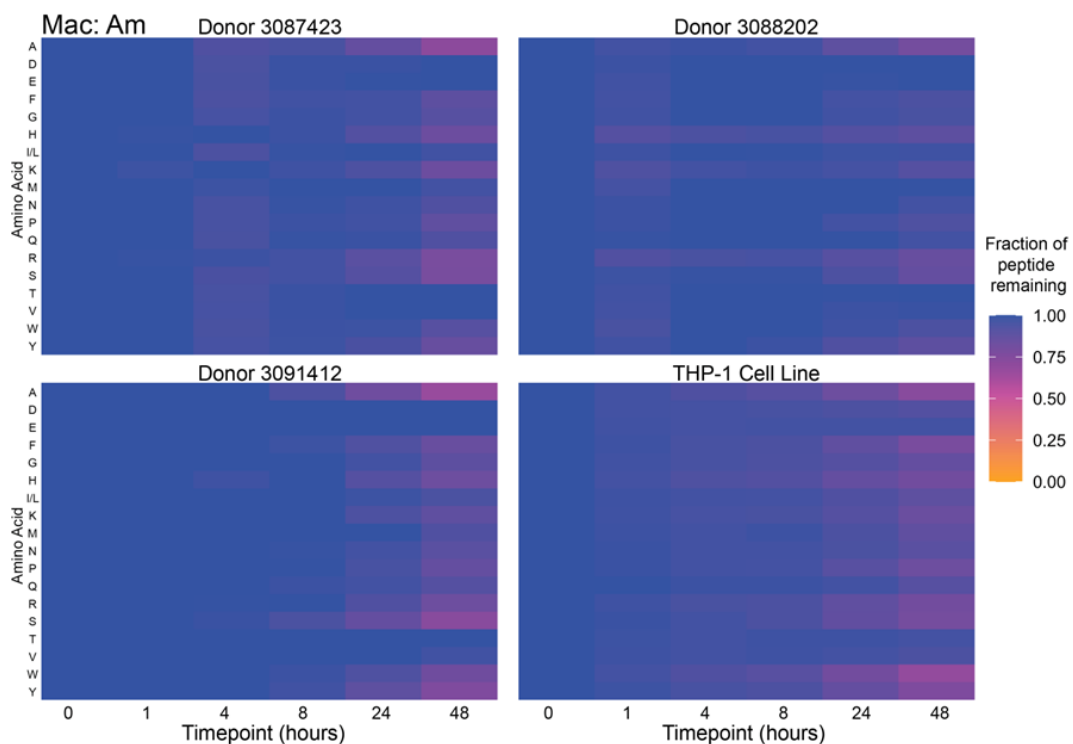


Figure 43 - Comparison of peptide degradation by different donors. Macrophages were cultured with RGEFV libraries containing end group Am.

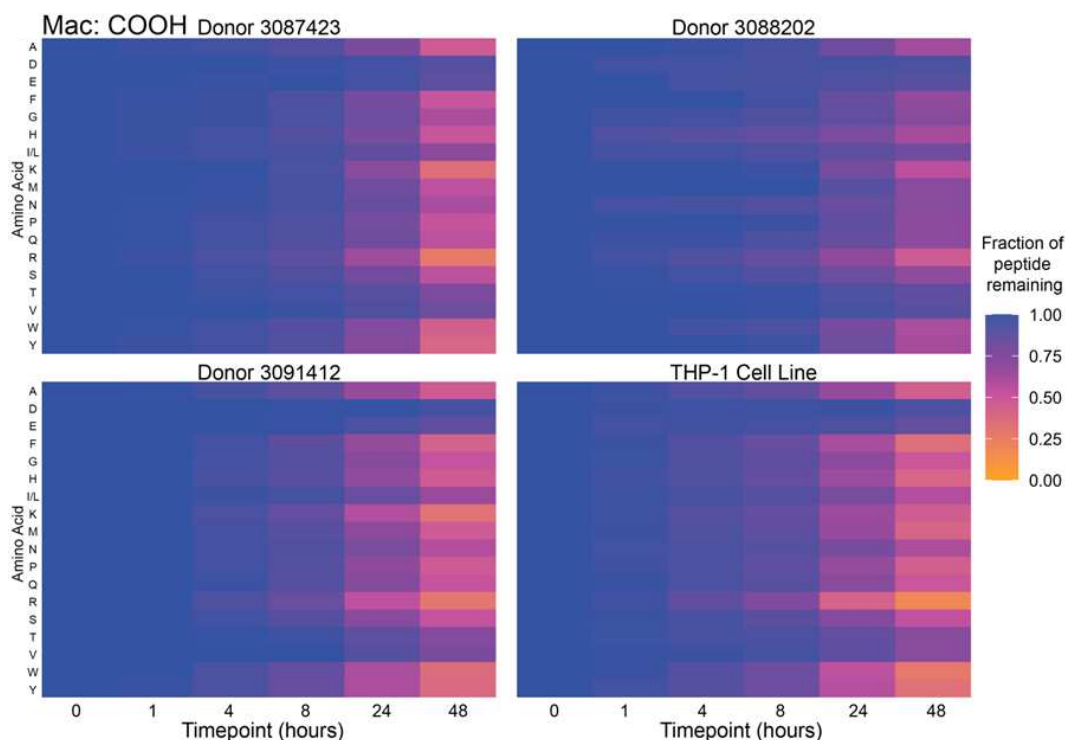


Figure 44 – Comparison of peptide degradation by different donors. Macrophages were cultured with RGEFV libraries containing end group COOH.

3.3.3 Sequence Specific Degradation

Initial peptide libraries were derivatives of an RGEFV peptide based upon the RGD cell adhesion peptide. To ensure that the results are not specific to this sequence we synthesized two other peptide libraries, an IVKVA peptide based upon the IKVAV laminin-mimetic peptide¹⁴⁰, and an LIAANK based upon the LIAANK TGF- β mimetic peptide¹⁴¹. We made peptides with each of the terminal chemistries having glycine at the terminus (Appendix Figure 127 - 140), since both LIAANK and IVKVA peptides do not have any special chemical groups and had degradation in the RGEFV peptides near the average for each condition (Figure 50 - Figure 50). The same broad trends held, with most peptides having more C-terminal degradation in the COOH condition, and acetylating the N-terminus, either Ac or Ac- β A reduced N-terminal degradation.

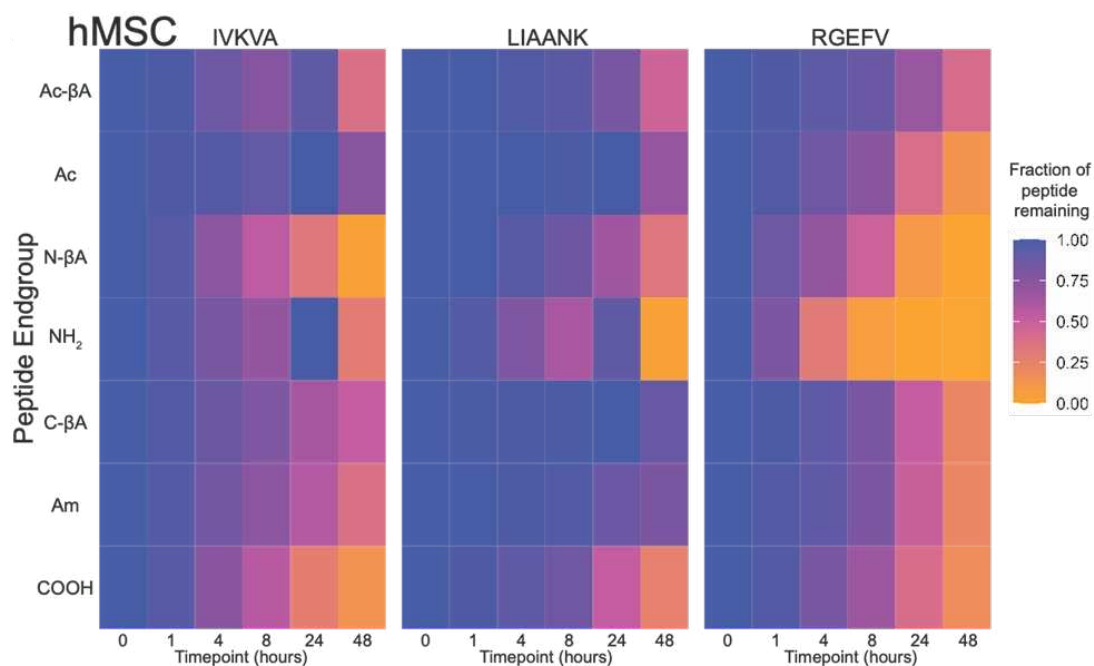


Figure 45 - Effects of different peptide sequences on non-specific degradation. Degradation was quantified for cell type hMSC.

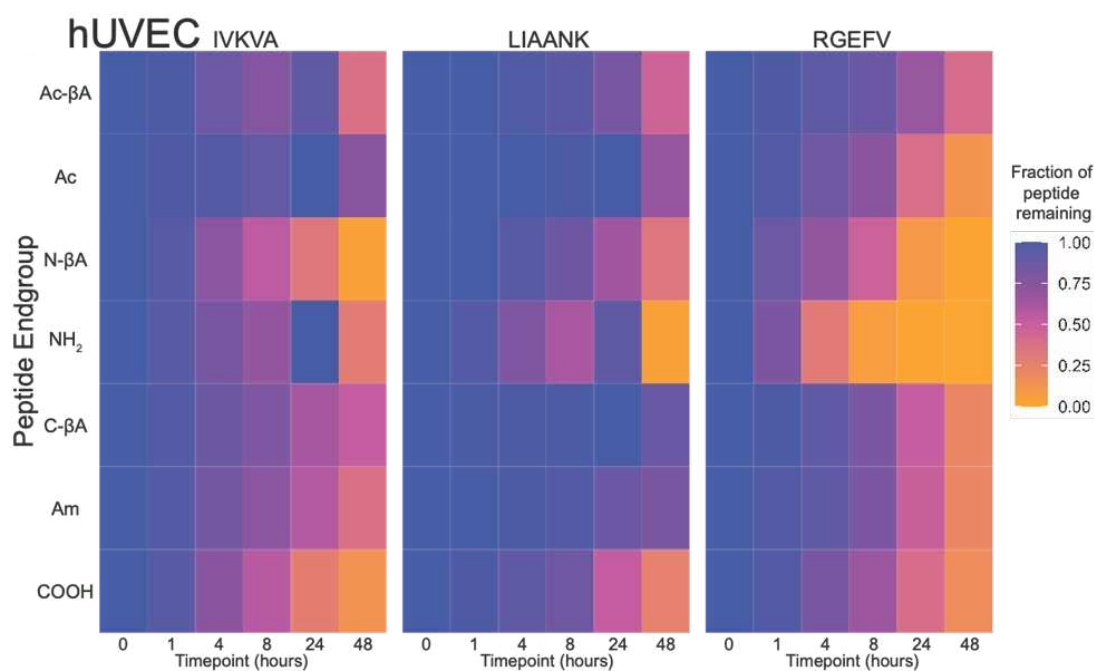


Figure 46 - Effects of different peptide sequences on non-specific degradation. Degradation was quantified for cell type hUVEC.

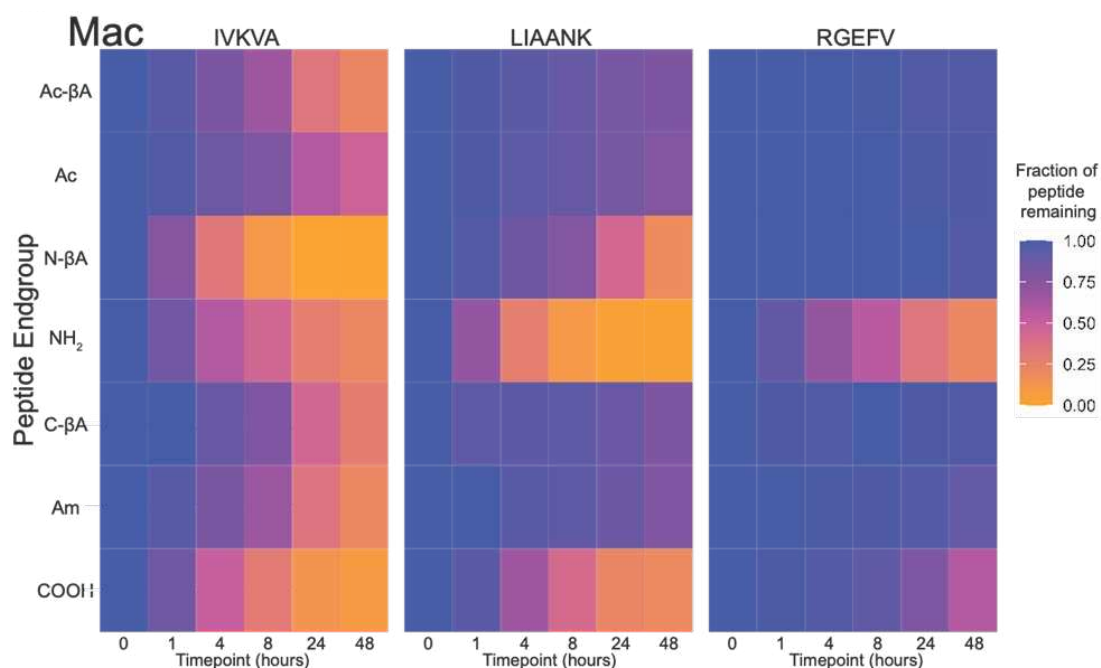


Figure 47 - Effects of different peptide sequences on non-specific degradation. Degradation was quantified for cell type Macrophage.

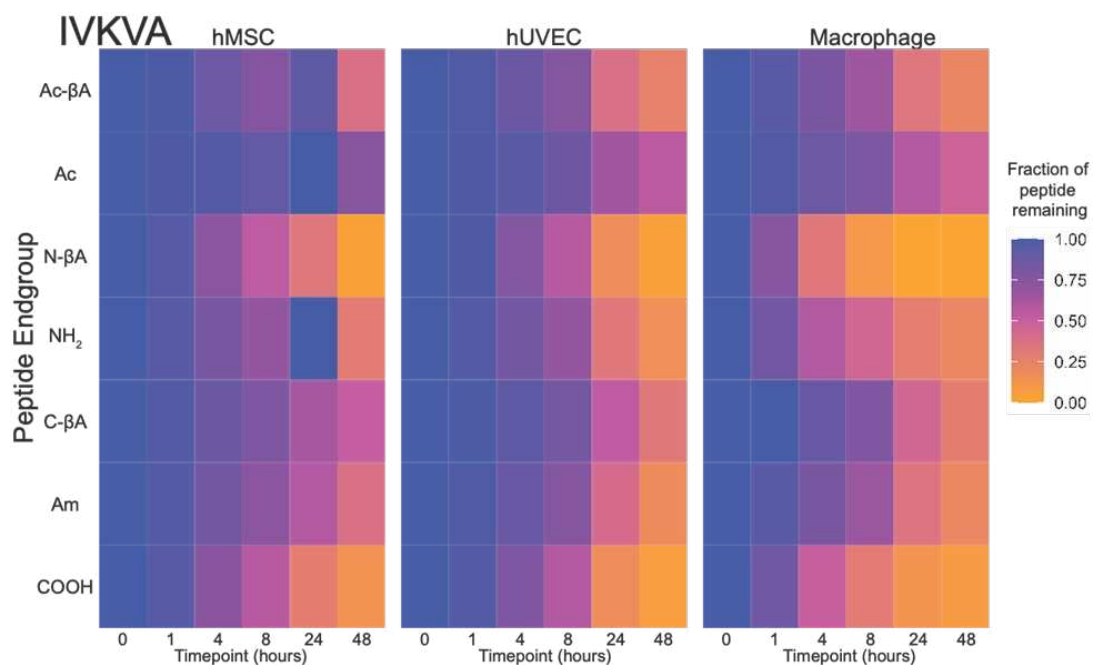


Figure 48 - Effects of different peptide sequences on non-specific degradation. Degradation was quantified for peptide IVKVA.

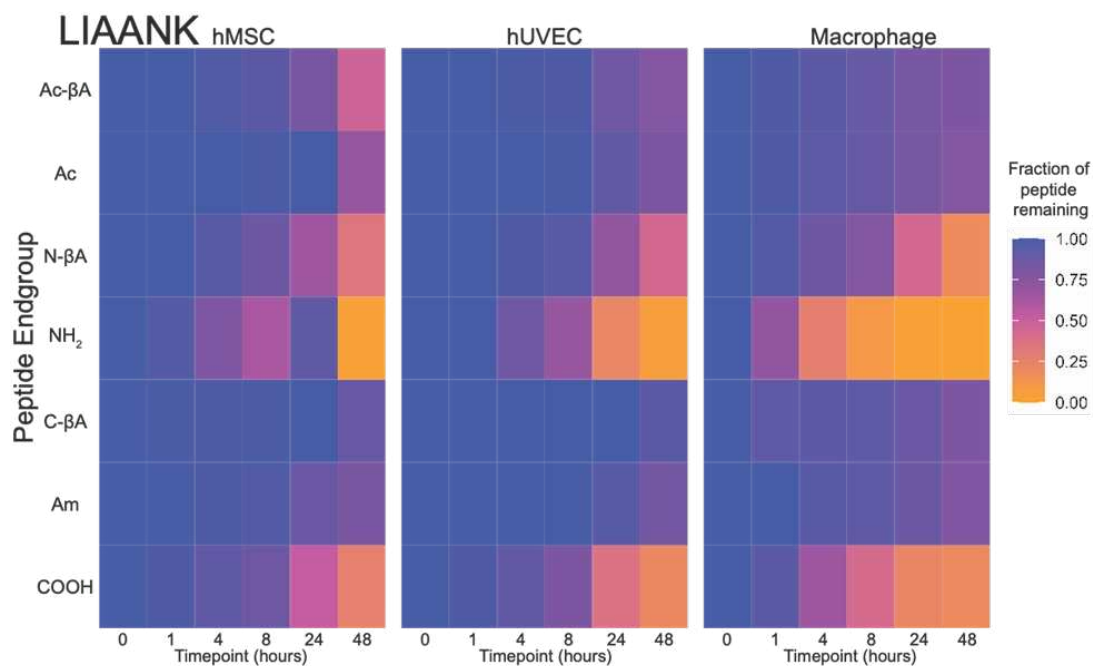


Figure 49 - Effects of different peptide sequences on non-specific degradation. Degradation was quantified for peptide LIAANK.

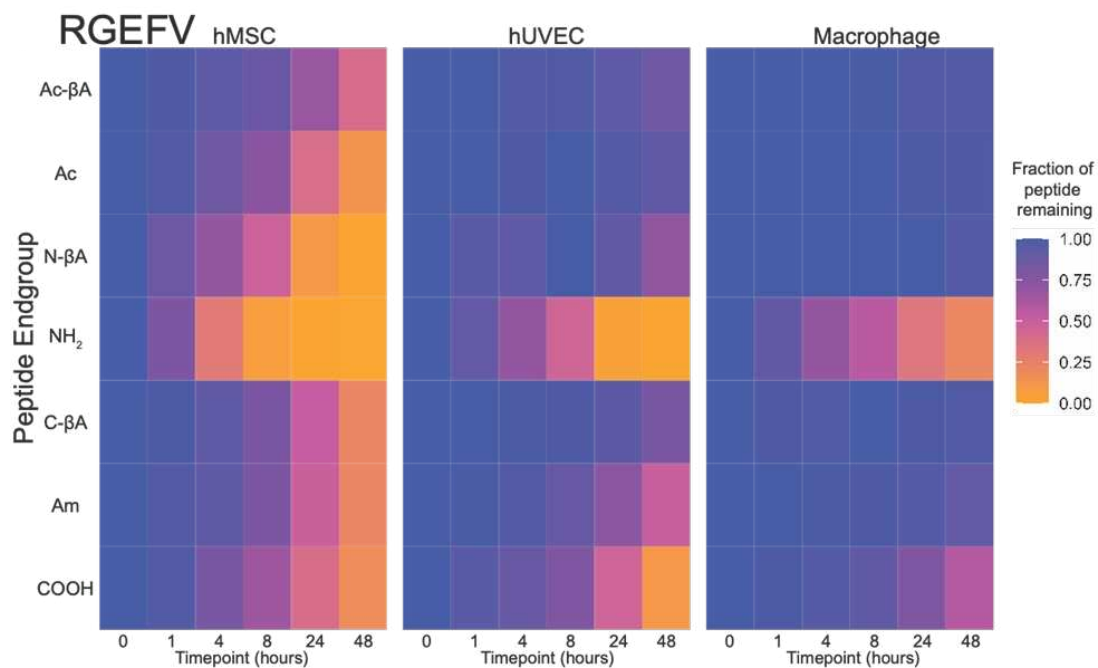


Figure 50 – Effects of different peptide sequences on non-specific degradation. Degradation was quantified for peptide RGEFV.

3.3.4 Statistical Analysis

Statistical analysis was done using multi-way analysis of variance (ANOVA) with a Tukey post-hoc test. All comparisons in this chapter are statistically significant ($p < 0.05$) unless otherwise noted. Statistical data can be found in Appendix Figure 173.A-D.

3.4 Conclusion

Here, the first comprehensive study on peptide degradation examining the effects of chain end chemistry was performed wherein each chain end was tested in libraries with all canonical amino acids immediately adjacent to the chain end. This indicates all quantified degradation within any given RGEFV library is paired, increasing confidence in accuracy of observed relative degradation within each library. First, hUVECs, hMSCs, and macrophages were all observed to degrade N-terminal amine and C-terminal carboxylic acid libraries faster than any other chain end for their respective termini. Second, hUVECs, hMSCs, and macrophages were all observed to degrade N-terminal acetylated β -alanine and C-terminal β -alanine libraries slower than any other chain end for their respective termini. The presence of positively charged amino acids (lysine and arginine) on the N-terminus of the peptide increased the degradation rate, and tryptophan was also degraded more rapidly across all N-terminal chemistries. Interestingly, proline slowed down degradation for N-terminal amines, but increased degradation for N-terminal β -alanines. For N-terminal amines the presence of negatively charged amino acids (glutamic acid or aspartic acid) reduced degradation rates. While acetylation was typically effective in preventing non-specific degradation of cells in gels, histidine was a significant exception and was substantially degraded by all three cell types. On the C-terminus tryptophan

increased the rate of degradation across all chemistries, and alanine, phenylalanine, lysine, and tyrosine had increased degradation for the carboxylic acid library, and aspartic acid, glutamic acid, and valine had decreased degradation. Third, hMSCs were observed to be the most proteolytically active while macrophages were observed to be the least proteolytically active. Chain-end dependent degradation was largely observed to be conserved when examined in regards to peptides LIAANK and IVKVA for all-three cell types tested, with the exception that for the IVKVA peptide in the context of an N-terminal β A appears to degrade faster than an N-terminal amine. These data support the notion peptides may not be stable in the presence of cells, chain end chemistry plays a role in peptide stability, and whenever peptides are used to impart function their stability should be taken into account.

Chapter 4: Other Methods of Modifying Degradation Rate

4.1 Introduction

This chapter has been adapted from work previously published. Reprinted with permission from *ACS Biomater. Sci. Eng.* 2024, XXXX, XXX, XXX-XXX. Publication Date: July 5, 2024. <https://doi.org/10.1021/acsbiomaterials.4c00736>. Copyright 2024 American Chemical Society.

Peptide are widely used in biomedical applications because of their biological selectivity, efficacy, and safety¹⁴². However, peptides are often more prone to degradation than proteins or other therapeutic molecules, and this remains a significant challenge in using peptide-based technologies¹⁴². Simple strategies can be used to improve the stability of peptides within biomaterials, such as increasing the initial peptide concentration of a peptide which decreases degradation rate¹⁴³, and modifying peptide with covalent chemistries, such as PEGylation, which can inhibit proteolytic degradation through steric hinderance^{142,144}. Increasing the concentration of a peptide within a hydrogel is a commonly done, however a drawback to this approach is that bioactive peptides frequently exhibit concentration-specific activity, and biomolecules degradation introduces a time-dependent variable into the system. PEGylation of peptides and proteins is a widely studied because presence of PEG chains has been shown to improve the stability and circulation time of protein drugs.^{145,146}. Notably, several PEG-protein conjugates have approved by the FDA and are used clinically.

Within the context of biomaterials, poly(ethylene glycol) is widely used as a polymer matrix within hydrogels. A key feature of PEG is that it resists protein adsorption, and as a result cells are typically unable to use adhesion proteins to bind PEG matrices. Most PEG hydrogels are modified with cell adhesion sequences, such as RGD, to enable cells to spread and migrate within these matrices. It is typically assumed that these adhesion peptides are stable throughout the lifetime of the hydrogel, however this is almost never quantified. Modifying soluble peptides with PEG chains can thus simulate the covalently bonded bioactive peptide to a PEG hydrogel, while enabling degradation to be easily quantified using methods we have already established for soluble peptides.

To examine the effects of concentration on peptide degradation, RGEFV peptides were synthesized with a glycine on either the C- or N- terminus of the peptide, with the end group chemistry being studied immediately adjacent to the terminal glycine. Glycine was chosen as a model peptide because it contains the peptide backbone but lacked any specific side group chemistry, having just a hydrogen atom, and had a degradation rate in the middle of all of the amino acids in our library studies. We incubated the glycine peptides with human mesenchymal stem/stromal cells (hMSCs), human umbilical vein endothelial cells (hUVECs), and pro-inflammatory macrophages and all N-terminal and C-terminal chemistries had slower degradation rates as the concentration of peptide increased. The presence of PEG modifications attenuated peptide degradation for all end group chemistries, however these peptides still showed degradation after 24 hours. PEGylating peptides does not perfectly recapitulate the covalent conjugation of peptides to hydrogel matrices because the PEG-peptide conjugates are still freely soluble in solution, unlike

peptides grafted onto a crosslinked polymer network. However, this system still gives insight into the influence that conjugation with bulky polymer chains can have on enzymatic activity against the peptide termini. While PEGylation did slow degradation, peptides containing an N-terminal amine or C-terminal carboxylic acid had increased degradation over other N-terminal and C-terminal chemistries, and those with an N-terminal Ac- β A and C-terminal β A were seen to degrade the slowest, consistent with results Chapter 3. These results imply a need for studying peptide stability in the context of hydrogels., This will reinforce generalized design rules to improve the design and bioactivity of peptides by preventing their non-specific degradation within peptide-functionalized hydrogels.

4.2 Experimental

4.2.1 Solid Phase Peptide Synthesis

The procedure for solid phase peptide synthesis remained the same as in section 3.2.1. All peptides used in this chapter can be found in Table 6 and have been validated via LC-MS in Appendix Figure 141 – 162.

Table 6 - List of all peptides used to evaluate other methods of modifying degradation rates. Note: N₃ stands for an azide moiety, and PEG₁₂ stands for monodisperse polyethylene glycol containing 12 monomers.

Peptide #	Amino Acid Sequence		Peptide #	Amino Acid Sequence
4.1	NH ₂ -βFβA ₆ -Amide		4.2	AcβA-GRGEFV-βA
4.3	Ac-GRGEFV-βA		4.4	βA-GRGEFV-βA
4.5	NH ₂ -GRGEFV-βA		4.6	AcβA-RGEFVG-Am
4.7	AcβA-RGEFVG-COOH		4.8	AcβA-RGEFVG-βA
4.9	AcβA-K(N ₃)GRGEFV-βA		4.10	Ac-K(N ₃)GRGEFV-βA
4.11	βA-K(N ₃)GRGEFV-βA		4.12	NH ₂ -K(N ₃)GRGEFV-βA
4.13	AcβA-GRGEFVK(N ₃)-Am		4.14	AcβA-GRGEFVK(N ₃)-COOH
4.15	AcβA-GRGEFVK(N ₃)-βA		4.16	AcβA-K(PEG ₁₂)GRGEFV-βA
4.17	Ac-K(PEG ₁₂)GRGEFV-βA		4.18	βA-K(PEG ₁₂)GRGEFV-βA
4.19	NH ₂ -K(PEG ₁₂)GRGEFV-βA		4.20	AcβA-(PEG ₁₂)-Am
4.21	AcβA-GRGEFVK(PEG ₁₂)-COOH		4.22	AcβA-GRGEFVK(triazole-PEG ₁₂)-βA

4.2.2 Peptide Cleavage from Solid Phase

The procedure for Peptide cleavage from solid phase remained the same as in section 3.2.2

4.2.3 Reagent Preparation for peptides of different concentrations.

After purification and lyophilization, peptides were dissolved and, if needed, pH adjusted to 7 using 2M ammonium hydroxide, then validated using LCMS (Table 6, peptides 4.2 – 4.8). Peptides were then lyophilized a second time peptides and dissolved at 50 mM in cell media containing 10 mM of standard NH₂-βF(βA)₆-NH₂ to be used in the degradation study. Since degradation was performed using seven RGEFV variants degraded by three cell-types, this is 21 solutions. Each solution was diluted 4X a total of 5 times, using the corresponding cell media containing 10 mM standard NH₂-βF(βA)₆-NH₂ as the diluent, for

final concentrations of: 1) 50 mM, 2) 12.5 mM 3.12 mM 780 μ M 195 μ M for a total of 105 different solutions.

4.2.4 PEGylation of peptides

Chain end chemistries studied remain the same as in Chapter 3. N-terminal chemistries of interest are an Acetylated β -Alanine, acetyl group, β -Alanine, and an amine. C-terminal chemistries of interest are an amide, carboxylic acid, and β -Alanine. Immediately adjacent to the chain-end chemistry of interest, on the N or C terminus of RGEFV peptide, an Fmoc-Azidolysine-OH was added (Table 6, 4.9 - 4.15). Once seven variations of the azidolysine functionalized RGEFV peptides were synthesized, HPLC purified, and dissolved in water at 10mM, and verified via LCMS, they were PEGylated. PEGylation was performed by aliquoting 20 mg of peptide into new conical 15 mL centrifuge tubes. In the manufacture provided vial, 100 mg of m-dPEG12-DBCO was dissolved in 1ml of reverse osmosis double distilled water and evenly distributed seven ways amongst all azide-functionalized RGEFV peptides previously aliquoted. The strained alkyne from the DBCO was allowed to click to the azide-functionalized peptides overnight on the wrist action shaker (Table 6. 4.16 – 4.22). The next day, the PEGylated peptides were HPLC purified, lyophilized, dissolved at 10 mM, and validated via LCMS.

4.2.5 Degradation of Peptides by Human Umbilical Vein Endothelial Cells on Tissue Culture Plastic

Human umbilical vein endothelial cells (hUVECs) (Lifecell Technology) at passage 2 were seeded into 24 well plates at a seeding density of 150,000 cells per well in 1ml of expansion media (Lifeline Cell Technology, LM-0002) containing ascorbic acid, hydrocortisone,

FBS, L-Glutamine, rh-EGF, heparin, and EnGS-US (All supplements LifeFactors, LS-1122). After 24 hour the media was replaced with 900 μ L. 24 hours later a glycine RGEFV peptides and the non- degradable $\text{NH}_2\text{-}\beta\text{F}(\beta\text{A})_6\text{-Amide}$ internal standard, were added to the cell media for final concentrations of 5000 μ M, 1250 μ M, 312 μ M, 78 μ M, and 19.5 μ M per peptide, with the standard held constant at 100 μ M. Each peptide was tested simultaneously, in triplicate with three technical repeats for a total of 9 wells/conditions 40 μ l samples were collected from the media at hours 0, 1, 4, 8, 24, and 48. Samples were frozen -80°C until they were ready for analysis by LC-MS. The cell donor used for this study was from Lot 04608 from an African American male.

The above protocol was used to study was slightly modified to study the degradation of peptide libraries containing LIAANK and IVKVA peptides. The peptides were added at a concentration of 37.5 μ M, the same concentration used in the RGEFV library degradation from chapter 3.

4.2.6 Degradation of Peptides by Human Mesenchymal Stem Cells on Tissue Culture Plastic

Human mesenchymal stem cells (hMSCs) (Rooster Bio) at passage 3 were seeded into 24 well plates at a seeding density of 75,000 cells per well in 1ml of RoosterBasal™-MSC-CC (RoosterBio, SU-022) containing RoosterBooster™-MSC (RoosterBio SU-003). After 24 hour the media was changed. 24 hours later a glycine RGEFV peptides and the non- degradable $\text{NH}_2\text{-}\beta\text{F}(\beta\text{A})_6\text{-Amide}$ internal standard, were added to the cell media for final concentrations of 5000 μ M, 1250 μ M, 312 μ M, 78 μ M, and 19.5 μ M per peptide, with the standard held constant at 100 μ M. Each peptide was tested simultaneously, in triplicate

with three technical repeats for a total of 9 wells/conditions. 40 µl samples were collected from the media at hours 0, 1, 4, 8, 24, and 48. Samples were frozen -80°C until they were ready for analysis by LC-MS. For these studies hMSC Lot 310268 a 19-year-old Eritrean/east African female was used.

4.2.7 Degradation of Peptides by THP-1 Derived Macrophages on Tissue Culture Plastic

THP-1 cells were placed into a 24 well plate with a seeding density of one million cells per well using RPMI (Cytiva, SJ30027.1) containing 10% FBS and 1% anti-anti, with PMA at a concentration of 100ng/ml for two days. After day 2 the media was changed to RPMI containing IFN- γ , 20 ng/ml MCSF, and 100 ng/ml LPS and allowed to polarize for three days (Day 5 of culture). After six days the media was changed to macrophage serum free media with L-Glutamine (Gibco 12065-074). After 24 hour the media was changed. 24 hours later a glycine RGEFV peptides and the non- degradable NH₂- β F(β A)₆-Amide internal standard, were added to the cell media for final concentrations of 5000 µM, 1250 µM, 312 µM, 78 µM, and 19.5 µM per peptide, with the standard held constant at 100 µM. Each peptide was tested simultaneously, in triplicate with three technical repeats for a total of 9 wells/conditions. 40 µl samples were collected from the media at hours 0, 1, 4, 8, 24, and 48. Samples were frozen -80°C until they were ready for analysis by LC-MS. The THP-1 cell line was used for initial degradation experiments on tissue culture plastic and all other cell studies.

4.2.8 Liquid Chromatography – Mass Spectrometry

For LIAANK and IVKVA peptides the LC-MS was performed as previously described.

Immediately after the 96-well sample plate were removed from the -80°C freezer, 4 µL of neat acetic acid was added to each well to acidify the media and prevent further peptide degradation by proteases. From each sample, 10 µL of crude solution was introduced by the LC-MS through an Thermo Scientific Vanquish LC System (Thermo Fisher Scientific) which outputted to a Thermo Scientific LTQ XL Linear Ion Trap Mass Spectrometer (Thermo Fisher Scientific). The sampled mixture was trapped on a column (ProntoSIL C18 AQ, 120 Å, 3 µm, 2.0 x 50 mm HPLC Column, PN 0502F184PS030, MAC-MOD Analytical Inc.). The samples were loaded onto the column with a solvent containing acetonitrile/water, 5:95 (v/v) containing 1% acetic acid at a flow rate of 300 µL/min and held for one minute. The sample was then eluted from the column with a linear gradient of 5-30% Solvent B (1% acetic acid in acetonitrile) at the same flow rate for one minute. This was followed by a 1 min ramp up to 100% Solvent B, where it was re-equilibrated with Solvent A (1% acetic acid) to 5% solvent B over the course of 1 min and held there for 2 min. The column temperature was a constant 29 °C. The mass spectrometer was operated in positive ion mode. Using a heated ESI, the source voltage was set to 4.1 kV, and the capillary temperature was 350 °C.

Data analysis was also performed as previously described for all peptides.

4.3 Results and Discussion

4.3.1 Concentration effects of Peptides on Degradation

Degradation studies were performed using an individual RGEFV peptide with a glycine at the terminus being studied at concentrations ranging from 19.5 µM to 5,000 µM. It was

generally observed that peptides at lower concentrations were more rapidly degraded than peptides at higher concentrations (Figure 53 - Figure 54) and is in agreement with the literature¹⁴³. The effects of terminal chemistry on peptide degradation were broadly conserved across concentration ranges, with peptides having N-terminal amine-Gly being rapidly degraded even at 5 millimolar concentrations. After 48 hours only 5% of amine-Gly-terminated RGEFV peptides remained after starting with an initial concentration was 5,000 μM in hMSCs and Macrophages (Figure 53.D & Figure 53.D). C-terminal degradation was also observed to be rapid with only 26% of the initial peptide remained of an initial concentration of 5,000 μM Gly-COOH terminated peptide when cultured with hUVECs (Figure 52.G). It is notable that C-terminated Gly-COOH peptides were mostly degraded by 48 hours when cultured with hMSCs and hUVECs, but only showed modest degradation when cultured with THP-1-derived macrophages (Figure 51, Figure 52.G and Figure 53.G respectively). Overall, these results indicate that increasing peptide concentration leads to a slower degradation rate and a higher amount of peptide at later time points; however, modifying the chemistry at the terminus is a more effective method for controlling concentration of peptide after 48 hours. In addition, general degradation profiles are consistent with those observed in Chapter 3.

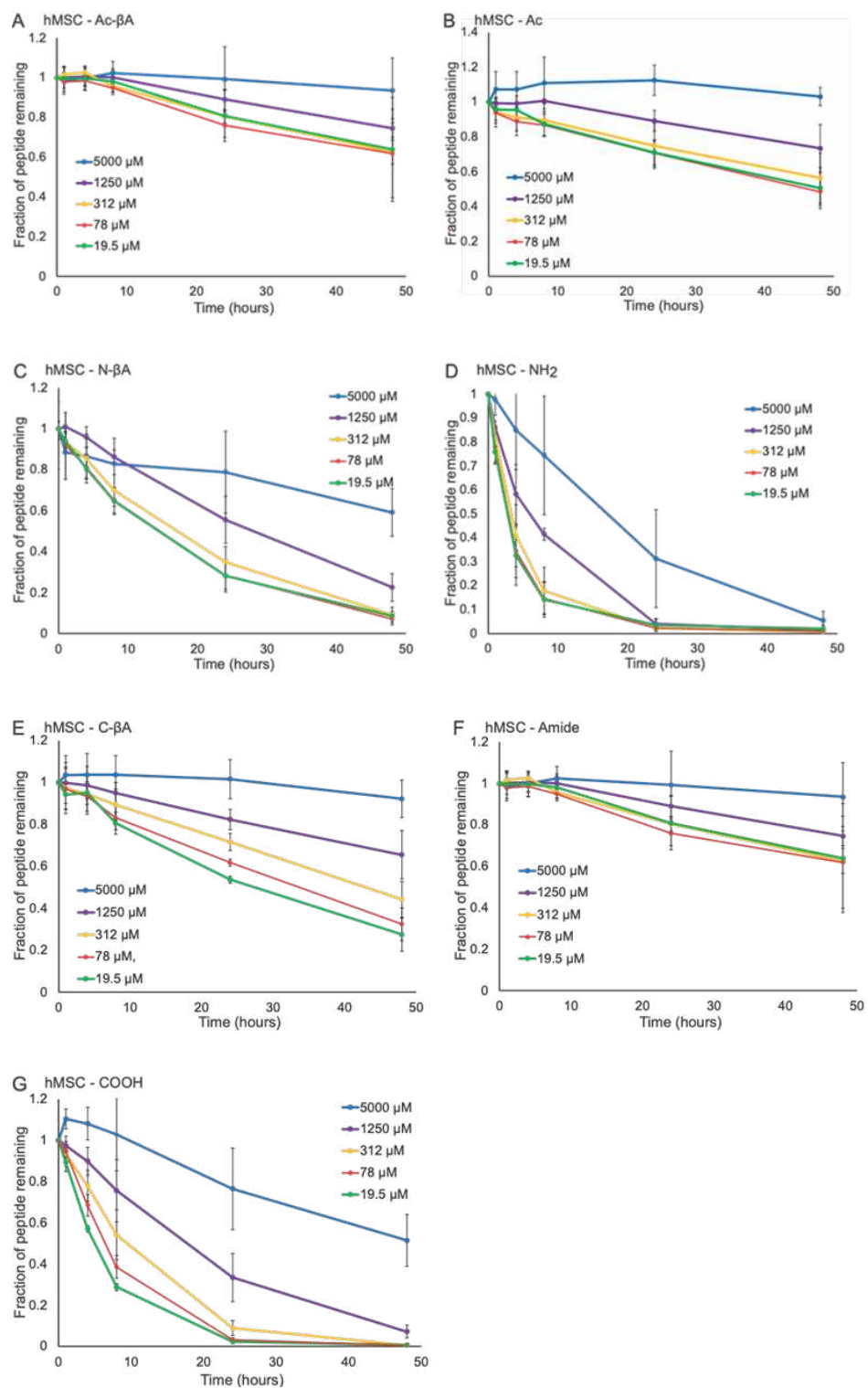


Figure 51 - Degradation of peptides at different concentrations. Data was quantified for hMSCs (A) Ac-βA, (B) Ac, (C) N-βA, (D) NH₂, (E) C-βA, (F) Am, (G) COOH

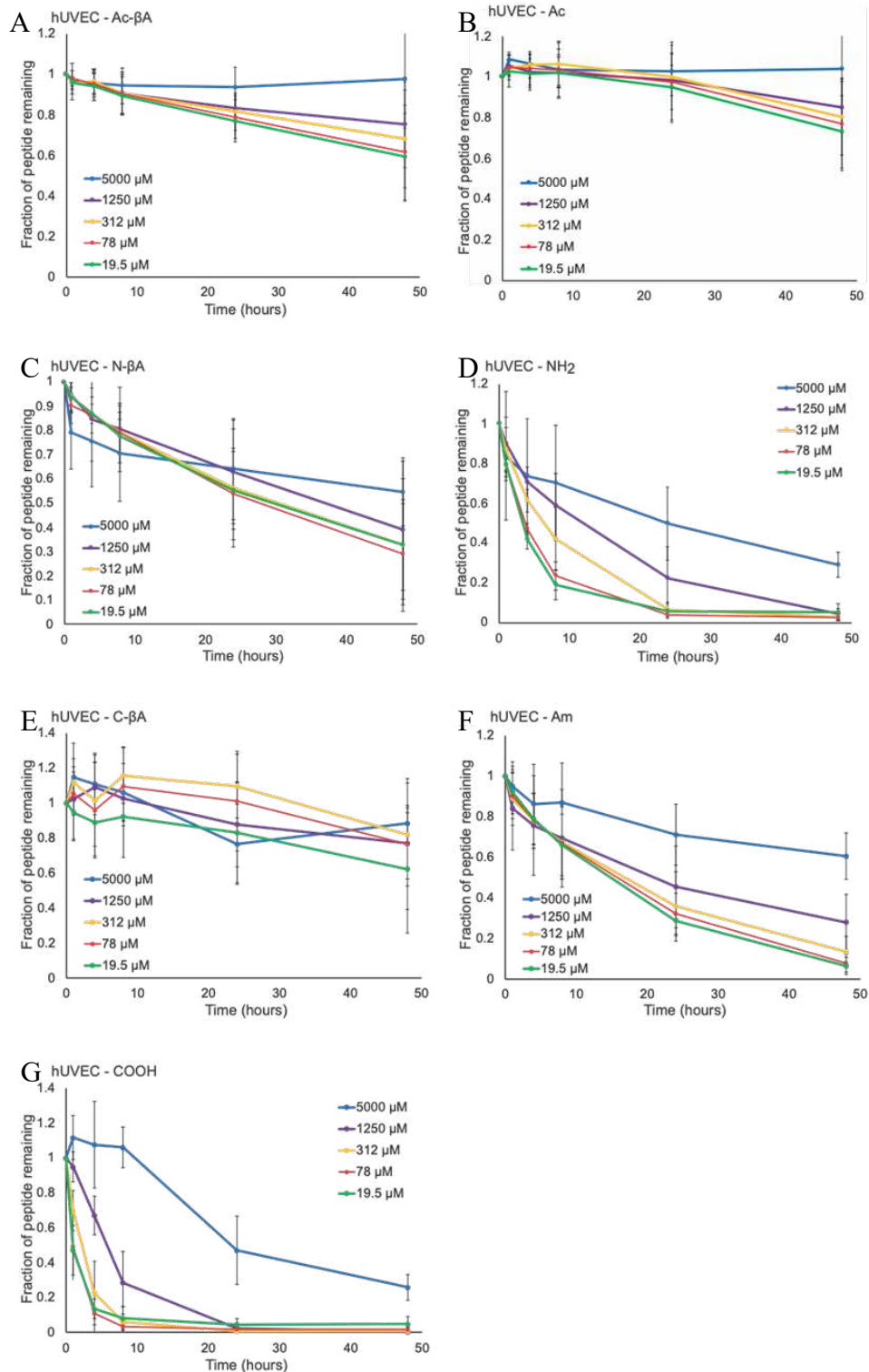


Figure 52 - Degradation of peptides at different concentrations. Data was quantified for hUVECs (A) Ac-βA, (B) Ac, (C) N-βA, (D) NH₂, (E) C-βA, (F) Am, (G) COOH.

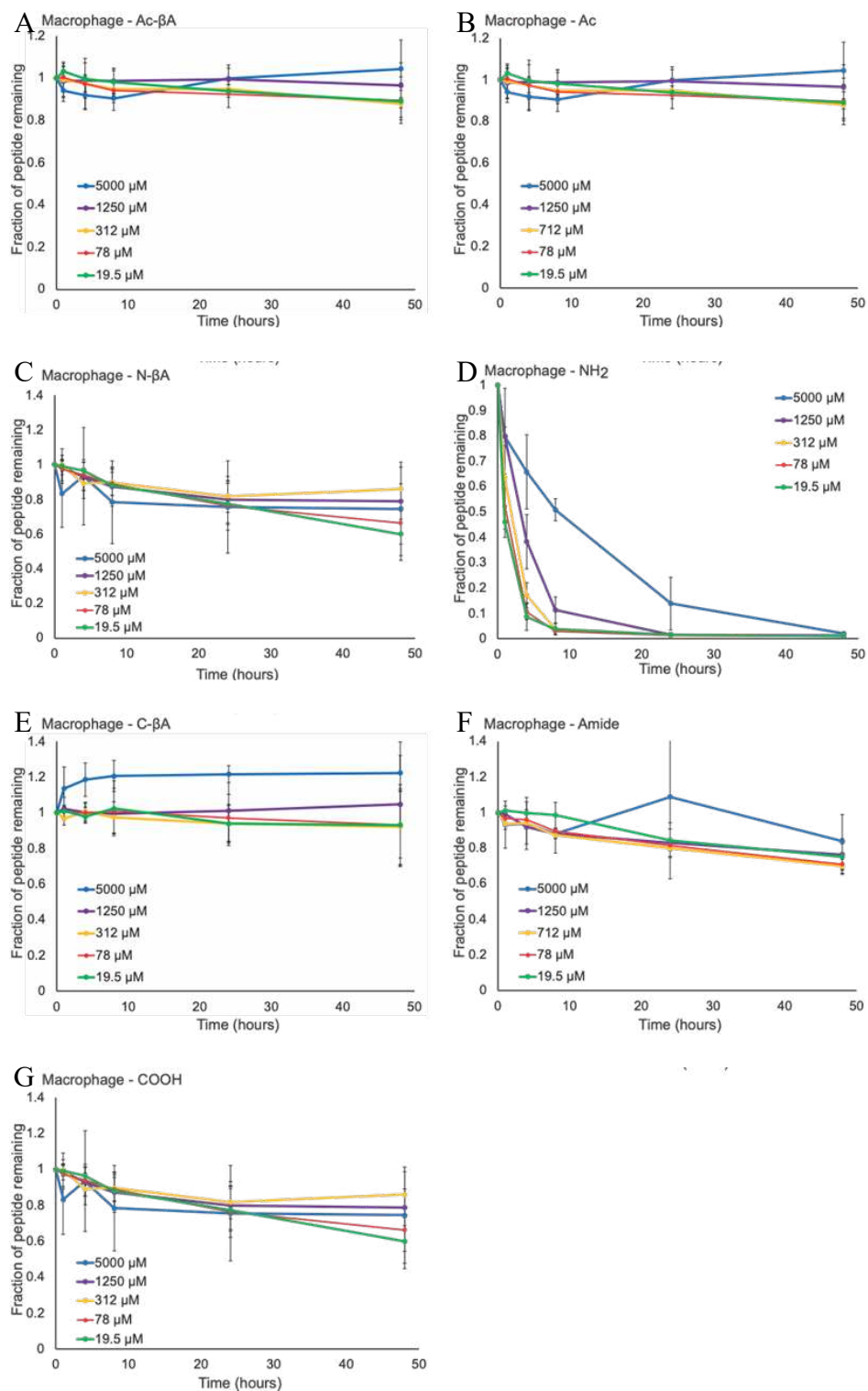


Figure 53 – Degradation of peptides at different concentrations. Data was quantified for macrophages (A) Ac- βA , (B) Ac, (C) N- βA , (D) NH_2 , (E) C- βA , (F) Am, (G) COOH.

4.3.2 PEGylation/Matrix Mimicking effects on Peptide Degradation

In addition to their roles as adhesion ligands or growth factor mimetic peptides, peptides are also widely used to crosslink hydrogel matrices^{87,147}. This is often done by utilizing chemistries that can react with canonical amino acids, such as thiol-maleimide reactions¹⁴⁸ or incorporating non-natural chemistries into the peptide side chain, such as azides, which

can then undergo click reactions with reactive groups present on polymers¹⁴⁹. To better understand how these peptide modifications influence degradation kinetics, A

series peptides were synthesized, and an azido-lysine was placed on either the N-terminus or C-

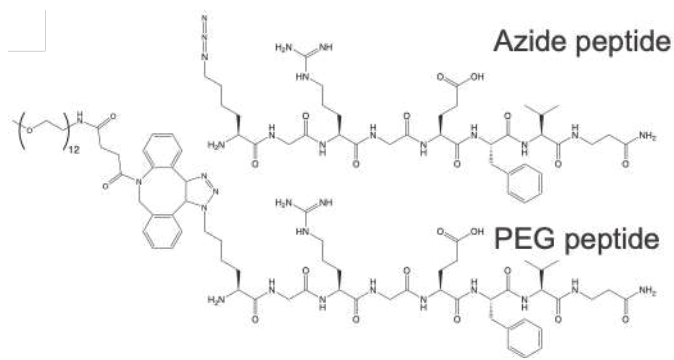


Figure 54 – Example of RGEFV peptide with different terminal chemistries. Peptides were synthesized with azides (top) on either the N- or C- terminus. A portion were modified with a (PEG)₁₂-DBCO (bottom). The amine version of the RGEFV peptide is displayed.

terminus immediately adjacent to each of the seven different terminal chemistries being studied (Figure 54.top). A portion of these peptides were then functionalized with a (PEG)₁₂ chain modified with a dibenzocyclooctyne (DBCO) group (Figure 54.bottom) that is commonly used in biomaterial synthesis. Also, azide-containing peptides and PEG-modified peptides were added to cell culture media and quantified degradation by hMSCs, hUVECs, and macrophages (Figure 55). PEG modification slowed peptide degradation for every N-terminal and C-terminal chemistry across hMSCs, hUVECs, and macrophages. Quantifying peptides covalently attached to hydrogels remains challenging, however, PEGylation of peptides provides a convenient methodology to gain insight as to what

happens when peptides are attached to PEG hydrogels. These results indicate that non-specific peptide degradation depends upon both the end group chemistry of the peptide and also the presence of bulky groups which can slow or prevent the degradation of peptides conjugated to matrices, such as crosslinking peptides.

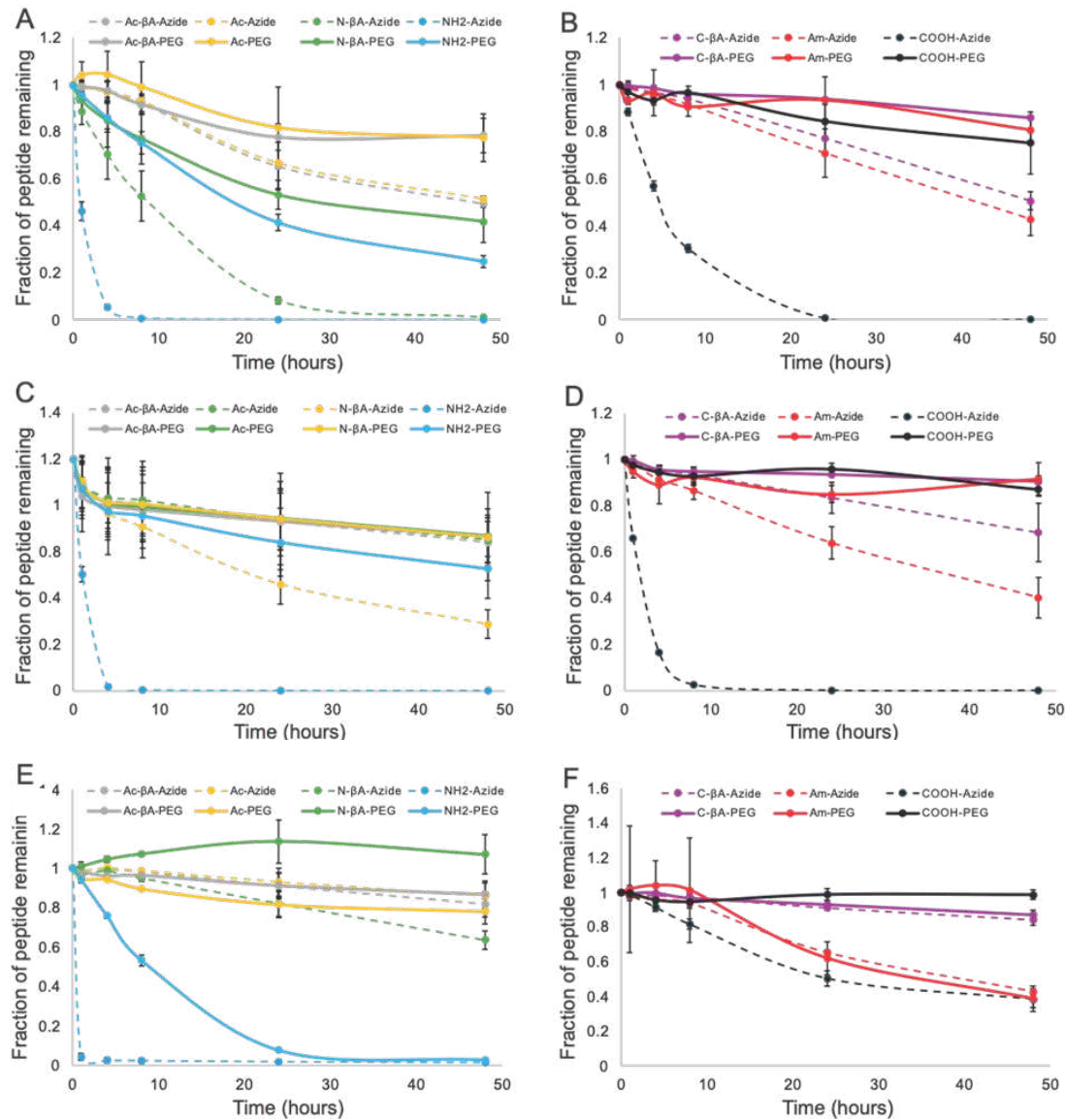


Figure 55 – PEG conjugation to peptides slows degradation across endgroups and cell types. (A) hMSC N-terminal chemistries, (B) hMSC C-terminal chemistries, (C) hUVEC N-terminal chemistries, (D) hUVEC C-terminal chemistries, (E) macrophage N-terminal chemistries, (F) macrophage C-terminal chemistries.

4.4 Conclusion

In conclusion, peptides were synthesized and degraded in the presence of hUVECs, hMSCs and macrophages to better understand the influence of substrate concentration, modification with an azide, and PEGylation. Generally, increasing concentration had the expected result of decreasing degradation rate; however, this was not as effective as changing the end group chemistry. Azide functionalized peptides had a did not appear to decrease degradation rate, and followed degradation trends observed in Chapter 3. PEGylation, while a well-accepted method of slowing degradation rate, its effectiveness is still determined by end group chemistry and the cell-type degrading the peptide. This is readily apparent when observing the $\text{NH}_2\text{-K(PEG}_{12}\text{)-RGEFV-}\beta\text{A}$ being degraded down to about 10% by macrophages within a 24-hour period. Highlighting that non-specific degradation is context dependent on end group chemistry, adjacent PEG functionalization, and cell type present. While PEGylation can inhibit degradation, it is not fully effective in all cases. Indicating peptide degradation within hydrogels may be occurring.

Chapter 5: Cells in Gels influence Peptide Degradation, and Peptide Degradation influences Cells in Gels

5.1 Introduction

This chapter has been adapted from work previously published. Reprinted with permission from *ACS Biomater. Sci. Eng.* 2024, XXXX, XXX, XXX-XXX. Publication Date: July 5, 2024. <https://doi.org/10.1021/acsbiomaterials.4c00736>. Copyright 2024 American Chemical Society.

2D cell culture is an attractive method because of its simplicity, since nearly all products for culturing and analyzing cells *in vitro* have been optimized for cells grown on tissue culture plastic. However, it is well understood that cell-cell and cell-ECM interactions are substantially different in within the complex 3D environment found within tissues^{150,151}. Some of these differences include proliferation, differentiation, gene expression¹⁵⁰, cell morphology, polarity, and method of division¹⁵¹ have been both observed. To better understand how non-specific peptide degradation occurs in a more physiologically relevant system, a 3D hydrogel environment was engineered and used for evaluation of degradation and biologic impact of peptide stability.

It is well understood that molecular and mechanical cues are an important in recapitulating important features of the ECM¹⁵². Since peptides are commonly used to improve cell adhesion and signaling, their stability in culture is important for biological activity. Utilization of proteolytically sensitive crosslinkers such as a Pan-MMP sensitive peptide allows cell mobility by creating space in the matrix via protease mediated cleavage of the

crosslinker¹⁵³. Additionally the local microenvironment of 3D cell culture is a deterministic factor of cell adhesion and mobility¹⁵⁴. It has also been shown that hydrogels with multiple peptide functionalities will outperform materials with single functionality¹⁵³, such as inclusion of an adhesion peptide with a cleavable crosslinking peptide. Studies were designed using two such peptides in a 3D-PEG model system in order to better understand how peptide degradation is impacted by environment, and how this environment influences cells.

Peptides are frequently incorporated into hydrogels to improve physiological relevance. This includes cell adhesion peptides, such as a cyclic GRGDSK(N₃), and peptides that are substrates for MMPs, such as the Pan-MMP peptide N₃KKGPQGIWGQKK(N₃), which enables cells to spread and migrate within covalently crosslinked networks. These peptides were incorporated into 3D PEG hydrogel microenvironment for cell culture. Notably, while the PanMMP peptides is designed to be degraded by cells, RGD peptides are widely used to improve cell adhesion, but is not typically intended to be degraded during cell culture. hMSCs, hUVECs, and macrophages were each introduced into this 3D culture environment, and the soluble libraries used in Chapter 41 were degraded. Degradation was then quantified to assess if a 3D microenvironment impacts the degradation rate of soluble peptides. Next, we sought to better understand if the non-specific degradation of cell adhesion peptides impacts the bioactivity of hydrogel matrices. We fabricated a series of hydrogels conjugated with one of three different RGD molecules: a cyclic RGD which has no peptide termini and is not susceptible to degradation by exopeptidases, a “fast degrading” RGD peptide with an N-terminal amine, and a “slow degrading” RGD peptide

with an acetylated β -alanine on the N-terminus. Our results indicate that peptide stability within hydrogels does impact cell behavior, and that there is a trend for reduced spreading in gels with rapidly degrading adhesion sequences.

5.2 Experimental

5.2.1 8-Arm PEG evaluation

20 kDa 8-arm PEG-DBCO which dissolved in water in under 30 seconds were used as received. Otherwise, the PEG was quickly purified by dissolving them in isopropanol and removing impurities using a 10 kDa Amicon centrifugal filter. Approximately 200 mg of PEG was dissolved in 5 mLs of isopropanol and it was centrifuged at 4,500 RPM until there was less than one milliliter of PEG-DBCO/isopropanol left in the filter. This was repeated twice, and then the filtrate was lyophilized and used.

5.2.2 2-Azidoacetic Acid

Synthesis of 2-azidoacetic acid was based on a procedure by Li¹⁵⁵ (Figure 56). Sodium Azide (6.5g, 100 mmol) and bromoacetic acid (13.9g, 100 mmol) was dissolved in water (50ml). The reaction was stirred at room temperature under ambient conditions overnight. After which the reaction was acidified to pH 1 with 6M HCl and extracted with diethyl ether (3 x 100ml). The organics were combined, dried over MgSO₄, and concentrated to afford 2-azidoacetic acid as a colorless oil. Note: 2-azidoacetic acid was added to peptides on resin using the same HCTU chemistry as with Fmoc-amino acids.

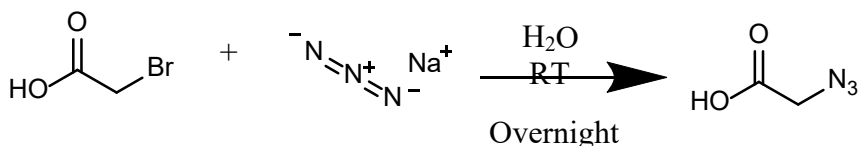


Figure 56 – Schematic of 2-Azidoacetic Acid Synthesis

5.2.3 Solid Phase Peptide Synthesis

The procedure for solid phase peptide synthesis remained the same as in section 3.2.1. All peptides used in this chapter can be found in Table 7 and have been validated via LC-MS in Appendix Figure 1-126 and Appendix Figure 163 - 167.

Table 7 - List of all peptides used to demonstrate how chain end modification modulates non-specific degradation of peptides. Asides from peptide 5.1, four N-terminal modifications including an acetylated β -Alanine (Ac β A), a β -Alanine (β A), Acetylation (Ac), and amine (NH₂). Three C-terminal modifications include amidation (Am), a carboxylic acid (COOH), and a β -Alanine (β A). For peptide libraries, X represents a variable amino acid which includes: A, D, E, F, G, H, I, K, L, M, N, P, Q, R, S, T, V, W, and Y. An Azide moiety is shown as N₃.

Peptide/Peptide Library #	Amino Acid Sequence	Peptide/Peptide Library #	
5.1	NH ₂ - β F β A6-Amide	5.2	Ac β A-X-RGEFV- β A
5.3	Ac-X-RGEFV- β A	5.4	β A-X-RGEFV- β A
5.5	NH ₂ -X-RGEFV- β A	5.6	Ac β A-RGEFV-X-Am
5.7	Ac β A-RGEFV-X-COOH	5.8	Ac β A-RGEFV-X- β A
5.9	N ₃ -KGPQGIWGQK(N ₃)-NH ₂	5.10	NH ₂ -GRGDSK(N ₃)-NH ₂
5.11	Ac β A-GRGDSK(N ₃)-NH ₂	5.12	Cyclic GRGDSK(N ₃)

5.2.4 Peptide Cyclization

Cyclic GRGDSK(N₃) was synthesized on 2-chlorotrityl Chloride resin as described previously. After synthesis, the peptide was cleaved from the resin using a mild acidic solution of 5% TFA with 2.5% triisopropylsilane in DCM for 5 minutes and collected. This

process was repeated until the resin turned dark red/black. The liquid was then precipitated in ether, dissolved in 50% acetonitrile in water, neutralized using 1M ammonium hydroxide, and lyophilized. The protected peptide was then cyclized by dissolution in DMF at a concentration of 1 mg/mL and adding 3 molar equivalents of HATU, and adding DIPEA at a ratio of 260 μ l/mmol of HATU. After 6 hours the peptide was concentrated using rotary evaporation at 65°C, precipitated in diethyl ether and washed 3X in diethyl ether. Protecting groups were removed using 95% TFA with 2.5% TIPS and 2.5% DI water, followed by precipitation in diethyl ether. After washing 3X more times in diethyl ether the cyclic peptide was purified using HPLC as previously described.

5.2.5 Degradation of Peptides by Human Umbilical Vein Endothelial Cells in PEG hydrogels

hUVECs at passage 2 were seeded into T75 flasks in basal media containing ascorbic acid, hydrocortisone, FBS, L-Glutamine, rh EGF, heparin, and EnGS-US (All supplements - LifeFactors, LS-1122) until they were 80-90% confluent. Cells were then washed with PBS and trypsinized with 2 mL of 0.25% Trypsin in Hank's Buffered Salt Solution with EDTA and incubated for 5 minutes. Once cells had detached they were centrifuged at 0.2 RCF for 5 minutes and counted using a hemocytometer. At this time, they were seeded into 28 μ l of 3.5% (W/V) 8-arm-PEG-DBCO (MW 20,000 KDa) hydrogels at a density of 150,000 cells per gel with 35% of PEG arms crosslinked with PanMMP degradable peptide N₃-KGPQGIWGQKK(N₃), and 10% of the arms are tethered with cyclic GRGDSK(N₃) using copper free click chemistry of the strained alkyne, DBCO, with the azides. After 24 hours peptide libraries were added to the cell media for a final concentration of 37 μ M per

peptide. Each library was tested simultaneously, in triplicate for a total of 9 wells per library per celltype. 40 μ l samples were collected from the media at hours 0, 1, 4, 8, 24, and 48. In-between timepoints samples were frozen -80°C. After 48 hours, samples were kept frozen and thawed just prior to LCMS.

5.2.6 Degradation of Peptides by Human Mesenchymal Stem Cells in PEG hydrogels

hMSCs at passage 3 were seeded into T-75 flasks until they 80-90% confluent. Cells were then washed with PBS and trypsinized in 2 mL of trypsin and incubated for 5 minutes. Once the cells had detached they were centrifuged at 0.2 RCF for 5 minutes and counted using a hemocytometer. At this time, they were seeded into 28 μ l of 3.5% (W/V) 8-arm-peg-DBCO (MW 20,000 KDa) hydrogels at a density of 75,000 cells per gel with 35% of PEG arms crosslinked with a PanMMP peptide N₃-KGPQGIWGQKK(N₃), and 10% of the arms are tethered with cyclic GRGDSK(N₃) using copper free click chemistry of the strained alkyne DBCO with the azides. After 24 hours peptide libraries were added to the cell media for a final concentration of 37 μ M per peptide. Each library was tested simultaneously, in triplicate for a total of 21 wells per study. 40 μ l samples were collected from the media at hours 0, 1, 4, 8, 24, and 48. In-between timepoints samples were frozen -80°C. After 48 hours, samples were kept frozen and thawed just prior to LCMS.

5.2.7 Degradation of Peptides by THP1 Derived Macrophages in PEG hydrogels

THP1 cells were placed into untreated six well plates with RPMI containing 10% FBS and 1% anti-anti, with PMA at a concentration of 100 ng/ml for two days. After day 2 the media was changed to RPMI containing IFN- γ , MCSF, and LPS and allowed to polarize for three

days (Day 5 of culture). On day six, the media was changed to fresh RPMI and detached using a cell scraper. They were then centrifuged at 0.2 RCF for 5 minutes, counted using a hemocytometer and seeded into 40uL gels at a density of 1million cells per gel containing 28 uL of 3.5% (W/V) 8-arm-PEG-DBCO (MW 20,000 KDa) hydrogels at a density of 75,000 cells per gel with 35% of PEG arms crosslinked with a PanMMP sensitive peptide N3KGPQGIWGQKK(N₃), and 10% of the arms are tethered with cyclic GRGDSK(N₃) using copper free click chemistry of the strained alkyne DBCO with the azides. After 24 hours peptide libraries were added to the cell media for a final concentration of 37 μ M per peptide. Each library was tested simultaneously, in triplicate for a total of 21 wells. 40 samples were collected from the media at hours 0, 1, 4, 8, 24, and 48. In-between timepoints samples were frozen -80°C. After 48 hours, samples were kept frozen and thawed just prior to LCMS.

5.2.8 Liquid Chromatography – Mass Spectrometry

All LC-MS samples were collected as described previously in Chapter 3: Chain End Modification Modulates Non-Specific Degradation of Peptides.

5.2.9 Imaging hMSCs in Gels Containing Fast and Slow Degrading Cell-Adhesion Peptides

hMSCs were cultured in PEG hydrogels as described above, except the gels were pipetted onto cover slips and contained different cell-adhesion peptides: 1) no-RGD, 2) cyclic GRGDSK(N₃) ,3) NH₂-GRGDSK(N₃), or 4) Ac β A-GRGDSK(N₃). At day 7, gels were washed two times with 1 \times PBS and stained in 10% NBF for 15 min and washed three times with 1 \times PBS. Cells were then permeabilized with 100% methanol at 4°C for 30 min,

washed two times with 1× PBS and permeabilized with 0.5% Triton-X-100 for 15 min at RT. Gels were washed two times with 1× PBS and blocked using blocking solution (1% BSA, 0.3 M glycine, and 0.01% Triton-X-100) for one hour. Cells were then incubated with anti-pan actin mouse monoclonal antibody (AANO2, Cytoskeleton inc.) (1:500) in blocking solution and agitated overnight at 4°C. Gels were washed with 0.1% Triton X-100 in 1× PBS, and then three times with 1× PBS. Cells were then incubated with Goat anti-mouse IgG2b-AF555 (1091-32, SouthernBiotech) (1:400) in blocking solution for 60 min at RT in the dark. Gels were washed three times with 1X PBS and then incubated in DAPI (Anaspec AS-83210) (1:10,000) in 1× PBS for 20 min at RT. Cells were mounted on coverslips just prior to imaging. Cells were imaged using a confocal microscopy (Nikon Eclipse Ti). Cell area was quantified by first importing a Z-stack into the FIJI distribution of ImageJ2. The Z-stack was then projected into two dimensional space using the maximum projection function. After splitting the color channels, the threshold was adjusted such that the only the DAPI or the phalloidin staining was applied. Last, the “analyze particles” function was applied to gain two pieces of information: 1) the number of particles taken from the DAPI channel, and the total particle area taken from the phalloidin area. Should two nuclei be very close and be counted as one particle, the particle count was adjusted manually for accuracy. The total actin particle area was then normalized to the number of DAPI particles to get an average area per cell. Each group tested was done using three replicates, each done in triplicate for 9 measurements in total.

5.2.10 Viability Assay

Cells were cultured in gels as described above. An alamar blue working solution was made by diluting the alamarBlue dye (Y00-100, Thermo Scientific) (1:10) with the same media cells were cultured in. The media the cells were in was replaced with one ml of working solution. One mL of working solution was also placed into 3 blank wells. The cells were then placed in the incubator 36°C, 5% CO₂ for 3 hours. After 3 hours, 100 µL of the solution was sampled and placed into a 96 well plate, and fluorescence intensity was measured using a Tecan plate reader using 560Ex/590Em nm filter settings, reading from the bottom of the plate. Immediately after measurement, the alamar blue working solution was washed three times with appropriate media for each cell type being measured and placed back in the incubator. The same cells were used for each measurement during Days 0, 3, and 7.

5.2.11 DNA Quantification Assay

Cells were cultured in gels as described above. However, gels were placed on SilGuard coated 24 well plates to prevent cell adhesion to the tissue culture plastic, ensuring the origin of the quantified DNA are exclusively taken from cells located within the gels. To coat plates in Sylgard, the Sylgard 184 elastomer was mixed with its curing agent in a 1:10 ratio. Subsequently, the mixture was poured into each well of a 24-well plate. The elastomer was allowed to cure at room temperature overnight for all experiments. Following the curing process, an alcohol-based reagent was applied through spraying, and the samples were subjected to UV sterilization for 24 hours.

A two-step procedure was used to quantify the double-stranded DNA (dsDNA): 1) sample homogenization, and 2) dsDNA quantification. Sample homogenization was performed via enzymatic digestion of the gel and cellular components using Papain (P4762-50mg, Sigma-Aldrich). Papain was reconstituted to a concentration of 10 mg/mL using PBS, 300 μ L was aliquoted into Eppendorf tubes, and the papain stock solution was stored in -20°C until needed. L-cysteine (25-7210-00, Chemical Dynamics Co.) was prepared at a concentration of 24.2 mg/mL in DI water, placed into 0.5 ml aliquots and stored at -20°C until use. EDTA was prepared into a stock of 0.333M in DI water and stored at 4°C in the fridge until needed (shelf life 3 months). Papain solution was prepared fresh just prior to homogenization by combining and diluting papain, L-cysteine, and EDTA to a final concentration of 125 μ g/ml, 0.242 mg/ml, and 0.333 M respectively with PBS. 300 μ L of papain digestion solution was used per 28 μ L gel. Each gel was then incubated at overnight at 4°C. The next day, homogenization was verified by pipetting samples up and down, noting absence of crosslinked gel material.

Double Stranded DNA was quantified using the Quantifluor dsDNA System (E2670, Promega). 1 \times TE buffer was prepared by diluting the stock TE buffer 20 fold with microbial cell culture grade water (BP2820-100, Fisher BioReagents). The Quantifluor dsDNA dye was then diluted 400 fold with 1 \times TE buffer to create the working dye solution. 200 μ L. A standard curve was prepared in a 96 well plate by placing 2 μ L of DNA standard into 200 μ L of the working dye solution for a total amount of 200 ng of dsDNA standard. Then a 1:4 dilution series was performed down to 0.05 ng of dsDNA standard using the working dye solution as the diluent, and a blank containing just 2 μ L of 1 \times TE buffer in

the working dye solution. This was performed in triplicate. 15 μ L of the homogenized samples were placed into an empty well of the plate, and 185 μ L of the working dye solution was added on top of the unknown samples. Samples were protected from light and incubated for 5-10 minutes, and the fluorescence (504nmEx/531nmEm) was measured using a plate reader (SpectraMax iD3, Molecular Devices). The three standard curves were averaged, and then used to calculate the total dsDNA present within each sample.

5.3 Results and Discussions

5.3.1 Peptides degraded by cells in hydrogels.

We found that RGEFV peptide library degradation with hUVECs was similar between tissue culture plastic (Figure 11 - Figure 22. all center panes) and within hydrogels (Figure 58). Macrophages also had similar peptide degradation kinetics when soluble peptides were added to cells on tissue culture plastic (Figure 11 - Figure 22.all right panes) or cells in gels (Figure 59). Interestingly, hMSCs had significantly less non-specific degradation of peptides when cultured in gels (Figure 67) compared to cells cultured on tissue culture plastic (Figure 11 - Figure 22.all left panes). This observation is also highlighted in (Figure 67). While acetylation of the N-terminus was largely effective at reducing non-specific degradation, peptides with an N-terminal histidine were an exception, and peptides with an acetylated histidine were cleaved for all three cell types when cultured in gels (Figure 11 - Figure 22). Overall the same broad peptide degradations trends held for cells in gels, with N-terminal amines undergoing significant degradation for all three cell types versus other N-terminal functionalization's, and C-terminal carboxylic acids being significantly degraded by hMSCs and hUVECs compared to other terminal chemistries after 48 hours

(Figure 67 & Figure 58). Macrophages cultured on tissue culture plastic had significantly reduced degradation of C-terminal libraries compared to the two other cell types (Figure 11 - Figure 23), but were still only had 59% of peptides remaining after 24 hours across amino acids. However, macrophages encapsulated in hydrogels had greater than 96% remaining of all C-terminal peptide chemistries after 48 hours in culture (Figure 59).

While the effects of the N-terminal and C-terminal amino acids tended to be much smaller than the chemistry of the termini, there were some trends seen across cell types in both the cells on tissue culture plastic and cells encapsulated within PEG hydrogels. In addition, the degradation trends observed when cells were encapsulated inside hydrogels showed the same trends as when cells were cultured on tissue culture plastic shown in Chapter 3. Of note, positively charged amino acids on the N terminus increased degradation rate. Amine terminated peptides on the N-terminus strongly degraded except for negatively charged amino acids, glutamic and aspartic acid. This suggests that at least some of the proteases present are mechanistically electrostatic in nature. While acetylation was typically effective in preventing non-specific degradation of cells in gels, histidine was a significant exception and was substantially degraded by all three cell types on TCP and gels (Figure 67) except for hUVECs on TCP (See Chapter 3).

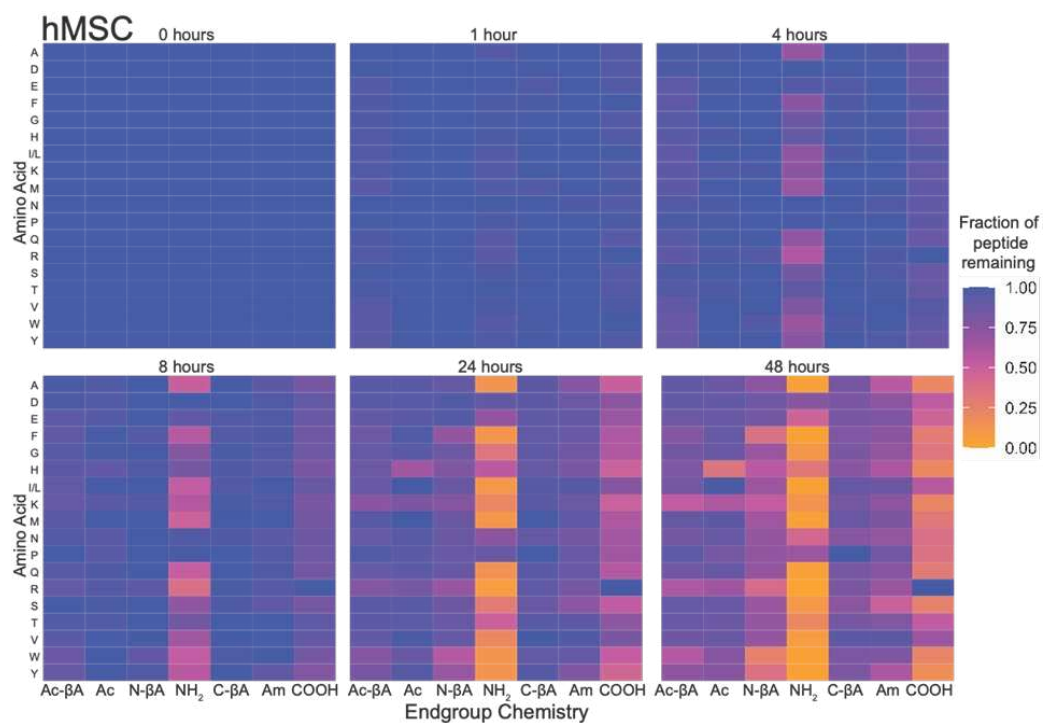


Figure 57 - Degradation of soluble peptide libraries by hMSCs in PEG hydrogels.

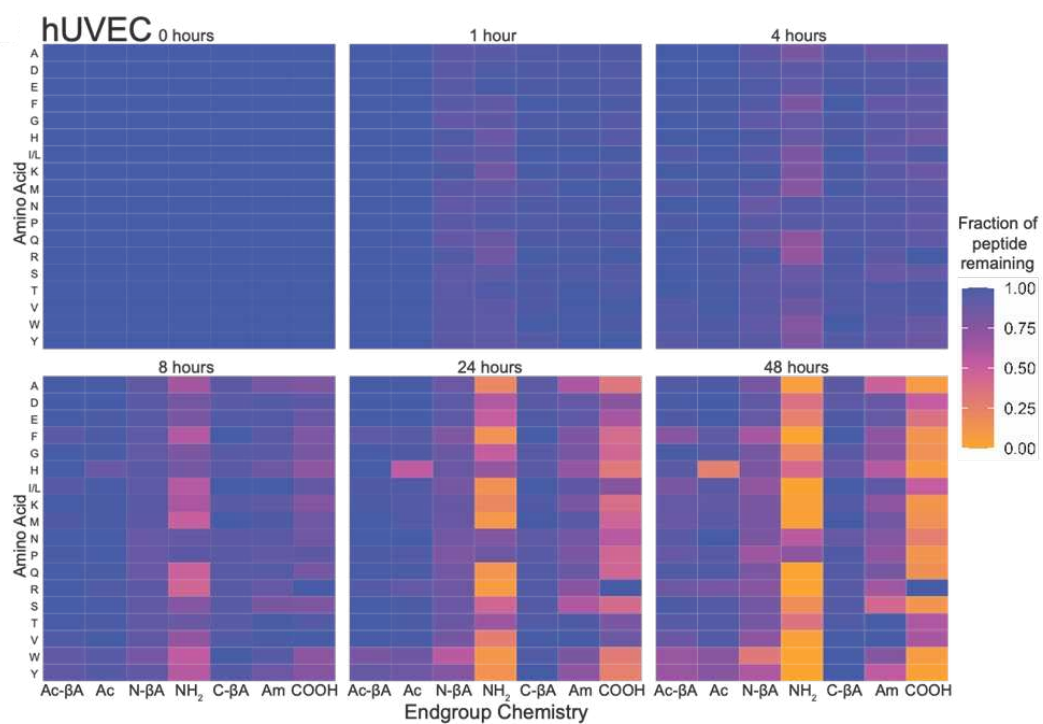


Figure 58 - Degradation of soluble peptide libraries by hUVECs in PEG hydrogels.

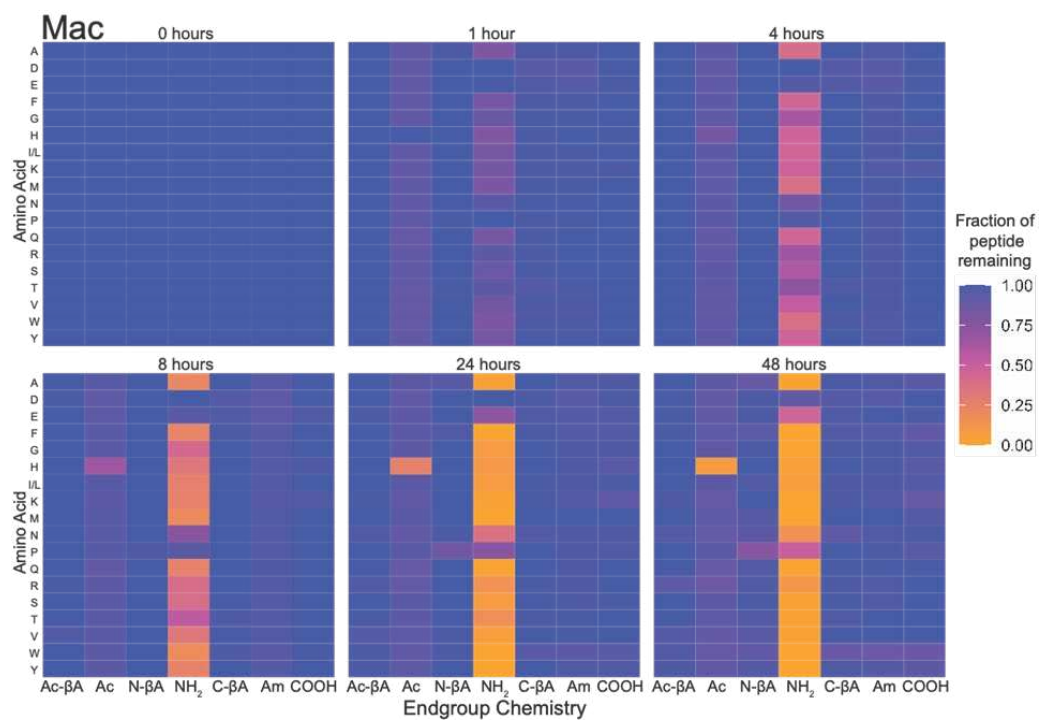


Figure 59 - Degradation of soluble peptide libraries by macrophages in PEG hydrogels.

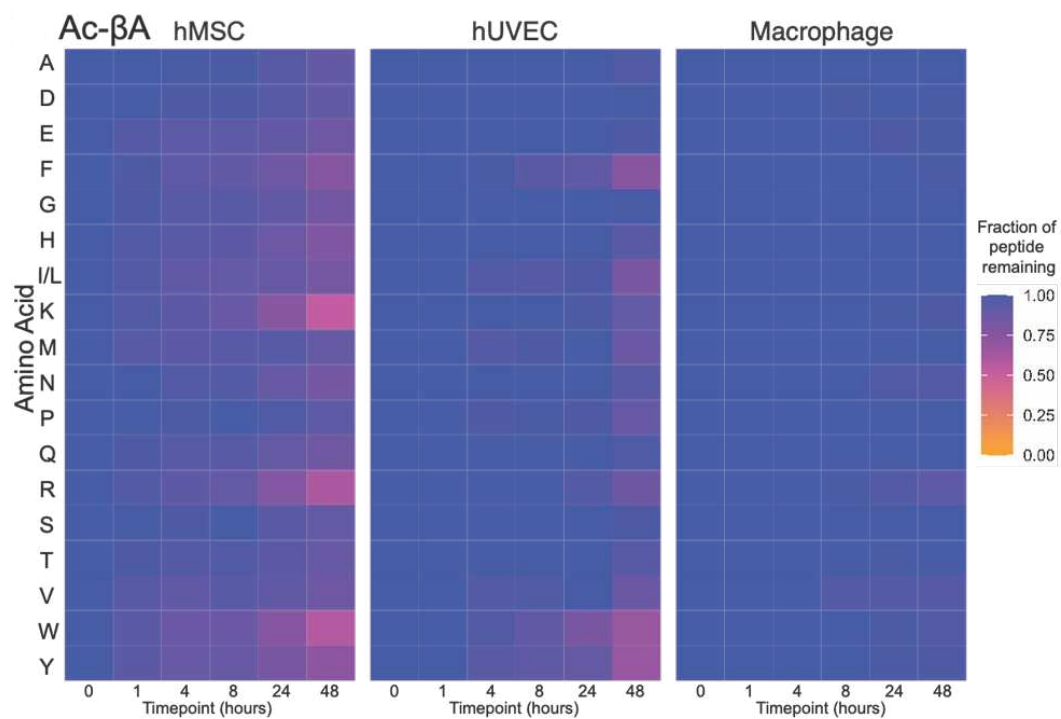


Figure 60 - Degradation of soluble Ac-βA peptide libraries by cells in PEG hydrogels.

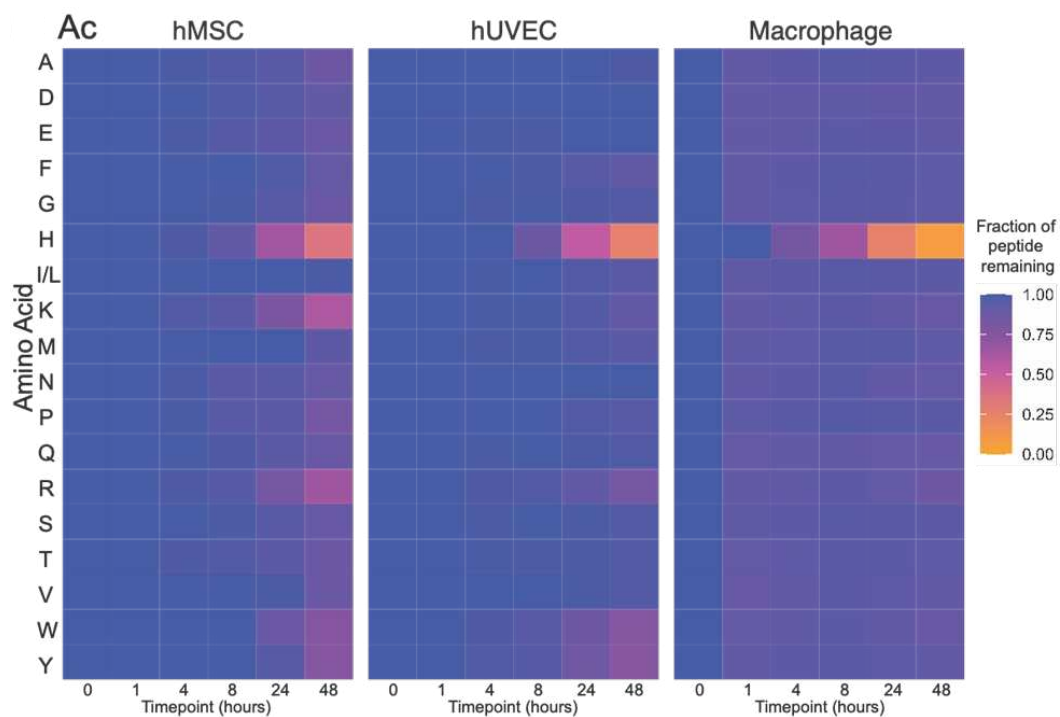


Figure 61 - Degradation of soluble Ac peptide libraries by cells in PEG hydrogels.

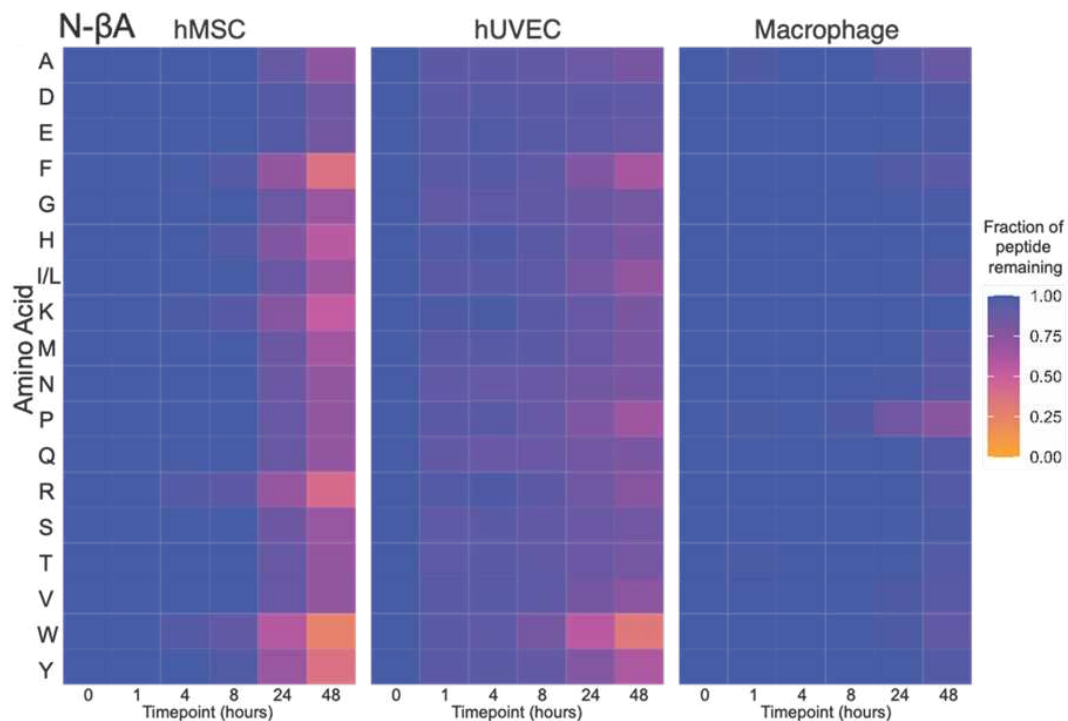


Figure 62 - Degradation of soluble N-βA peptide libraries by cells in PEG hydrogels.

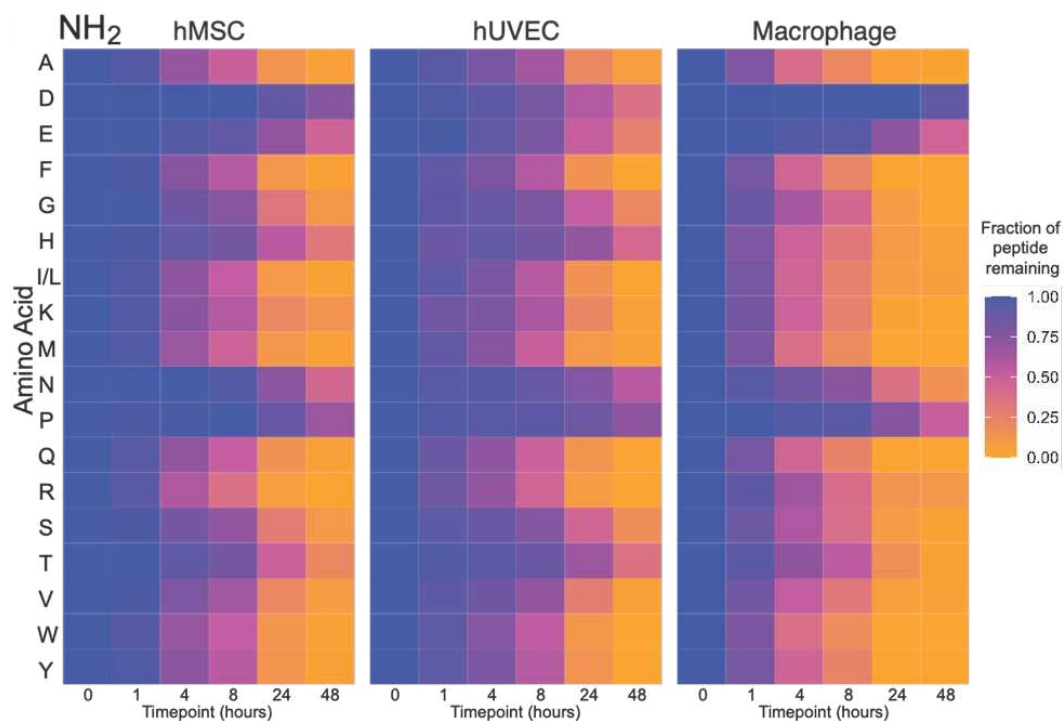


Figure 63 - Degradation of soluble NH₂ peptide libraries by cells in PEG hydrogels.

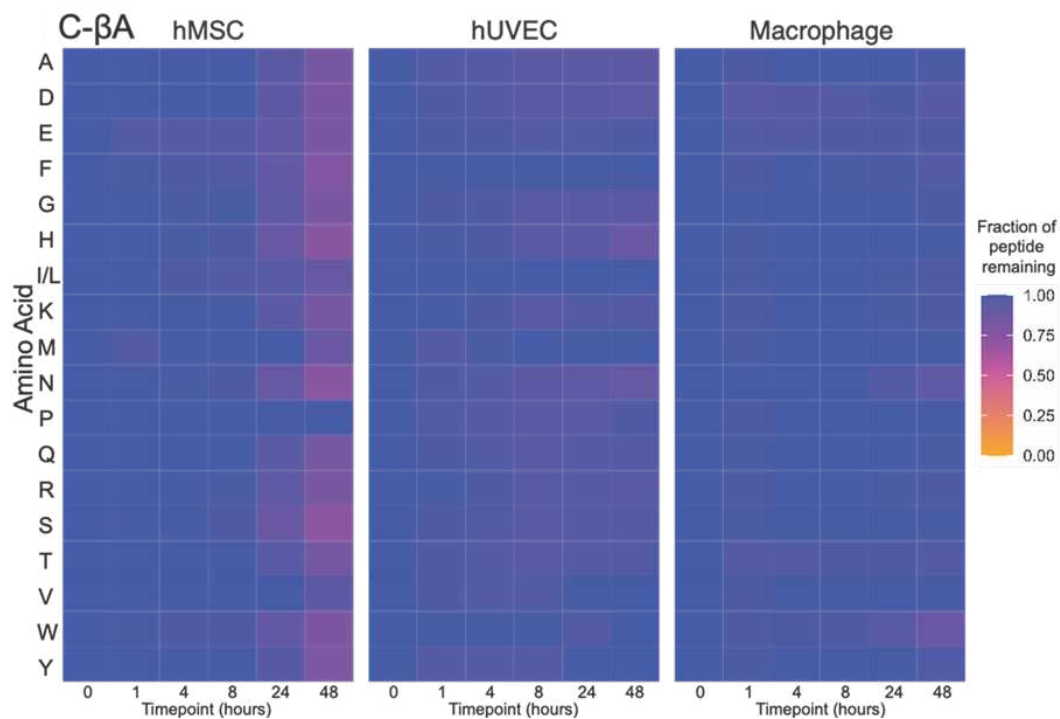


Figure 64 - Degradation of soluble C-βA peptide libraries by cells in PEG hydrogels.

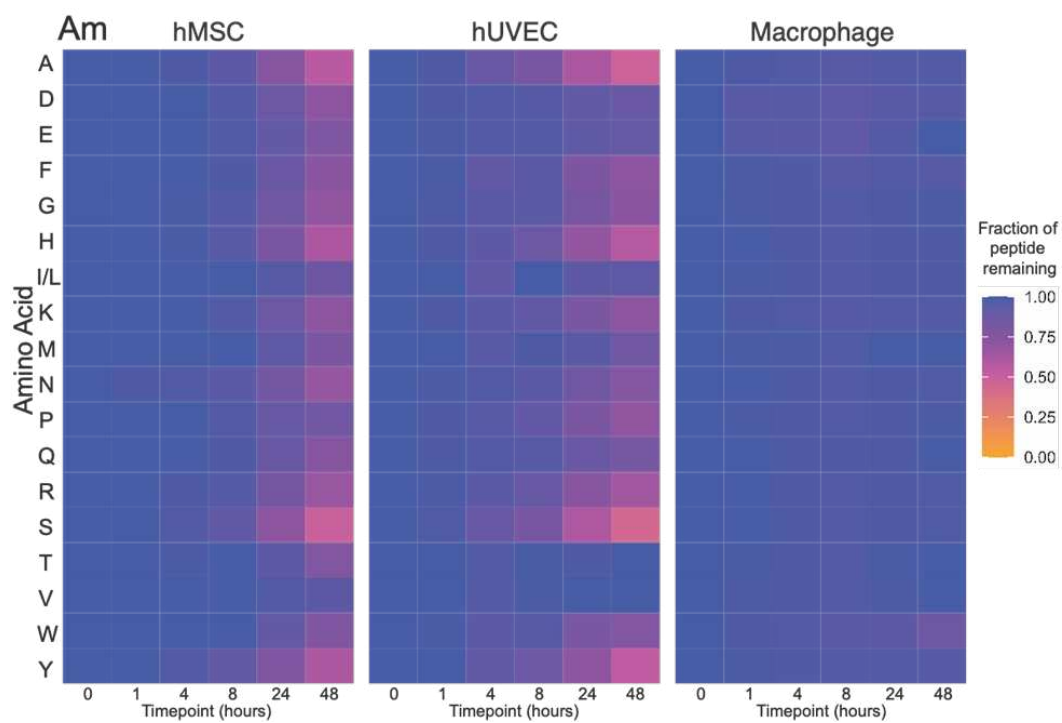


Figure 65 - Degradation of soluble Am peptide libraries by cells in PEG hydrogels.

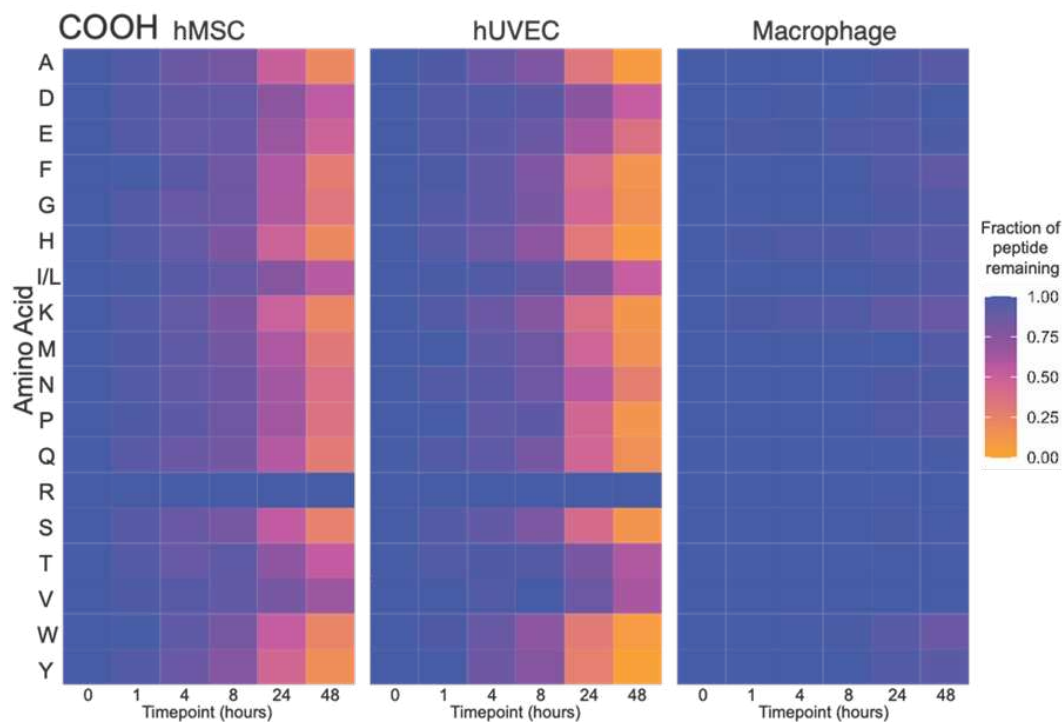


Figure 66 - Degradation of soluble COOH peptide libraries by cells in PEG hydrogels.

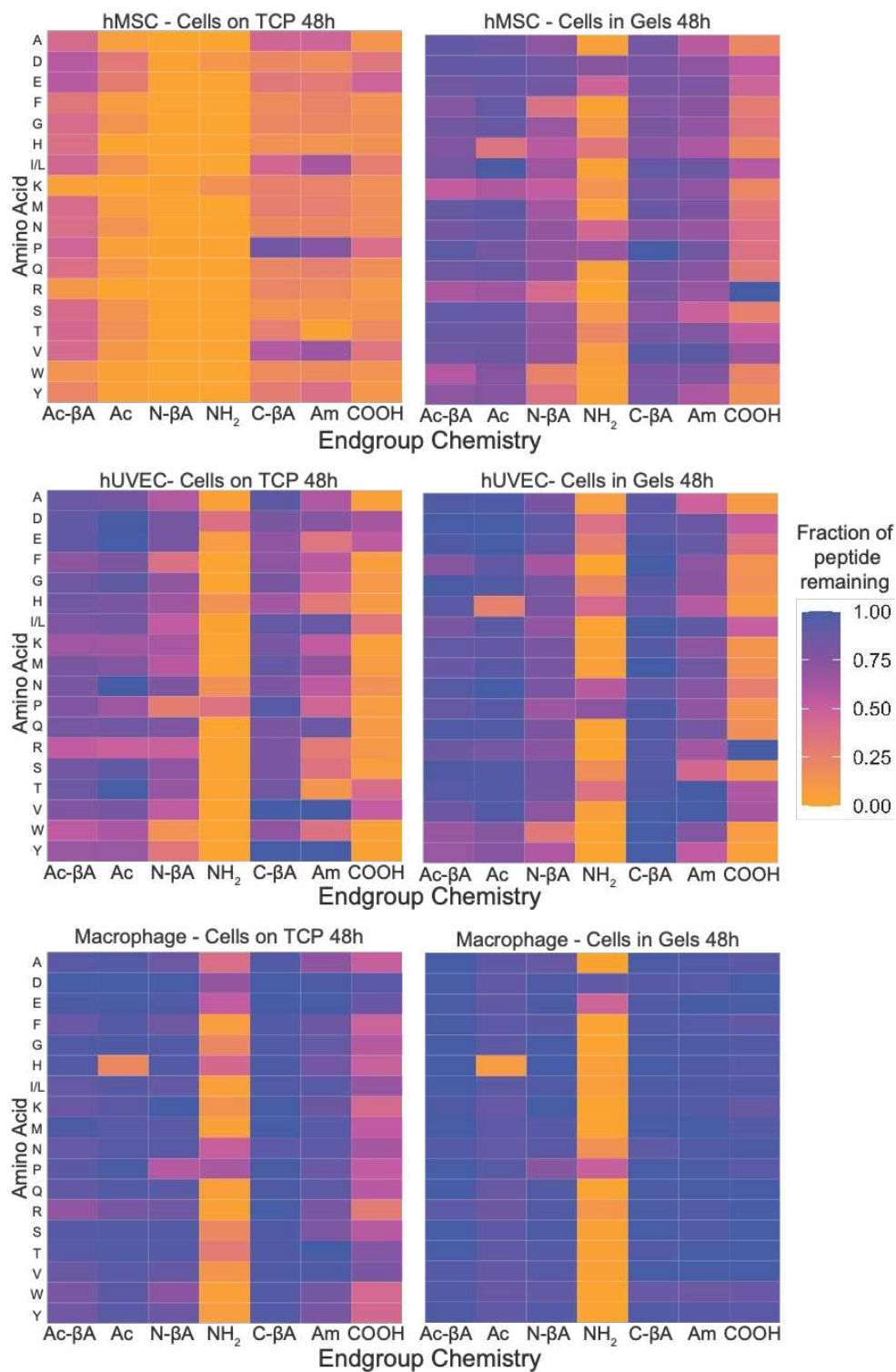


Figure 67 - Comparison of peptide library degradation by cells on tissue culture plastic and cells in gels.

5.3.2 Effects of RGD End Group Chemistry on Cell Behavior in Hydrogels

To better understand how the presence of fast and slow degrading RGD sequences

influenced cell behavior and peptide degradation when covalently coupled to a hydrogel. To do this we made hydrogels with both a “Fast” degrading cell adhesion peptide, NH₂-GRGDS and slow degrading cell adhesion Ac- β A-GRGDS peptides. As a positive control we used a cyclic RGD peptide (cRGD), which does not have a terminus and is not susceptible to non-specific degradation by exopeptidases. We also included a negative control which consisted of gels without any RGD peptides. To better understand the effects of RGD stability on cell morphology, hMSC spreading was quantified at Day 7 in hydrogels with

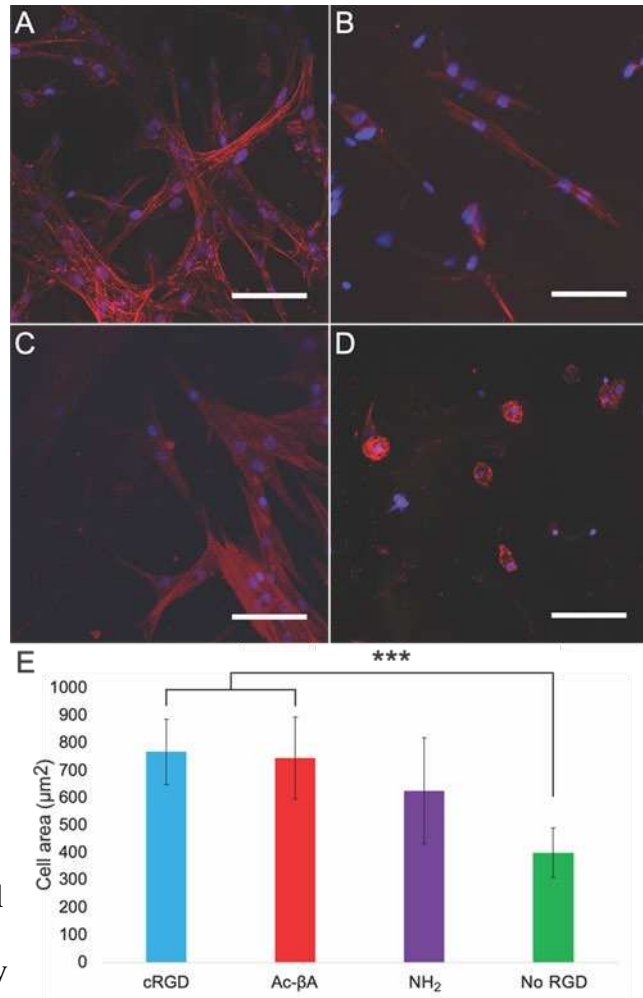


Figure 68 - RGD is required for cell spreading and viability within hydrogels. (A) Ac- β A-GRGDS, (B) NH₂-GRGDS, (C) cyclic RGDS (cRGD), and (D) no added RGDS. (E) hMSC spreading was increased in hydrogels which were functionalized with RGD peptides. Red is actin and blue is the nuclei. Scale bar is 100 μm and * indicates $p < 0.05$, *** indicates $p < 0.001$ by Tukey's post hoc test.

cyclic RGD, slow-degrading Ac- β A-GRGDS, fast degrading NH₂-GRGDS and gels with no RGD peptides (Figure 68 and S9). hMSCs in the cRGD gels had the most spreading

($769 \pm 119 \mu\text{m}^2$), followed by the Ac- β A-GRGDS ($746 \pm 149 \mu\text{m}^2$), NH₂-GRGDS ($626 \pm 193 \mu\text{m}^2$), and gels without RGD ($400 \pm 91 \mu\text{m}^2$). Hydrogels with cRGD and Ac- β A-GRGDS had more spreading than gels with either NH₂-GRGDS or no RGD, although the differences with the NH₂-GRGDS were not statistically significant ($p > 0.05$). Also, viability within gels was primarily dependent upon the presence of RGD, however this varied by cell type (Appendix Figure 169). Gels containing the cyclic RGD peptide had the greatest viability across all cell types, which was also seen in Live/Dead staining (Appendix Figure 170 - 172). This could be due to both the inability of cyclic peptides to undergo exopeptidase degradation, or the beneficial effect that the cyclization of RGD sequences can have on adhesion. Finally, the presence of different RGD ligands did not appear to significantly influence the macroscopic degradation of the hydrogels (Appendix Figure 168).

5.3.3 Statistical Analysis

Statistical analysis was done using multi-way analysis of variance (ANOVA) with a Tukey post-hoc test. All comparisons in this chapter are statistically significant ($p < 0.05$) unless otherwise noted. Statistical data can be found in Appendix Figure 173.E-G.

5.4 Conclusions

To better understand the influence of culture substrate on peptide degradation, cells were cultured on 3D PEG substrates, in contrast to the 2D cell culture on TCP seen in Chapter 3. Most notably, non-specific peptide degradation was seen to attenuate significantly when cells were cultured in 3D PEG hydrogels. In addition, many earlier conclusions are

reinforced: 1) of the chain ends tested, peptides containing N- and C - terminal amines and carboxylic acids respectively degrade most rapidly; 2) peptides containing N- and C – Ac β A and β A respectively degrade most slowly, and 3) of the cell types examined, hMSCs non-specifically degrade peptide more rapidly than hUVECs and THP-1 derived macrophages in that order. N-terminal acetylation is also capable of protecting peptides except when an N-terminal histidine is present. In all cases, except for hUVECs cultured on TCP, peptides containing an N-terminal acetylation and an N-terminal histidine are notably degraded by 48h. Using GRGDS as a model cell adhesion peptide it was shown that cell spreading trended in order, from most-to-least cell-spreading from slowest-fastest degrading peptide. The slow degrading cell-adhesion peptide Ac β A-GRGDS approached the cell spreading of the cyclic cell-adhesion peptide, and the fast-degrading cell-adhesion peptide NH₂-GRGDS approached the cell spreading when to cell-adhesion peptide was present. These results reinforce design principles discovered in Chapter 3 regarding the effects of chain-end chemistry on peptide are applicable when cells are cultured within 3D engineered scaffolds, and these degradation characteristics play a role in cell behavior.

Chapter 6: Overall Conclusions and Future Directions

6.1 Overall Conclusions

This thesis presents a novel and facile LC-MS based method for multiplex quantification of peptide degradation by cells. In chapter 2 we performed an in-depth analysis of a peptide libraries, which demonstrates the power of this method to simultaneously quantify the degradation of numerous peptides. We identified a peptide-based internal standard that was capable of surviving incubation with cells is necessary to account for changes in media concentration via evaporation, variances in pipetting, injection amount into the LC-MS, and other factors within a workflow. The incorporation of this internal standard into degradation studies improves the accuracy and reproducibility of the experiments. The peptide standard, NH₂-βFβA6-Amide, has been demonstrated to be stable enough to enable the quantification of peptides incubated with hMSCs, hUVECs, and macrophages for 48 hours. However, this may not be the case with other cell types or longer periods of time and their combinations of non-canonical amino acids may need to be explored depending on the application.

Liquid chromatography is sensitive to the composition of the injected sample, and we found that the addition of salts and acetic acid had a minimal impact on chromatography, while adding organic solvents can be detrimental to analyte retention. Specifically, accurate quantification requires a single analyte peak that binds the column, and peak splitting in which the analyte comes off at multiple points during a run is considered undesirable. Second, evaluation of the internal standard chosen should be performed with the cell-type

of interest within the desired time-frame, and for a seven day study the standard should be stable throughout the entirety of the study.. If these studies require medium changes, the analyte(s) and internal standard should be introduced to a stock solution of medium, and included in the medium changes. A sample should be taken immediately prior to media changes and then again after the media change to benchmark how much peptide has been degraded throughout each period of cell culture, and how much fresh peptide has been added to the solution.

Non-specific peptide degradation within biomaterials has the potential to reduce the bioactivity of the biomaterial, and therefore it's function. However, quantification of the stability of bioactive peptides such as RGD is not typically done, which highlights an important gap in the literature. This work contributes to the biomaterials field by developing liquid-chromatography-mass spectrometry (LC-MS) methods which are subsequently used to study cell-peptide interactions. These cell-peptide interactions were then quantified to make peptide degradation more visible to the biomaterials community and generate easy to apply design principles for mitigating non-specific peptide degradation. This work also deviates from the norm by studying peptides degraded by all proteases secreted by cell, generating a more functional perspective. This powerful technique enables high-throughput design of experiment to study how peptide substrate relates to stability among varying cells, cultured on both soft and hard substrates, and predict impact of stability on cell behavior.

Chain end chemistry was concluded to be the biggest factor that contributes to peptide stability in a 3D culture. It was found that an acetylated or an acetylated- β -alanine

functionalized to the the N-terminus offered the greatest protection to non-specific degradation, while an amine offered the least amount of protection. Similarly, a β -alanine functionalized C-terminus offered the most amount of protection to non-specific degradation, while a carboxylic acid offered the least amount of protection. Notably, while N-terminal acetylation was shown to broadly inhibit proteolytic degradation, there was one striking exemption to this rule. An acetylated histidine not only degrades, but degrades as fast as some amine-terminated peptides. A key advantage of the acetylated- β -alanine library is that it appears to broadly protect all adjacent amino acids from degradation including the histidine. Lessons learned from these discoveries have already been utilized to discover peptide sequences that are degraded in a cell-type specific manor¹⁵⁶, which in the presence of multiple cell types was designed for cell-type specific invasion applications.

Ultimately, peptide stability was demonstrated to influence cell behavior. By incorporating fast and slow degrading cell-adhesion peptides into hydrogels, cell area was quantified and trend in the direction that faster degrading peptide incorporated into hydrogels induce less cell spreading than slower degrading cell-adhesion peptides. Indicating that when peptides are covalently bonded to materials, their stability is not guaranteed, and degradation of this function-imparting molecule is not a negligible event.

6.2 Future Directions

6.2.1 HPLC Column performance tracking

The non-specific degradation of peptides within biomaterials has the potential to alter the structure of the biomaterial, and therefore its function. However, quantification peptide stability within biomaterials is rarely studied within the community. This work contributes to the biomaterials field by developing liquid chromatography-mass spectrometry (LC-MS) methods which are subsequently used to study cell-peptide interactions. These cell-peptide interactions were then quantified to make peptide degradation more visible to the biomaterials community and generate easily adoptable design principles for mitigating non-specific peptide degradation. This work also deviates from the norm by studying the functional degradation of peptides by total proteolytic activity of cells, including dozens of proteases, inhibitors, and cofactors. This powerful technique enables high-throughput design of experiment to study how peptide substrate relates to stability among varying cells, cultured on both soft and hard substrates, and predict impact of stability on cell behavior.

To the best of this author's knowledge, this is the first presentation of a peptide based internal standard, $\text{NH}_2\text{-}\beta\text{F}(\beta\text{A})_6\text{-Amide}$, for use in cell-culture that is non-isotopically labelled and demonstrated to be stable within a 48-hour period of cell culture with human mesenchymal stem cells (hMSCs), human umbilical vein endothelial cells (hUVECs), peripheral blood mononuclear cell (PBMC) derived macrophages, and Tohoku hospital pediatrics-1 (THP-1) derived macrophages for use with LC-MS based quantification.

Being able to pair the internal standard with the analytes of interest within a cell culture context increases confidence in data by reducing variability between samples.

Chain end chemistry was concluded to be the biggest factor that contributes to the stability of soluble peptides in a 3D culture. It was found that an acetylated or an acetylated- β -alanine functionalized to the N-terminus offered the greatest protection to non-specific degradation, while an amine offered the least amount of protection. Similarly, a β -alanine functionalized C-terminus offered the most amount of protection to non-specific degradation, while a carboxylic acid offered the least amount of protection. The chemistry of the peptide termini was the primary variable that influenced the rate of peptide degradation, however the specific amino acid at the termini could have an important effect. While N-terminal acetylation was shown to broadly inhibit proteolytic degradation, an acetylated histidine not only degrades, but degrades as fast as some amine-terminated peptides. A key advantage of the acetylated- β -alanine library is that it appears to broadly protect all adjacent amino acids from degradation including the histidine. The lessons learned from these discoveries have already been utilized to discover peptide sequences that are degraded in a cell-type specific manner¹⁵⁶, which in the presence of multiple cell types was designed for cell-type specific invasion applications.

Ultimately, peptide stability was demonstrated to influence cell behavior. By incorporating fast and slow degrading cell-adhesion peptides into hydrogels, cell area was quantified and trend in the direction that faster degrading peptide incorporated into hydrogels induce less cell spreading than slower degrading cell-adhesion peptides. Indicating that when peptides

are covalently bonded to materials, their stability is not guaranteed, and degradation of this function-imparting molecule is not a negligible event.

6.2.2 HPLC Column performance tracking

An LC-MS based method of quantifying peptide degradation was described earlier. As was previously shown in Chapter 2, repeated injections of biological samples on the HPLC column eventually lead to column failure. However, identification of this failure remains a challenge, and uncertainties around column performance leads to conservative use and frequent column replacements to ensure data-quality. Development of methods to track column performance in real time would help optimize column lifetime, would indicate what analytes could be accurately quantified, and would increase the overall confidence in the data collected. This could easily be done by creating a β -amino acid standard library with varying hydrophilicities that will track column performance as a function of elution time.

6.2.3 Expand on Non-Specific Degradation Profile of More Cell Types & Chain End Chemistries

This work is limited in that only three cell types were tested: hMSCs, hUVECs, and THP-1 derived pro-inflammatory macrophages. There are an estimated 200-500¹⁵⁷ different cell types in the human body depending on how one classifies a cell-type. To further verify generalizations made within this thesis, it is of interest to quantify functional proteolytic activity within a larger sampling of these cell-types.

Three methods of modifying the activity of proteases on protease substrate peptides was achieved through modification of: 1) chain end chemistry, 2) PEGylation, 3) and concentration. Chain end modification was found to be the most effective method of modifying chain-end chemistry. Effectively 133 different chain end peptides were evaluated (7 chain ends each coupled to 19 different peptides). It would be beneficial to examine a large variety of chain-end chemistries to further fine-tune desired relative degradation characteristics of an engineered application.

6.2.4 Structure-Function Relationship of Acetylated Histidine

An acetylated histidine shows a clear and isolated deviation from the generalizable rule that acetylation offers protection from non-specific degradation and is worth deeper investigation. As 80% of human proteins contain an acetylated N-termini¹³⁰, which is associated with the shielding proteins from degradation¹⁵⁸, a regulatory role of protease-based protein modification/stability of acetylated histidine is theorized and worth investigating.

6.2.5 Functional investigation of Proteolytic Activity on Implanted Devices

Tissue culture substrate was demonstrated to influence protease activity. In Chapter 3 degradation of RGEFV peptide libraries was quantified while cells were cultured on tissue culture plastic. In Chapter 5 degradation of those same libraries was performed while cells were cultured in PEG hydrogels. Interestingly, the softer PEG hydrogel influenced less degradation of the RGEFV libraries.

Dental implants lead to peri-implant inflammation of up to 20% for peri-implantitis and 40% for peri-implant mucositis¹⁵⁹. The modulus of the elastic modulus of the native oral mucosa ranges from 0.1-680 MPa, the periodontal ligaments range from 0.07-1.75 GPa, and various bone tissues ranging from 0.2-17.5 GPa¹⁶⁰. Dental implants are made of materials containing moduli between 53 – 113 GPa¹⁶¹, representing a much stiffer substrate as compared to the native tissue. Proteomic analysis of the gingival crevicular fluid identified 21 proteases related to inflammation such as cathepsin G or neutrophil elastase¹⁵⁹. LC-MS quantification of cells cultured with dental implants have the ability to help validate an *in vitro* model which can be used to deduce mechanisms of endopeptidase mediated proteolytic regulation, and further design better engineered strategies for dental implants and inflammation.

6.2.6 Comparative Functional Proteolytic Activity in Cancer versus Healthy Cells

It is well documented that cancers significantly increase protease activity^{162–164}. The importance of proteases in cancer development and progression is highlighted by interest in using protease inhibitors for cancer therapy¹⁶⁵. Most protease inhibitors which have undergone pre-clinical/clinical trials have failed due to poor pharmacological effects and outcome^{165–167}. A functional perspective of protease activity comparing cancer cells and native tissue would help isolate therapeutic inhibitor mechanisms to modulate to achieve more desired outcomes.

6.2.7 Development of Functional Intracellular Protease Activity.

Also noted is the role of intracellular proteases in carcinogenesis, which may occur within the cytoplasm, or other organelles¹⁶⁵. Adaption of the peptide degradation assay presented

in this thesis to isolate differences in protease activity from different intracellular organelles would also help with the functional design of protease inhibitor-based cancer strategies and therapeutics. This problem may be tackled in two ways by focusing on technological developments on: peptide delivery into cells, or 2) figuring out how to get proteases out of cells while maintaining native activity.

6.2.8 How cell interaction through coculture influences proteolytic activity within biomaterials

Cells are known to signal other cells through paracrine, endocrine, juxtacrine, and autocrine signaling processes¹⁶⁸. These cell-cell communications alter gene expression¹⁶⁸, which have potential for altering functional protease activity. Just because a protease is present does not mean it is active. For example, tissue inhibitors of metalloproteinases (TIMPs) were have been shown to inhibit matrix metalloproteinases (MMPs)¹⁶⁹. Coculture of human keratinocytes and fibroblasts was shown to significantly alter the amount of MMPs and TIMPs via paracrine signaling¹⁷⁰ demonstrating proteolytic activity is changed in the presence of other cells. This provides motivation to develop systems to mimic these different signaling mechanisms. As a biomaterials lab coculturing multiple cell types in gels is of interest to better mimic the physiological or pathological environment to study the functional degradation of peptides by all proteases secreted by all cells of a given process (e.g., wound healing).

6.2.9 In-depth Evaluation of how the Non-Specific Degradation of Adhesion Peptides Influences Cells in Gels

Peptide bioactivity was examined assessed in Chapter 5 using cell-spreading as an metric for the functionality of cell-adhesion peptides. Adding other independent assays would help to confirm the influence that non-specific proteolytic degradation has on cell function. For example, gaining an understanding of how peptides that are designed to degrade at different rates changes the integrin-YAP-TAZ-JNK mechano-transduction pathway will give a deeper understanding of the degree to which non-specific proteolytic degradation effects cells.

References

- (1) Pranantyo, D.; Yeo, C. K.; Wu, Y.; Fan, C.; Xu, X.; Yip, Y. S.; Vos, M. I. G.; Mahadevegowda, S. H.; Lim, P. L. K.; Yang, L.; Hammond, P. T.; Leavesley, D. I.; Tan, N. S.; Chan-Park, M. B. Hydrogel Dressings with Intrinsic Antibiofilm and Antioxidative Dual Functionalities Accelerate Infected Diabetic Wound Healing. *Nat Commun* **2024**, *15* (1), 954. <https://doi.org/10.1038/s41467-024-44968-y>.
- (2) Hoare, T. R.; Kohane, D. S. Hydrogels in Drug Delivery: Progress and Challenges. *Polymer* **2008**, *49* (8), 1993–2007. <https://doi.org/10.1016/j.polymer.2008.01.027>.
- (3) Camacho, P.; Busari, H.; Seims, K. B.; Schwarzenberg, P.; Dailey, H. L.; Chow, L. W. 3D Printing with Peptide–Polymer Conjugates for Single-Step Fabrication of Spatially Functionalized Scaffolds. *Biomater. Sci.* **2019**, *7* (10), 4237–4247. <https://doi.org/10.1039/C9BM00887J>.
- (4) Bercea, M. Bioinspired Hydrogels as Platforms for Life-Science Applications: Challenges and Opportunities. *Polymers* **2022**, *14* (12), 2365. <https://doi.org/10.3390/polym14122365>.
- (5) Kragstrup, T. W.; Kjaer, M.; Mackey, A. L. Structural, Biochemical, Cellular, and Functional Changes in Skeletal Muscle Extracellular Matrix with Aging. *Scandinavian Journal of Medicine & Science in Sports* **2011**, *21* (6), 749–757. <https://doi.org/10.1111/j.1600-0838.2011.01377.x>.
- (6) Frantz, C.; Stewart, K. M.; Weaver, V. M. The Extracellular Matrix at a Glance. *J Cell Sci* **2010**, *123* (24), 4195–4200. <https://doi.org/10.1242/jcs.023820>.
- (7) Järveläinen, H.; Sainio, A.; Koulu, M.; Wight, T. N.; Penttinen, R. Extracellular Matrix Molecules: Potential Targets in Pharmacotherapy. *Pharmacol Rev* **2009**, *61* (2), 198–223. <https://doi.org/10.1124/pr.109.001289>.
- (8) Dai, Z.; Lee, A. J.; Roberts, S.; Sysoeva, T. A.; Huang, S.; Dzuricky, M.; Yang, X.; Zhang, X.; Liu, Z.; Chilkoti, A.; You, L. Versatile Biomanufacturing through Stimulus-Responsive Cell–Material Feedback. *Nat Chem Biol* **2019**, *15* (10), 1017–1024. <https://doi.org/10.1038/s41589-019-0357-8>.
- (9) Rosso, F.; Giordano, A.; Barbarisi, M.; Barbarisi, A. From Cell–ECM Interactions to Tissue Engineering. *Journal of Cellular Physiology* **2004**, *199* (2), 174–180. <https://doi.org/10.1002/jcp.10471>.
- (10) Winkler, J.; Abisoye-Ogunniyan, A.; Metcalf, K. J.; Werb, Z. Concepts of Extracellular Matrix Remodelling in Tumour Progression and Metastasis. *Nat Commun* **2020**, *11* (1), 5120. <https://doi.org/10.1038/s41467-020-18794-x>.

- (11) Lu, P.; Takai, K.; Weaver, V. M.; Werb, Z. Extracellular Matrix Degradation and Remodeling in Development and Disease. *Cold Spring Harb Perspect Biol* **2011**, *3* (12), a005058. <https://doi.org/10.1101/cshperspect.a005058>.
- (12) Järveläinen, H.; Sainio, A.; Koulu, M.; Wight, T. N.; Penttinen, R. Extracellular Matrix Molecules: Potential Targets in Pharmacotherapy. *Pharmacol Rev* **2009**, *61* (2), 198–223. <https://doi.org/10.1124/pr.109.001289>.
- (13) Sedo, A.; Mandys, V.; Krepela, E. Cell Membrane-Bound Proteases: Not “Only” Proteolysis. *Physiol Res* **1996**, *45* (3), 169–176.
- (14) Daviran, M.; Caram, H. S.; Schultz, K. M. Role of Cell-Mediated Enzymatic Degradation and Cytoskeletal Tension on Dynamic Changes in the Rheology of the Pericellular Region Prior to Human Mesenchymal Stem Cell Motility. *ACS Biomater Sci Eng* **2018**, *4* (2), 468–472. <https://doi.org/10.1021/acsbiomaterials.7b01005>.
- (15) McGlynn, J. A.; Druggan, K. J.; Croland, K. J.; Schultz, K. M. Human Mesenchymal Stem Cell-Engineered Length Scale Dependent Rheology of the Pericellular Region Measured with Bi-Disperse Multiple Particle Tracking Microrheology. *Acta Biomater* **2021**, *121*, 405–417. <https://doi.org/10.1016/j.actbio.2020.11.048>.
- (16) Mayer, J. E.; Iatridis, J. C.; Chan, D.; Qureshi, S. A.; Gottesman, O.; Hecht, A. C. Genetic Polymorphisms Associated with Intervertebral Disc Degeneration. *The Spine Journal* **2013**, *13* (3), 299–317. <https://doi.org/10.1016/j.spinee.2013.01.041>.
- (17) Pierschbacher, M. D.; Ruoslahti, E. Cell Attachment Activity of Fibronectin Can Be Duplicated by Small Synthetic Fragments of the Molecule. *Nature* **1984**, *309* (5963), 30–33. <https://doi.org/10.1038/309030a0>.
- (18) Craig, D.; Gao, M.; Schulten, K.; Vogel, V. Tuning the Mechanical Stability of Fibronectin Type III Modules through Sequence Variations. *Structure* **2004**, *12* (1), 21–30. <https://doi.org/10.1016/j.str.2003.11.024>.
- (19) Perera, T. H.; Lu, X.; Howell, S. M.; Kurosu, Y. E.; Smith Callahan, L. A. Combination of IKVAV, LRE, and GPQGIWGQ Bioactive Signaling Peptides Increases Human Induced Pluripotent Stem Cell Derived Neural Stem Cells Extracellular Matrix Remodeling and Neurite Extension. *Advanced Biosystems* **2020**, *4* (8), 2000084. <https://doi.org/10.1002/adbi.202000084>.
- (20) Lee, J. S.; Lee, J. S.; Murphy, W. L. Modular Peptides Promote Human Mesenchymal Stem Cell Differentiation on Biomaterial Surfaces. *Acta Biomater* **2010**, *6* (1), 21–28. <https://doi.org/10.1016/j.actbio.2009.08.003>.
- (21) Ligorio, C.; Mata, A. Synthetic Extracellular Matrices with Function-Encoding Peptides. *Nat Rev Bioeng* **2023**, *1* (7), 518–536. <https://doi.org/10.1038/s44222-023-00055-3>.

- (22) Tajhya, R. B.; Patel, R. S.; Beeton, C. Detection of Matrix Metalloproteinases by Zymography. *Methods Mol Biol* **2017**, *1579*, 231–244. https://doi.org/10.1007/978-1-4939-6863-3_12.
- (23) Ihssen, J.; Faccio, G.; Yao, C.; Sirec, T.; Spitz, U. Fluorogenic in Vitro Activity Assay for the Main Protease Mpro from SARS-CoV-2 and Its Adaptation to the Identification of Inhibitors. *STAR Protoc* **2021**, *2* (3), 100793. <https://doi.org/10.1016/j.xpro.2021.100793>.
- (24) Böttger, R.; Hoffmann, R.; Knappe, D. Differential Stability of Therapeutic Peptides with Different Proteolytic Cleavage Sites in Blood, Plasma and Serum. *PLoS one* **2017**, *12* (6), e0178943.
- (25) Deshmukh, A. A.; Weist, J. L.; Leight, J. L. Detection of Proteolytic Activity by Covalent Tethering of Fluorogenic Substrates in Zymogram Gels. *BioTechniques* **2018**, *64* (5), 203–210. <https://doi.org/10.2144/btn-2018-0005>.
- (26) Rozans, S. J.; Moghaddam, A. S.; Wu, Y.; Atanasoff, K.; Nino, L.; Dunne, K.; Pashuck, E. T. Quantifying and Controlling the Proteolytic Degradation of Cell Adhesion Peptides. *ACS Biomater. Sci. Eng.* **2024**. <https://doi.org/10.1021/acsbiomaterials.4c00736>.
- (27) Liu, A. P.; Appel, E. A.; Ashby, P. D.; Baker, B. M.; Franco, E.; Gu, L.; Haynes, K.; Joshi, N. S.; Kloxin, A. M.; Kouwer, P. H. J.; Mittal, J.; Morsut, L.; Noireaux, V.; Parekh, S.; Schulman, R.; Tang, S. K. Y.; Valentine, M. T.; Vega, S. L.; Weber, W.; Stephanopoulos, N.; Chaudhuri, O. The Living Interface between Synthetic Biology and Biomaterial Design. *Nat Mater* **2022**, *21* (4), 390–397. <https://doi.org/10.1038/s41563-022-01231-3>.
- (28) Hua, K.; Rocha, I.; Zhang, P.; Gustafsson, S.; Ning, Y.; Strømme, M.; Mihranyan, A.; Ferraz, N. Transition from Bioinert to Bioactive Material by Tailoring the Biological Cell Response to Carboxylated Nanocellulose. *Biomacromolecules* **2016**, *17* (3), 1224–1233. <https://doi.org/10.1021/acs.biomac.6b00053>.
- (29) Brovold, M.; Almeida, J. I.; Pla-Palacín, I.; Sainz-Arnal, P.; Sánchez-Romero, N.; Rivas, J. J.; Almeida, H.; Royo Dachary, P.; Serrano-Aulló, T.; Soker, S.; Baptista, P. M. Naturally-Derived Biomaterials for Tissue Engineering Applications. *Adv Exp Med Biol* **2018**, *1077*, 421–449. https://doi.org/10.1007/978-981-13-0947-2_23.
- (30) Passaniti, A.; Kleinman, H. K.; Martin, G. R. Matrigel: History/Background, Uses, and Future Applications. *J Cell Commun Signal* **2022**, *16* (4), 621–626. <https://doi.org/10.1007/s12079-021-00643-1>.
- (31) Funaki, M.; Janmey, P. A. Chapter 23 - Technologies to Engineer Cell Substrate Mechanics in Hydrogels. In *Biology and Engineering of Stem Cell Niches*; Vishwakarma, A., Karp, J. M., Eds.; Academic Press: Boston, 2017; pp 363–373. <https://doi.org/10.1016/B978-0-12-802734-9.00023-8>.

- (32) Sodek, K. L.; Brown, T. J.; Ringuette, M. J. Collagen I but Not Matrigel Matrices Provide an MMP-Dependent Barrier to Ovarian Cancer Cell Penetration. *BMC Cancer* **2008**, 8 (1), 223. <https://doi.org/10.1186/1471-2407-8-223>.
- (33) Chrisnandy, A. Engineering Hydrogel Microenvironments for Epithelial Organoid Culture, EPFL, Lausanne, 2024. <https://doi.org/10.5075/epfl-thesis-10261>.
- (34) Polykandriotis, E.; Arkudas, A.; Horch, R. E.; Kneser, U.; Mitchell, G. To Matrigel or Not to Matrigel. *The American Journal of Pathology* **2008**, 172 (5), 1441–1442. <https://doi.org/10.2353/ajpath.2008.071215>.
- (35) He, Z.-J.; Huang, B.; Cai, L.-H. Bottlebrush Polyethylene Glycol Nanocarriers Translocate across Human Airway Epithelium via Molecular Architecture-Enhanced Endocytosis. *ACS Nano* **2024**, 18 (27), 17586–17599. <https://doi.org/10.1021/acsnano.4c01983>.
- (36) Zhu, J. Bioactive Modification of Poly(Ethylene Glycol) Hydrogels for Tissue Engineering. *Biomaterials* **2010**, 31 (17), 4639–4656. <https://doi.org/10.1016/j.biomaterials.2010.02.044>.
- (37) Peppas, N. A.; Keys, K. B.; Torres-Lugo, M.; Lowman, A. M. Poly(Ethylene Glycol)-Containing Hydrogels in Drug Delivery. *Journal of Controlled Release* **1999**, 62 (1), 81–87. [https://doi.org/10.1016/S0168-3659\(99\)00027-9](https://doi.org/10.1016/S0168-3659(99)00027-9).
- (38) Lin, C.-C.; Anseth, K. S. PEG Hydrogels for the Controlled Release of Biomolecules in Regenerative Medicine. *Pharm Res* **2009**, 26 (3), 631–643. <https://doi.org/10.1007/s11095-008-9801-2>.
- (39) Kong, X.; Tang, Q.; Chen, X.; Tu, Y.; Sun, S.; Sun, Z. Polyethylene Glycol as a Promising Synthetic Material for Repair of Spinal Cord Injury. *Neural Regen Res* **2017**, 12 (6), 1003–1008. <https://doi.org/10.4103/1673-5374.208597>.
- (40) Sun, S.; Cui, Y.; Yuan, B.; Dou, M.; Wang, G.; Xu, H.; Wang, J.; Yin, W.; Wu, D.; Peng, C. Drug Delivery Systems Based on Polyethylene Glycol Hydrogels for Enhanced Bone Regeneration. *Front Bioeng Biotechnol* **2023**, 11, 1117647. <https://doi.org/10.3389/fbioe.2023.1117647>.
- (41) Qin, Y.; Zhu, Y.; Luo, X.; Liang, S.; Wang, J.; Zhang, L. End Group Modification of Polyethylene Glycol (PEG): A Novel Method to Mitigate the Supercooling of PEG as Phase Change Material. *International Journal of Energy Research* **2019**, 43 (2), 1000–1011. <https://doi.org/10.1002/er.4356>.
- (42) Li, K.; Fong, D.; Meichsner, E.; Adronov, A. A Survey of Strain-Promoted Azide–Alkyne Cycloaddition in Polymer Chemistry. *Chemistry – A European Journal* **2021**, 27 (16), 5057–5073. <https://doi.org/10.1002/chem.202003386>.
- (43) Landel, R. F.; Nielsen, L. E. *Mechanical Properties of Polymers and Composites*; CRC Press, 1993.

- (44) Weber, L. M.; Lopez, C. G.; Anseth, K. S. Effects of PEG Hydrogel Crosslinking Density on Protein Diffusion and Encapsulated Islet Survival and Function. *Journal of Biomedical Materials Research Part A* **2009**, *90A* (3), 720–729. <https://doi.org/10.1002/jbm.a.32134>.
- (45) Hagel, V.; Haraszti, T.; Boehm, H. Diffusion and Interaction in PEG-DA Hydrogels. *Biointerphases* **2013**, *8* (1), 36. <https://doi.org/10.1186/1559-4106-8-36>.
- (46) Ehrbar, M.; Sala, A.; Lienemann, P.; Ranga, A.; Mosiewicz, K.; Bittermann, A.; Rizzi, S. C.; Weber, F. E.; Lutolf, M. P. Elucidating the Role of Matrix Stiffness in 3D Cell Migration and Remodeling. *Biophys J* **2011**, *100* (2), 284–293. <https://doi.org/10.1016/j.bpj.2010.11.082>.
- (47) Wang, Y.; Rencus-Lazar, S.; Zhou, H.; Yin, Y.; Jiang, X.; Cai, K.; Gazit, E.; Ji, W. Bioinspired Amino Acid Based Materials in Bionanotechnology: From Minimalistic Building Blocks and Assembly Mechanism to Applications. *ACS Nano* **2024**, *18* (2), 1257–1288. <https://doi.org/10.1021/acsnano.3c08183>.
- (48) Qin, S.-Y.; Feng, J.-Q.; Cheng, Y.-J.; Liu, W.-L.; Zhang, A.-Q.; Wang, L.; Wang, H.; Zhang, X.-Z. A Comprehensive Review on Peptide-Bearing Biomaterials: From Ex Situ to in Situ Self-Assembly. *Coordination Chemistry Reviews* **2024**, *502*, 215600. <https://doi.org/10.1016/j.ccr.2023.215600>.
- (49) Krishna, O. D.; Kiick, K. L. Protein- and Peptide-Modified Synthetic Polymeric Biomaterials. *Peptide Science* **2010**, *94* (1), 32–48. <https://doi.org/10.1002/bip.21333>.
- (50) Merrifield, R. B. Solid Phase Peptide Synthesis. I. The Synthesis of a Tetrapeptide. *J. Am. Chem. Soc.* **1963**, *85* (14), 2149–2154. <https://doi.org/10.1021/ja00897a025>.
- (51) Carpino, L. A.; Han, G. Y. 9-Fluorenylmethoxycarbonyl Function, a New Base-Sensitive Amino-Protecting Group. *J. Am. Chem. Soc.* **1970**, *92* (19), 5748–5749. <https://doi.org/10.1021/ja00722a043>.
- (52) Rink, H. Solid-Phase Synthesis of Protected Peptide Fragments Using a Trialkoxy-Diphenyl-Methylester Resin. *Tetrahedron Letters* **1987**, *28* (33), 3787–3790. [https://doi.org/10.1016/S0040-4039\(00\)96384-6](https://doi.org/10.1016/S0040-4039(00)96384-6).
- (53) 任连兵; 王勇; 陈继伟; 黎秋萍; 刘宏红. Preparation Method of Rink Amide Resin. CN104292394A, January 21, 2015. <https://patents.google.com/patent/CN104292394A/en> (accessed 2024-07-10).
- (54) Chatzi, K. Barlos. O.; Gatos, D.; Stavropoulos, G. 2-Chlorotrityl Chloride Resin. *International Journal of Peptide and Protein Research* **1991**, *37* (6), 513–520. <https://doi.org/10.1111/j.1399-3011.1991.tb00769.x>.

- (55) Wang, S.-Sun. P-Alkoxybenzyl Alcohol Resin and p-Alkoxybenzyloxycarbonylhydrazide Resin for Solid Phase Synthesis of Protected Peptide Fragments. *J. Am. Chem. Soc.* **1973**, 95 (4), 1328–1333. <https://doi.org/10.1021/ja00785a602>.
- (56) Sieber, P. A New Acid-Labile Anchor Group for the Solid-Phase Synthesis of C-Terminal Peptide Amides by the Fmoc Method. *Tetrahedron Letters* **1987**, 28 (19), 2107–2110. [https://doi.org/10.1016/S0040-4039\(00\)96055-6](https://doi.org/10.1016/S0040-4039(00)96055-6).
- (57) Merrifield, R. B.; Stewart, J. M. Automated Peptide Synthesis. *Nature* **1965**, 207 (4996), 522–523. <https://doi.org/10.1038/207522a0>.
- (58) *The Nobel Prize in Chemistry 1984*. NobelPrize.org. <https://www.nobelprize.org/prizes/chemistry/1984/summary/> (accessed 2024-07-10).
- (59) Bicho, D.; Ajami, S.; Liu, C.; Reis, R. L.; Oliveira, J. M. Peptide-Biofunctionalization of Biomaterials for Osteochondral Tissue Regeneration in Early Stage Osteoarthritis: Challenges and Opportunities. *J. Mater. Chem. B* **2019**, 7 (7), 1027–1044. <https://doi.org/10.1039/C8TB03173H>.
- (60) Hamley, I. W. Small Bioactive Peptides for Biomaterials Design and Therapeutics. *Chem. Rev.* **2017**, 117 (24), 14015–14041. <https://doi.org/10.1021/acs.chemrev.7b00522>.
- (61) Morwood, A. J.; El-Karim, I. A.; Clarke, S. A.; Lundy, F. T. The Role of Extracellular Matrix (ECM) Adhesion Motifs in Functionalised Hydrogels. *Molecules* **2023**, 28 (12), 4616. <https://doi.org/10.3390/molecules28124616>.
- (62) Li, Y.; Hoffman, M. D.; Benoit, D. S. W. Matrix Metalloproteinase (MMP)-Degradable Tissue Engineered Periosteum Coordinates Allograft Healing via Early Stage Recruitment and Support of Host Neurovasculature. *Biomaterials* **2021**, 268, 120535. <https://doi.org/10.1016/j.biomaterials.2020.120535>.
- (63) Tashiro, K.; Sephel, G. C.; Weeks, B.; Sasaki, M.; Martin, G. R.; Kleinman, H. K.; Yamada, Y. A Synthetic Peptide Containing the IKVAV Sequence from the A Chain of Laminin Mediates Cell Attachment, Migration, and Neurite Outgrowth. *J Biol Chem* **1989**, 264 (27), 16174–16182.
- (64) Spicer, C. D.; Pashuck, E. T.; Stevens, M. M. Achieving Controlled Biomolecule–Biomaterial Conjugation. *Chem. Rev.* **2018**, 118 (16), 7702–7743. <https://doi.org/10.1021/acs.chemrev.8b00253>.
- (65) Agard, N. J.; Prescher, J. A.; Bertozzi, C. R. A Strain-Promoted [3 + 2] Azide-Alkyne Cycloaddition for Covalent Modification of Biomolecules in Living Systems. *J Am Chem Soc* **2004**, 126 (46), 15046–15047. <https://doi.org/10.1021/ja044996f>.
- (66) Xing, H.; Lee, H.; Luo, L.; Kyriakides, T. R. Extracellular Matrix-Derived Biomaterials in Engineering Cell Function. *Biotechnol Adv* **2020**, 42, 107421. <https://doi.org/10.1016/j.biotechadv.2019.107421>.

- (67) Vaheri, A.; Ruoslahti, E. Disappearance of a Major Cell-Type Specific Surface Glycoprotein Antigen (SF) after Transformation of Fibroblasts by Rous Sarcoma Virus. *International Journal of Cancer* **1974**, *13* (5), 579–586. <https://doi.org/10.1002/ijc.2910130502>.
- (68) Hynes, R. O.; Bye, J. M. Density and Cell Cycle Dependence of Cell Surface Proteins in Hamster Fibroblasts. *Cell* **1974**, *3* (2), 113–120. [https://doi.org/10.1016/0092-8674\(74\)90114-7](https://doi.org/10.1016/0092-8674(74)90114-7).
- (69) Hynes, R. O.; Destree, A. T. 10 Nm Filaments in Normal and Transformed Cells. *Cell* **1978**, *13* (1), 151–163. [https://doi.org/10.1016/0092-8674\(78\)90146-0](https://doi.org/10.1016/0092-8674(78)90146-0).
- (70) Ludwig, B. S.; Kessler, H.; Kossatz, S.; Reuning, U. RGD-Binding Integrins Revisited: How Recently Discovered Functions and Novel Synthetic Ligands (Re-)Shape an Ever-Evolving Field. *Cancers (Basel)* **2021**, *13* (7), 1711. <https://doi.org/10.3390/cancers13071711>.
- (71) Notni, J. RGD Forever!—Past, Present, and Future of a 3-Letter-Code in Radiopharmacy and Life Sciences. *Pharmaceuticals (Basel)* **2022**, *16* (1), 56. <https://doi.org/10.3390/ph16010056>.
- (72) Bellis, S. L. Advantages of RGD Peptides for Directing Cell Association with Biomaterials. *Biomaterials* **2011**, *32* (18), 4205–4210.
- (73) Hersel, U.; Dahmen, C.; Kessler, H. RGD Modified Polymers: Biomaterials for Stimulated Cell Adhesion and Beyond. *Biomaterials* **2003**, *24* (24), 4385–4415. [https://doi.org/10.1016/S0142-9612\(03\)00343-0](https://doi.org/10.1016/S0142-9612(03)00343-0).
- (74) Okamoto, K.; Matsuura, T.; Hosokawa, R.; Akagawa, Y. RGD Peptides Regulate the Specific Adhesion Scheme of Osteoblasts to Hydroxyapatite but Not to Titanium. *J Dent Res* **1998**, *77* (3), 481–487. <https://doi.org/10.1177/00220345980770030701>.
- (75) Porto de Souza Vandenberghe, L.; Karp, S. G.; Binder Pagnoncelli, M. G.; von Linsingen Tavares, M.; Libardi Junior, N.; Valladares Diestra, K.; Viesser, J. A.; Soccol, C. R. Chapter 2 - Classification of Enzymes and Catalytic Properties. In *Biomass, Biofuels, Biochemicals*; Singh, S. P., Pandey, A., Singhania, R. R., Larroche, C., Li, Z., Eds.; Elsevier, 2020; pp 11–30. <https://doi.org/10.1016/B978-0-12-819820-9.00002-8>.
- (76) Pashuck, E. T. Designing Enzyme-Responsive Biomaterials. In *Peptide-based Biomaterials*; Guler, M. O., Ed.; The Royal Society of Chemistry, 2020; pp 76–125. <https://doi.org/10.1039/9781839161148-00076>.
- (77) McDonald, J. K. An Overview of Protease Specificity and Catalytic Mechanisms: Aspects Related to Nomenclature and Classification. *Histochem J* **1985**, *17* (7), 773–785. <https://doi.org/10.1007/BF01003313>.
- (78) Sanz, Y. Aminopeptidases. Industrial enzymes: Structure, function and applications **2007**, 243–260.

- (79) Klein, T.; Bischoff, R. Physiology and Pathophysiology of Matrix Metalloproteases. *Amino Acids* **2011**, *41* (2), 271–290. <https://doi.org/10.1007/s00726-010-0689-x>.
- (80) Tu, Z.; Zhong, Y.; Hu, H.; Shao, D.; Haag, R.; Schirner, M.; Lee, J.; Sullenger, B.; Leong, K. W. Design of Therapeutic Biomaterials to Control Inflammation. *Nat Rev Mater* **2022**, *7* (7), 557–574. <https://doi.org/10.1038/s41578-022-00426-z>.
- (81) Zhang, C.; Jiang, G.; Gao, X. Matrix Metalloproteinase-Responsive Drug Delivery Systems. *Bioconjugate Chem.* **2023**, *34* (8), 1349–1365. <https://doi.org/10.1021/acs.bioconjchem.3c00266>.
- (82) ter Mors, B.; Spieler, V.; Merino Asumendi, E.; Gantert, B.; Lühmann, T.; Meinel, L. Bioresponsive Cytokine Delivery Responding to Matrix Metalloproteinases. *ACS Biomater. Sci. Eng.* **2024**, *10* (1), 29–37. <https://doi.org/10.1021/acsbiomaterials.2c01320>.
- (83) Patterson, J.; Hubbell, J. A. Enhanced Proteolytic Degradation of Molecularly Engineered PEG Hydrogels in Response to MMP-1 and MMP-2. *Biomaterials* **2010**, *31* (30), 7836–7845. <https://doi.org/10.1016/j.biomaterials.2010.06.061>.
- (84) Lutolf, M. P.; Weber, F. E.; Schmoekel, H. G.; Schense, J. C.; Kohler, T.; Müller, R.; Hubbell, J. A. Repair of Bone Defects Using Synthetic Mimetics of Collagenous Extracellular Matrices. *Nat Biotechnol* **2003**, *21* (5), 513–518. <https://doi.org/10.1038/nbt818>.
- (85) Metzger, S.; Blache, U.; Lienemann, P. S.; Karlsson, M.; Weber, F. E.; Weber, W.; Ehrbar, M. Cell-Mediated Proteolytic Release of Growth Factors from Poly(Ethylene Glycol) Matrices. *Macromolecular Bioscience* **2016**, *16* (11), 1703–1713. <https://doi.org/10.1002/mabi.201600223>.
- (86) Kwon, M. Y.; Vega, S. L.; Gramlich, W. M.; Kim, M.; Mauck, R. L.; Burdick, J. A. Dose and Timing of N-Cadherin Mimetic Peptides Regulate MSC Chondrogenesis within Hydrogels. *Adv Healthc Mater* **2018**, *7* (9), e1701199. <https://doi.org/10.1002/adhm.201701199>.
- (87) Lutolf, M. P.; Lauer-Fields, J. L.; Schmoekel, H. G.; Metters, A. T.; Weber, F. E.; Fields, G. B.; Hubbell, J. A. Synthetic Matrix Metalloproteinase-Sensitive Hydrogels for the Conduction of Tissue Regeneration: Engineering Cell-Invasion Characteristics. *Proc Natl Acad Sci U S A* **2003**, *100* (9), 5413–5418. <https://doi.org/10.1073/pnas.0737381100>.
- (88) Jansen, L. E.; Kim, H.; Hall, C. L.; McCarthy, T. P.; Lee, M. J.; Peyton, S. R. A Poly(Ethylene Glycol) Three-Dimensional Bone Marrow Hydrogel. *Biomaterials* **2022**, *280*, 121270. <https://doi.org/10.1016/j.biomaterials.2021.121270>.

- (89) Schultz, K. M.; Kyburz, K. A.; Anseth, K. S. Measuring Dynamic Cell–Material Interactions and Remodeling during 3D Human Mesenchymal Stem Cell Migration in Hydrogels. *Proceedings of the National Academy of Sciences* **2015**, *112* (29), E3757–E3764. <https://doi.org/10.1073/pnas.1511304112>.
- (90) VAN DER VELDEN; HULSMANN, A. R. Peptidases: Structure, Function and Modulation of Peptide-mediated Effects in the Human Lung. *Clin Exp Allergy* **1999**, *29* (4), 445–456. <https://doi.org/10.1046/j.1365-2222.1999.00462.x>.
- (91) Mathur, D.; Prakash, S.; Anand, P.; Kaur, H.; Agrawal, P.; Mehta, A.; Kumar, R.; Singh, S.; Raghava, G. P. S. PEPLife: A Repository of the Half-Life of Peptides. *Sci Rep* **2016**, *6* (1), 36617. <https://doi.org/10.1038/srep36617>.
- (92) Tasdemiroglu, Y.; Gourdie, R. G.; He, J.-Q. In Vivo Degradation Forms, Anti-Degradation Strategies, and Clinical Applications of Therapeutic Peptides in Non-Infectious Chronic Diseases. *European Journal of Pharmacology* **2022**, *932*, 175192. <https://doi.org/10.1016/j.ejphar.2022.175192>.
- (93) Werle, M.; Bernkop-Schnürch, A. Strategies to Improve Plasma Half Life Time of Peptide and Protein Drugs. *Amino Acids* **2006**, *30* (4), 351–367. <https://doi.org/10.1007/s00726-005-0289-3>.
- (94) Caliri, S. R.; Burdick, J. A. A Practical Guide to Hydrogels for Cell Culture. *Nat Methods* **2016**, *13* (5), 405–414. <https://doi.org/10.1038/nmeth.3839>.
- (95) Binaymotlagh, R.; Chronopoulou, L.; Palocci, C. Peptide-Based Hydrogels: Template Materials for Tissue Engineering. *J Funct Biomater* **2023**, *14* (4), 233. <https://doi.org/10.3390/jfb14040233>.
- (96) Liu, S. Q.; Tay, R.; Khan, M.; Ee, P. L. R.; Hedrick, J. L.; Yang, Y. Y. Synthetic Hydrogels for Controlled Stem Cell Differentiation. *Soft Matter* **2009**, *6* (1), 67–81. <https://doi.org/10.1039/B916705F>.
- (97) Zouani, O. F.; Chollet, C.; Guillotin, B.; Durrieu, M.-C. Differentiation of Pre-Osteoblast Cells on Poly(Ethylene Terephthalate) Grafted with RGD and/or BMPs Mimetic Peptides. *Biomaterials* **2010**, *31* (32), 8245–8253. <https://doi.org/10.1016/j.biomaterials.2010.07.042>.
- (98) Pagano, M. Application of Electrophoresis and Related Methods, Such as Western Blotting and Zymography to the Study of Some Proteins and Enzymes. *Analytica Chimica Acta* **1999**, *383* (1), 119–125. [https://doi.org/10.1016/S0003-2670\(98\)00493-0](https://doi.org/10.1016/S0003-2670(98)00493-0).
- (99) Frankowski, H.; Gu, Y.-H.; Heo, J. H.; Milner, R.; del Zoppo, G. J. Use of Gel Zymography to Examine Matrix Metalloproteinase (Gelatinase) Expression in Brain Tissue or in Primary Glial Cultures. *Methods Mol Biol* **2012**, *814*, 221–233. https://doi.org/10.1007/978-1-61779-452-0_15.

- (100) Rani, V.; Aggarwal, K.; Varshney, S.; Atale, N. Zymographic Techniques. In *Handbook of Oxidative Stress in Cancer: Mechanistic Aspects*; Chakraborti, S., Ray, B. K., Roychoudhury, S., Eds.; Springer Nature: Singapore, 2022; pp 327–340. https://doi.org/10.1007/978-981-15-9411-3_26.
- (101) Rauh, M. LC–MS/MS for Protein and Peptide Quantification in Clinical Chemistry. *Journal of Chromatography B* **2012**, 883–884, 59–67. <https://doi.org/10.1016/j.jchromb.2011.09.030>.
- (102) Hewavitharana, A. K. Internal Standard—Friend or Foe? *Critical Reviews in Analytical Chemistry* **2009**, 39 (4), 272–275. <https://doi.org/10.1080/10408340903001201>.
- (103) McNally, M. E.; Usher, K.; Hansen, S. W.; Amoo, J. S.; Bernstein, A. P. Precision of Internal Standard and External Standard Methods in High Performance Liquid Chromatography. **2015**, 33, 40–46.
- (104) Wieling, J. LC-MS-MS Experiences with Internal Standards. *Chromatographia* **2002**, 55 (1), S107–S113. <https://doi.org/10.1007/BF02493365>.
- (105) Klont, F.; Bras, L.; Wolters, J. C.; Ongay, S.; Bischoff, R.; Halmos, G. B.; Horvatovich, P. Assessment of Sample Preparation Bias in Mass Spectrometry-Based Proteomics. *Anal. Chem.* **2018**, 90 (8), 5405–5413. <https://doi.org/10.1021/acs.analchem.8b00600>.
- (106) Sanders, B. C.; Pokhrel, S.; Labbe, A. D.; Mathews, I. I.; Cooper, C. J.; Davidson, R. B.; Phillips, G.; Weiss, K. L.; Zhang, Q.; O'Neill, H.; Kaur, M.; Schmidt, J. G.; Reichard, W.; Surendranathan, S.; Parvathareddy, J.; Phillips, L.; Rainville, C.; Sterner, D. E.; Kumaran, D.; Andi, B.; Babnigg, G.; Moriarty, N. W.; Adams, P. D.; Joachimiak, A.; Hurst, B. L.; Kumar, S.; Butt, T. R.; Jonsson, C. B.; Ferrins, L.; Wakatsuki, S.; Galanie, S.; Head, M. S.; Parks, J. M. Potent and Selective Covalent Inhibition of the Papain-like Protease from SARS-CoV-2. *Nat Commun* **2023**, 14 (1), 1733. <https://doi.org/10.1038/s41467-023-37254-w>.
- (107) Furka, A.; Sebestyen, F.; Asgedom, M.; Dibo, G. General Method for Rapid Synthesis of Multicomponent Peptide Mixtures. *Int J Pept Protein Res* **1991**, 37 (6), 487–493. <https://doi.org/10.1111/j.1399-3011.1991.tb00765.x>.
- (108) Stokvis, E.; Rosing, H.; Beijnen, J. H. Stable Isotopically Labeled Internal Standards in Quantitative Bioanalysis Using Liquid Chromatography/Mass Spectrometry: Necessity or Not? *Rapid Communications in Mass Spectrometry* **2005**, 19 (3), 401–407. <https://doi.org/10.1002/rcm.1790>.
- (109) Jones, W. B.; Donati, G. L.; Calloway, C. P. Jr.; Jones, B. T. Standard Dilution Analysis. *Anal. Chem.* **2015**, 87 (4), 2321–2327. <https://doi.org/10.1021/ac504152x>.

- (110) Fu, Y.; Barkley, D.; Li, W.; Picard, F.; Flarakos, J. Evaluation, Identification and Impact Assessment of Abnormal Internal Standard Response Variability in Regulated LC–MS Bioanalysis. *Bioanalysis* **2020**, *12* (8), 545–559. <https://doi.org/10.4155/bio-2020-0058>.
- (111) Frackenpohl, J.; Arvidsson, P. I.; Schreiber, J. V.; Seebach, D. The Outstanding Biological Stability of β - and γ -Peptides toward Proteolytic Enzymes: An In Vitro Investigation with Fifteen Peptidases. *ChemBioChem* **2001**, *2* (6), 445–455. [https://doi.org/10.1002/1439-7633\(20010601\)2:6<445::AID-CBIC445>3.0.CO;2-R](https://doi.org/10.1002/1439-7633(20010601)2:6<445::AID-CBIC445>3.0.CO;2-R).
- (112) Seebach, D.; Overhand, M.; Kühnle, F. N. M.; Martinoni, B.; Oberer, L.; Hommel, U.; Widmer, H. β -Peptides: Synthesis by Arndt-Eistert Homologation with Concomitant Peptide Coupling. Structure Determination by NMR and CD Spectroscopy and by X-Ray Crystallography. Helical Secondary Structure of a β -Hexapeptide in Solution and Its Stability towards Pepsin. *Helvetica Chimica Acta* **1996**, *79* (4), 913–941. <https://doi.org/10.1002/hlca.19960790402>.
- (113) Gopi, H. N.; Ravindra, G.; Pal, P. P.; Pattanaik, P.; Balaram, H.; Balaram, P. Proteolytic Stability of β -Peptide Bonds Probed Using Quenched Fluorescent Substrates Incorporating a Hemoglobin Cleavage Site. *FEBS Letters* **2003**, *535* (1), 175–178. [https://doi.org/10.1016/S0014-5793\(02\)03885-1](https://doi.org/10.1016/S0014-5793(02)03885-1).
- (114) Araujo, P. Key Aspects of Analytical Method Validation and Linearity Evaluation. *Journal of Chromatography B* **2009**, *877* (23), 2224–2234. <https://doi.org/10.1016/j.jchromb.2008.09.030>.
- (115) Tan, A.; Boudreau, N.; Lévesque, A. Internal Standards for Quantitative LC-MS Bioanalysis. In *LC-MS in Drug Bioanalysis*; Xu, Q. A., Madden, T. L., Eds.; Springer US: Boston, MA, 2012; pp 1–32. https://doi.org/10.1007/978-1-4614-3828-1_1.
- (116) Schlüter, H. Chapter 3 - Reversed-Phase Chromatography. In *Journal of Chromatography Library*; Kastner, M., Ed.; Protein Liquid Chromatography; Elsevier, 2000; Vol. 61, pp 147–234. [https://doi.org/10.1016/S0301-4770\(08\)60531-X](https://doi.org/10.1016/S0301-4770(08)60531-X).
- (117) Alpert, A. J. Effect of Salts on Retention in Hydrophilic Interaction Chromatography. *Journal of Chromatography A* **2018**, *1538*, 45–53. <https://doi.org/10.1016/j.chroma.2018.01.038>.
- (118) Zheng, X.; Baker, H.; Hancock, W. S.; Fawaz, F.; McCaman, M.; Pungor Jr., E. Proteomic Analysis for the Assessment of Different Lots of Fetal Bovine Serum as a Raw Material for Cell Culture. Part IV. Application of Proteomics to the Manufacture of Biological Drugs. *Biotechnology Progress* **2006**, *22* (5), 1294–1300. <https://doi.org/10.1021/bp060121o>.

- (119) Kappelhoff, R.; Puente, X. S.; Wilson, C. H.; Seth, A.; López-Otín, C.; Overall, C. M. Overview of Transcriptomic Analysis of All Human Proteases, Non-Proteolytic Homologs and Inhibitors: Organ, Tissue and Ovarian Cancer Cell Line Expression Profiling of the Human Protease Degradome by the CLIP-CHIP™ DNA Microarray. *Biochimica et Biophysica Acta (BBA)-Molecular Cell Research* **2017**, *1864* (11), 2210–2219.
- (120) Pashuck, E. T.; Duchet, B. J.; Hansel, C. S.; Maynard, S. A.; Chow, L. W.; Stevens, M. M. Controlled Sub-Nanometer Epitope Spacing in a Three-Dimensional Self-Assembled Peptide Hydrogel. *ACS Nano* **2016**, *10* (12), 11096–11104. <https://doi.org/10.1021/acsnano.6b05975>.
- (121) Huettner, N.; Dargaville, T. R.; Forget, A. Discovering Cell-Adhesion Peptides in Tissue Engineering: Beyond RGD. *Trends Biotechnol* **2018**, *36* (4), 372–383. <https://doi.org/10.1016/j.tibtech.2018.01.008>.
- (122) Cai, L.; Dinh, C. B.; Heilshorn, S. C. One-Pot Synthesis of Elastin-like Polypeptide Hydrogels with Grafted VEGF-Mimetic Peptides. *Biomaterials science* **2014**, *2* (5), 757–765.
- (123) Álvarez, Z.; Kolberg-Edelbrock, A. N.; Sasselli, I. R.; Ortega, J. A.; Qiu, R.; Syrgiannis, Z.; Mirau, P. A.; Chen, F.; Chin, S. M.; Weigand, S.; Kiskinis, E.; Stupp, S. I. Bioactive Scaffolds with Enhanced Supramolecular Motion Promote Recovery from Spinal Cord Injury. *Science* **2021**, *374* (6569), 848–856. <https://doi.org/10.1126/science.abh3602>.
- (124) Hsu, C.-W.; Olabisi, R. M.; Olmsted-Davis, E. A.; Davis, A. R.; West, J. L. Cathepsin K-sensitive Poly (Ethylene Glycol) Hydrogels for Degradation in Response to Bone Resorption. *Journal of Biomedical Materials Research Part A* **2011**, *98* (1), 53–62.
- (125) Chandrawati, R. Enzyme-Responsive Polymer Hydrogels for Therapeutic Delivery. *Experimental Biology and Medicine* **2016**, *241* (9), 972–979.
- (126) Zhu, Y.; Shmidov, Y.; Harris, E. A.; Theus, M. H.; Bitton, R.; Matson, J. B. Activating Hidden Signals by Mimicking Cryptic Sites in a Synthetic Extracellular Matrix. *Nature communications* **2023**, *14* (1), 3635.
- (127) Gentilucci, L.; De Marco, R.; Cerisoli, L. Chemical Modifications Designed to Improve Peptide Stability: Incorporation of Non-Natural Amino Acids, Pseudo-Peptide Bonds, and Cyclization. *Current pharmaceutical design* **2010**, *16* (28), 3185–3203.
- (128) Cooper, B. M.; Iegre, J.; O'Donovan, D. H.; Halvarsson, M. Ö.; Spring, D. R. Peptides as a Platform for Targeted Therapeutics for Cancer: Peptide–Drug Conjugates (PDCs). *Chemical society reviews* **2021**, *50* (3), 1480–1494.

- (129) Marciano, Y.; Nayeem, N.; Dave, D.; Ulijn, R. V.; Contel, M. N-Acetylation of Biodegradable Supramolecular Peptide Nanofilaments Selectively Enhances Their Proteolytic Stability for Targeted Delivery of Gold-Based Anticancer Agents. *ACS Biomaterials Science & Engineering* **2023**.
- (130) Arnesen, T.; Van Damme, P.; Polevoda, B.; Helsens, K.; Evjenth, R.; Colaert, N.; Varhaug, J. E.; Vandekerckhove, J.; Lillehaug, J. R.; Sherman, F. Proteomics Analyses Reveal the Evolutionary Conservation and Divergence of N-Terminal Acetyltransferases from Yeast and Humans. *Proceedings of the National Academy of Sciences* **2009**, *106* (20), 8157–8162.
- (131) Powell, M. F.; Stewart, T.; Jr Otvos, L.; Urge, L.; Gaeta, F. C.; Sette, A.; Arrhenius, T.; Thomson, D.; Soda, K.; Colon, S. M. Peptide Stability in Drug Development. II. Effect of Single Amino Acid Substitution and Glycosylation on Peptide Reactivity in Human Serum. *Pharmaceutical research* **1993**, *10*, 1268–1273.
- (132) Mucha, A.; Drag, M.; Dalton, J. P.; Kafarski, P. Metallo-Aminopeptidase Inhibitors. *Biochimie* **2010**, *92* (11), 1509–1529.
- (133) Sapio, M. R.; Fricker, L. D. Carboxypeptidases in Disease: Insights from Peptidomic Studies. *PROTEOMICS–Clinical Applications* **2014**, *8* (5–6), 327–337.
- (134) Di, L. Strategic Approaches to Optimizing Peptide ADME Properties. *The AAPS journal* **2015**, *17*, 134–143.
- (135) Xiao, Q.; Zhang, F.; Nacev, B. A.; Liu, J. O.; Pei, D. Protein N-Terminal Processing: Substrate Specificity of Escherichia Coli and Human Methionine Aminopeptidases. *Biochemistry* **2010**, *49* (26), 5588–5599.
- (136) Rezania, A.; Healy, K. E. The Effect of Peptide Surface Density on Mineralization of a Matrix Deposited by Osteogenic Cells. *Journal of biomedical materials research* **2000**, *52* (4), 595–600.
- (137) Pfaff, M.; Tangemann, K.; Müller, B.; Gurrath, M.; Müller, G.; Kessler, H.; Timpl, R.; Engel, J. Selective Recognition of Cyclic RGD Peptides of NMR Defined Conformation by Alpha IIb Beta 3, Alpha V Beta 3, and Alpha 5 Beta 1 Integrins. *Journal of Biological Chemistry* **1994**, *269* (32), 20233–20238.
- (138) Chen, L.; Lin, Y.-L.; Peng, G.; Li, F. Structural Basis for Multifunctional Roles of Mammalian Aminopeptidase N. *Proceedings of the National Academy of Sciences* **2012**, *109* (44), 17966–17971.
- (139) Blainey, P.; Krzywinski, M.; Altman, N. Replication. *Nature Methods* **2014**, *11* (9), 879–880. <https://doi.org/10.1038/nmeth.3091>.
- (140) Silva, G. A.; Czeisler, C.; Niece, K. L.; Beniash, E.; Harrington, D. A.; Kessler, J. A.; Stupp, S. I. Selective Differentiation of Neural Progenitor Cells by High-Epitope Density Nanofibers. *Science* **2004**, *303* (5662), 1352–1355. <https://doi.org/10.1126/science.1093783>.

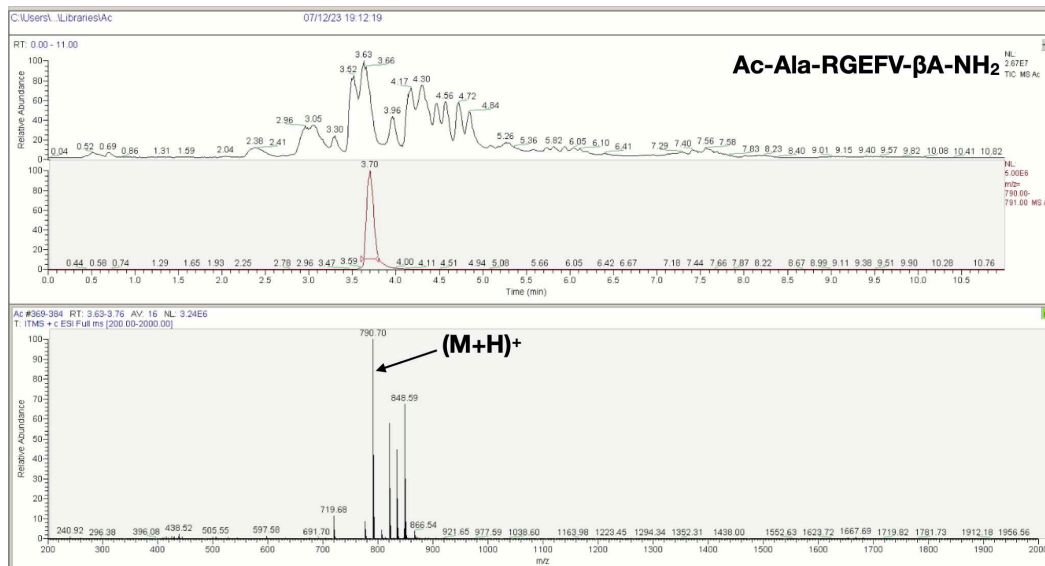
- (141) Seims, K. B.; Hunt, N. K.; Chow, L. W. Strategies to Control or Mimic Growth Factor Activity for Bone, Cartilage, and Osteochondral Tissue Engineering. *Bioconjugate Chemistry* **2021**, 32 (5), 861–878.
- (142) Fosgerau, K.; Hoffmann, T. Peptide Therapeutics: Current Status and Future Directions. *Drug Discovery Today* **2015**, 20 (1), 122–128. <https://doi.org/10.1016/j.drudis.2014.10.003>.
- (143) Ghale, G.; Kuhnert, N.; Nau, W. M. Monitoring Stepwise Proteolytic Degradation of Peptides by Supramolecular Domino Tandem Assays and Mass Spectrometry for Trypsin and Leucine Aminopeptidase. *Nat Prod Commun* **2012**, 7 (3), 343–348.
- (144) Veronese, F. M.; Pasut, G. PEGylation, Successful Approach to Drug Delivery. *Drug Discovery Today* **2005**, 10 (21), 1451–1458. [https://doi.org/10.1016/S1359-6446\(05\)03575-0](https://doi.org/10.1016/S1359-6446(05)03575-0).
- (145) Hamley, I. W. PEG–Peptide Conjugates. *Biomacromolecules* **2014**, 15 (5), 1543–1559. <https://doi.org/10.1021/bm500246w>.
- (146) Sachin, K.; Jadhav, V. H.; Kim, E.-M.; Kim, H. L.; Lee, S. B.; Jeong, H.-J.; Lim, S. T.; Sohn, M.-H.; Kim, D. W. F-18 Labeling Protocol of Peptides Based on Chemically Orthogonal Strain-Promoted Cycloaddition under Physiologically Friendly Reaction Conditions. *Bioconjugate Chem.* **2012**, 23 (8), 1680–1686. <https://doi.org/10.1021/bc3002425>.
- (147) Amer, L. D.; Bryant, S. J. The in Vitro and in Vivo Response to MMP-Sensitive Poly (Ethylene Glycol) Hydrogels. *Annals of biomedical engineering* **2016**, 44 (6), 1959–1969.
- (148) Darling, N. J.; Hung, Y.-S.; Sharma, S.; Segura, T. Controlling the Kinetics of Thiol-Maleimide Michael-Type Addition Gelation Kinetics for the Generation of Homogenous Poly (Ethylene Glycol) Hydrogels. *Biomaterials* **2016**, 101, 199–206.
- (149) DeForest, C. A.; Polizzotti, B. D.; Anseth, K. S. Sequential Click Reactions for Synthesizing and Patterning Three-Dimensional Cell Microenvironments. *Nat Mater* **2009**, 8 (8), 659–664. <https://doi.org/10.1038/nmat2473>.
- (150) Duval, K.; Grover, H.; Han, L.-H.; Mou, Y.; Pegoraro, A. F.; Fredberg, J.; Chen, Z. Modeling Physiological Events in 2D vs. 3D Cell Culture. *Physiology (Bethesda)* **2017**, 32 (4), 266–277. <https://doi.org/10.1152/physiol.00036.2016>.
- (151) Kapałczyńska, M.; Kolenda, T.; Przybyła, W.; Zajączkowska, M.; Teresiak, A.; Filas, V.; Ibbs, M.; Bliźniak, R.; Łuczewski, Ł.; Lamperska, K. 2D and 3D Cell Cultures – a Comparison of Different Types of Cancer Cell Cultures. *Arch Med Sci* **2018**, 14 (4), 910–919. <https://doi.org/10.5114/aoms.2016.63743>.
- (152) Pawluchin, A.; Galic, M. Moving through a Changing World: Single Cell Migration in 2D vs. 3D. *Front. Cell Dev. Biol.* **2022**, 10. <https://doi.org/10.3389/fcell.2022.1080995>.

- (153) Lin, C.-C. Recent Advances in Crosslinking Chemistry of Biomimetic Poly(Ethylene Glycol) Hydrogels. *RSC Adv.* **2015**, *5* (50), 39844–39853. <https://doi.org/10.1039/C5RA05734E>.
- (154) Doyle, A. D.; Carvajal, N.; Jin, A.; Matsumoto, K.; Yamada, K. M. Local 3D Matrix Microenvironment Regulates Cell Migration through Spatiotemporal Dynamics of Contractility-Dependent Adhesions. *Nat Commun* **2015**, *6* (1), 8720. <https://doi.org/10.1038/ncomms9720>.
- (155) Bioorthogonal chemistry for selective recognition, separation and killing bacteria over mammalian cells - Chemical Communications (RSC Publishing). <https://pubs.rsc.org/en/content/articlelanding/2016/cc/c5cc10625g> (accessed 2024-07-04).
- (156) Wu, Y.; Rozans, S. J.; Moghaddam, A. S.; Pashuck, E. T. Optimizing Peptide Crosslinks for Cell-Responsive Hydrogels. *bioRxiv* May 18, 2024, p 2024.05.16.594348. <https://doi.org/10.1101/2024.05.16.594348>.
- (157) Roy, A. L.; Conroy, R. S. Toward Mapping the Human Body at a Cellular Resolution. *Mol Biol Cell* **2018**, *29* (15), 1779–1785. <https://doi.org/10.1091/mbc.E18-04-0260>.
- (158) Varland, S.; Silva, R. D.; Kjosås, I.; Faustino, A.; Bogaert, A.; Billmann, M.; Boukhatmi, H.; Kellen, B.; Costanzo, M.; Drazic, A.; Osberg, C.; Chan, K.; Zhang, X.; Tong, A. H. Y.; Andreazza, S.; Lee, J. J.; Nedyalkova, L.; Ušaj, M.; Whitworth, A. J.; Andrews, B. J.; Moffat, J.; Myers, C. L.; Gevaert, K.; Boone, C.; Martinho, R. G.; Arnesen, T. N-Terminal Acetylation Shields Proteins from Degradation and Promotes Age-Dependent Motility and Longevity. *Nat Commun* **2023**, *14* (1), 6774. <https://doi.org/10.1038/s41467-023-42342-y>.
- (159) Halstenbach, T.; Nelson, K.; Iglhaut, G.; Schilling, O.; Fretwurst, T. Impact of Peri-Implantitis on the Proteome Biology of Crevicular Fluid: A Pilot Study. *Journal of Periodontology* **2023**, *94* (7), 835–847. <https://doi.org/10.1002/JPER.22-0461>.
- (160) Gasik, M.; Lambert, F.; Bacevic, M. Biomechanical Properties of Bone and Mucosa for Design and Application of Dental Implants. *Materials (Basel)* **2021**, *14* (11), 2845. <https://doi.org/10.3390/ma14112845>.
- (161) Brizuela, A.; Herrero-Climent, M.; Rios-Carrasco, E.; Rios-Santos, J. V.; Pérez, R. A.; Manero, J. M.; Gil Mur, J. Influence of the Elastic Modulus on the Osseointegration of Dental Implants. *Materials (Basel)* **2019**, *12* (6), 980. <https://doi.org/10.3390/ma12060980>.
- (162) Koblinski, J. E.; Ahram, M.; Sloane, B. F. Unraveling the Role of Proteases in Cancer. *Clinica Chimica Acta* **2000**, *291* (2), 113–135. [https://doi.org/10.1016/S0009-8981\(99\)00224-7](https://doi.org/10.1016/S0009-8981(99)00224-7).

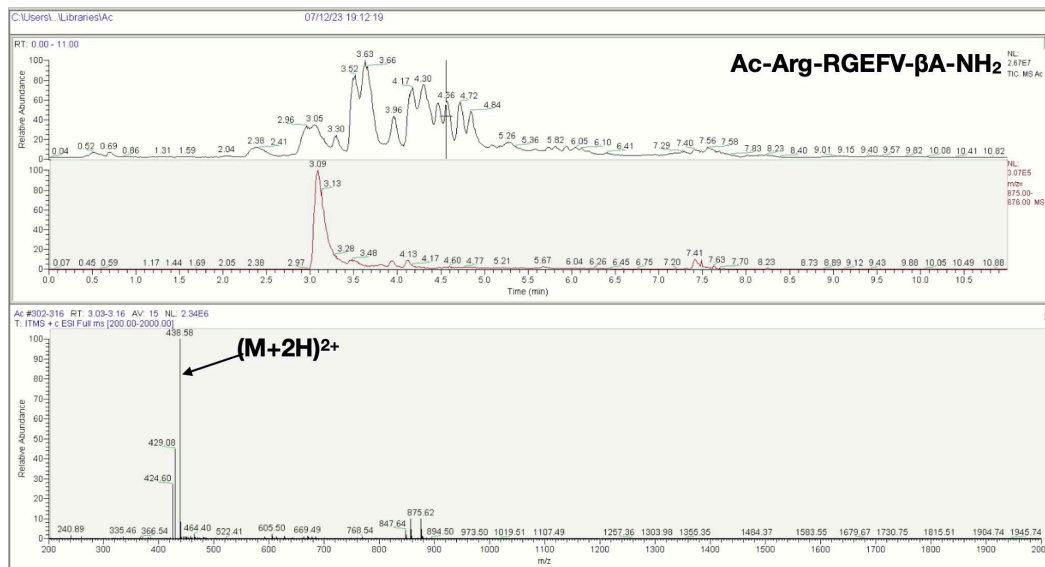
- (163) Radisky, E. S. Extracellular Proteolysis in Cancer: Proteases, Substrates, and Mechanisms in Tumor Progression and Metastasis. *Journal of Biological Chemistry* **2024**, *300* (6). <https://doi.org/10.1016/j.jbc.2024.107347>.
- (164) Vizovisek, M.; Ristanovic, D.; Menghini, S.; Christiansen, M. G.; Schuerle, S. The Tumor Proteolytic Landscape: A Challenging Frontier in Cancer Diagnosis and Therapy. *Int J Mol Sci* **2021**, *22* (5), 2514. <https://doi.org/10.3390/ijms22052514>.
- (165) Rudzińska, M.; Daglioglu, C.; Savvateeva, L. V.; Kaci, F. N.; Antoine, R.; Zamyatnin Jr, A. A. Current Status and Perspectives of Protease Inhibitors and Their Combination with Nanosized Drug Delivery Systems for Targeted Cancer Therapy. *Drug Des Devel Ther* **2021**, *15*, 9–20. <https://doi.org/10.2147/DDDT.S285852>.
- (166) Turk, B. Targeting Proteases: Successes, Failures and Future Prospects. *Nat Rev Drug Discov* **2006**, *5* (9), 785–799. <https://doi.org/10.1038/nrd2092>.
- (167) Winer, A.; Adams, S.; Mignatti, P. Matrix Metalloproteinase Inhibitors in Cancer Therapy: Turning Past Failures into Future Successes. *Mol Cancer Ther* **2018**, *17* (6), 1147–1155. <https://doi.org/10.1158/1535-7163.MCT-17-0646>.
- (168) Armingol, E.; Officer, A.; Harismendy, O.; Lewis, N. E. Deciphering Cell–Cell Interactions and Communication from Gene Expression. *Nat Rev Genet* **2021**, *22* (2), 71–88. <https://doi.org/10.1038/s41576-020-00292-x>.
- (169) Brew, K.; Nagase, H. The Tissue Inhibitors of Metalloproteinases (TIMPs): An Ancient Family with Structural and Functional Diversity. *Biochim Biophys Acta* **2010**, *1803* (1), 55–71. <https://doi.org/10.1016/j.bbamcr.2010.01.003>.
- (170) Tandara, A. A.; Mustoe, T. A. MMP- and TIMP-Secretion by Human Cutaneous Keratinocytes and Fibroblasts – Impact of Coculture and Hydration. *Journal of Plastic, Reconstructive & Aesthetic Surgery* **2011**, *64* (1), 108–116. <https://doi.org/10.1016/j.bjps.2010.03.051>.

Appendix

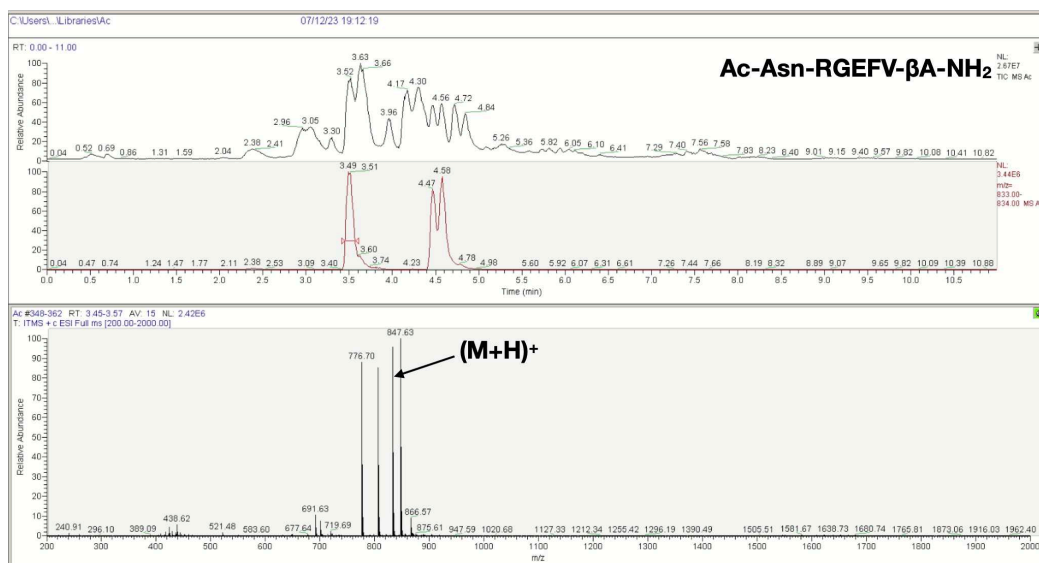
7.1 RGEFV Libraries



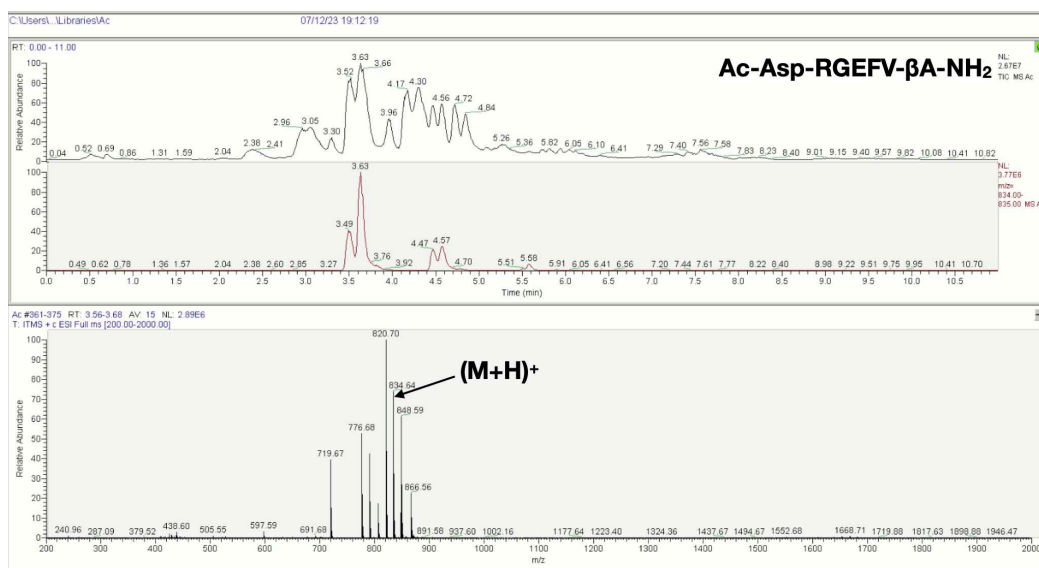
Appendix Figure 1 - LCMS spectra of the Ac-X-RGEFV-βA-NH₂ libraries, where X = Ala.



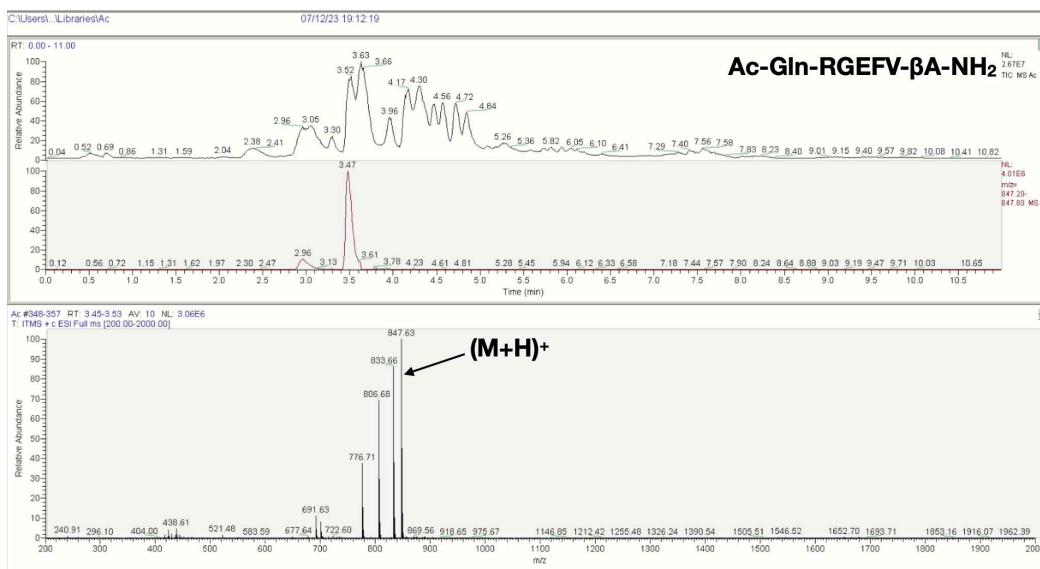
Appendix Figure 2 - LCMS spectra of the Ac-X-RGEFV-βA-NH₂ libraries, where X = Arg.



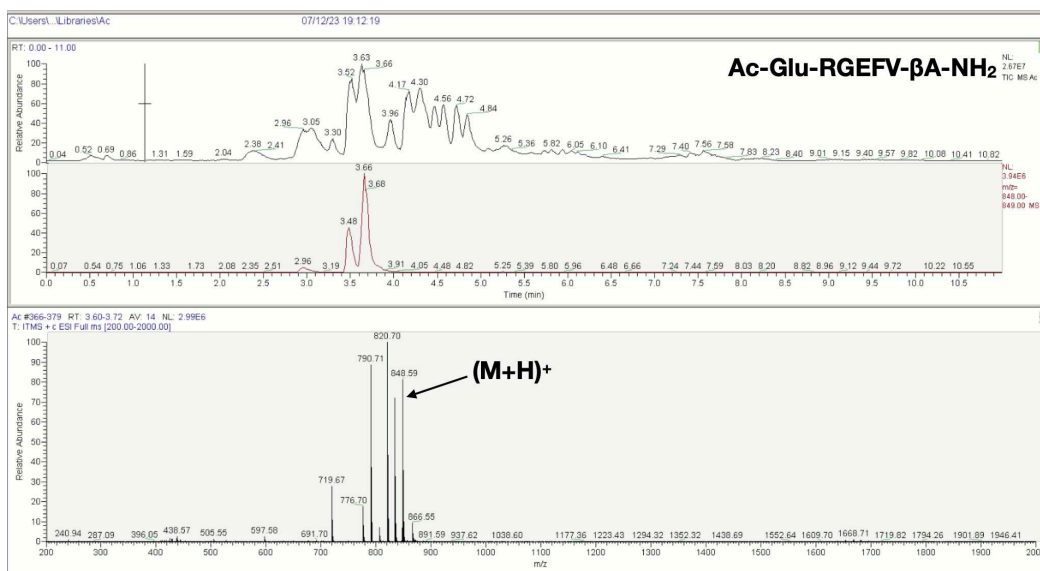
Appendix Figure 3 - LCMS spectra of the Ac-X-RGEFV-βA-NH₂ libraries, where X = Asn.



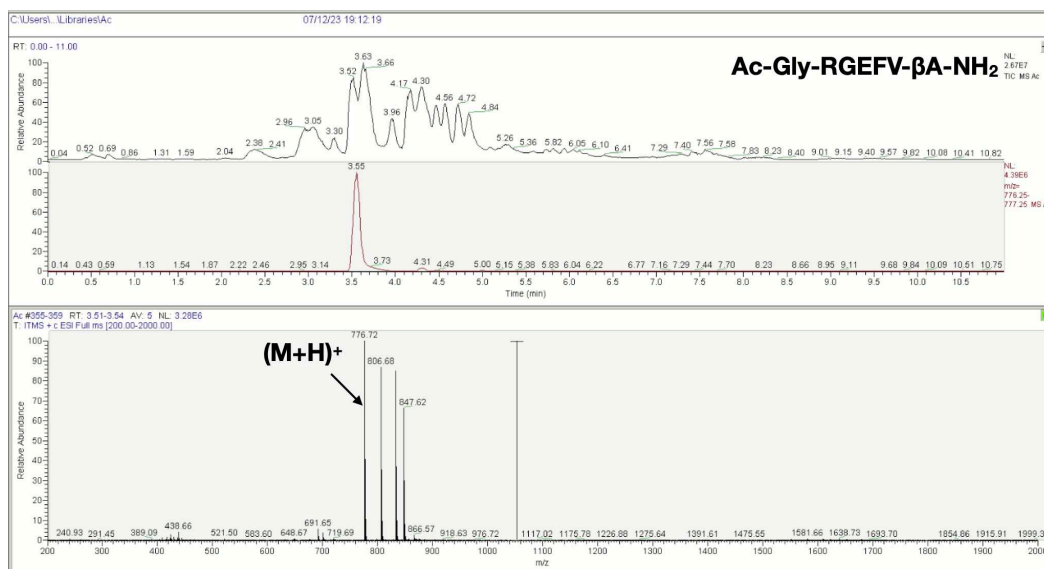
Appendix Figure 4 - LCMS spectra of the Ac-X-RGEFV-βA-NH₂ libraries, where X = Asp.



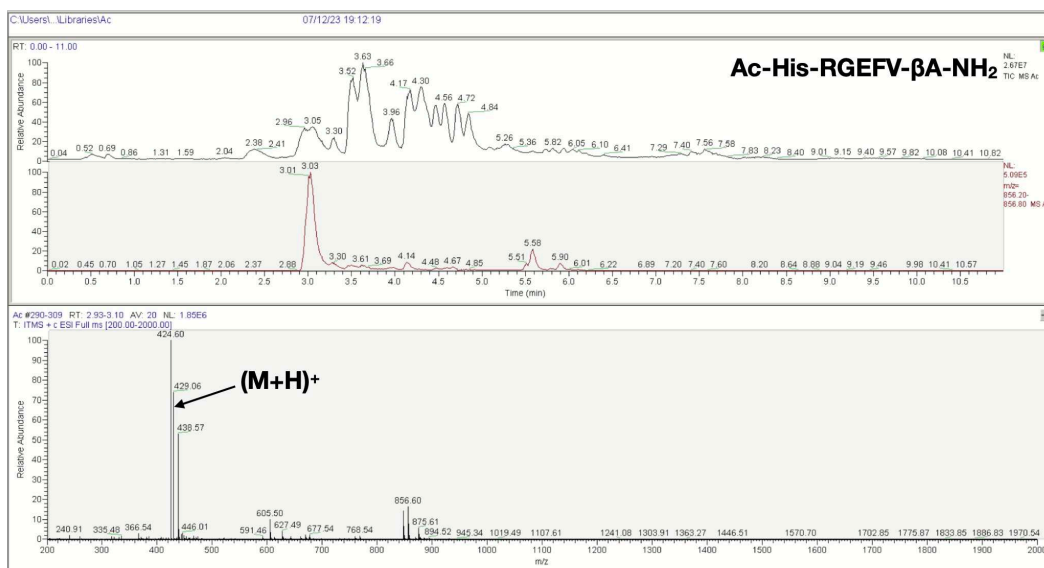
Appendix Figure 5 - LCMS spectra of the Ac-X-RGEFV-βA-NH₂ libraries, where X = Gln.



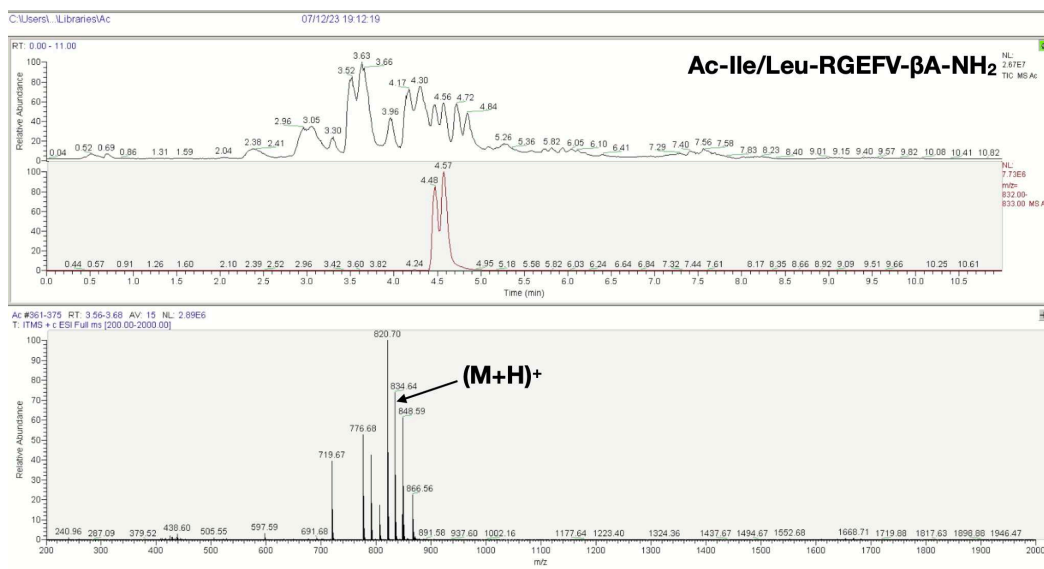
Appendix Figure 6 - LCMS spectra of the Ac-X-RGEFV-βA-NH₂ libraries, where X = Glu.



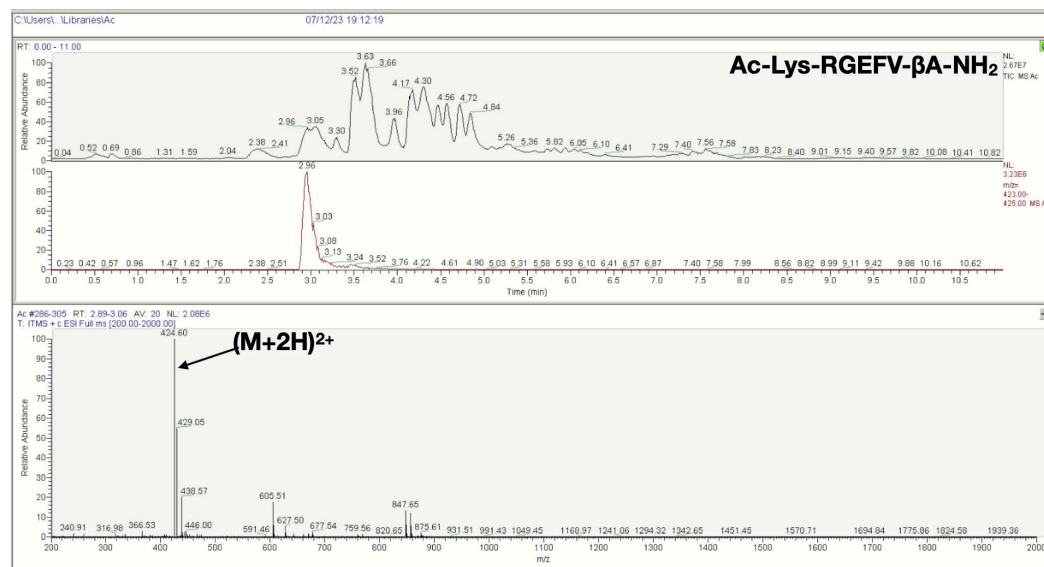
Appendix Figure 7 - LCMS spectra of the Ac-X-RGEFV-βA-NH₂ libraries, where X = Gly.



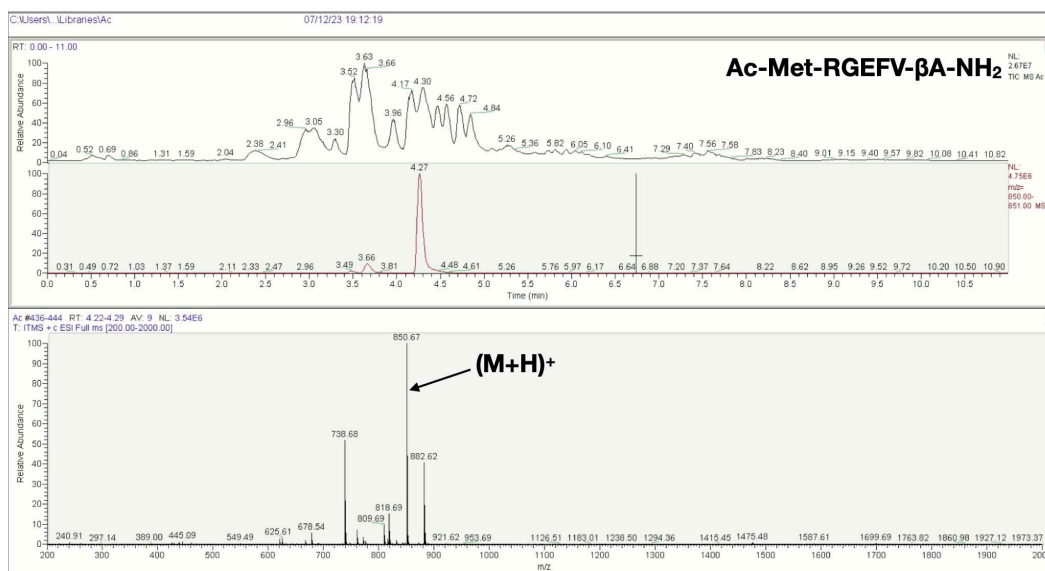
Appendix Figure 8 - LCMS spectra of the Ac-X-RGEFV-βA-NH₂ libraries, where X = His.



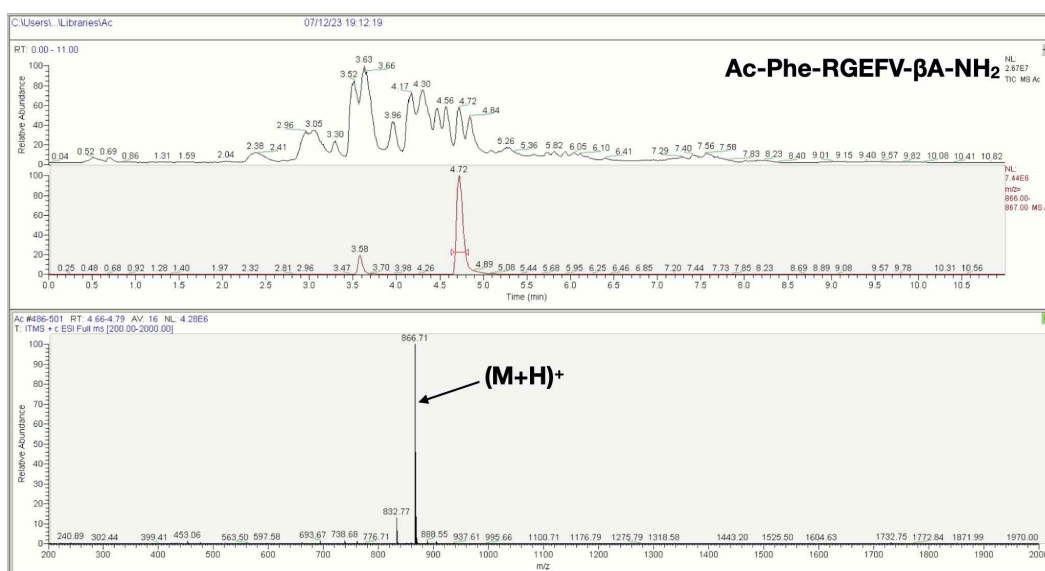
Appendix Figure 9 - LCMS spectra of the Ac-X-RGEFV-βA-NH₂ libraries, where X = Ile/Leu.



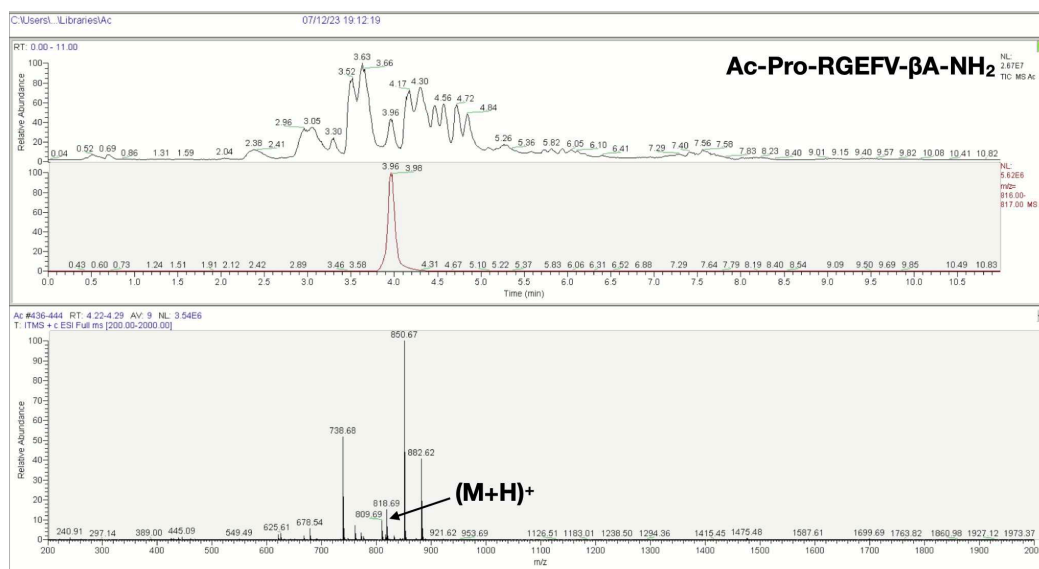
Appendix Figure 10 - LCMS spectra of the Ac-X-RGEFV-βA-NH₂ libraries, where X = Lys.



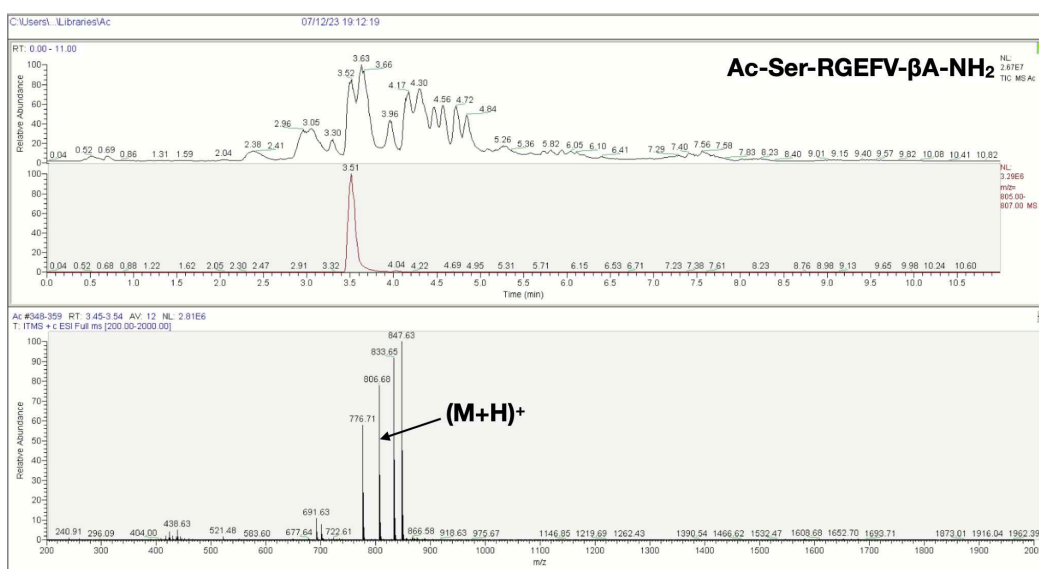
Appendix Figure 11 - LCMS spectra of the Ac-X-RGEFV-βA-NH₂ libraries, where X = Met.



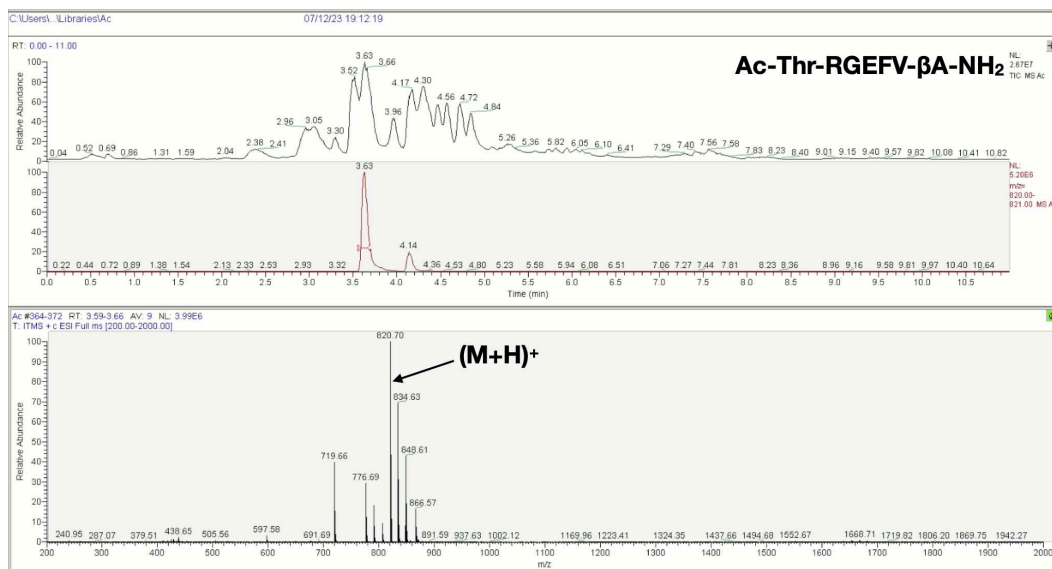
Appendix Figure 12 - LCMS spectra of the Ac-X-RGEFV-βA-NH₂ libraries, where X = Phe.



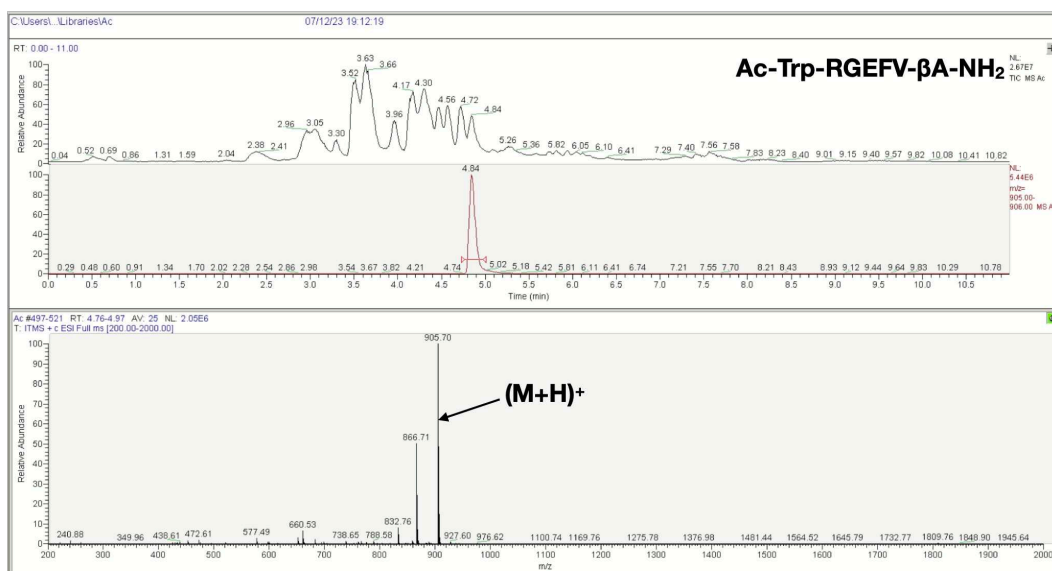
Appendix Figure 13 - LCMS spectra of the Ac-X-RGEFV-βA-NH₂ libraries, where X = Pro.



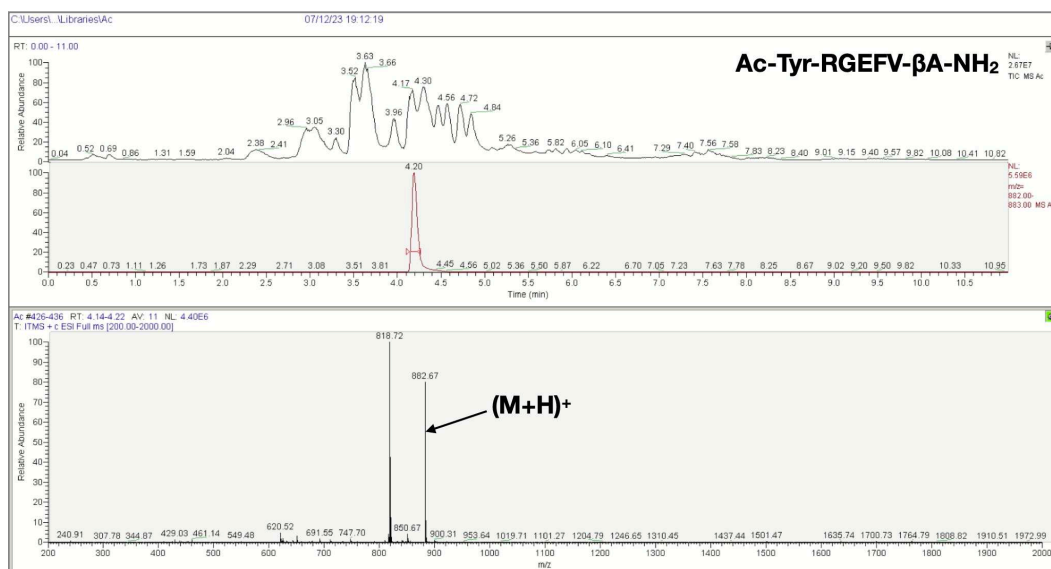
Appendix Figure 14 - LCMS spectra of the Ac-X-RGEFV-βA-NH₂ libraries, where X = Ser.



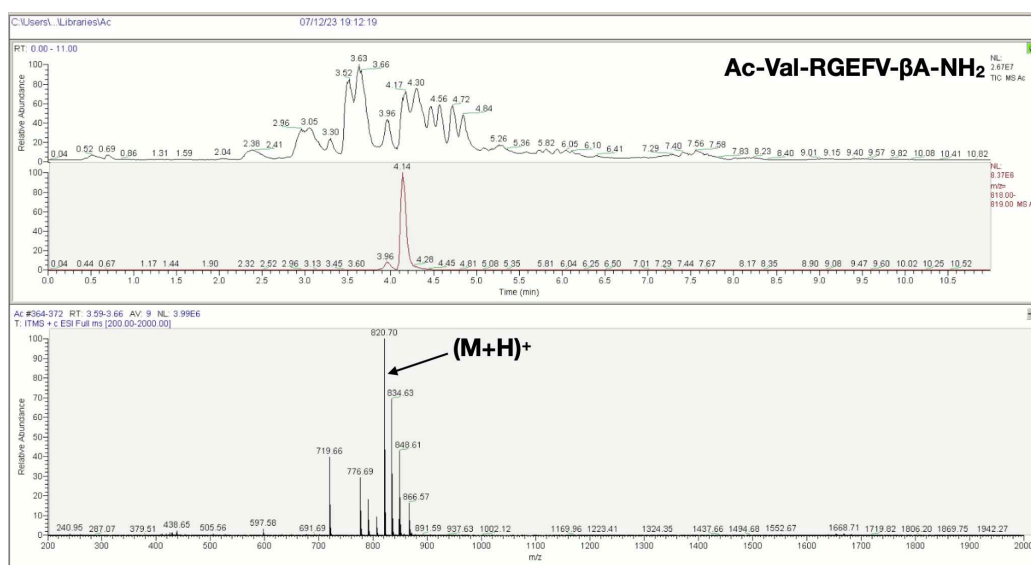
Appendix Figure 15 - LCMS spectra of the Ac-X-RGEFV-βA-NH₂ libraries, where X = Thr.



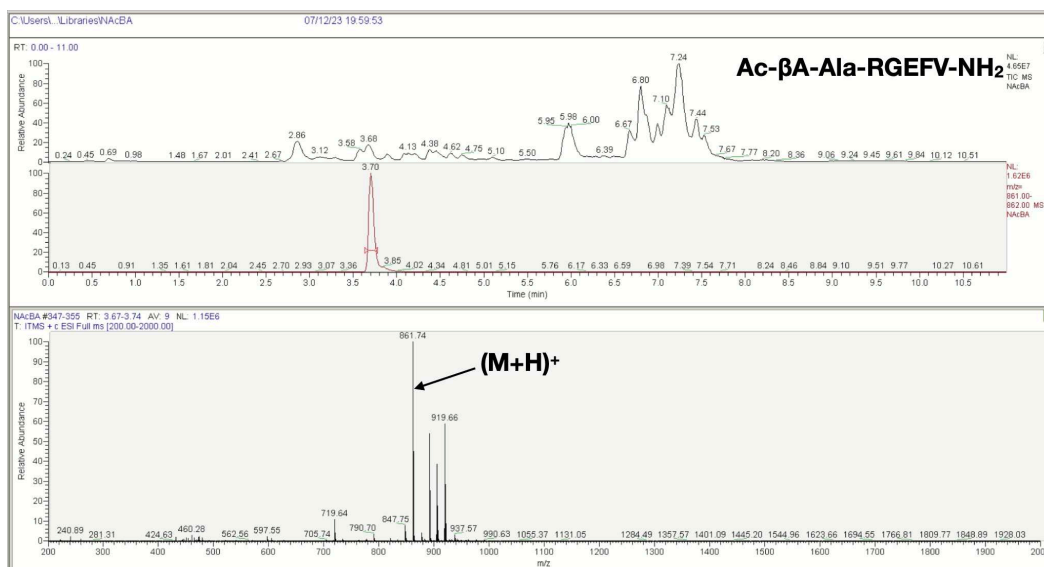
Appendix Figure 16 - LCMS spectra of the Ac-X-RGEFV-βA-NH₂ libraries, where X = Trp.



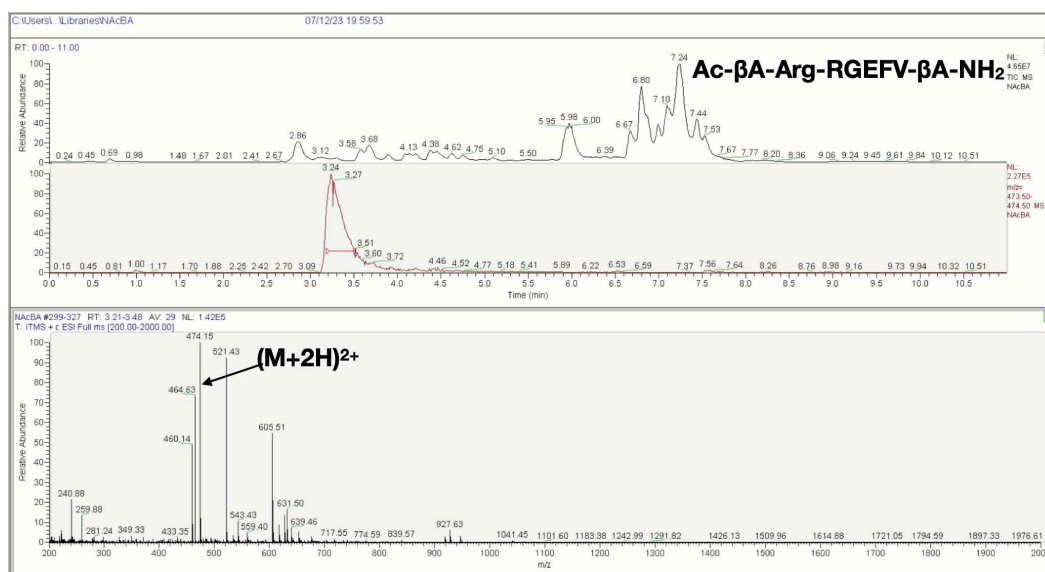
Appendix Figure 17 - LCMS spectra of the Ac-X-RGEFV-βA-NH₂ libraries, where X = Tyr.



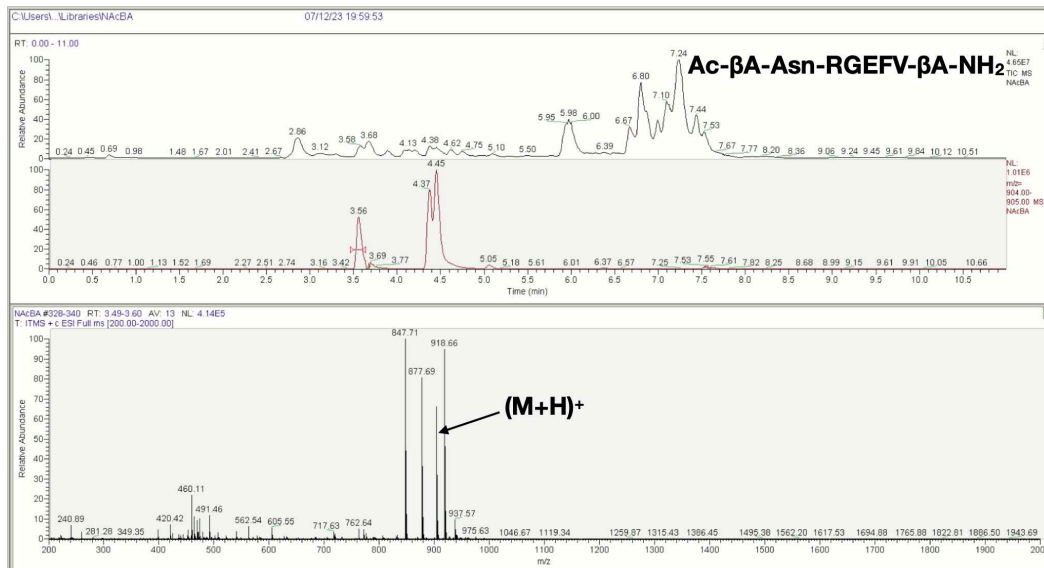
Appendix Figure 18 LCMS spectra of the Ac-X-RGEFV-βA-NH₂ libraries, where X = Val.



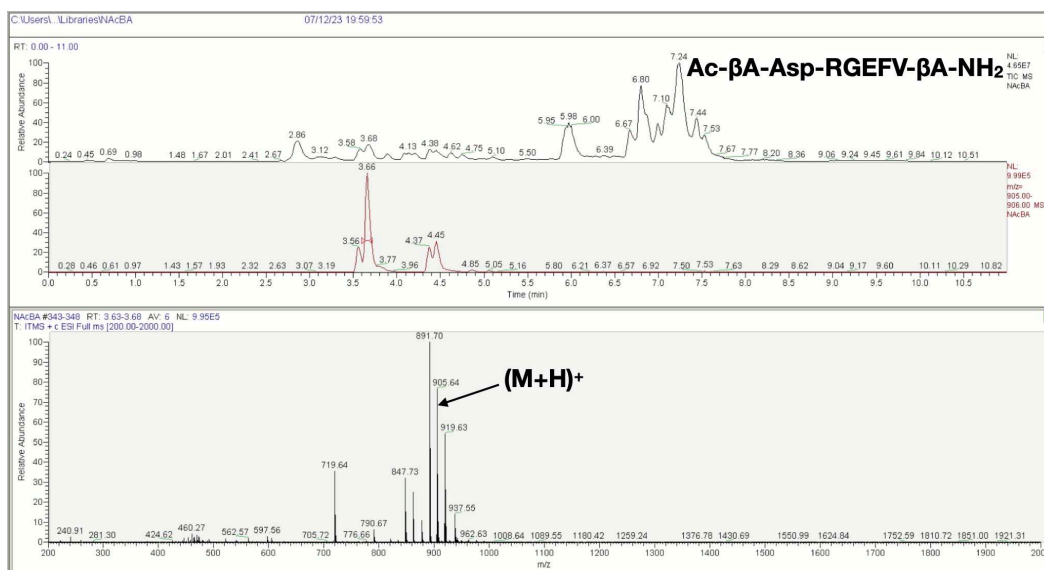
Appendix Figure 19 - LCMS spectra of the Ac-βA-X-RGEFV-βA-NH₂ libraries, where X = a) Ala.



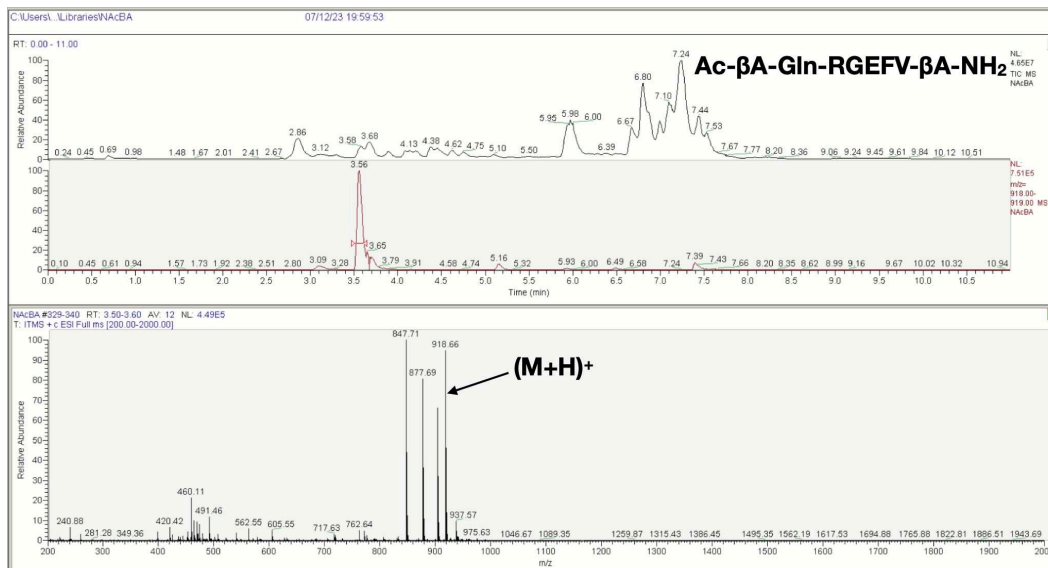
Appendix Figure 20 - LCMS spectra of the Ac-βA-X-RGEFV-βA-NH₂ libraries, where X = Arg.



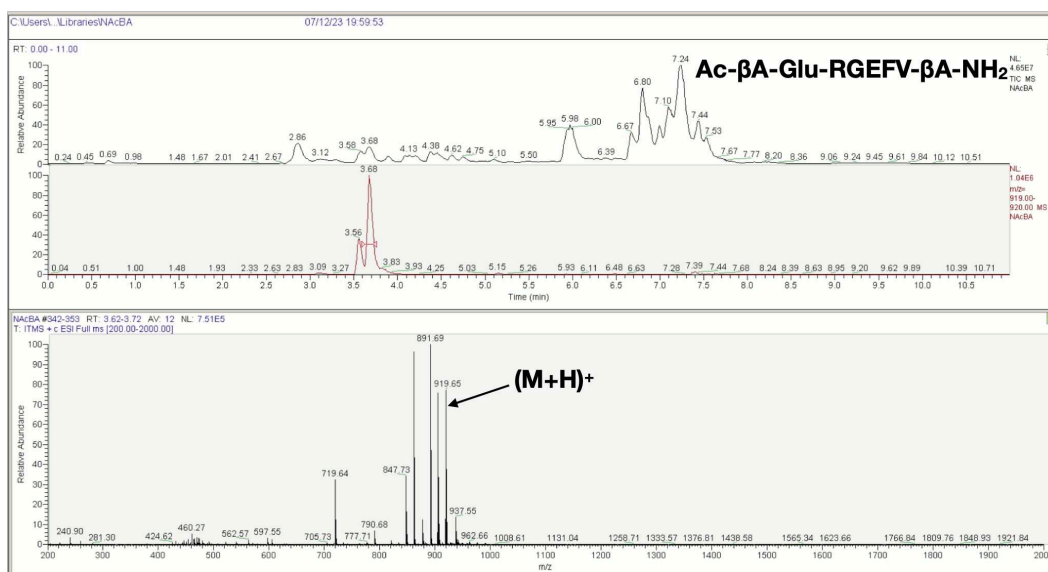
Appendix Figure 21 - LCMS spectra of the Ac-βA-X-RGEFV-βA-NH₂ libraries, where X = Asn.



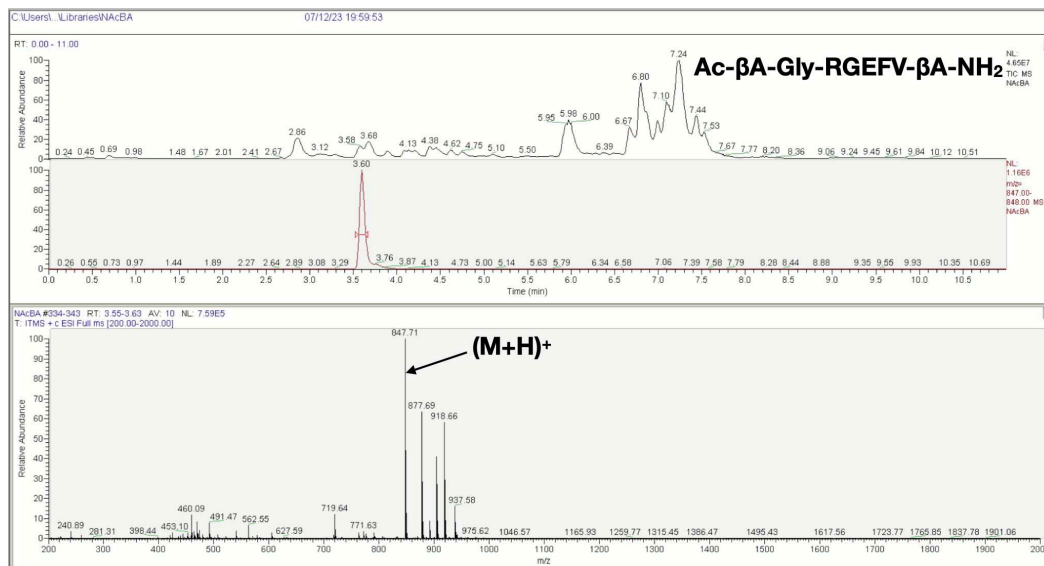
Appendix Figure 22 - LCMS spectra of the Ac-βA-X-RGEFV-βA-NH₂ libraries, where X = Asp



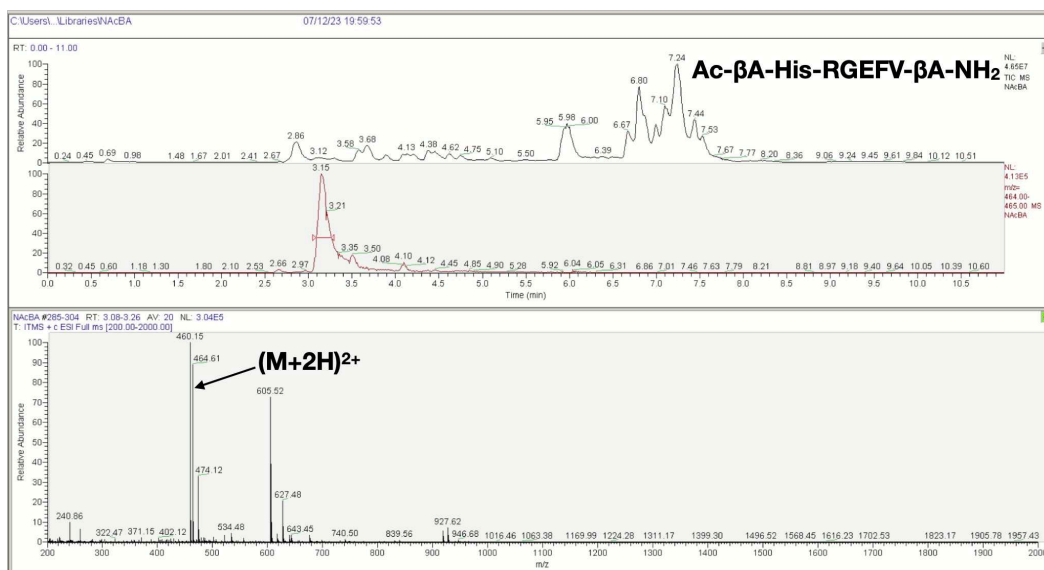
Appendix Figure 23 - LCMS spectra of the Ac-βA-X-RGEFV-βA-NH₂ libraries, where X = Gln.



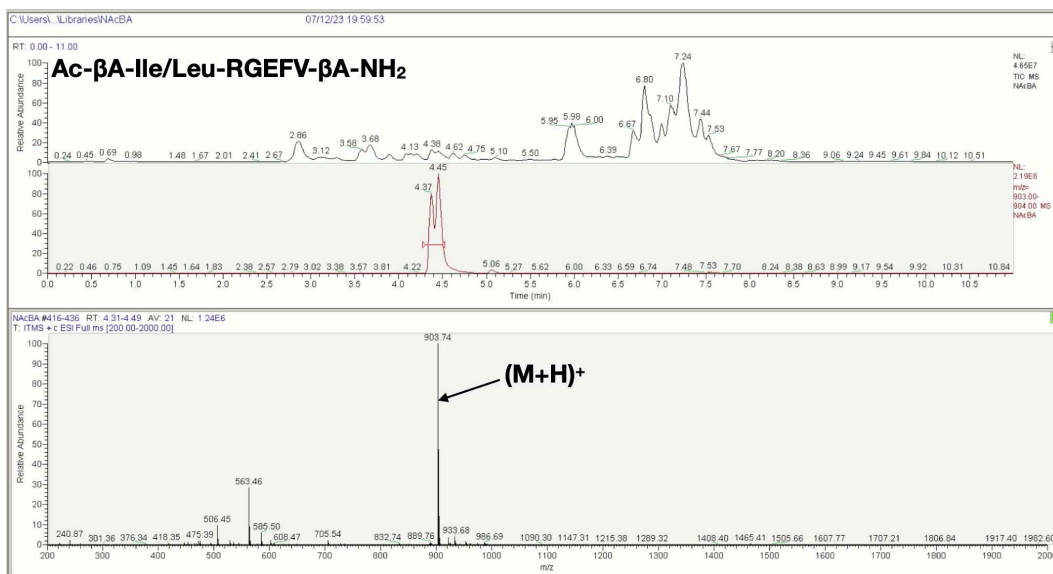
Appendix Figure 24 - LCMS spectra of the Ac-βA-X-RGEFV-βA-NH₂ libraries, where X = Glu.



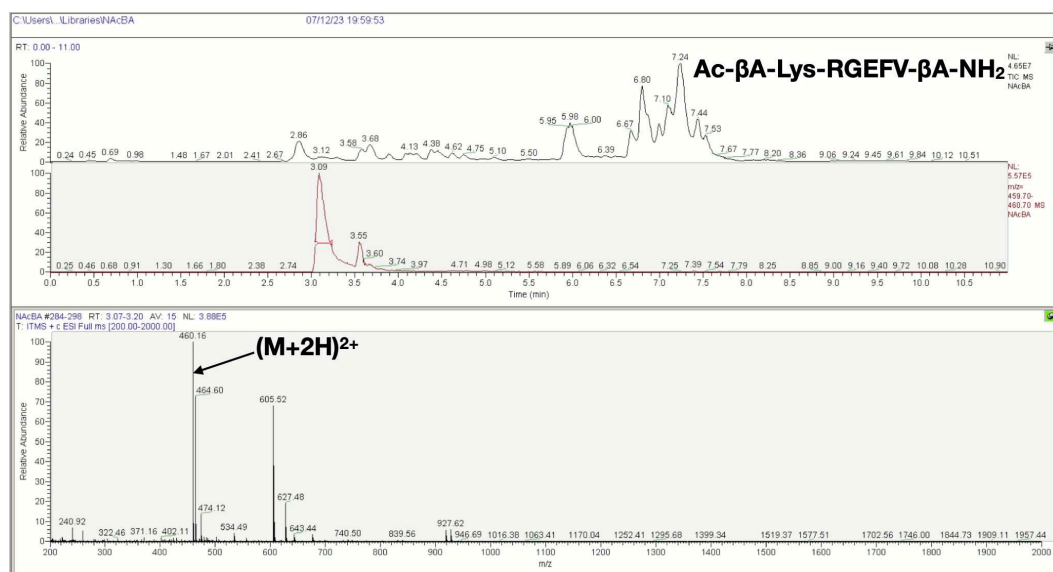
Appendix Figure 25 - LCMS spectra of the Ac-βA-X-RGEFV-βA-NH₂ libraries, where X = Gly.



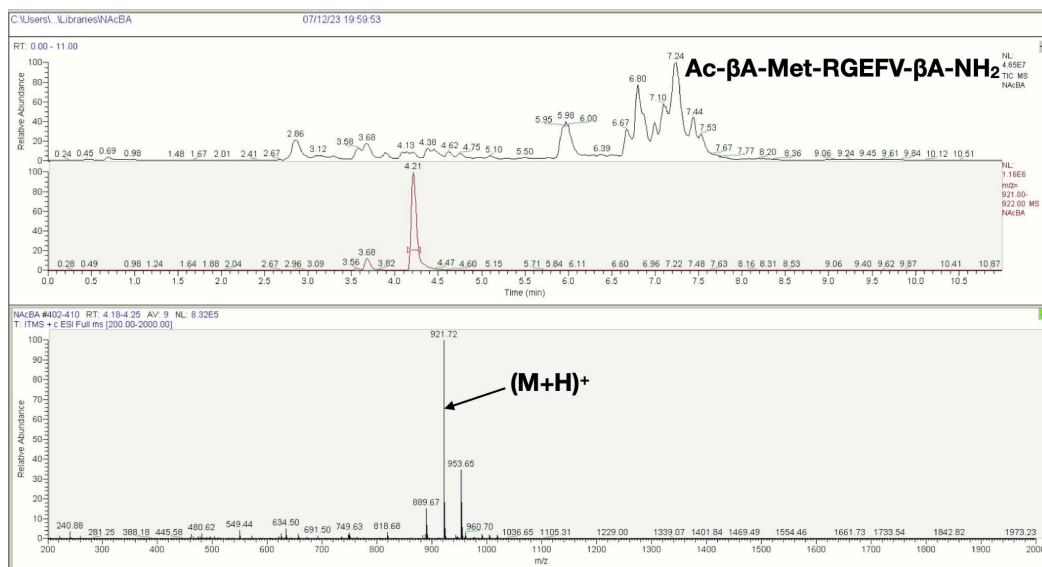
Appendix Figure 26 - LCMS spectra of the Ac-βA-X-RGEFV-βA-NH₂ libraries, where X = His.



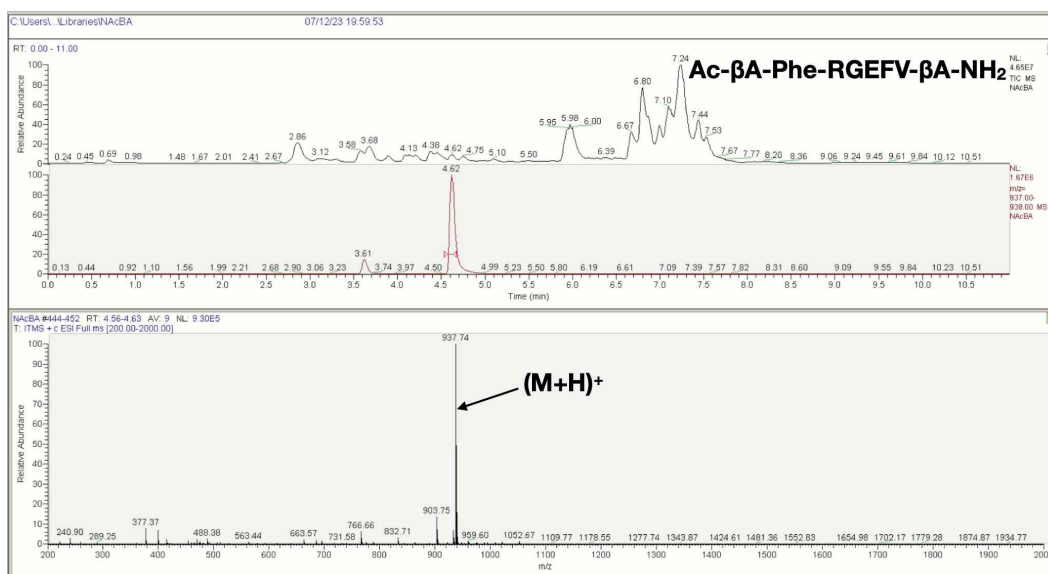
Appendix Figure 27 - LCMS spectra of the Ac-βA-X-RGEFV-βA-NH₂ libraries, where X = Ile/Leu.



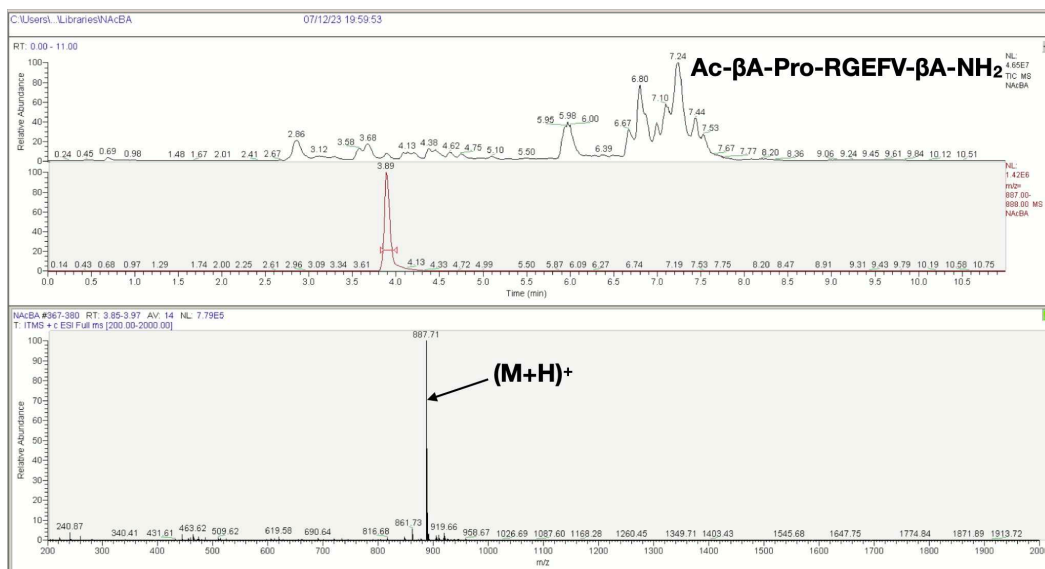
Appendix Figure 28 - LCMS spectra of the Ac-βA-X-RGEFV-βA-NH₂ libraries, where X = Lys.



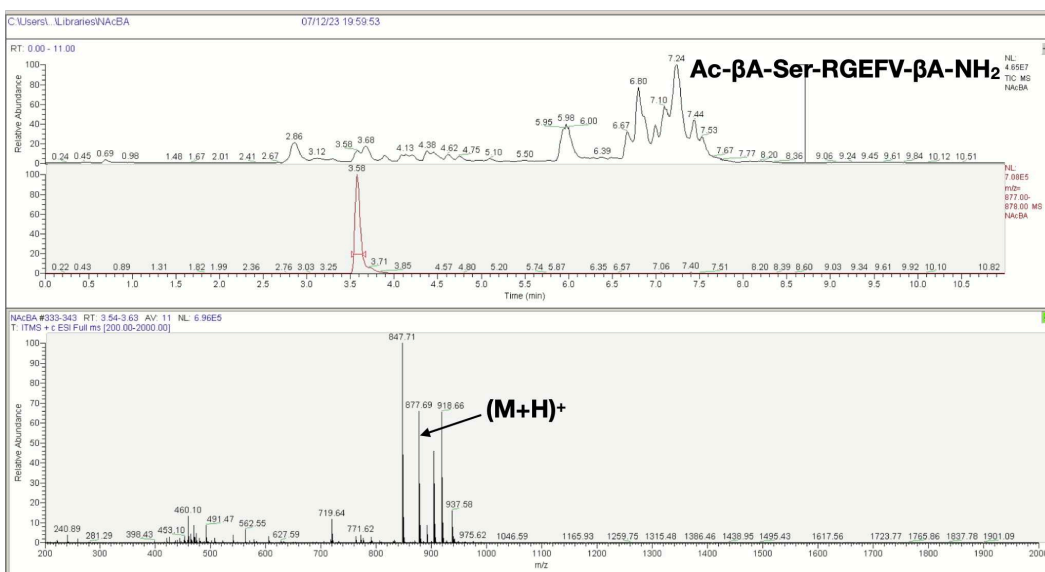
Appendix Figure 29 - LCMS spectra of the Ac-βA-X-RGEFV-βA-NH₂ libraries, where X = Met.



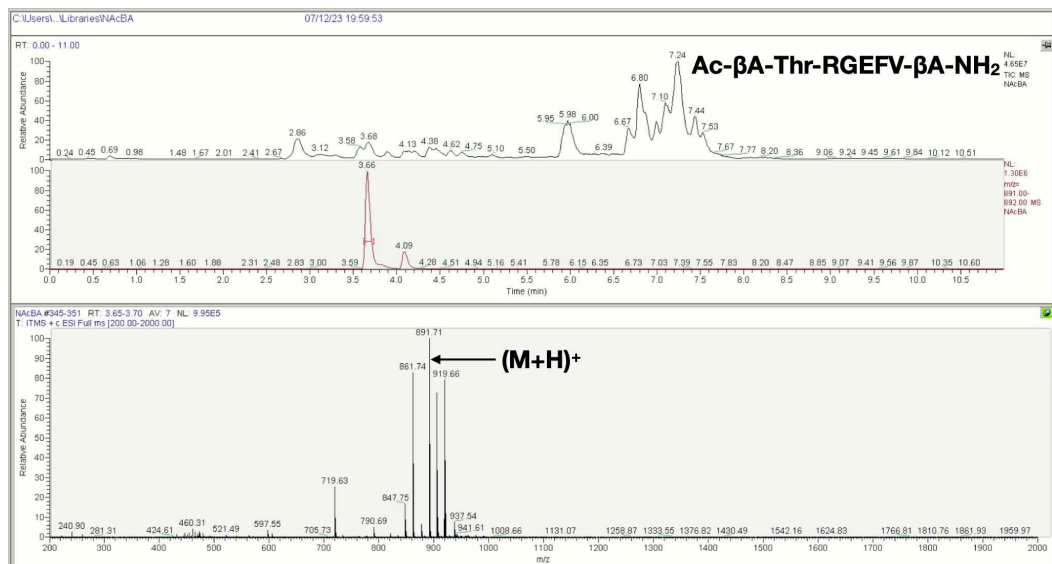
Appendix Figure 30 - LCMS spectra of the Ac-βA-X-RGEFV-βA-NH₂ libraries, where X = Phe.



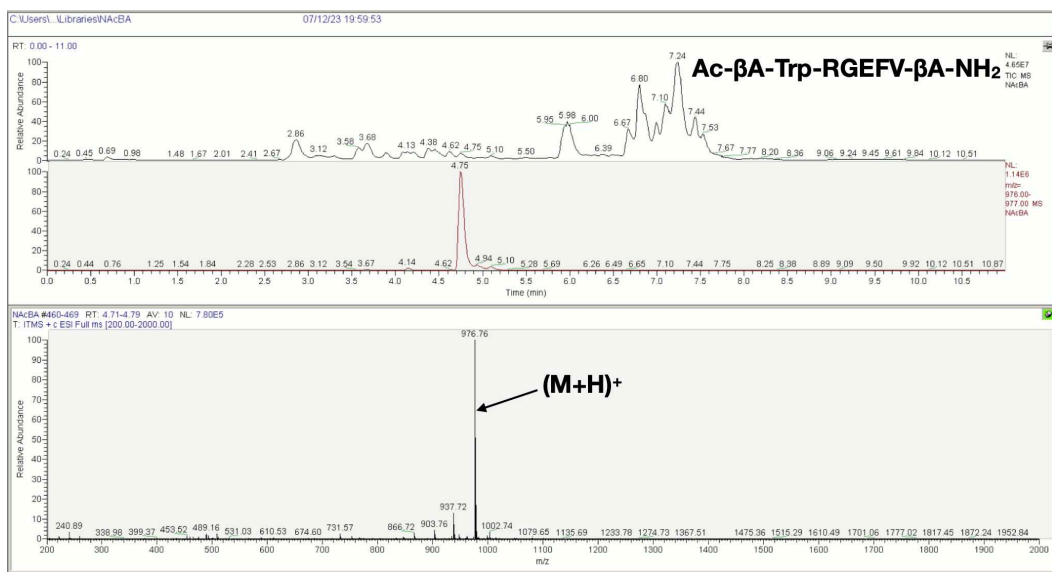
Appendix Figure 31 - LCMS spectra of the Ac-βA-X-RGEFV-βA-NH₂ libraries, where X = Pro.



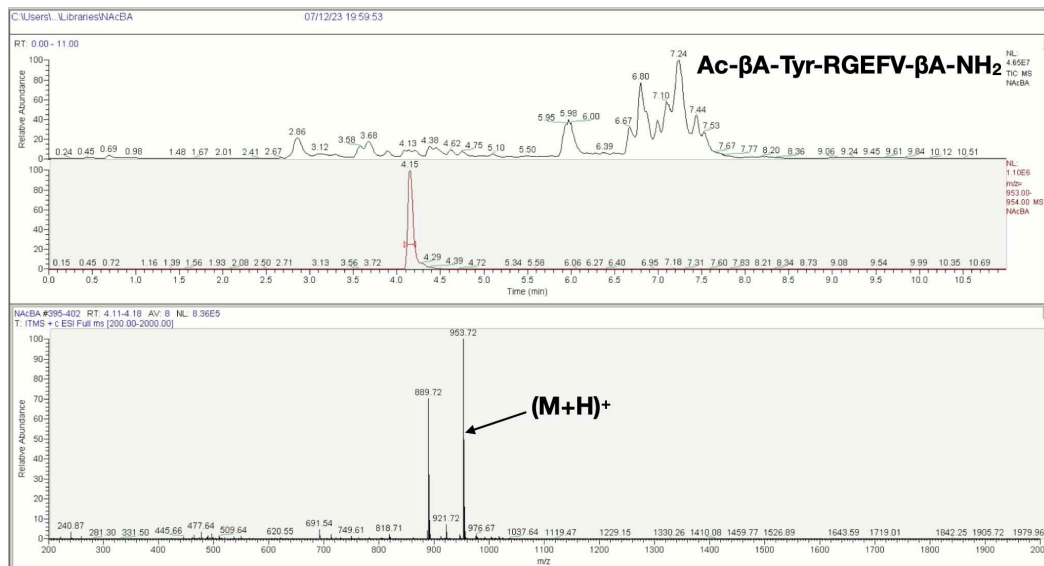
Appendix Figure 32 - LCMS spectra of the Ac-βA-X-RGEFV-βA-NH₂ libraries, where X = Ser.



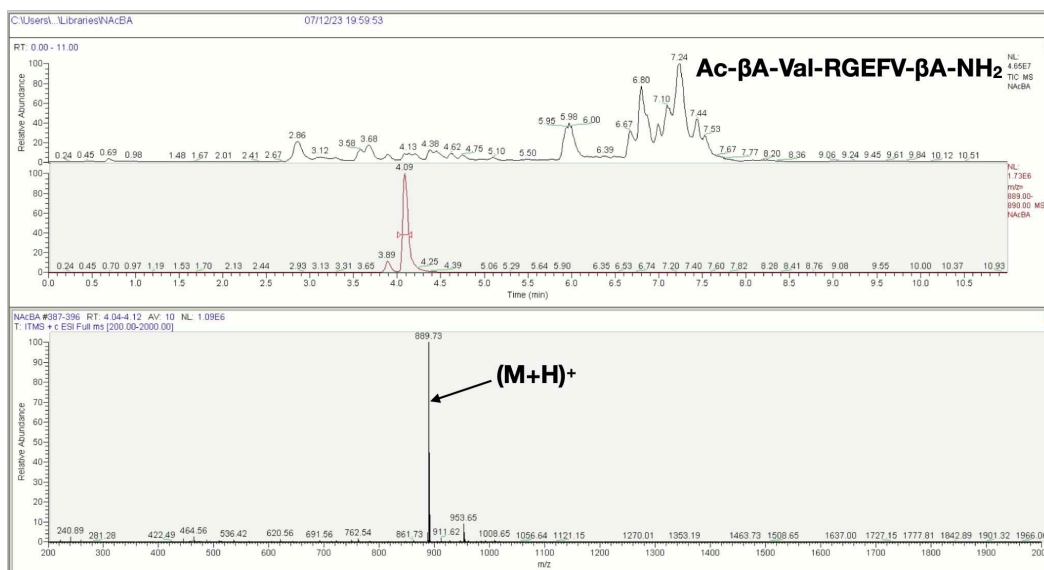
Appendix Figure 33 - LCMS spectra of the Ac-βA-X-RGEFV-βA-NH₂ libraries, where X = Thr.



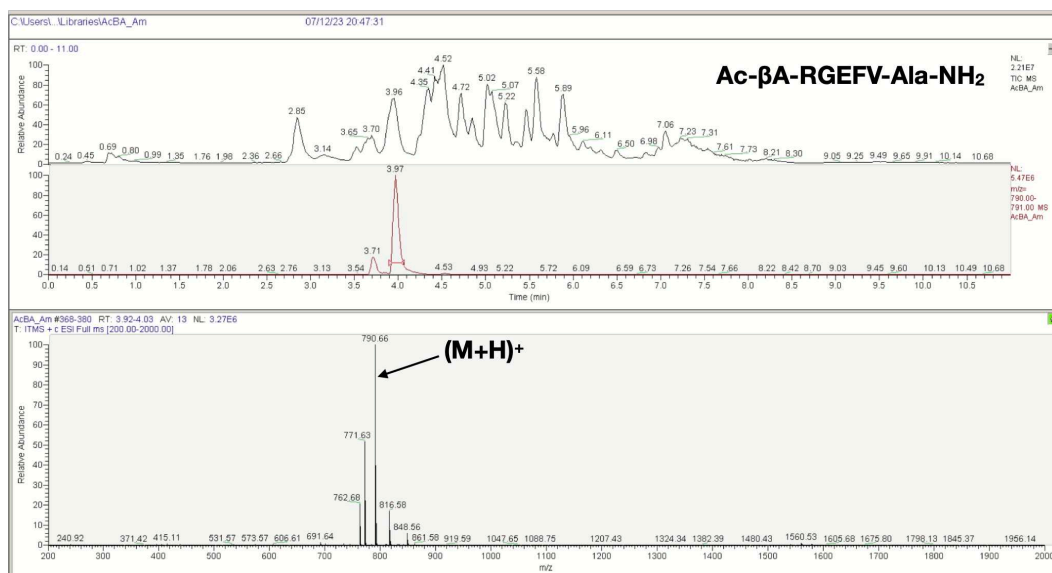
Appendix Figure 34 - LCMS spectra of the Ac-βA-X-RGEFV-βA-NH₂ libraries, where X = Trp.



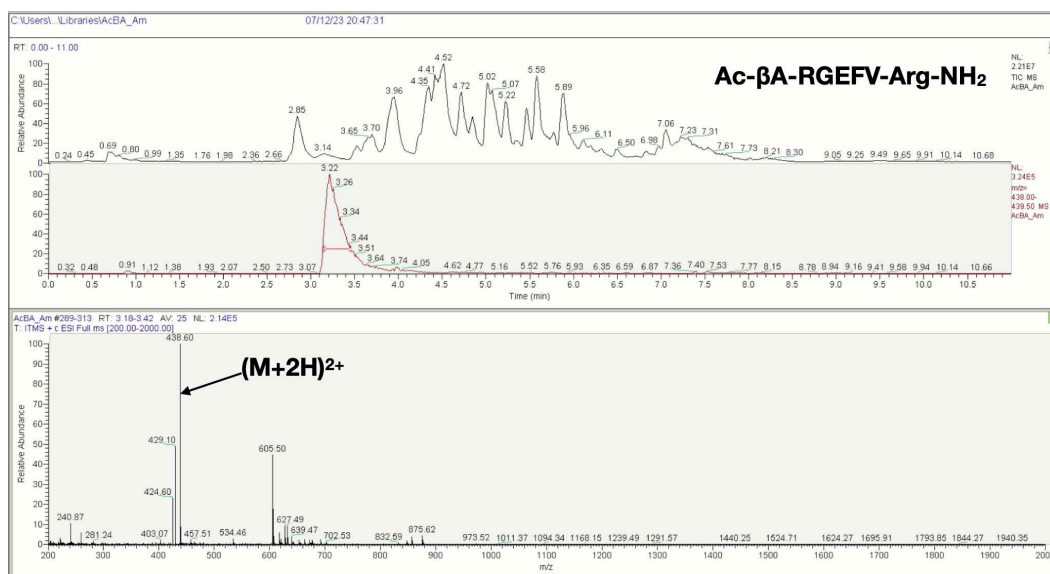
Appendix Figure 35 - LCMS spectra of the Ac-βA-X-RGEFV-βA-NH₂ libraries, where X = Tyr.



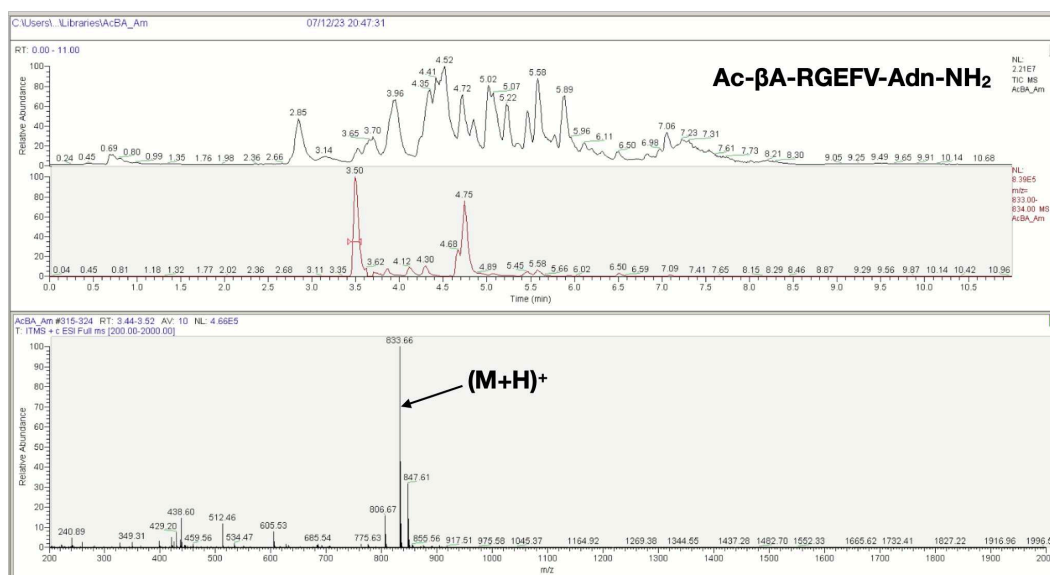
Appendix Figure 36 LCMS spectra of the Ac-βA-X-RGEFV-βA-NH₂ libraries, where X = Val.



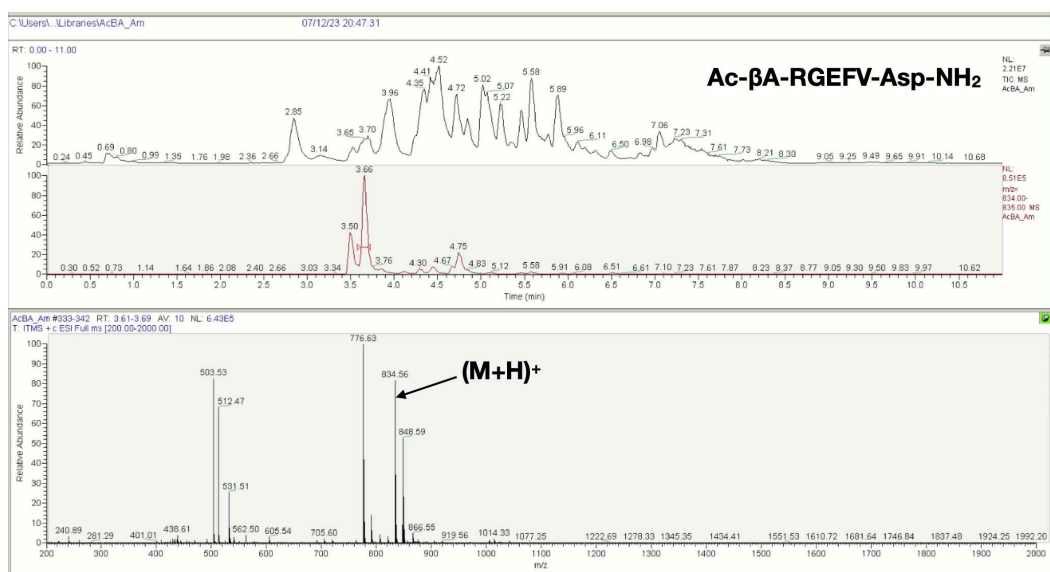
Appendix Figure 37 - LCMS spectra of the Ac-βA-RGEFV-X-NH₂ libraries, where X = Ala.



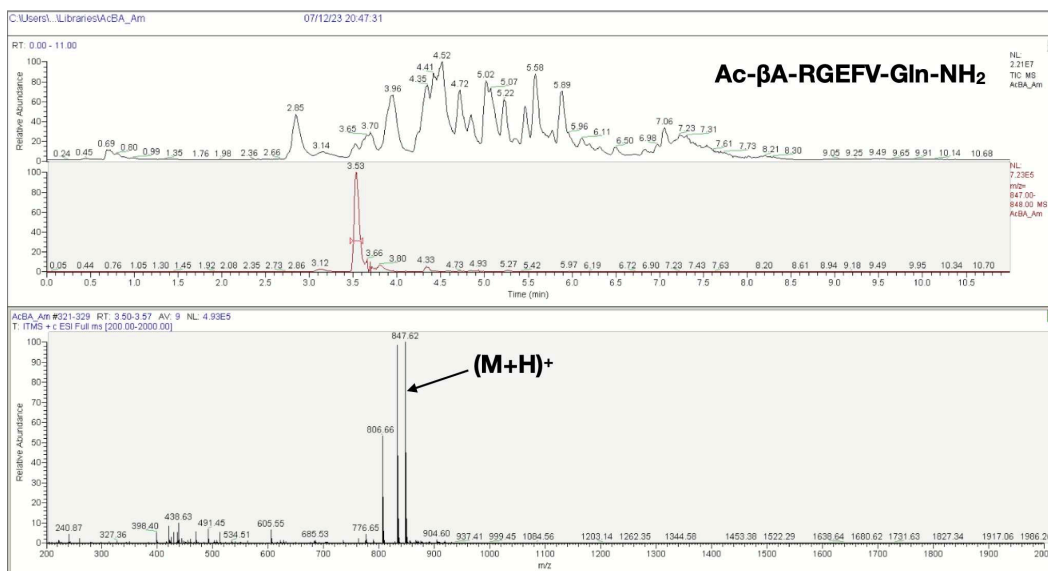
Appendix Figure 38 - LCMS spectra of the Ac-βA-RGEFV-X-NH₂ libraries, where X = Arg.



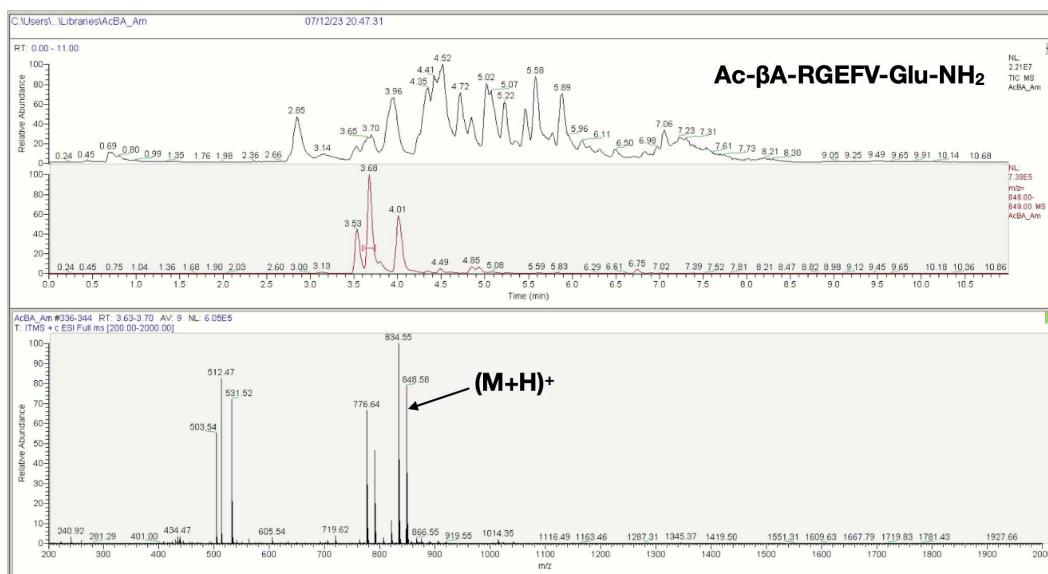
Appendix Figure 39 - LCMS spectra of the Ac-βA-RGEFV-X-NH₂ libraries, where X = Asn.



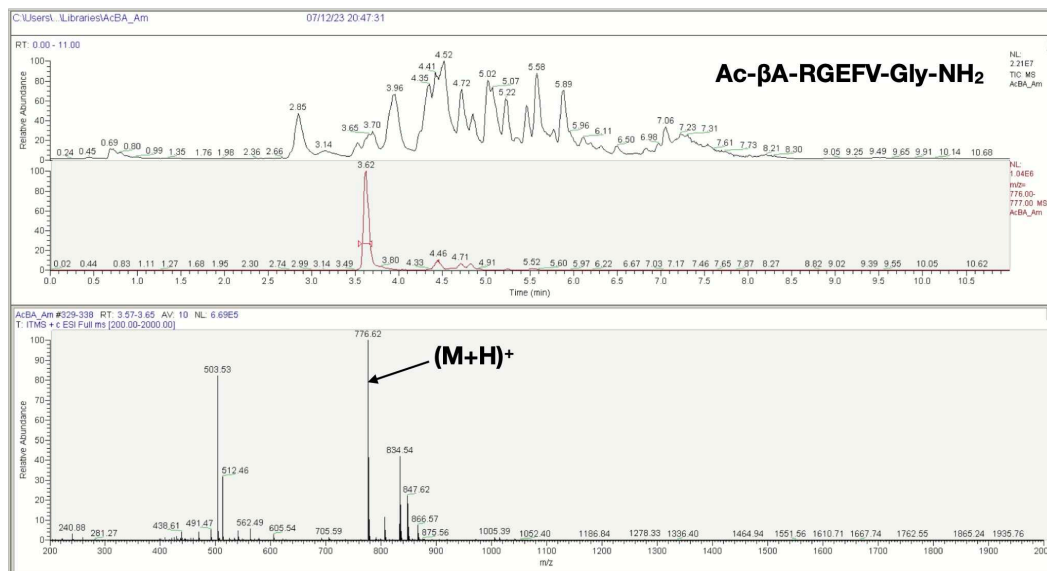
Appendix Figure 40 - LCMS spectra of the Ac-βA-RGEFV-X-NH₂ libraries, where X = Asp.



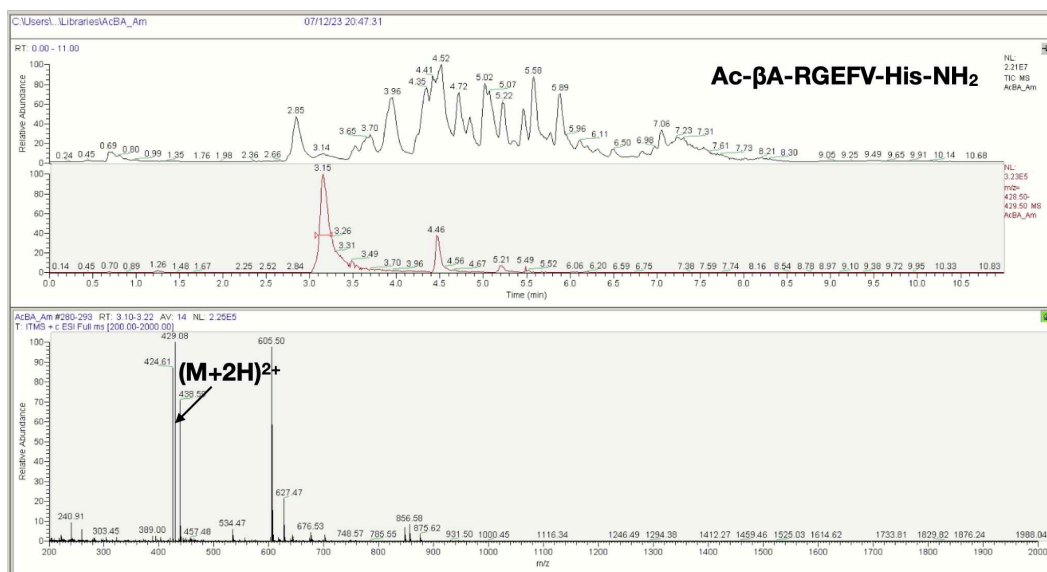
Appendix Figure 41 - LCMS spectra of the Ac-βA-RGEFV-X-NH₂ libraries, where X = Gln.



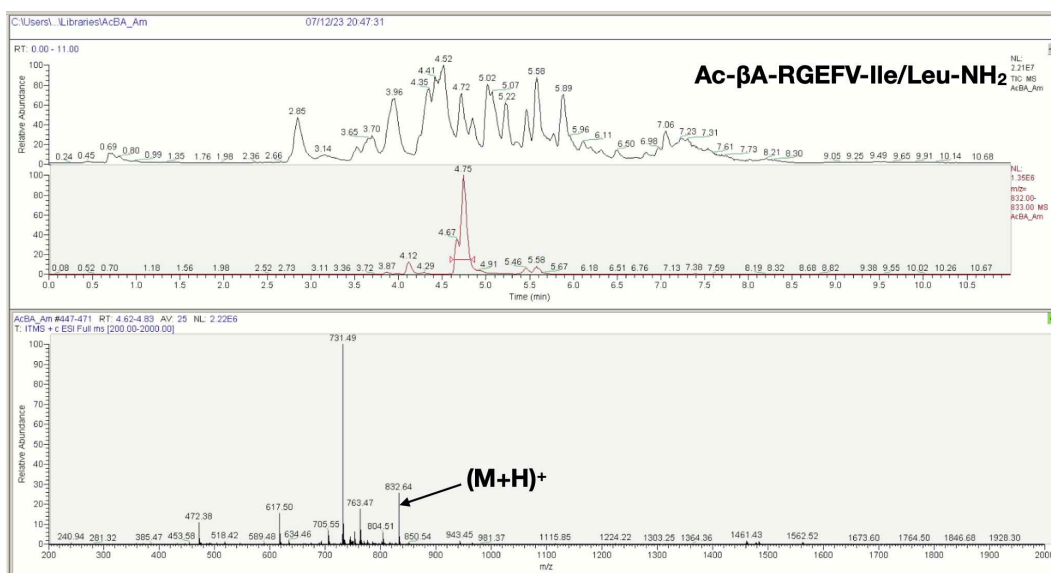
Appendix Figure 42 - LCMS spectra of the Ac-βA-RGEFV-X-NH₂ libraries, where X = Glu.



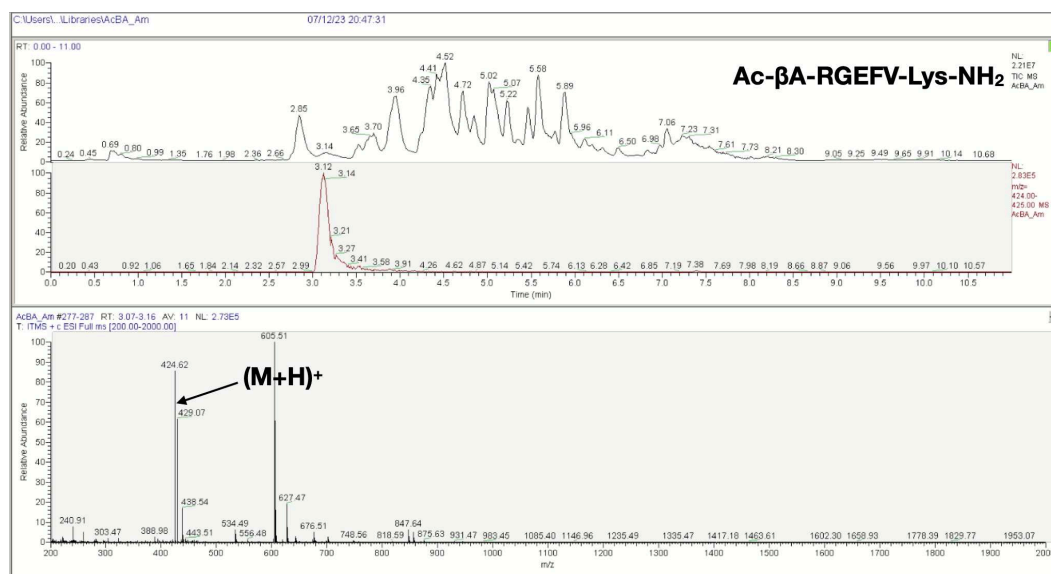
Appendix Figure 43 - LCMS spectra of the Ac-βA-RGEFV-X-NH₂ libraries, where X = Gly.



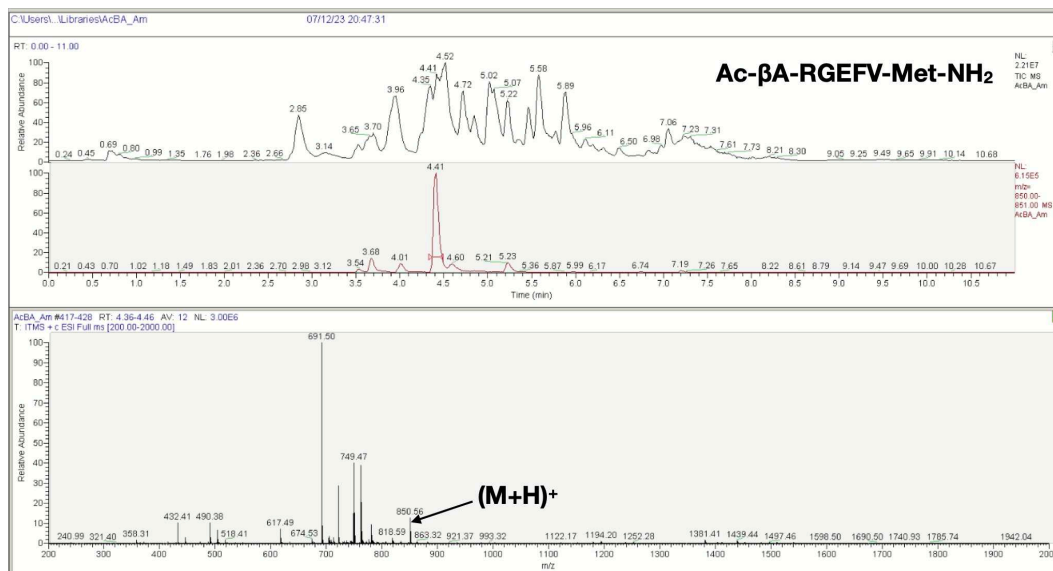
Appendix Figure 44 - LCMS spectra of the Ac-βA-RGEFV-X-NH₂ libraries, where X = His.



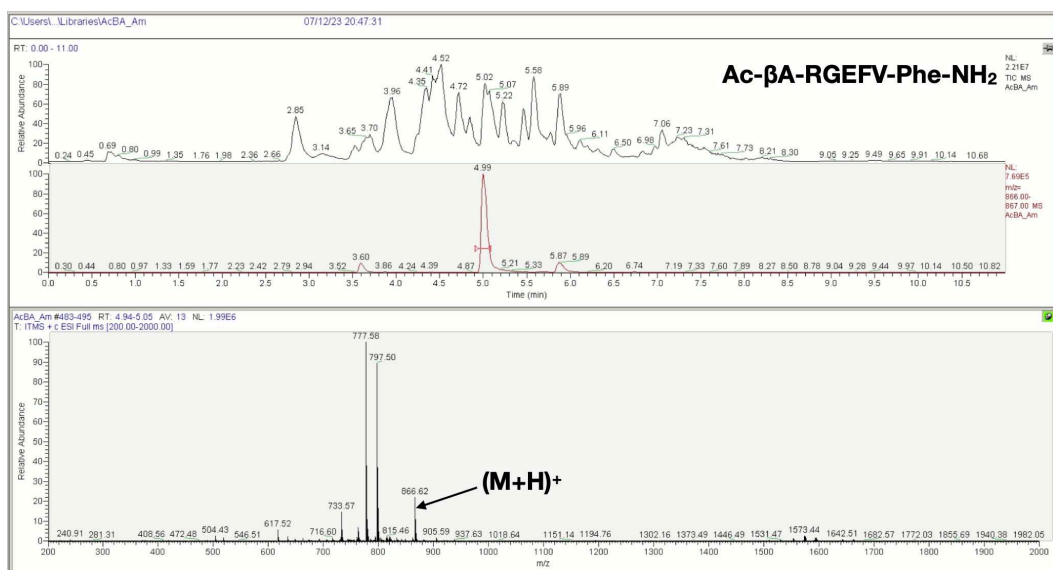
Appendix Figure 45 - LCMS spectra of the Ac-βA-RGEFV-X-NH₂ libraries, where X = Ile/Leu.



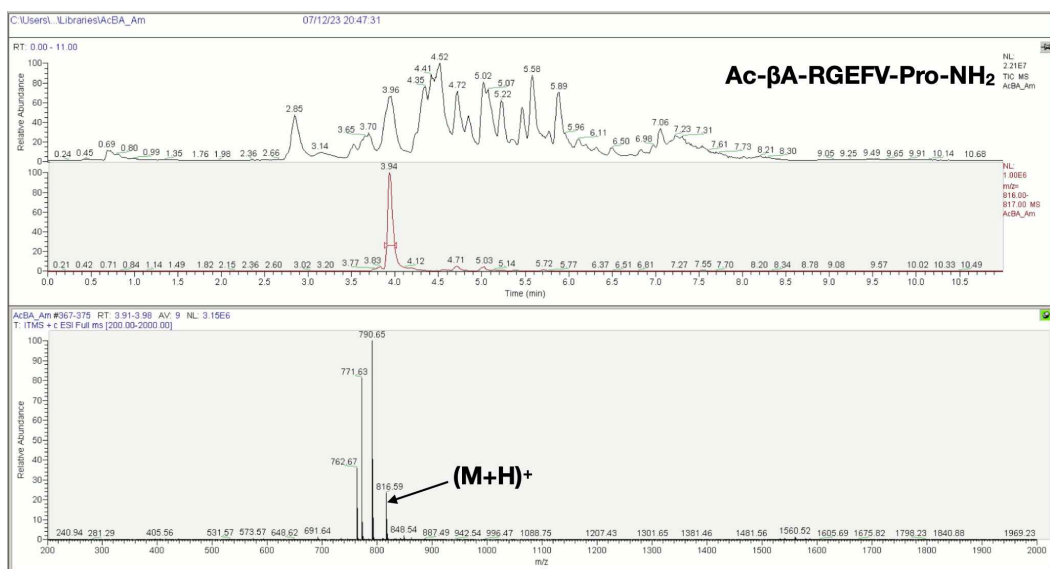
Appendix Figure 46 - LCMS spectra of the Ac-βA-RGEFV-X-NH₂ libraries, where X = Lys.



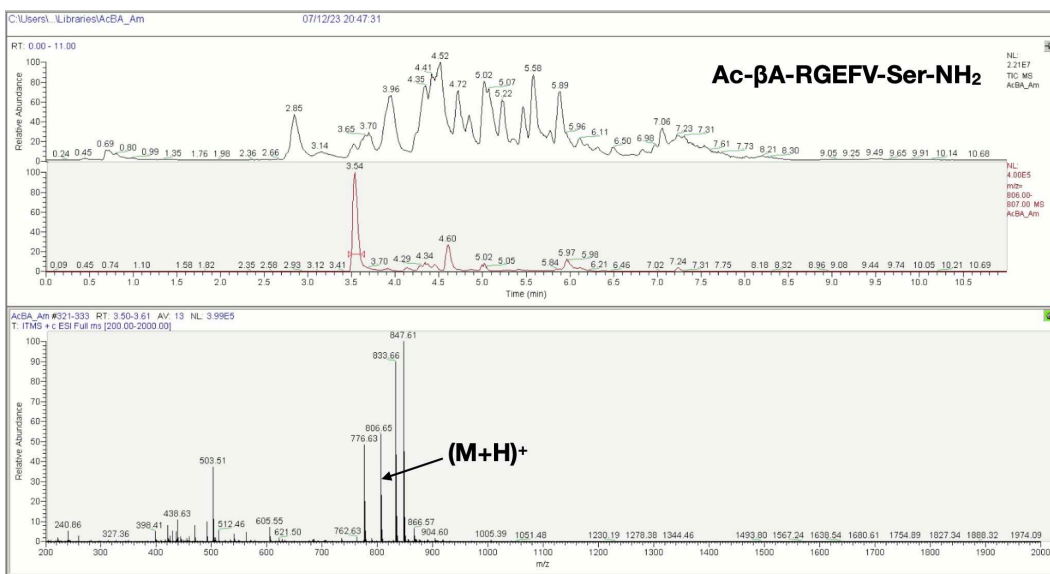
Appendix Figure 47 - LCMS spectra of the Ac-βA-RGEFV-X-NH₂ libraries, where X = Met.



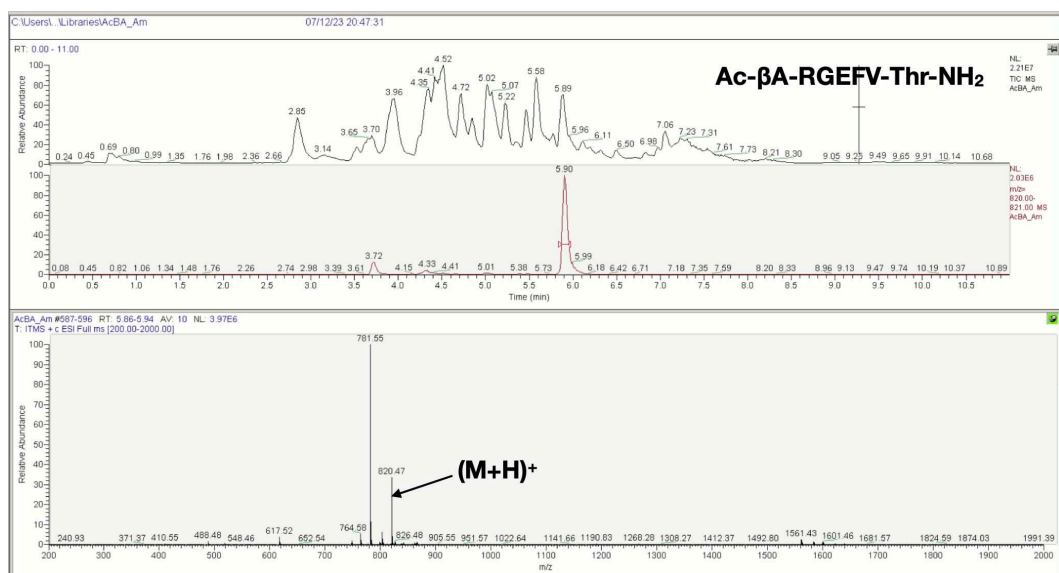
Appendix Figure 48 - LCMS spectra of the Ac-βA-RGEFV-X-NH₂ libraries, where X = Phe.



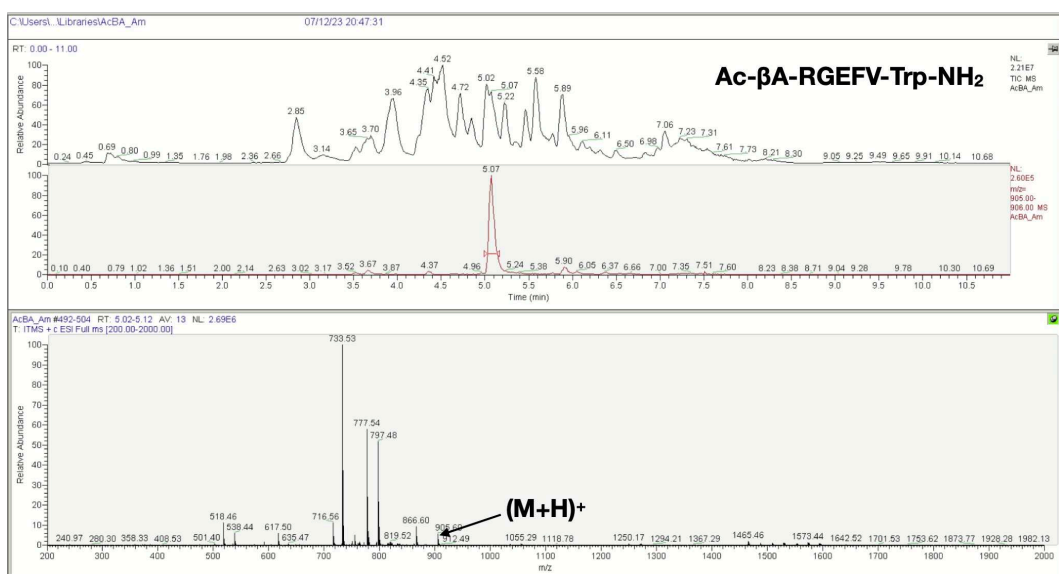
Appendix Figure 49 - LCMS spectra of the Ac-βA-RGEFV-X-NH₂ libraries, where X = Pro.



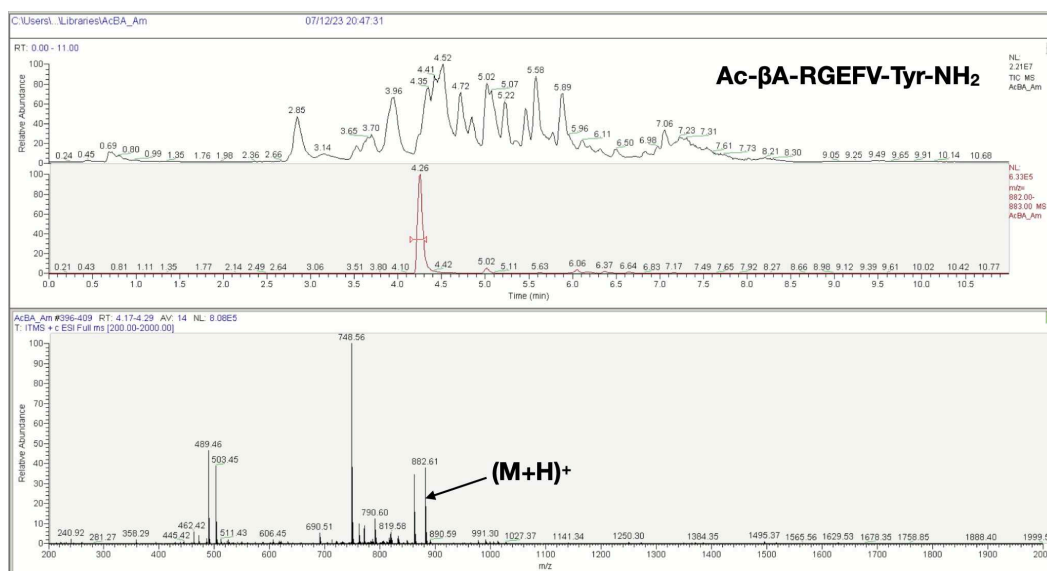
Appendix Figure 50 - LCMS spectra of the Ac-βA-RGEFV-X-NH₂ libraries, where X = Ser.



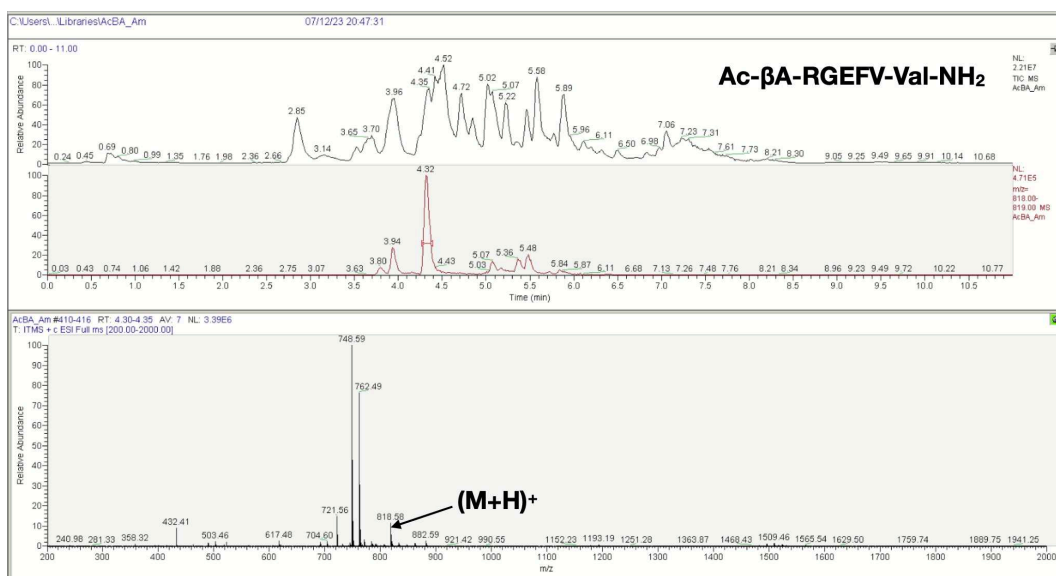
Appendix Figure 51 - LCMS spectra of the Ac-βA-RGEFV-X-NH₂ libraries, where X = Thr.



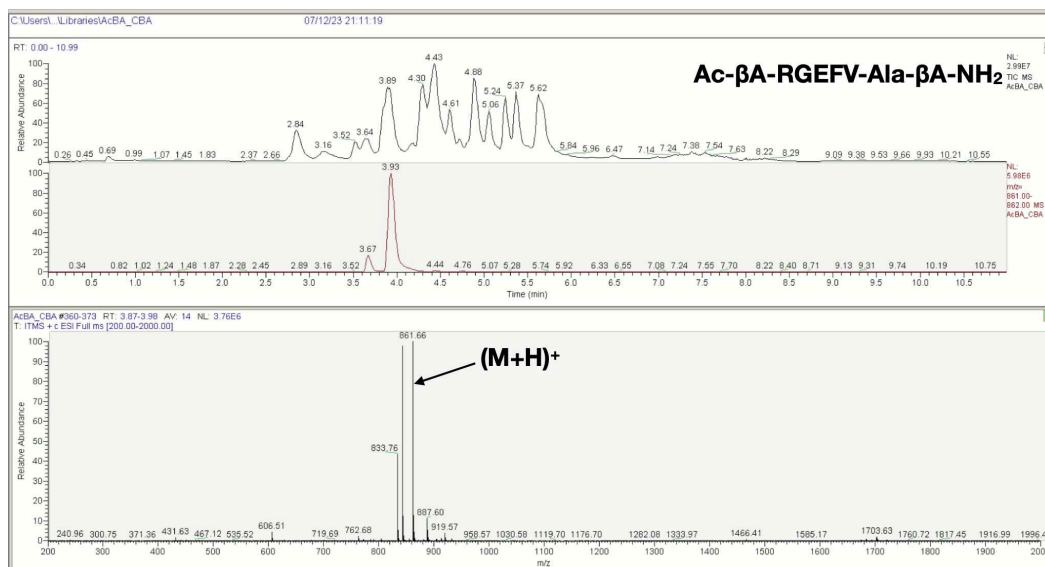
Appendix Figure 52 - LCMS spectra of the Ac-βA-RGEFV-X-NH₂ libraries, where X = Trp.



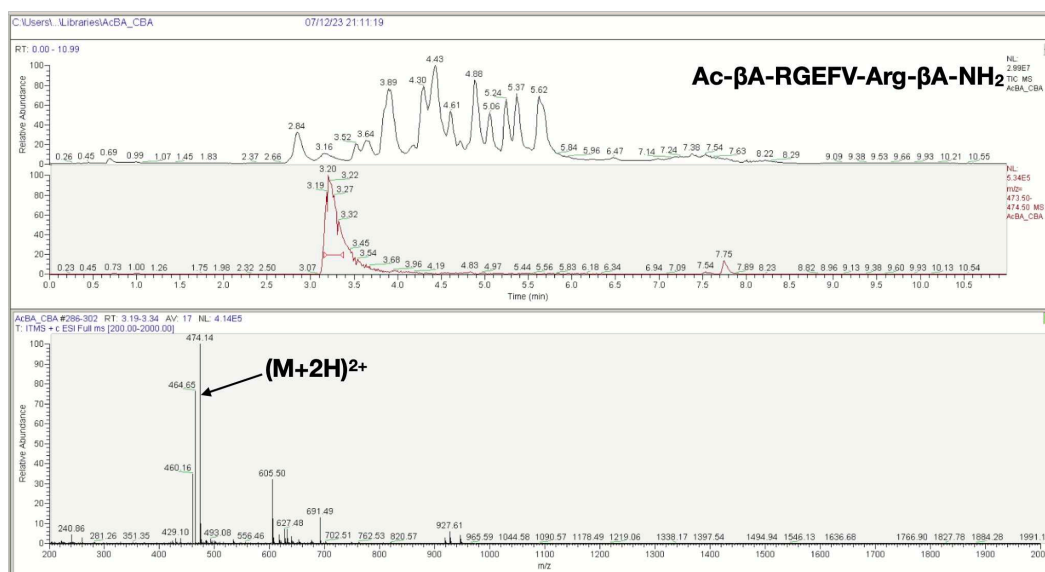
Appendix Figure 53 - LCMS spectra of the Ac-βA-RGEFV-X-NH₂ libraries, where X = Tyr.



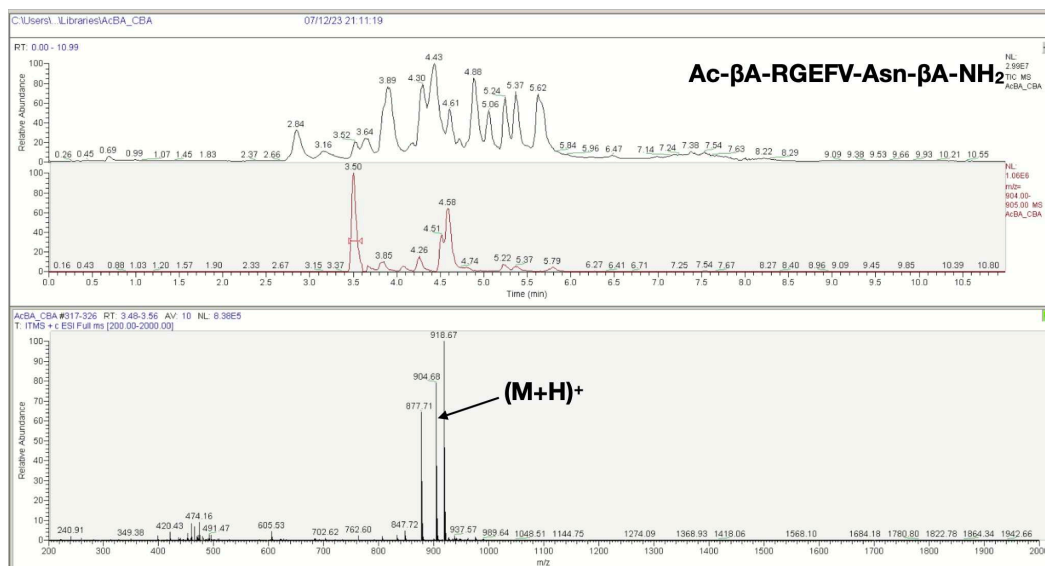
Appendix Figure 54 - LCMS spectra of the Ac-βA-RGEFV-X-NH₂ libraries, where X = Val.



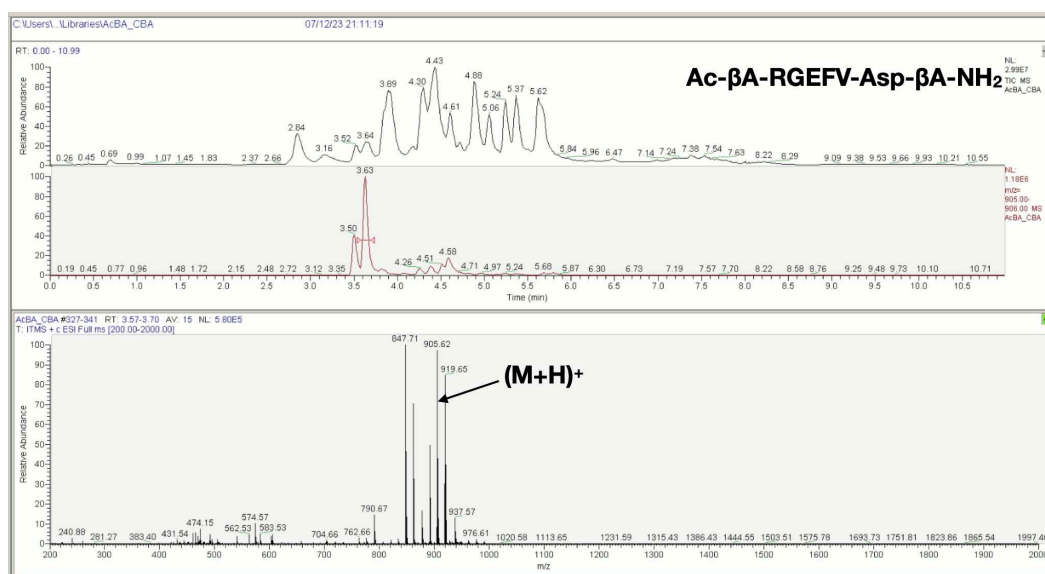
Appendix Figure 55 - LCMS spectra of the Ac-βA-RGEFV-X-βA-NH₂ libraries, where X = Ala.



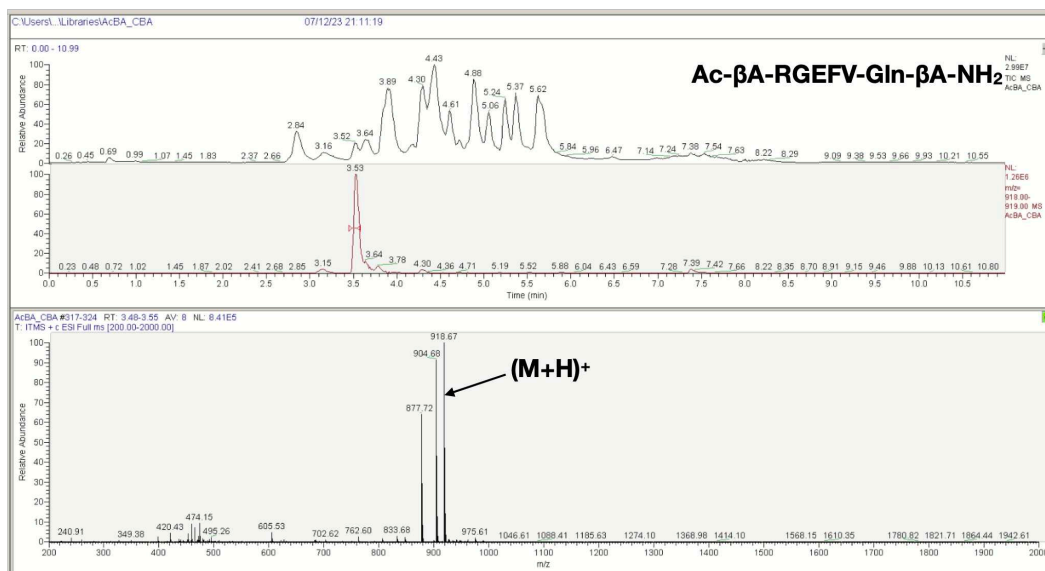
Appendix Figure 56 - LCMS spectra of the Ac-βA-RGEFV-X-βA-NH₂ libraries, where X = Arg.



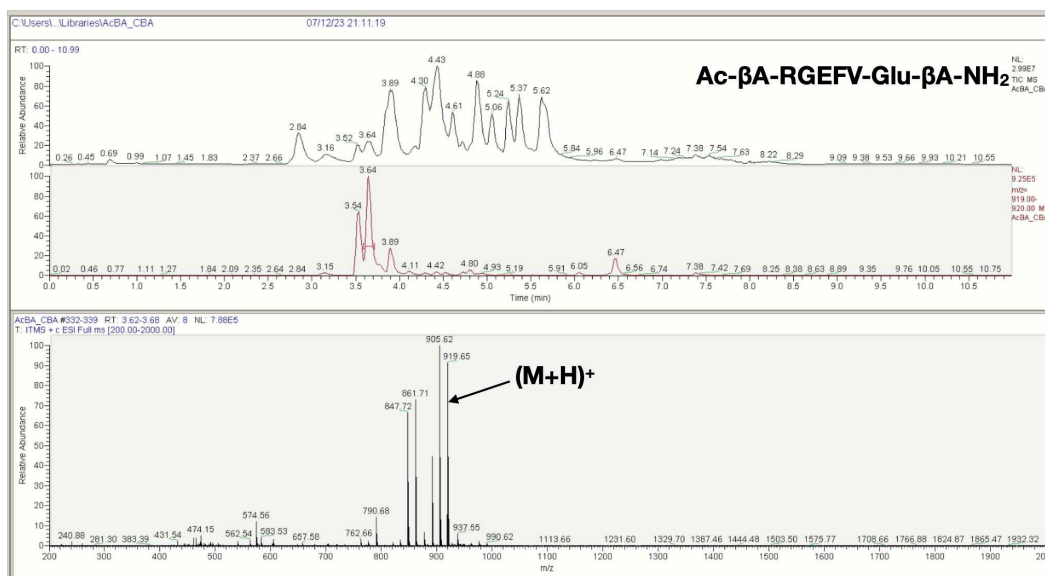
Appendix Figure 57 - LCMS spectra of the Ac-βA-RGEFV-X-βA-NH₂ libraries, where X = Asn.



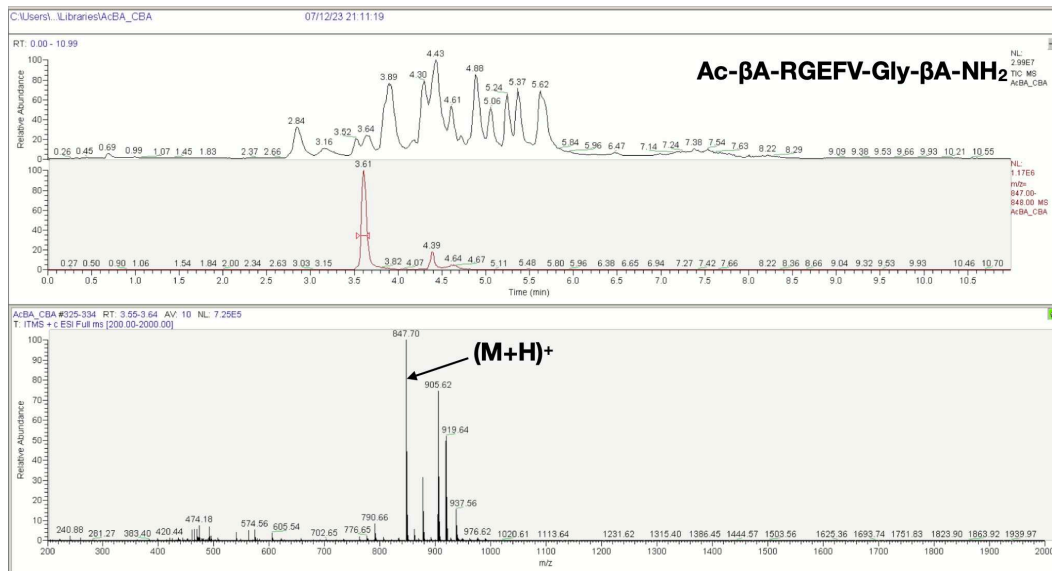
Appendix Figure 58 - LCMS spectra of the Ac-βA-RGEFV-X-βA-NH₂ libraries, where X = Asp.



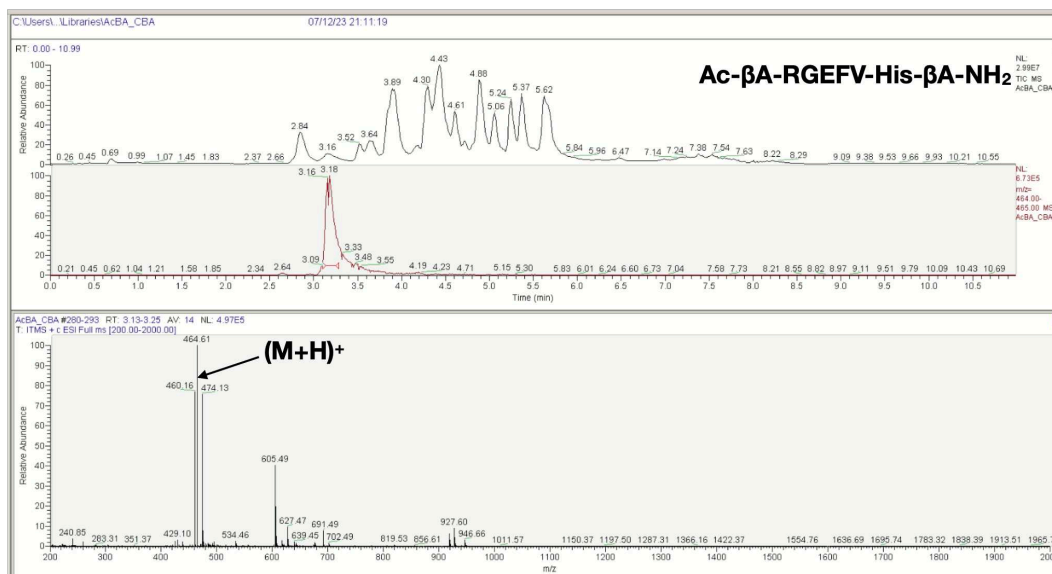
Appendix Figure 59 - LCMS spectra of the Ac-βA-RGEFV-X-βA-NH₂ libraries, where X = Gln.



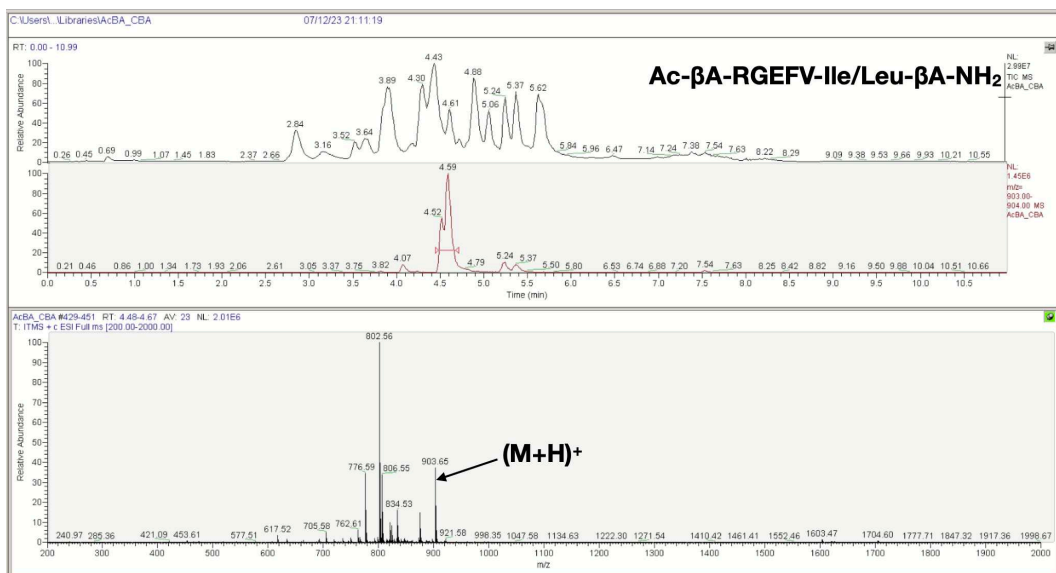
Appendix Figure 60 - LCMS spectra of the Ac-βA-RGEFV-X-βA-NH₂ libraries, where X = Glu.



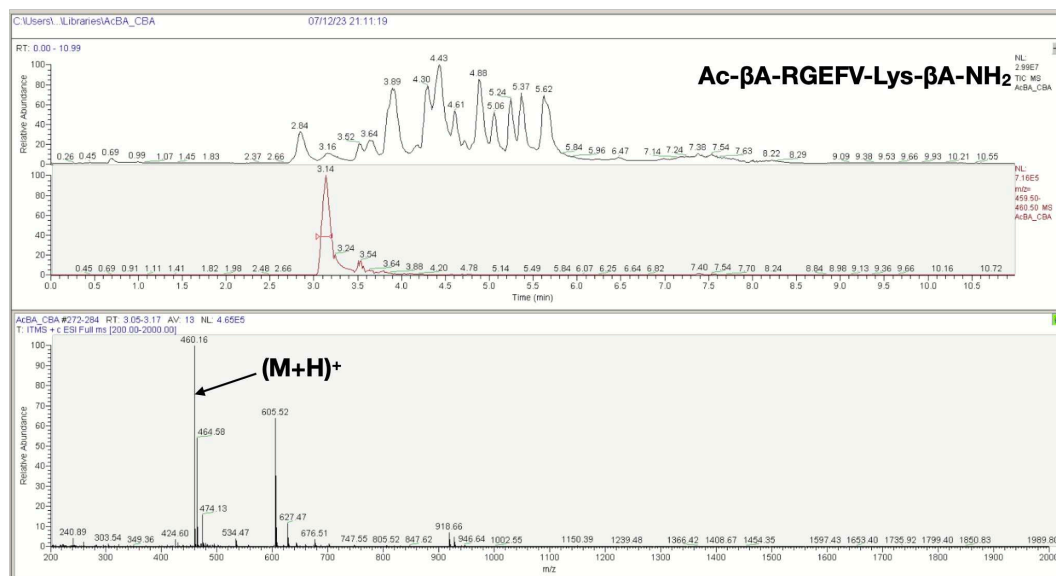
Appendix Figure 61 - LCMS spectra of the Ac-βA-RGEFV-X-βA-NH₂ libraries, where X = Gly.



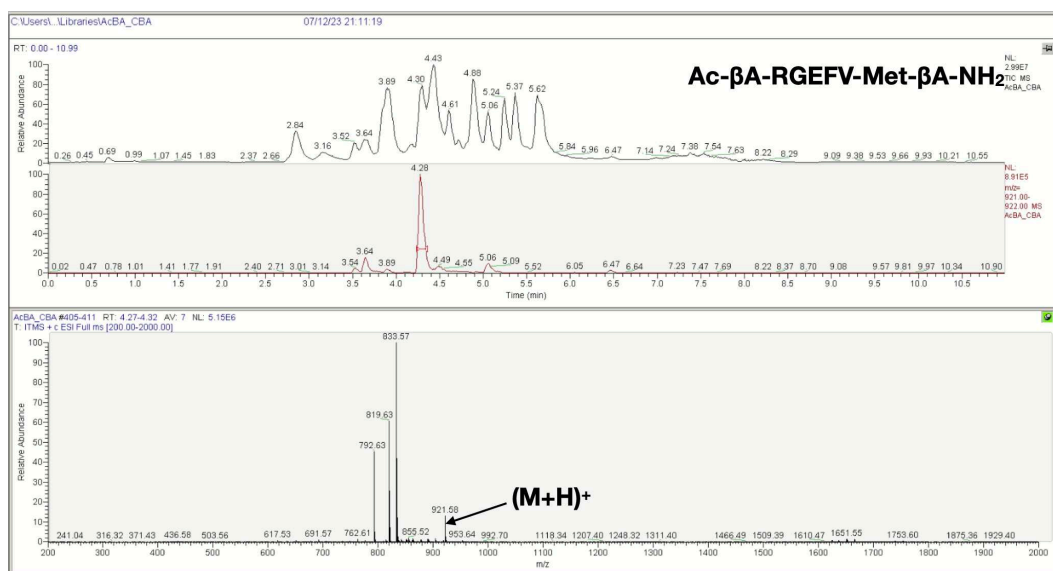
Appendix Figure 62 - LCMS spectra of the Ac-βA-RGEFV-X-βA-NH₂ libraries, where X = His.



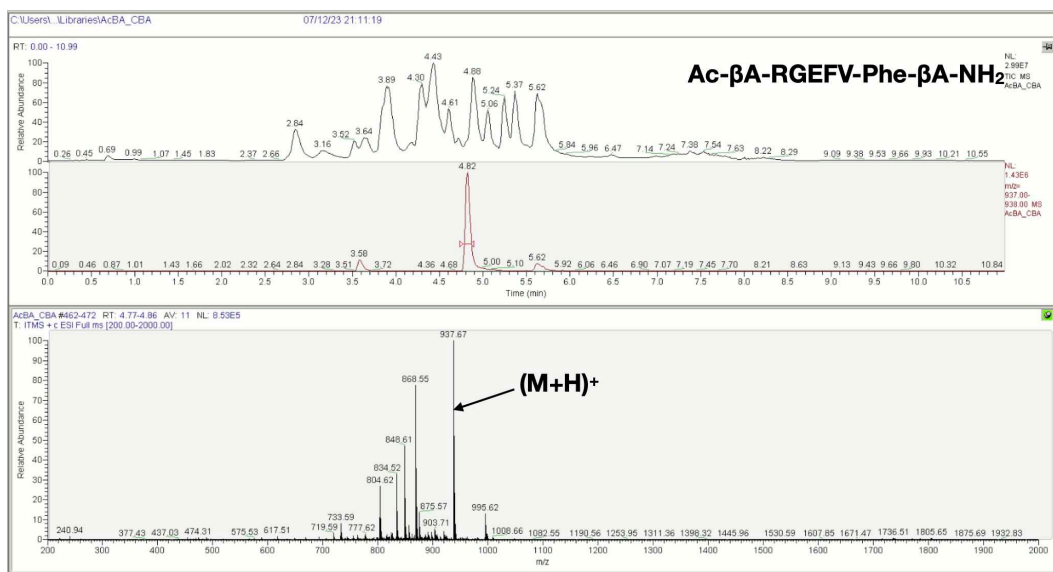
Appendix Figure 63 - LCMS spectra of the Ac-βA-RGEFV-X-βA-NH₂ libraries, where X = Ile/Leu.



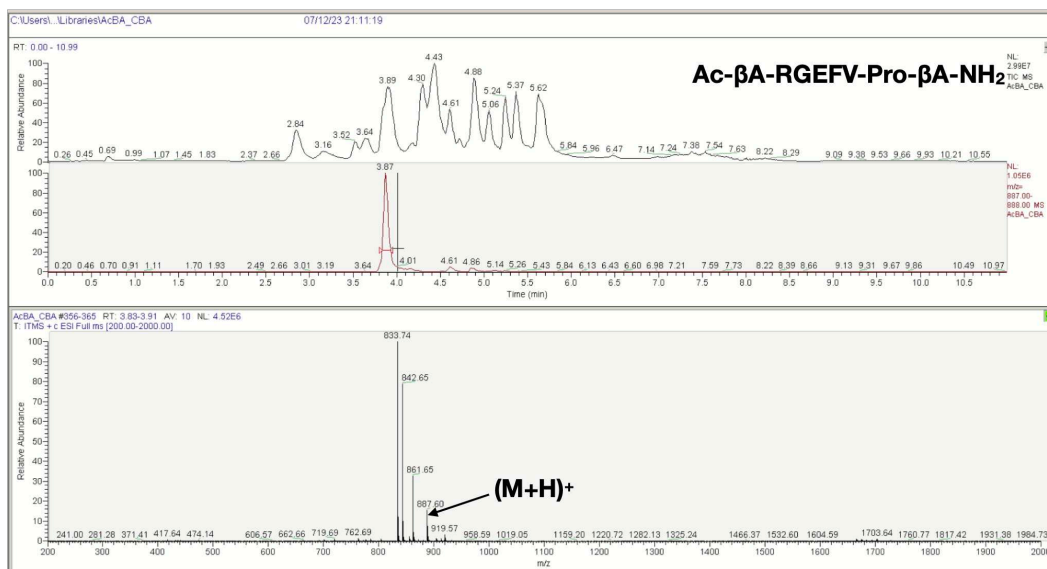
Appendix Figure 64 - LCMS spectra of the Ac-βA-RGEFV-X-βA-NH₂ libraries, where X = Lys.



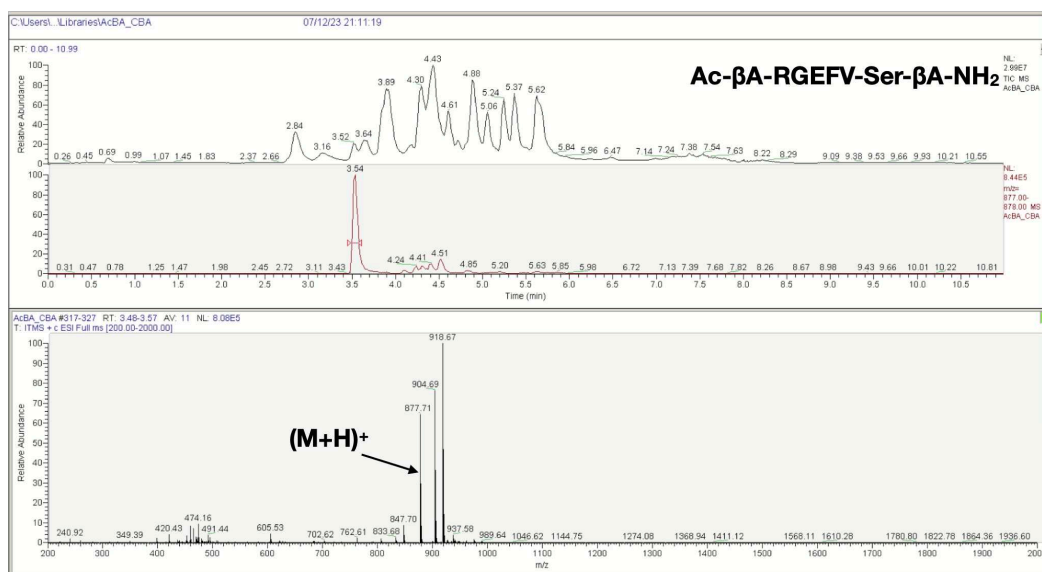
Appendix Figure 65 - LCMS spectra of the Ac-βA-RGEFV-X-βA-NH₂ libraries, where X = Met.



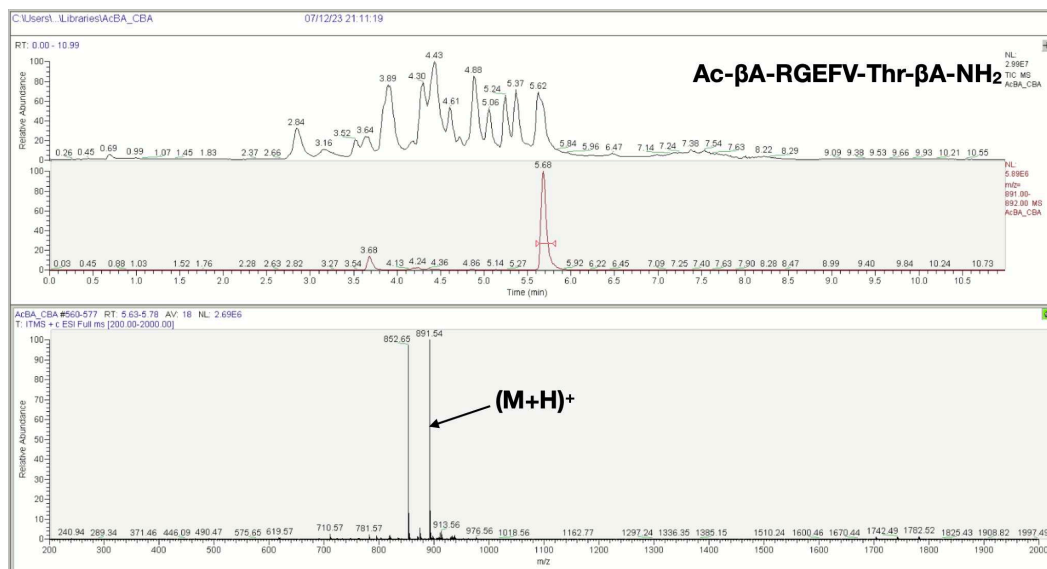
Appendix Figure 66 - LCMS spectra of the Ac-βA-RGEFV-X-βA-NH₂ libraries, where X = Phe.



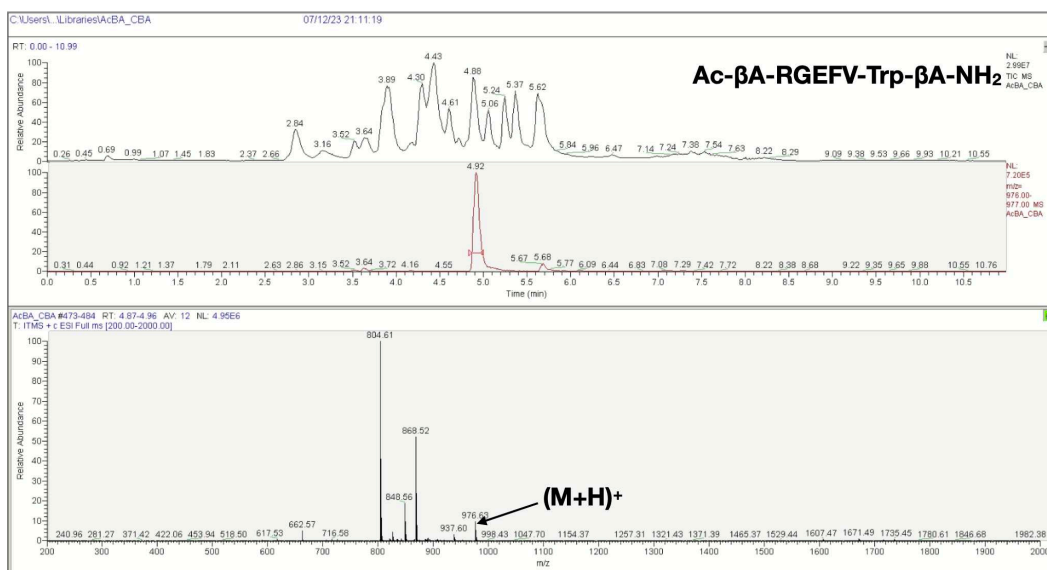
Appendix Figure 67 - LCMS spectra of the Ac-βA-RGEFV-X-βA-NH₂ libraries, where X = Pro.



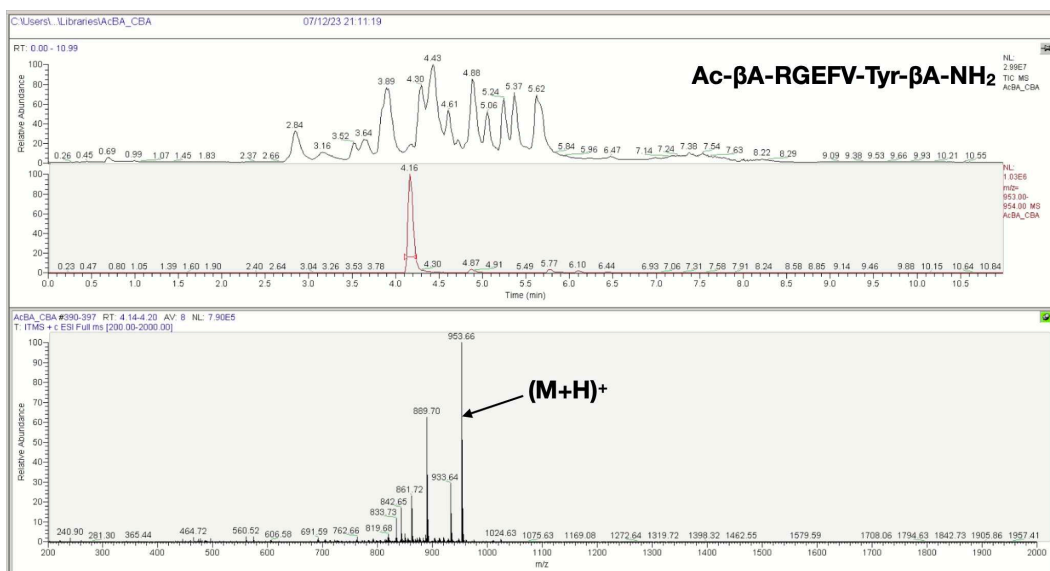
Appendix Figure 68 - LCMS spectra of the Ac-βA-RGEFV-X-βA-NH₂ libraries, where X = Ser.



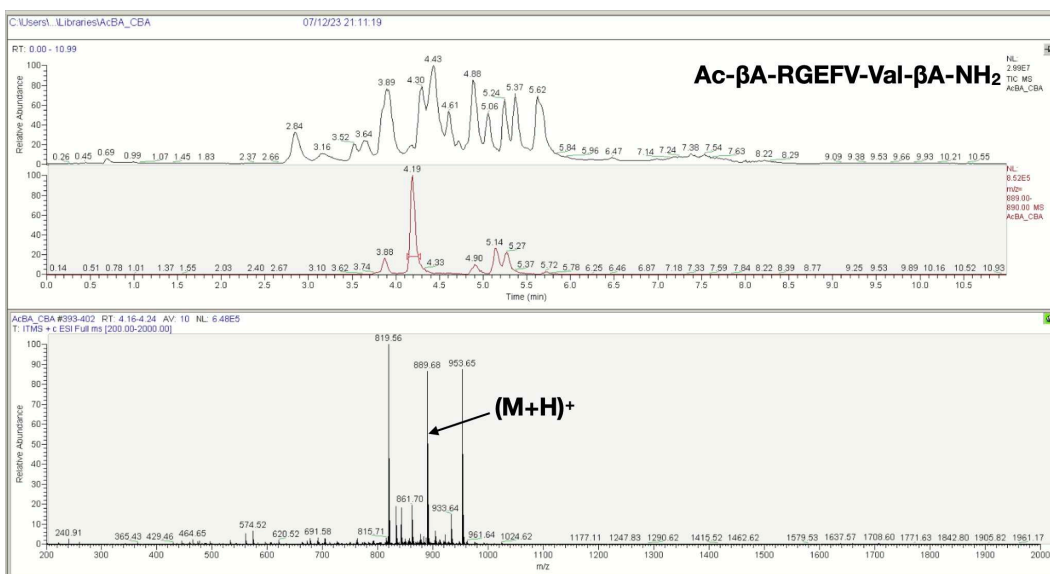
Appendix Figure 69 - LCMS spectra of the Ac-βA-RGEFV-X-βA-NH₂ libraries, where X = Thr.



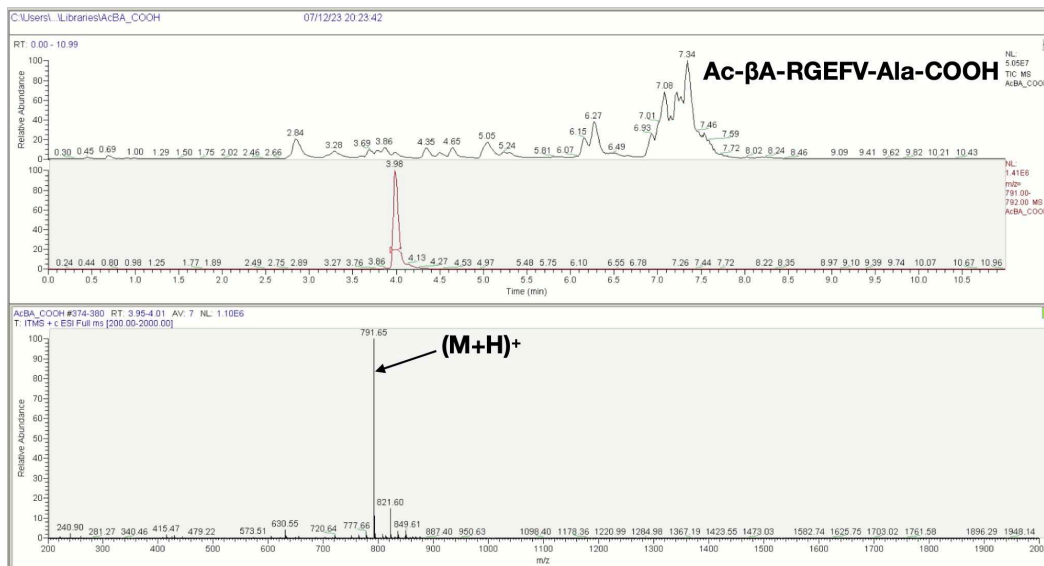
Appendix Figure 70 - LCMS spectra of the Ac-βA-RGEFV-X-βA-NH₂ libraries, where X = Trp.



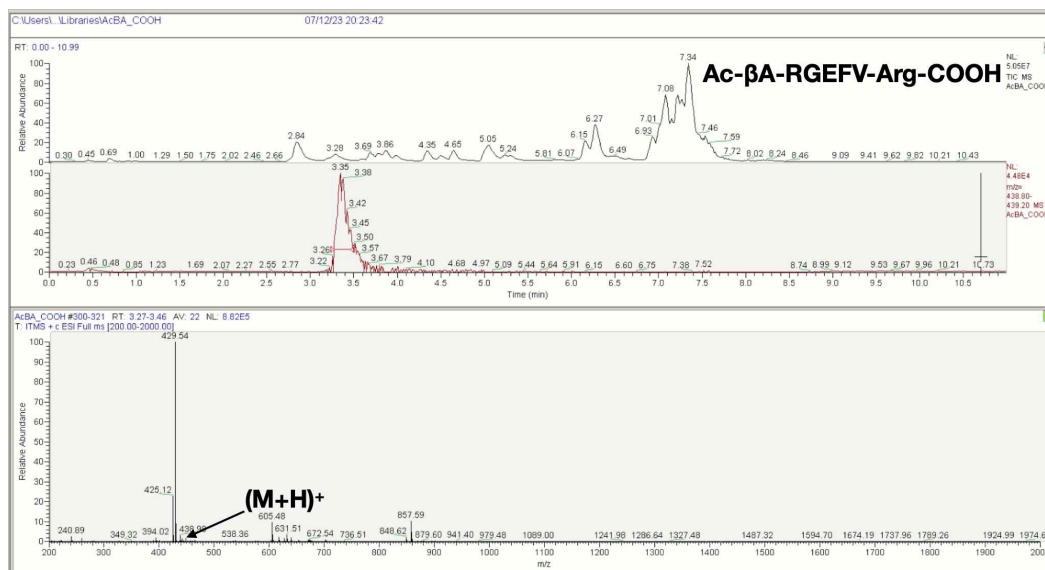
Appendix Figure 71 - LCMS spectra of the Ac-βA-RGEFV-X-βA-NH₂ libraries, where X = Tyr.



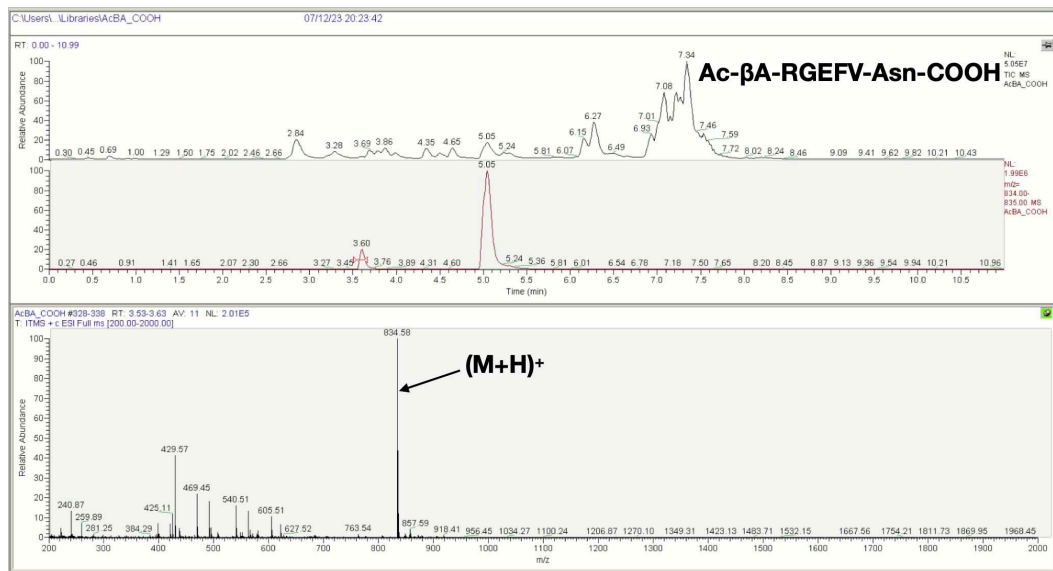
Appendix Figure 72 - LCMS spectra of the Ac-βA-RGEFV-X-βA-NH₂ libraries, where X = Val.



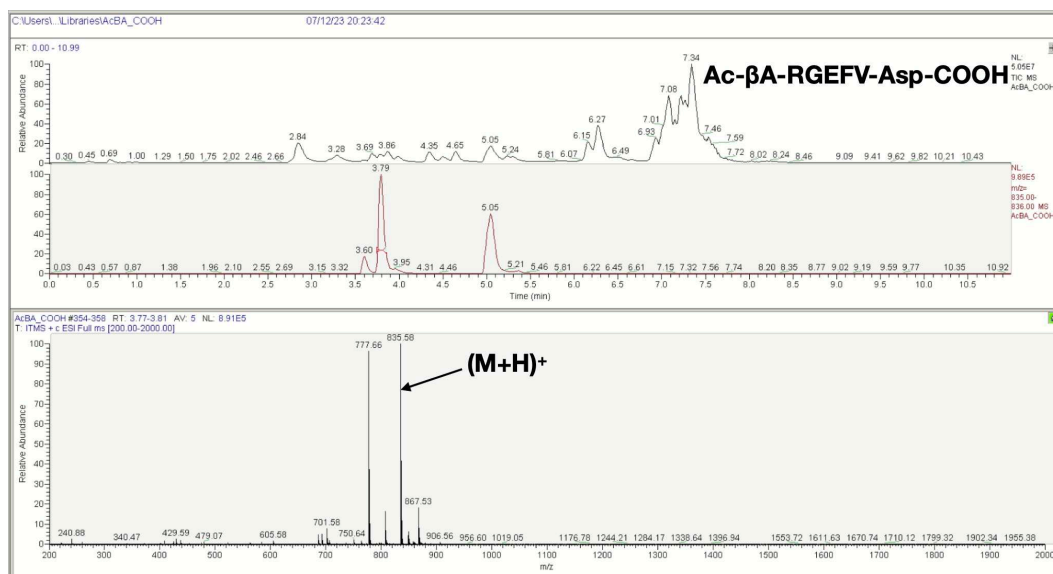
Appendix Figure 73 - LCMS spectra of the Ac-βA-RGEFV-X-COOH libraries, where X = Ala.



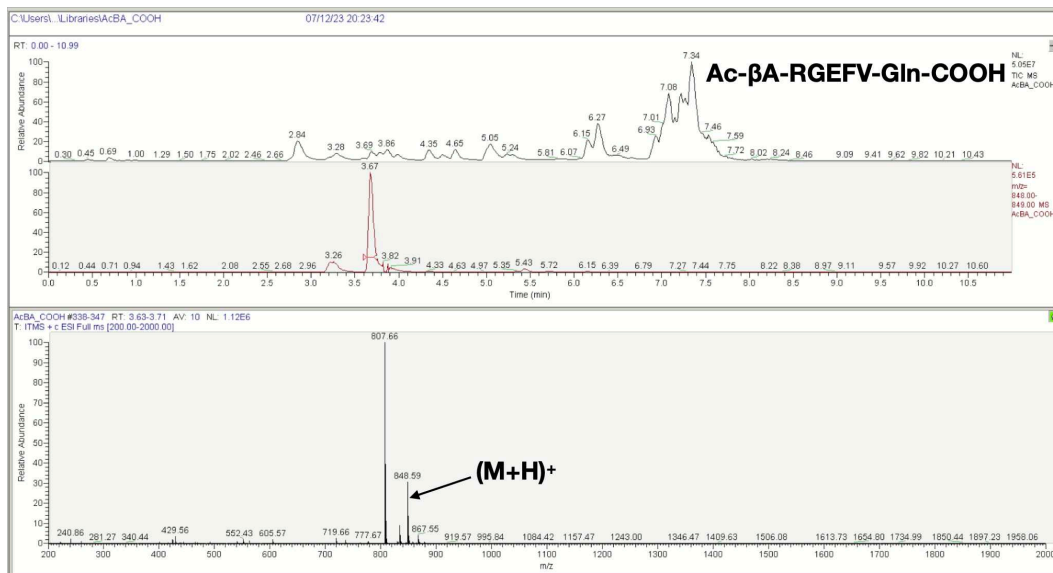
Appendix Figure 74 - LCMS spectra of the Ac-βA-RGEFV-X-COOH libraries, where X = Arg.



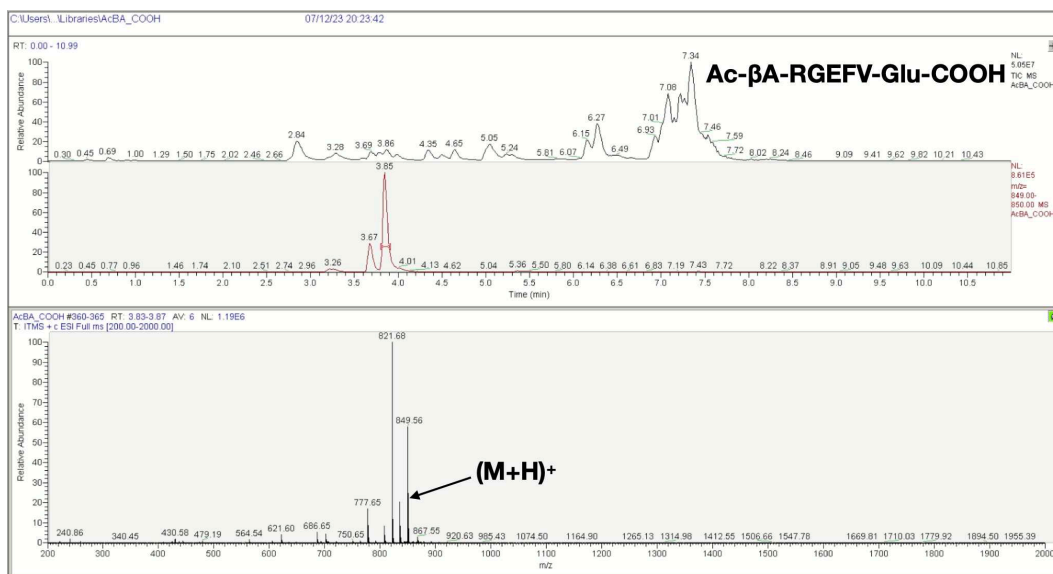
Appendix Figure 75 - LCMS spectra of the Ac-βA-RGEFV-X-COOH libraries, where X = Asn.



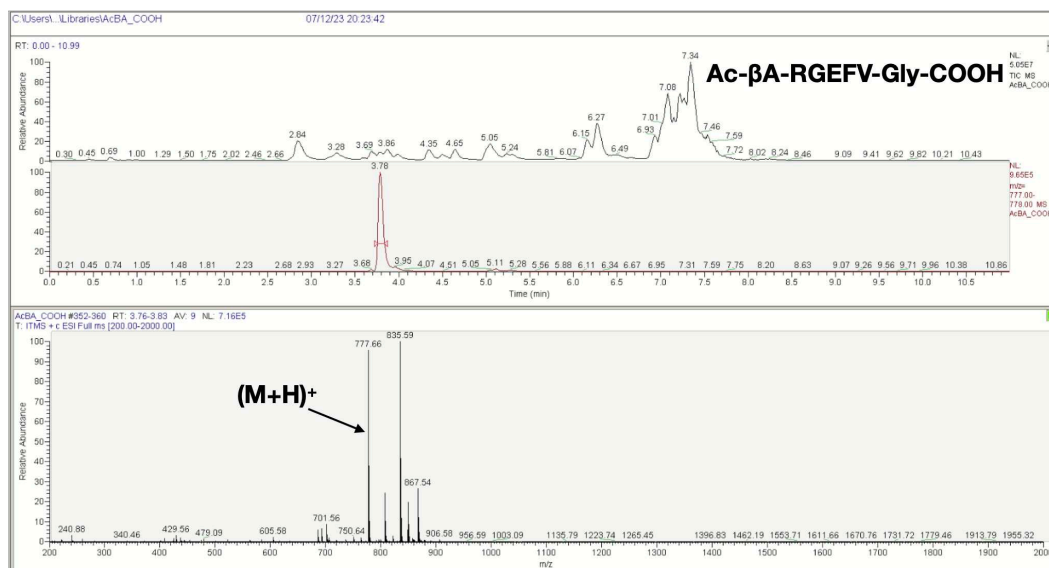
Appendix Figure 76 - LCMS spectra of the Ac-βA-RGEFV-X-COOH libraries, where X = Asp.



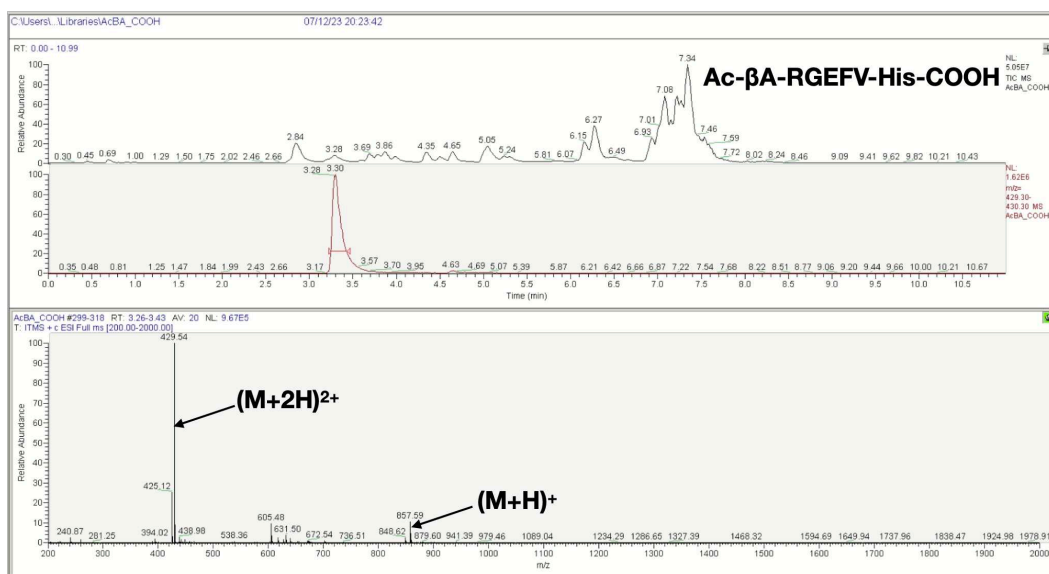
Appendix Figure 77 - LCMS spectra of the Ac-βA-RGEFV-X-COOH libraries, where X = Gln.



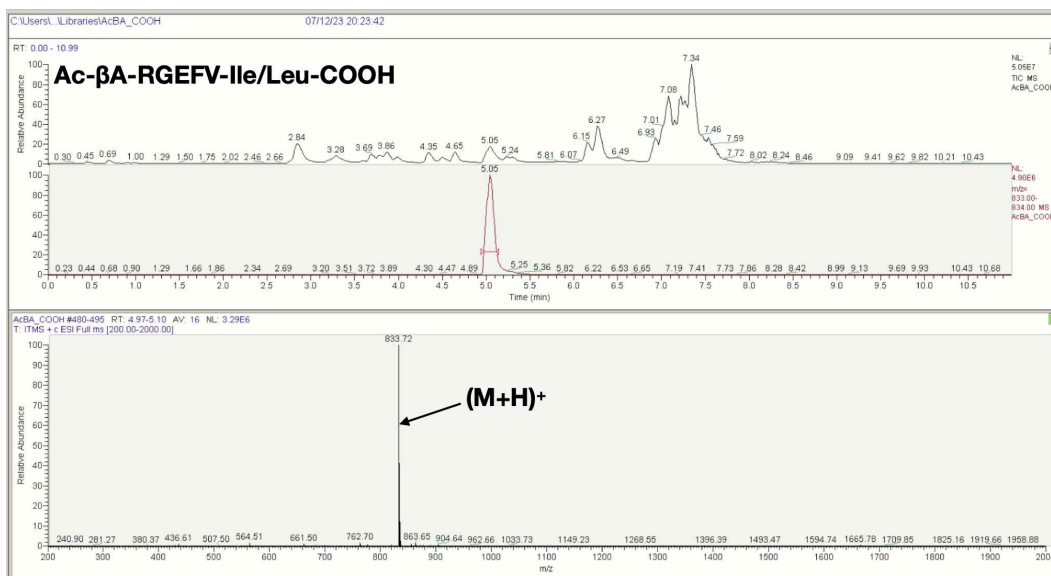
Appendix Figure 78 - LCMS spectra of the Ac-βA-RGEFV-X-COOH libraries, where X = Glu.



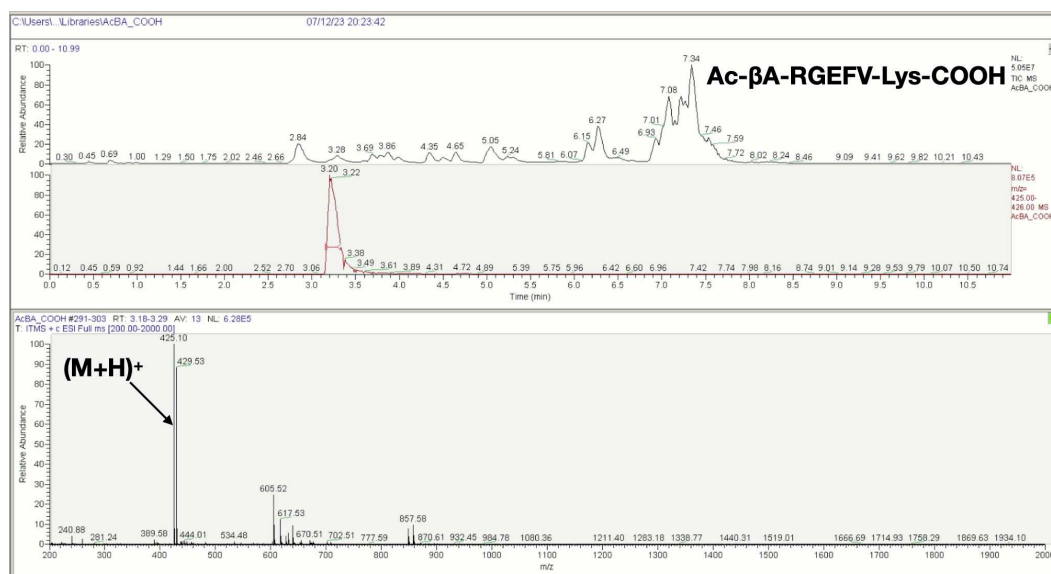
Appendix Figure 79 - LCMS spectra of the Ac-βA-RGEFV-X-COOH libraries, where X = Gly.



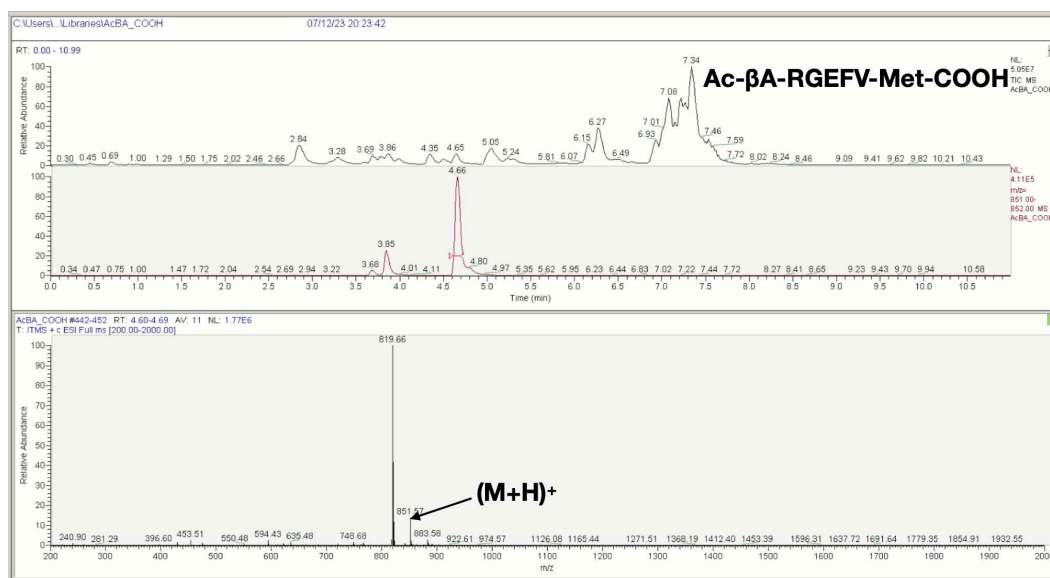
Appendix Figure 80 - LCMS spectra of the Ac-βA-RGEFV-X-COOH libraries, where X = His.



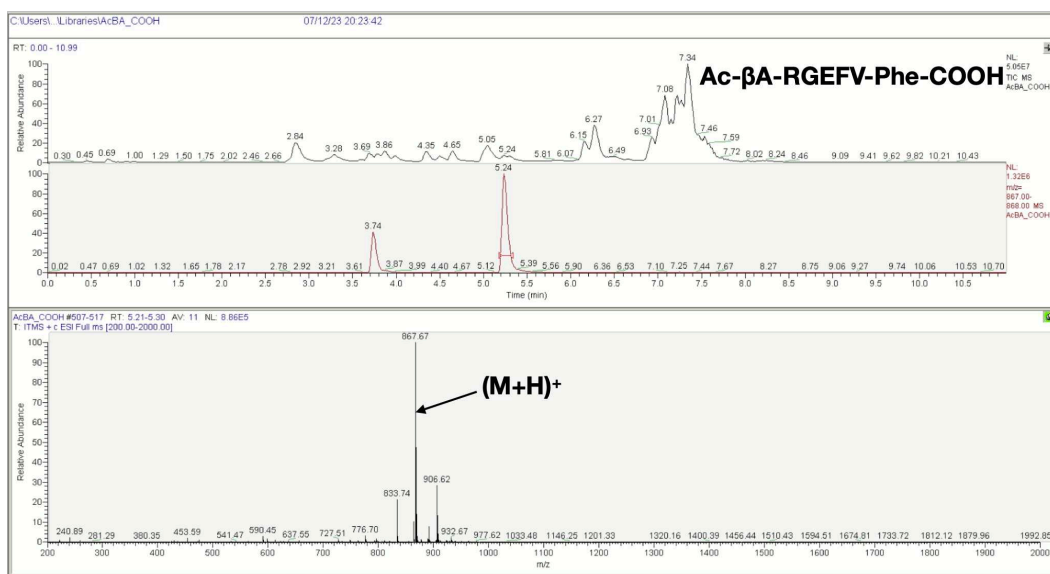
Appendix Figure 81 - LCMS spectra of the Ac-βA-RGEFV-X-COOH libraries, where X = Ile/Leu.



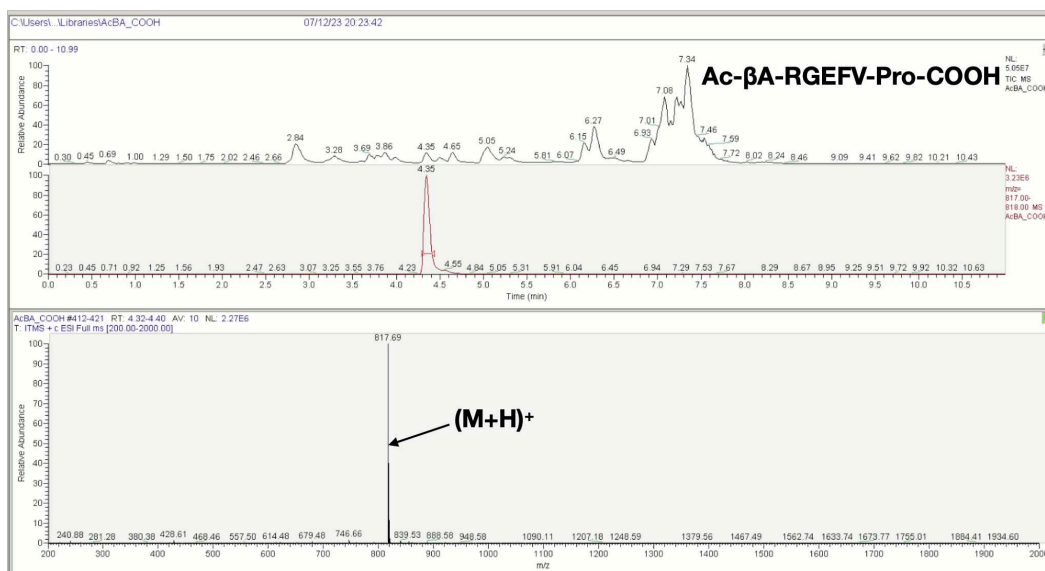
Appendix Figure 82 - LCMS spectra of the Ac-βA-RGEFV-X-COOH libraries, where X = Lys.



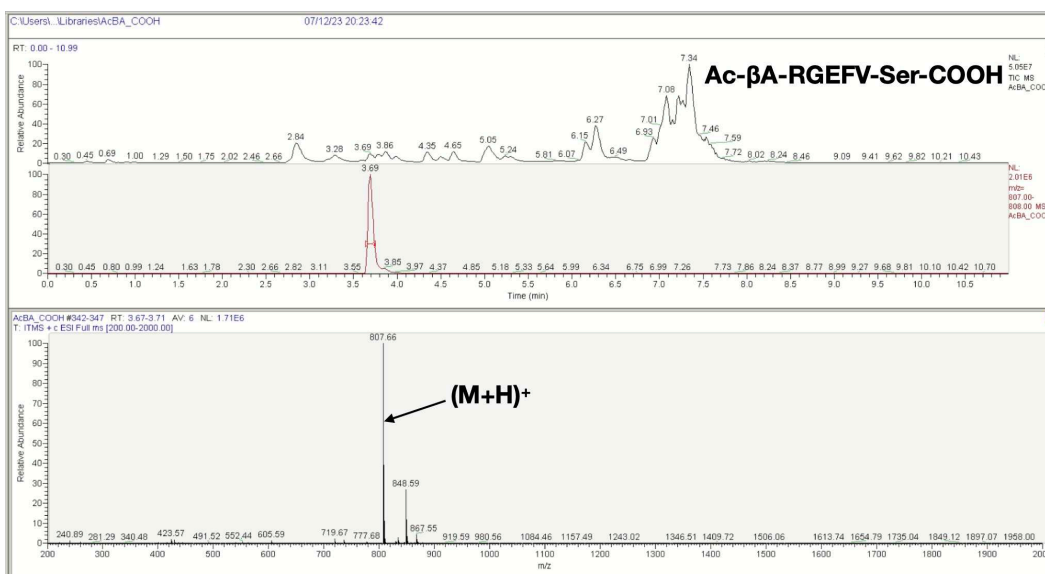
Appendix Figure 83 - LCMS spectra of the Ac-βA-RGEFV-X-COOH libraries, where X = Met.



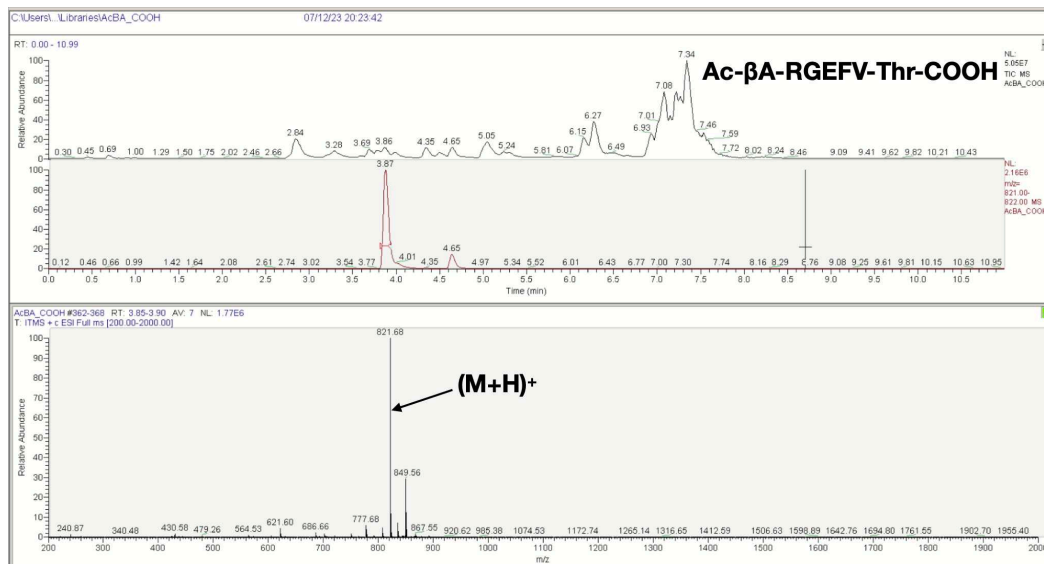
Appendix Figure 84 - LCMS spectra of the Ac-βA-RGEFV-X-COOH libraries, where X = Phe.



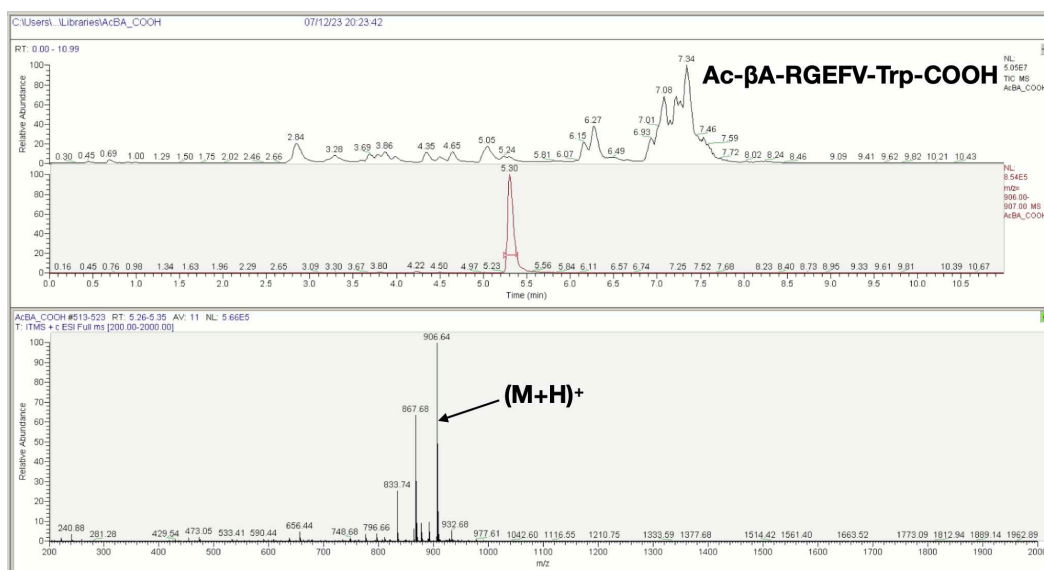
Appendix Figure 85 - LCMS spectra of the Ac- β A-RGEFV-X-COOH libraries, where X = Pro.



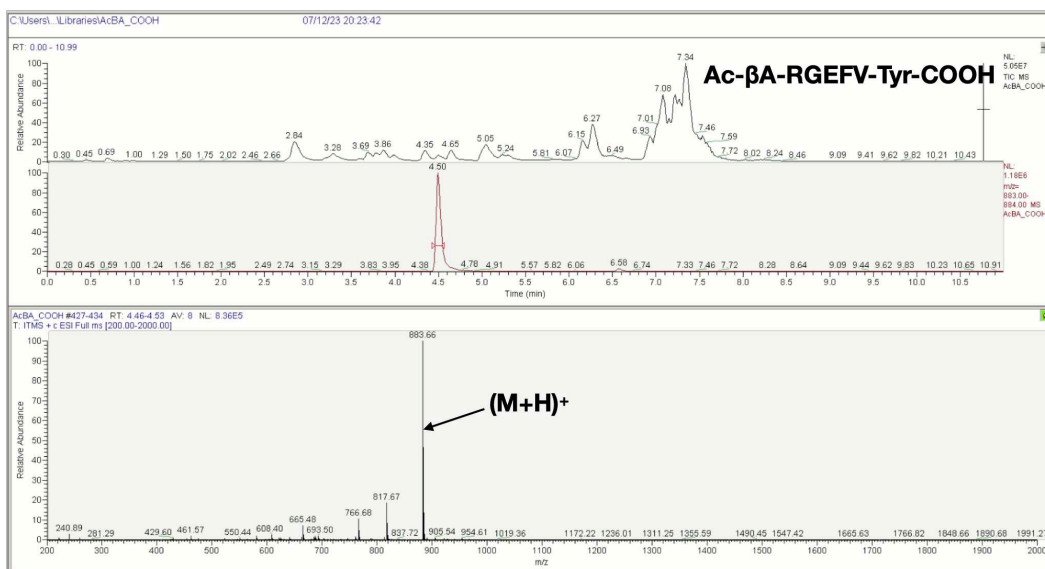
Appendix Figure 86 - LCMS spectra of the Ac- β A-RGEFV-X-COOH libraries, where X = Ser.



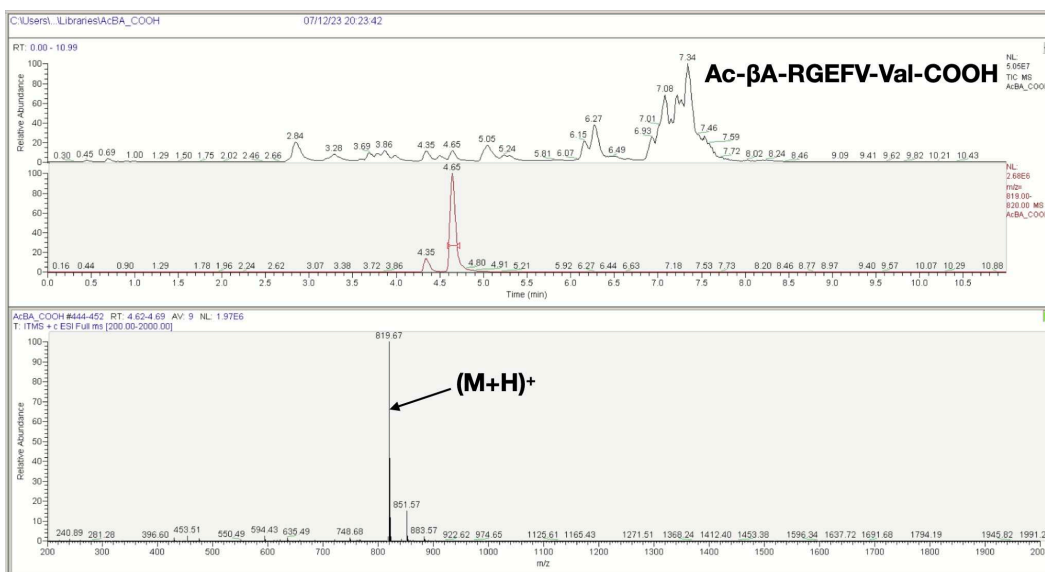
Appendix Figure 87 - LCMS spectra of the Ac-βA-RGEFV-X-COOH libraries, where X = Thr.



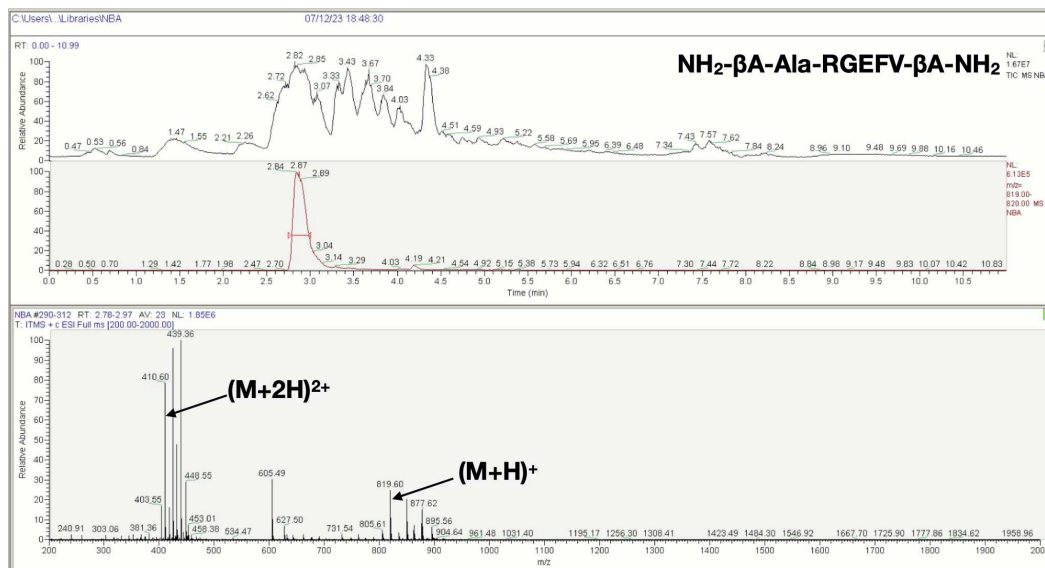
Appendix Figure 88 - LCMS spectra of the Ac-βA-RGEFV-X-COOH libraries, where X = Trp.



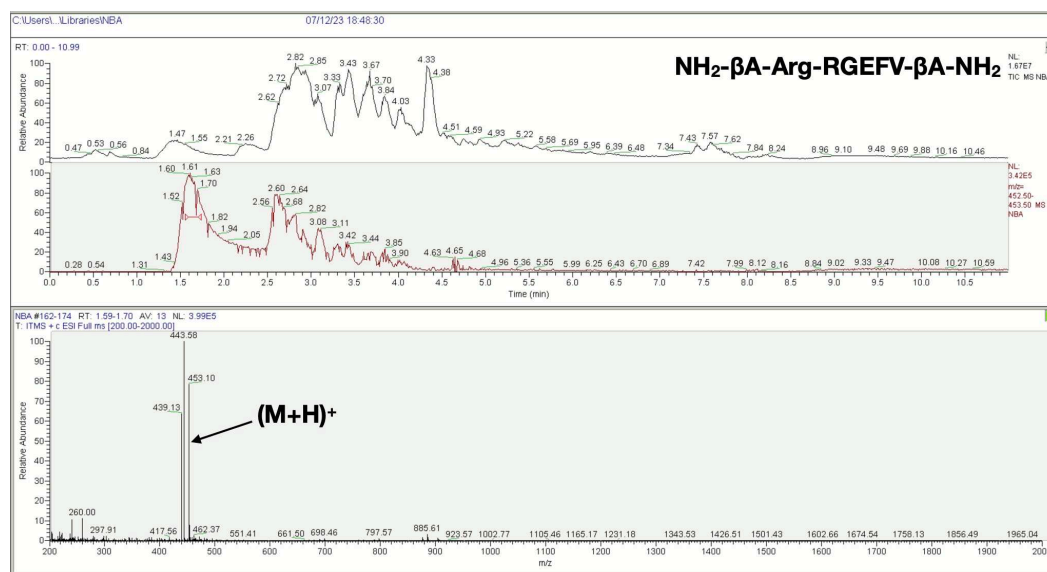
Appendix Figure 89- LCMS spectra of the Ac-βA-RGEFV-X-COOH libraries, where X = Tyr.



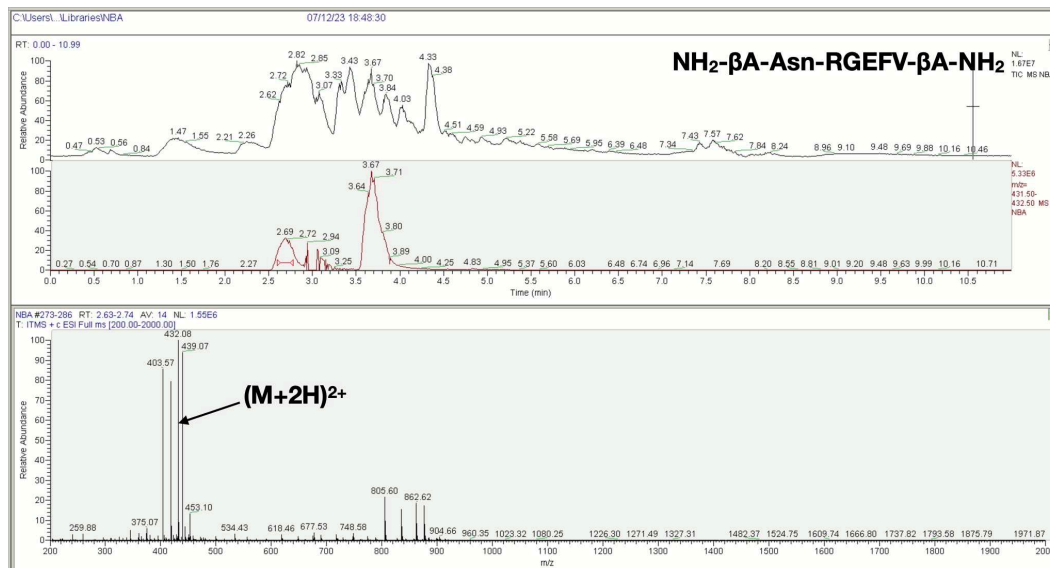
Appendix Figure 90 - LCMS spectra of the Ac-βA-RGEFV-X-COOH libraries, where X = Val.



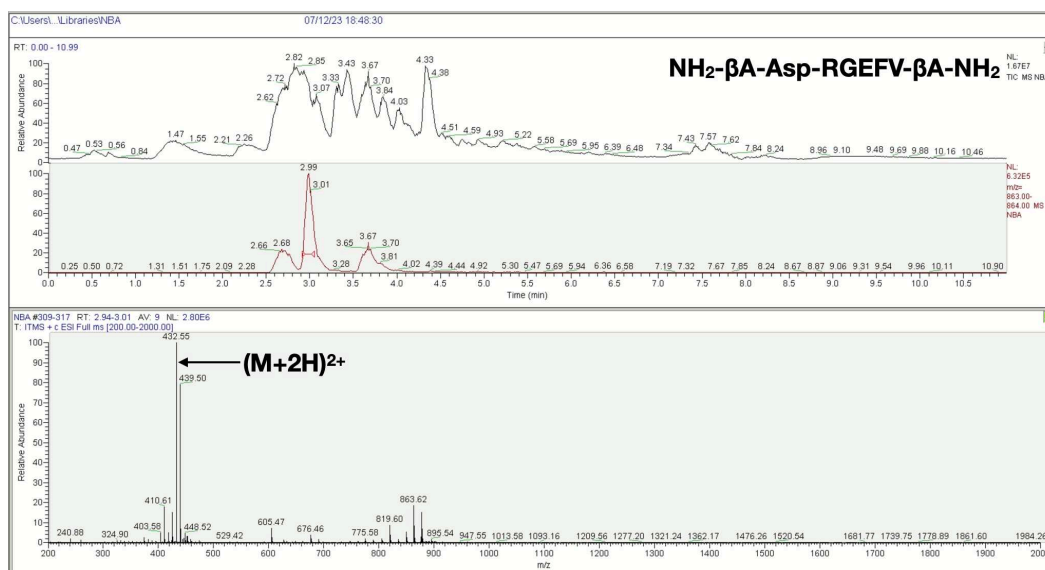
Appendix Figure 91 - LCMS spectra of the $\text{NH}_2\text{-}\beta\text{A-X-RGEFV-}\beta\text{A-NH}_2$ libraries, where X = Ala.



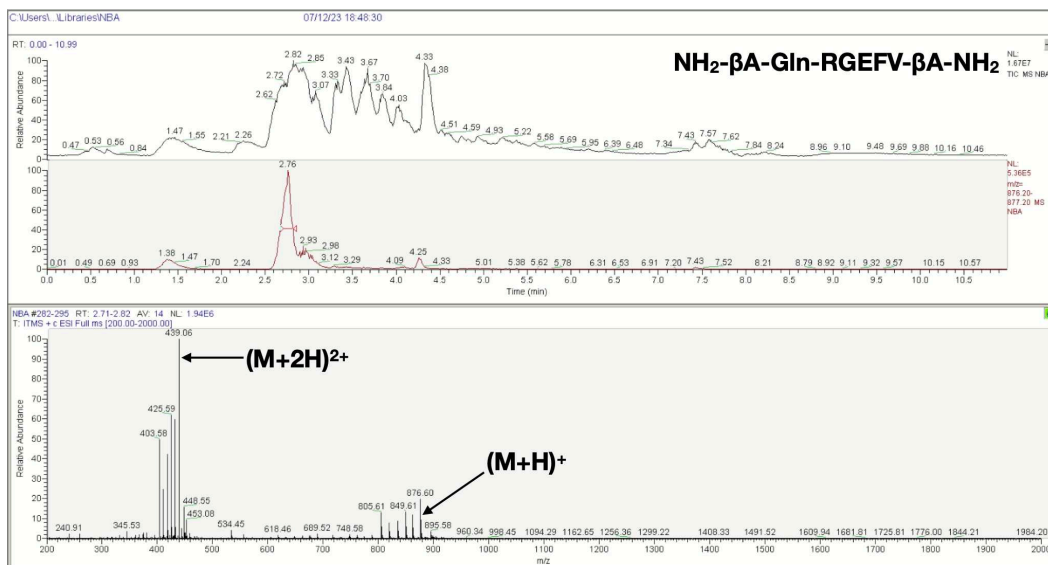
Appendix Figure 92 - LCMS spectra of the $\text{NH}_2\text{-}\beta\text{A-X-RGEFV-}\beta\text{A-NH}_2$ libraries, where X = Arg.



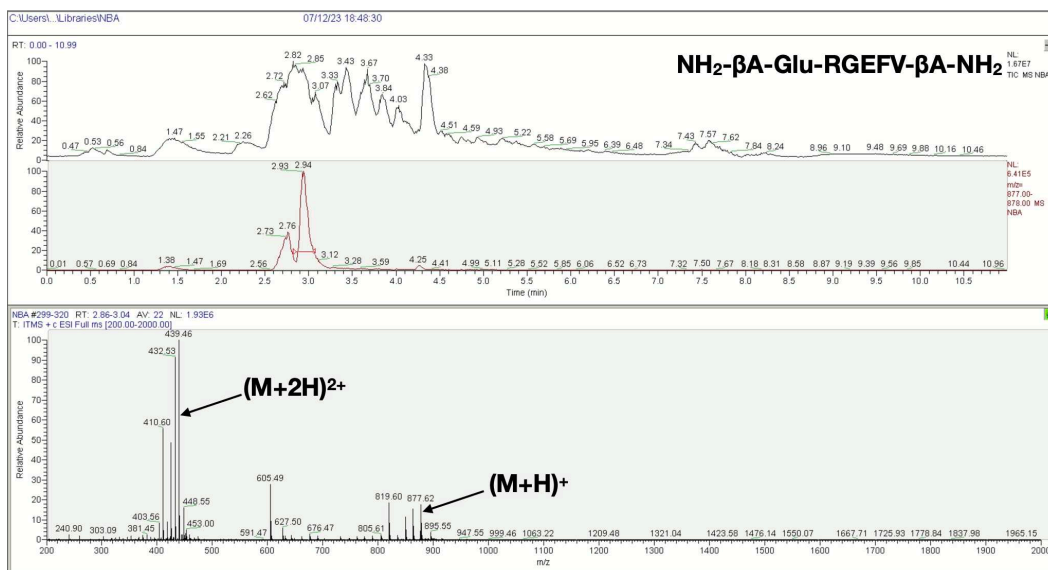
Appendix Figure 93 - LCMS spectra of the $\text{NH}_2\text{-}\beta\text{A-X-RGEFV-}\beta\text{A-NH}_2$ libraries, where X = Asn.



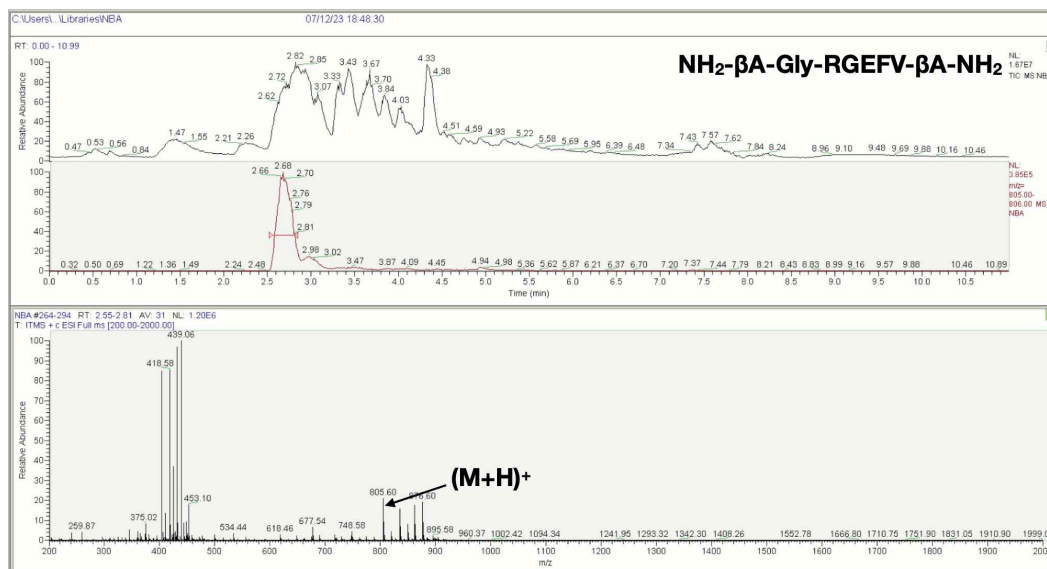
Appendix Figure 94 - LCMS spectra of the $\text{NH}_2\text{-}\beta\text{A-X-RGEFV-}\beta\text{A-NH}_2$ libraries, where X = Asp.



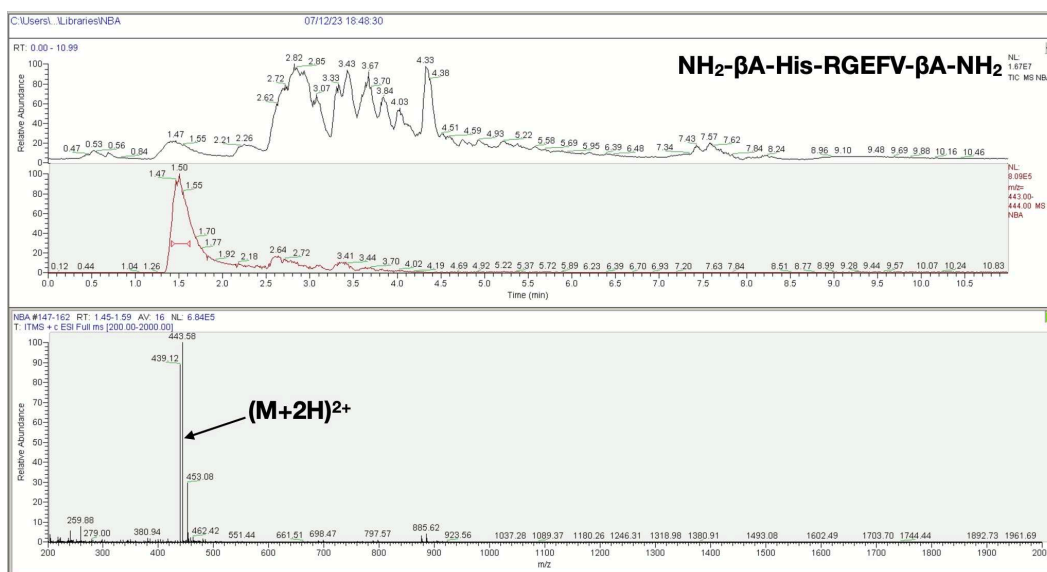
Appendix Figure 95 - LCMS spectra of the NH₂-βA-X-RGEFV-βA-NH₂ libraries, where X = Gln.



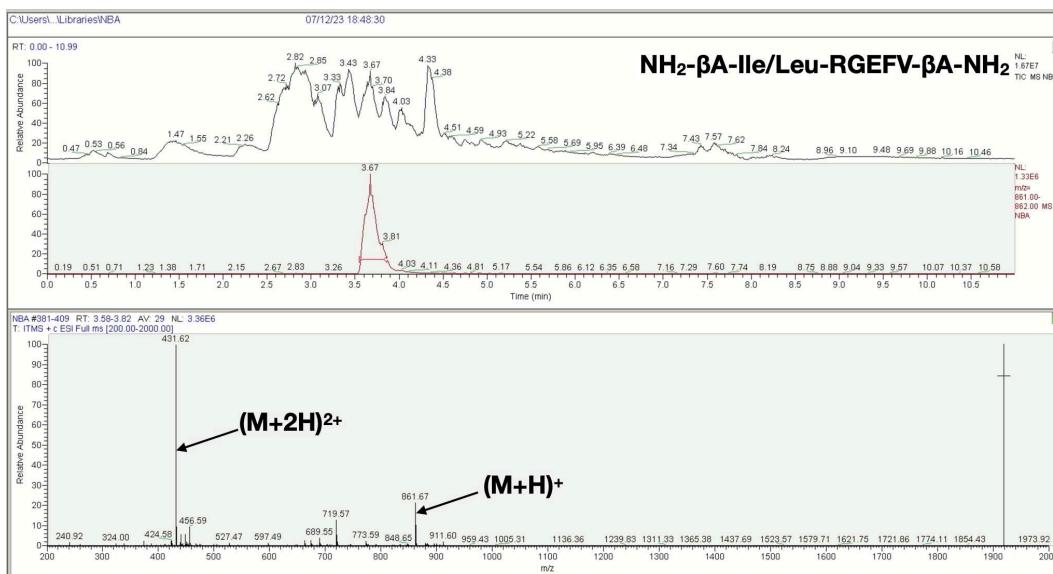
Appendix Figure 96 - LCMS spectra of the NH₂-βA-X-RGEFV-βA-NH₂ libraries, where X = Glu.



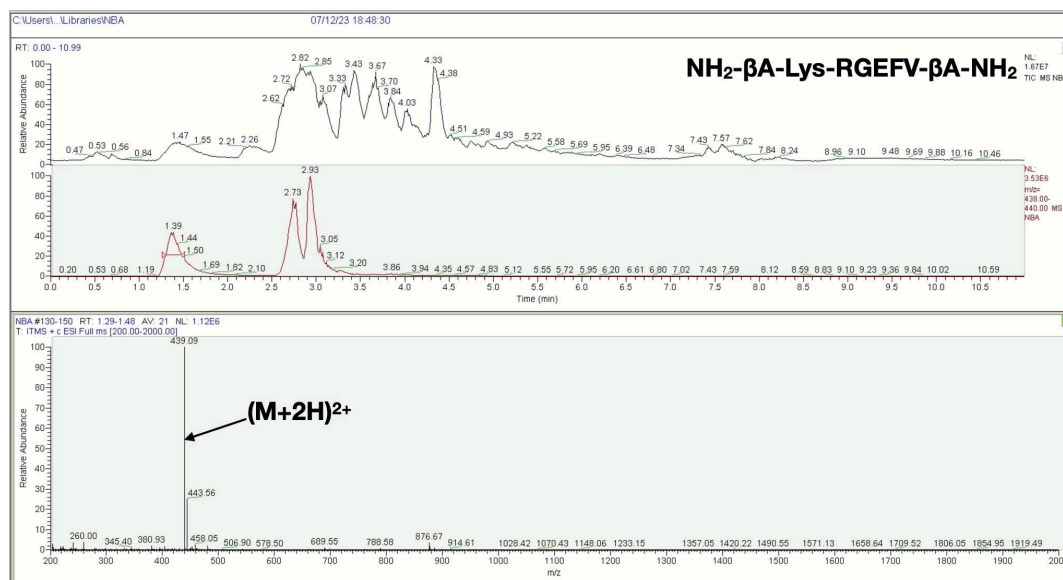
Appendix Figure 97 - LCMS spectra of the NH₂-βA-X-RGEFV-βA-NH₂ libraries, where X = Gly.



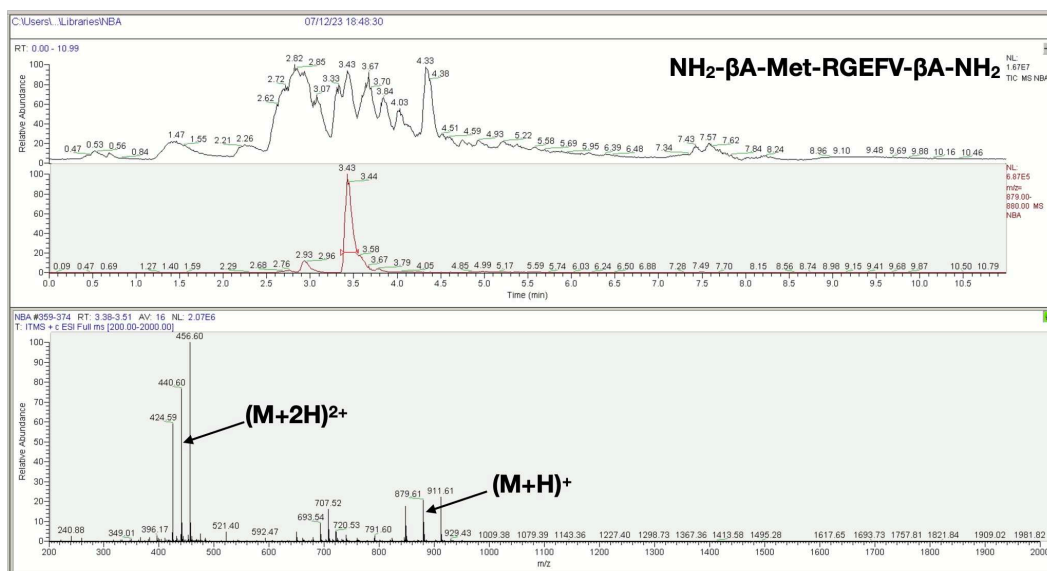
Appendix Figure 98 - LCMS spectra of the NH₂-βA-X-RGEFV-βA-NH₂ libraries, where X = His.



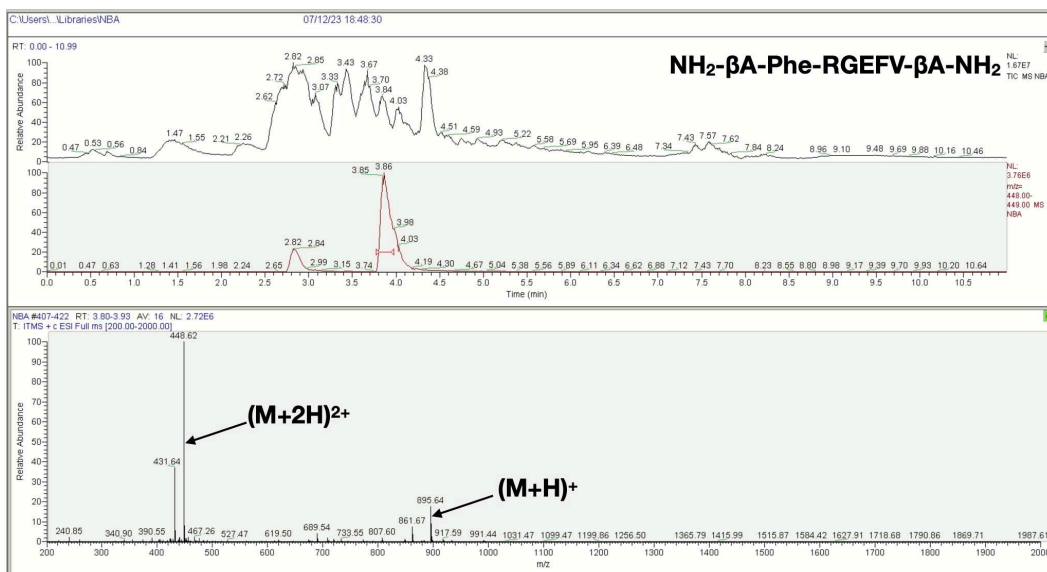
Appendix Figure 99 - LCMS spectra of the NH₂-βA-X-RGEFV-βA-NH₂ libraries, where X = Ile/Leu.



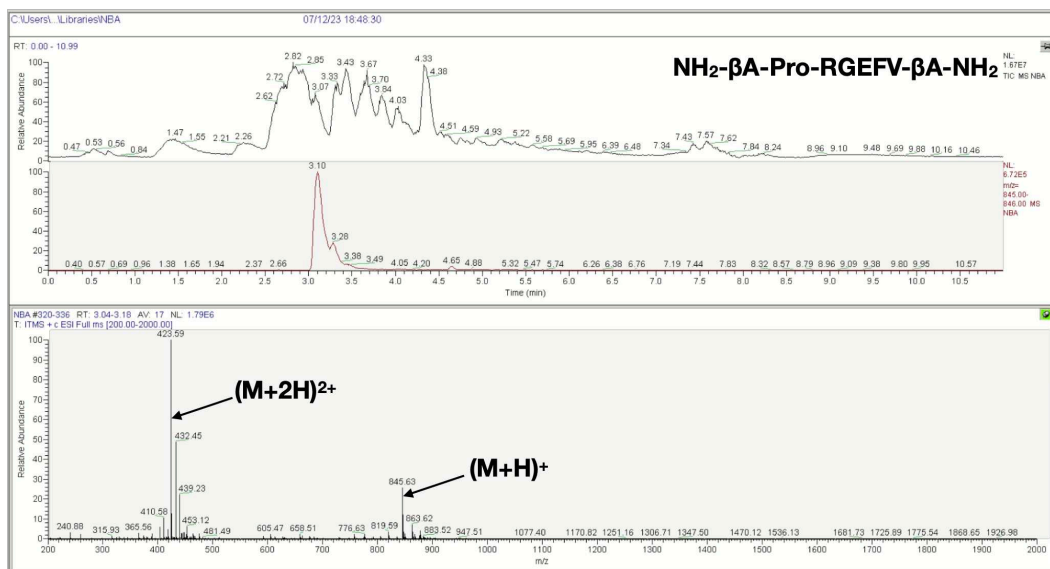
Appendix Figure 100 - LCMS spectra of the NH₂-βA-X-RGEFV-βA-NH₂ libraries, where X = Lys.



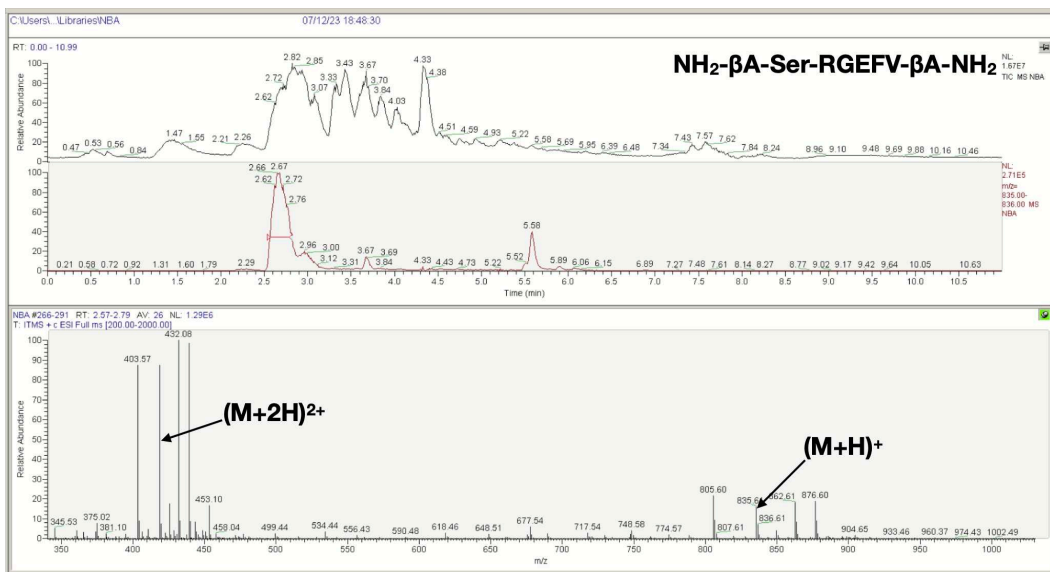
Appendix Figure 101 - LCMS spectra of the NH₂-βA-X-RGEFV-βA-NH₂ libraries, where X = Met.



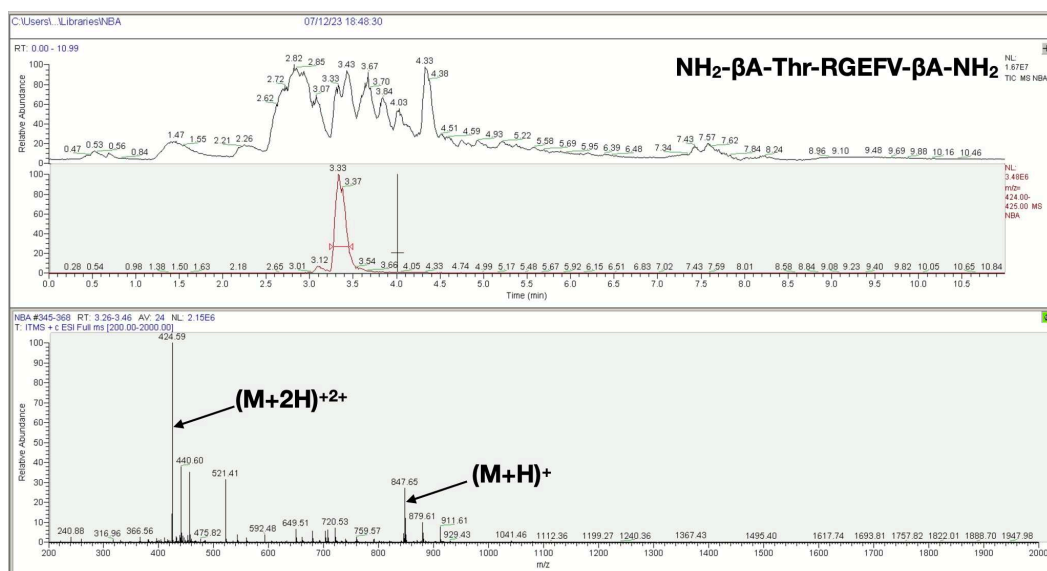
Appendix Figure 102 - LCMS spectra of the NH₂-βA-X-RGEFV-βA-NH₂ libraries, where X = Phe.



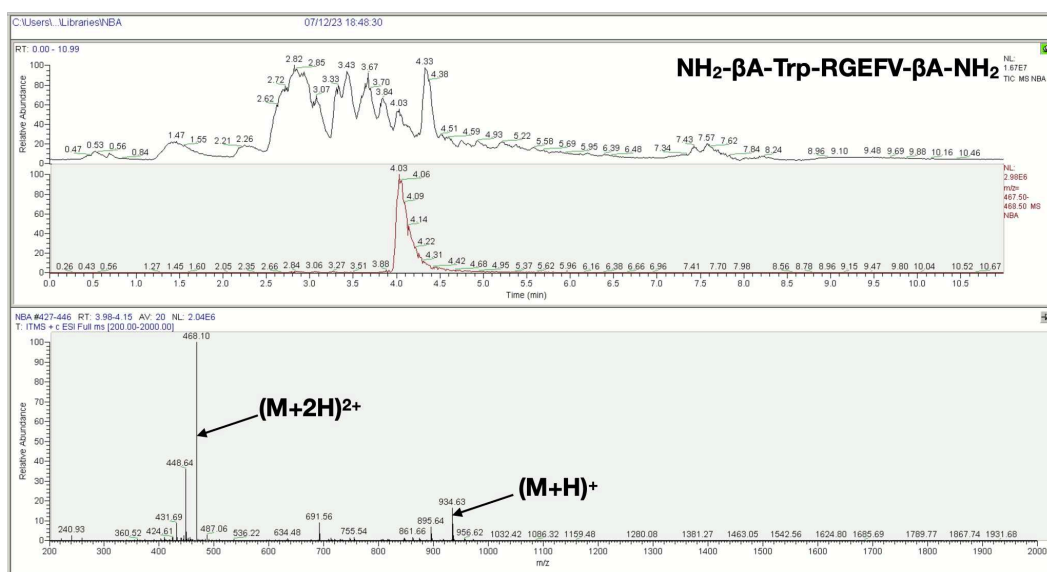
Appendix Figure 103 - LCMS spectra of the $\text{NH}_2\text{-}\beta\text{A-X-RGEFV-}\beta\text{A-NH}_2$ libraries, where X = Pro.



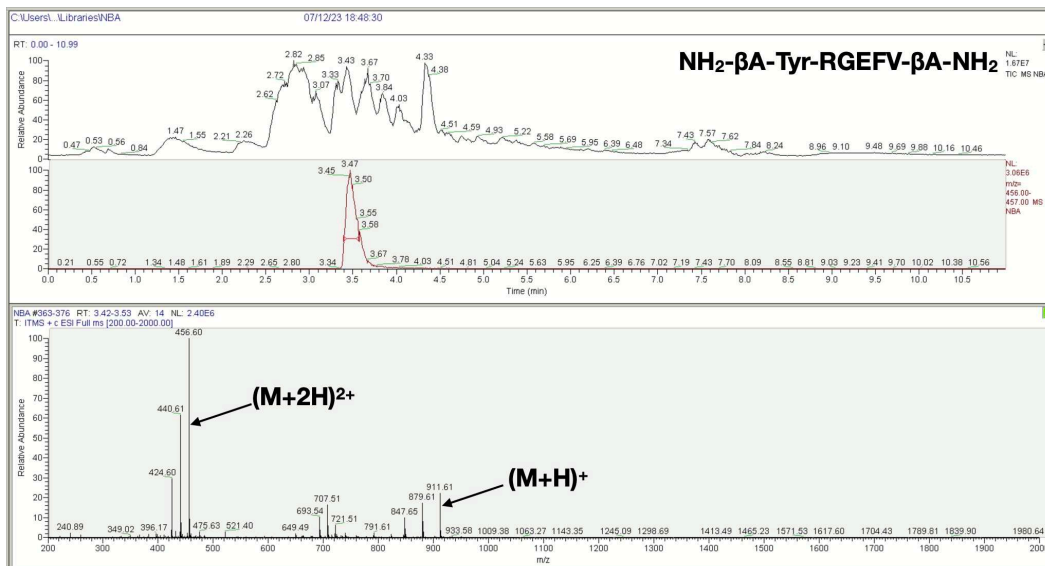
Appendix Figure 104 - LCMS spectra of the $\text{NH}_2\text{-}\beta\text{A-X-RGEFV-}\beta\text{A-NH}_2$ libraries, where X = Ser.



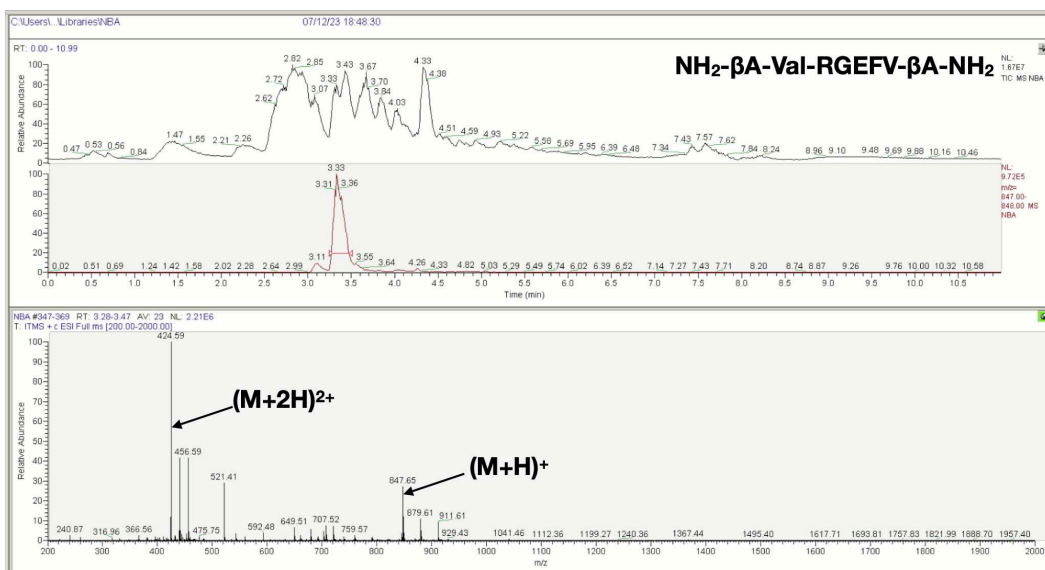
Appendix Figure 105 - LCMS spectra of the $\text{NH}_2\text{-}\beta\text{A-X-RGEFV-}\beta\text{A-NH}_2$ libraries, where X = Thr.



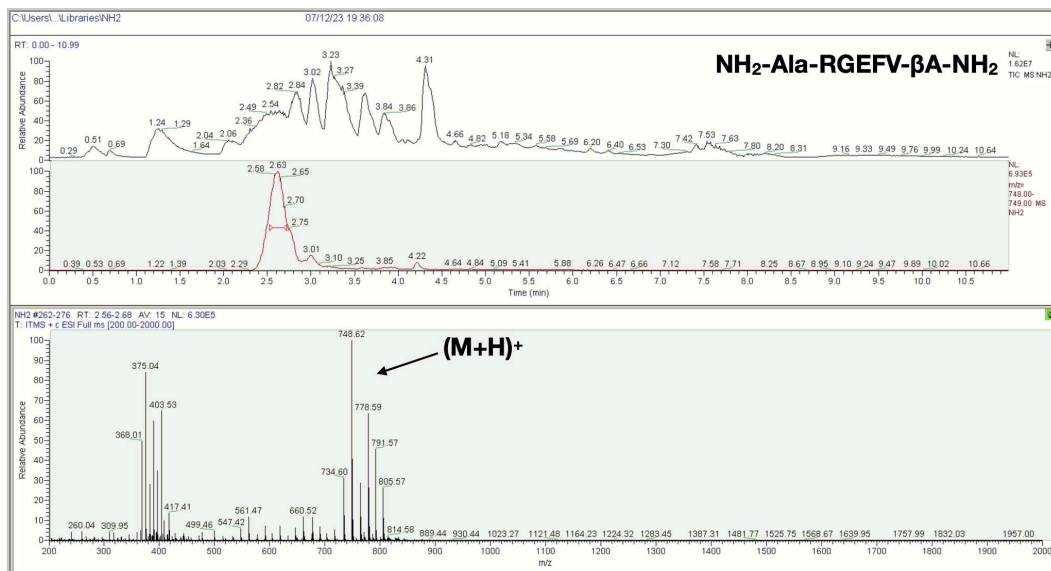
Appendix Figure 106 - LCMS spectra of the $\text{NH}_2\text{-}\beta\text{A-X-RGEFV-}\beta\text{A-NH}_2$ libraries, where X = Trp.



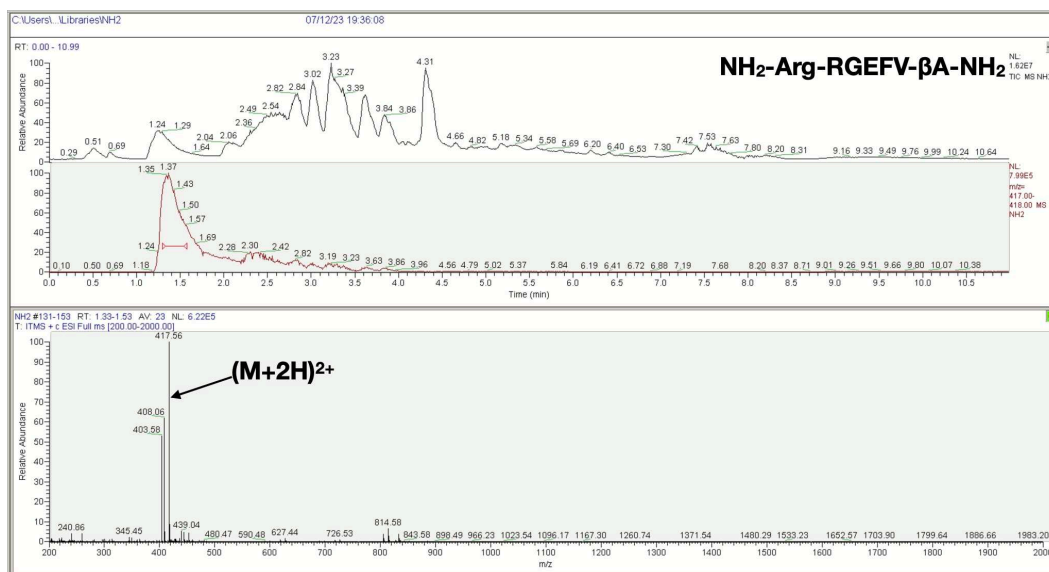
Appendix Figure 107 - LCMS spectra of the $\text{NH}_2\text{-}\beta\text{A-X-RGEFV-}\beta\text{A-NH}_2$ libraries, where X = q) Tyr.



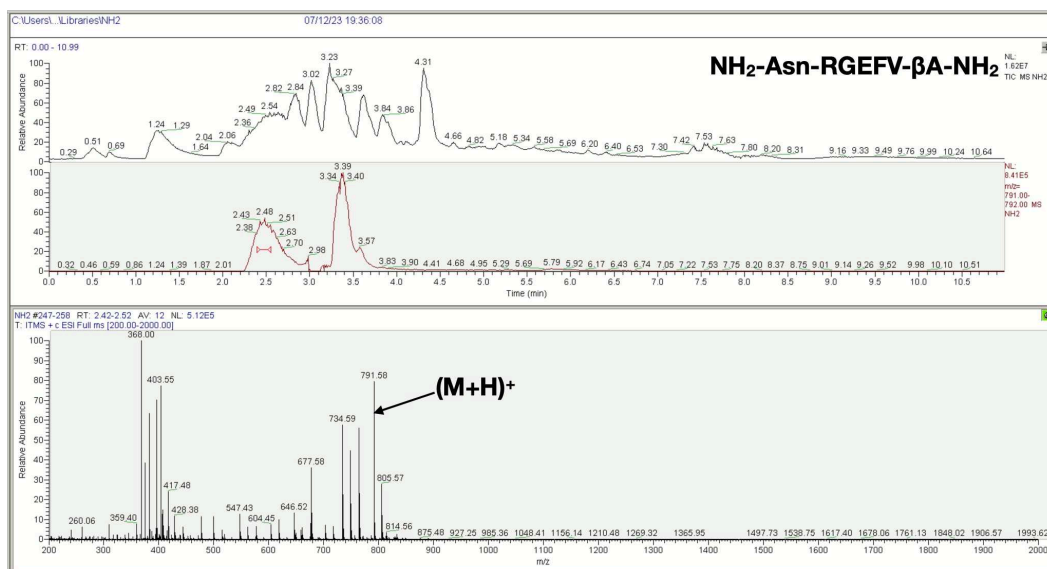
Appendix Figure 108 - LCMS spectra of the $\text{NH}_2\text{-}\beta\text{A-X-RGEFV-}\beta\text{A-NH}_2$ libraries, where X = Val.



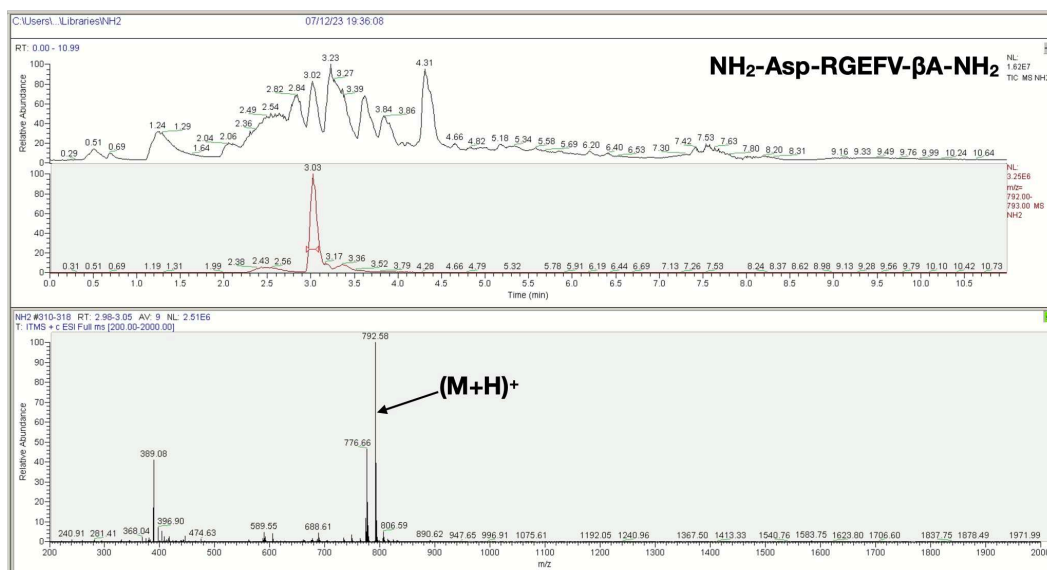
Appendix Figure 109 - LCMS spectra of the NH₂-X-RGEFV-βA-NH₂ libraries, where X = Ala.



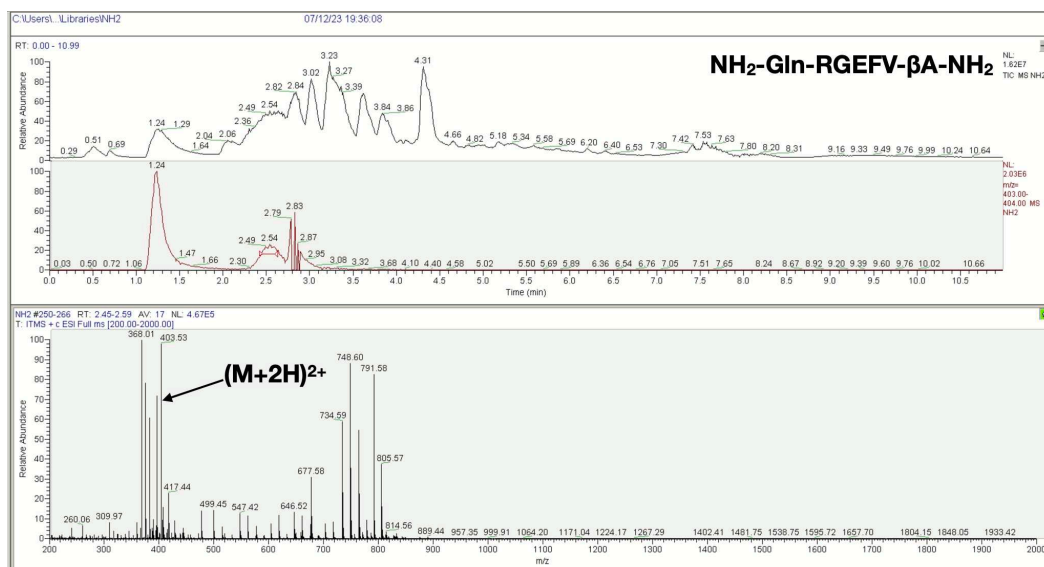
Appendix Figure 110 - LCMS spectra of the NH₂-X-RGEFV-βA-NH₂ libraries, where X = Arg.



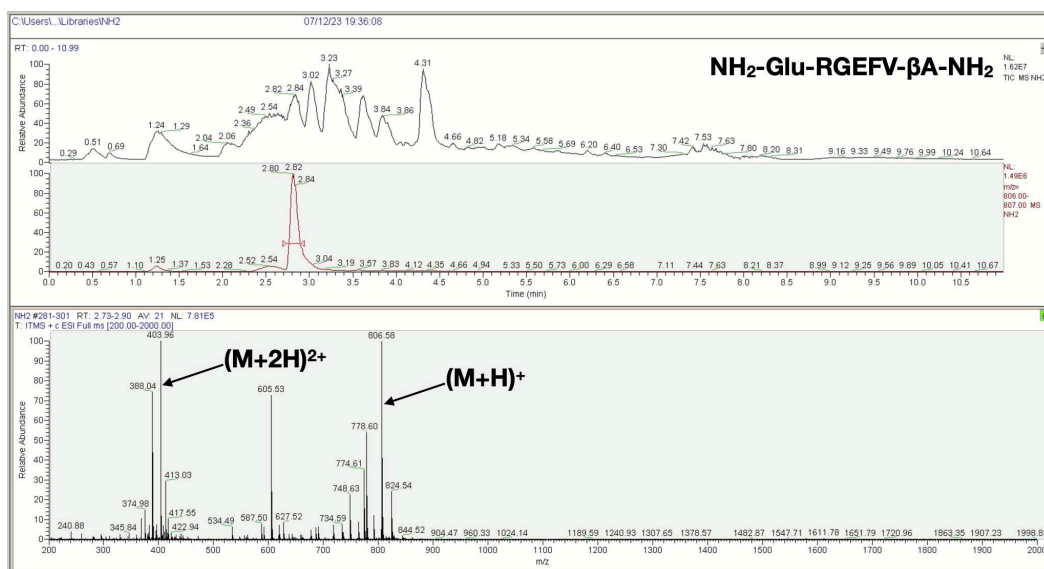
Appendix Figure 111 - LCMS spectra of the NH₂-X-RGEFV-βA-NH₂ libraries, where X = Asn.



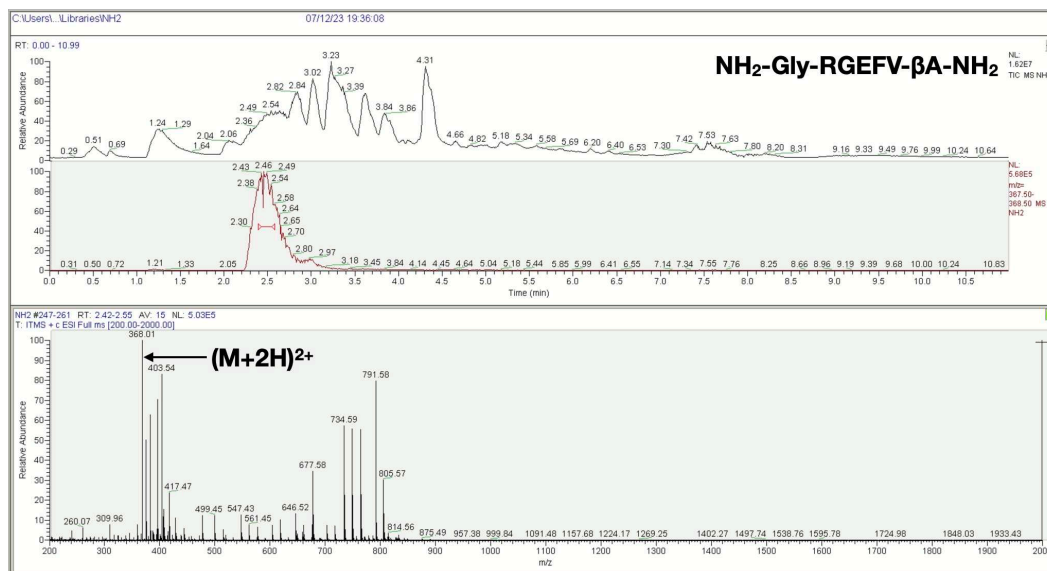
Appendix Figure 112 - LCMS spectra of the NH₂-X-RGEFV-βA-NH₂ libraries, where X = Asp.



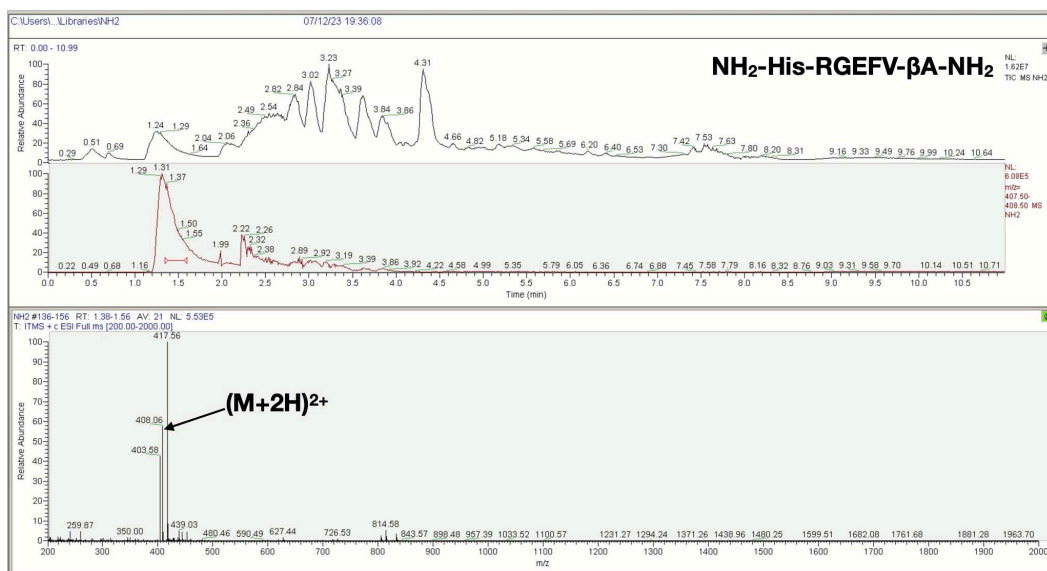
Appendix Figure 113 - LCMS spectra of the NH₂-X-RGEFV-βA-NH₂ libraries, where X = Gln.



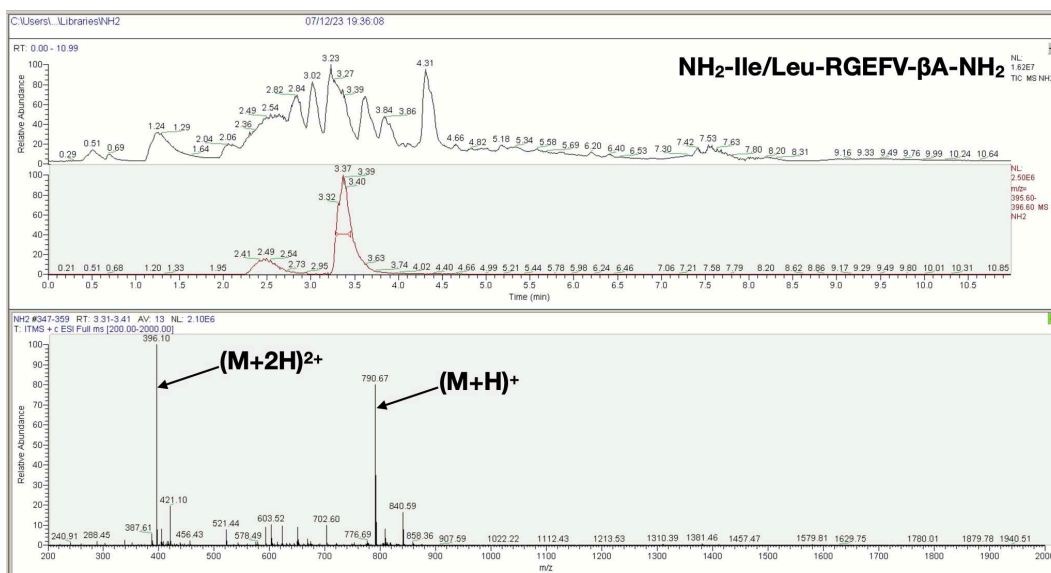
Appendix Figure 114 - LCMS spectra of the NH₂-X-RGEFV-βA-NH₂ libraries, where X = Glu.



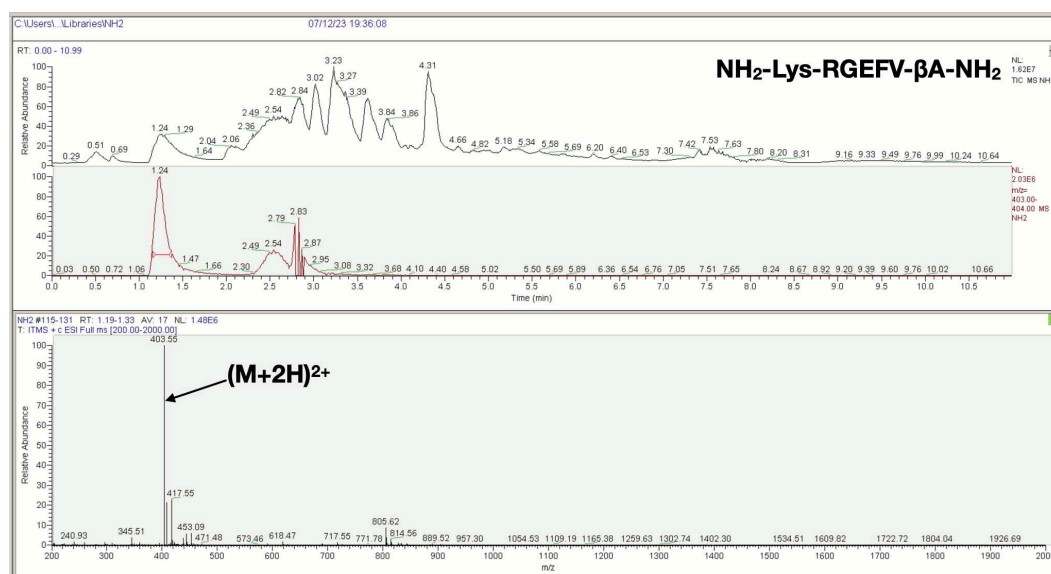
Appendix Figure 115 - LCMS spectra of the NH₂-X-RGEFV-βA-NH₂ libraries, where X = Gly.



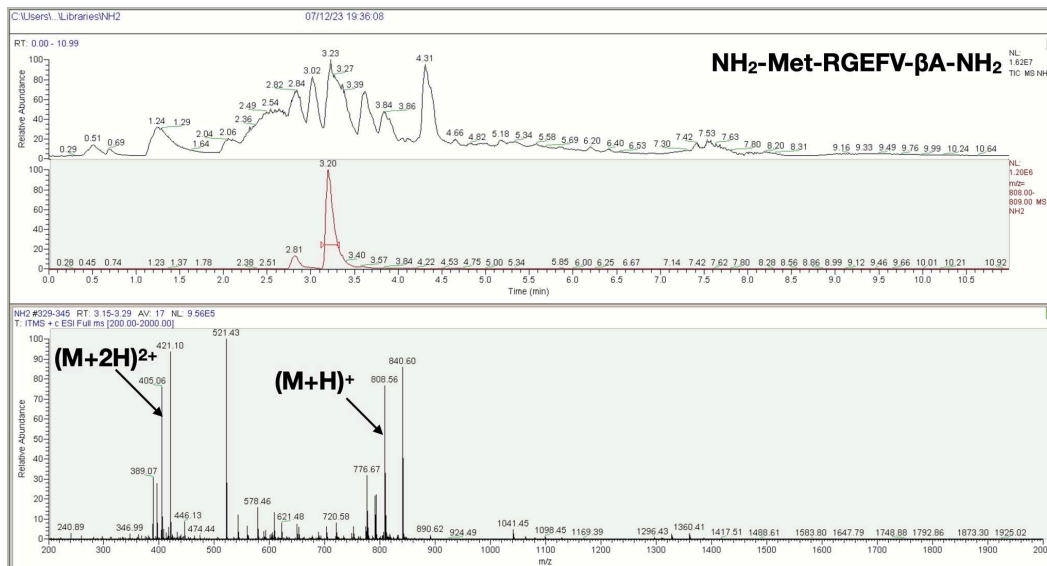
Appendix Figure 116 - LCMS spectra of the NH₂-X-RGEFV-βA-NH₂ libraries, where X = His.



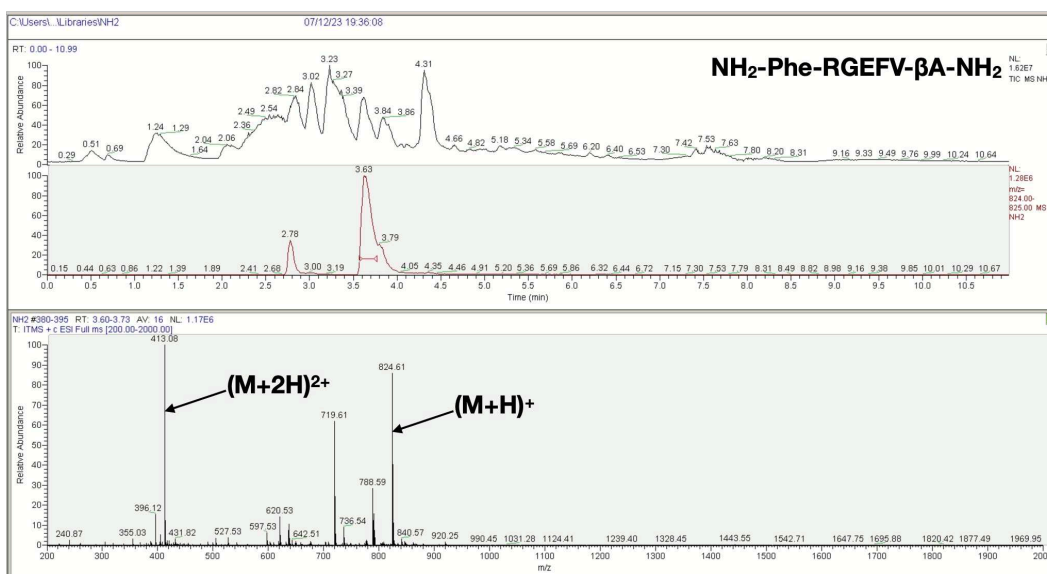
Appendix Figure 117 - LCMS spectra of the NH₂-X-RGEFV-βA-NH₂ libraries, where X = Ile/Leu.



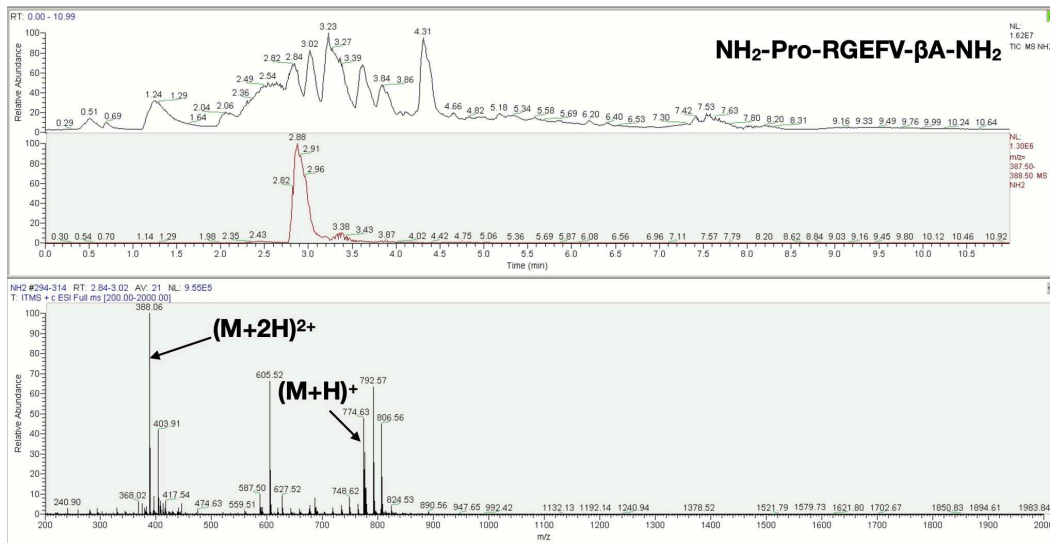
Appendix Figure 118 - LCMS spectra of the NH₂-X-RGEFV-βA-NH₂ libraries, where X = Lys.



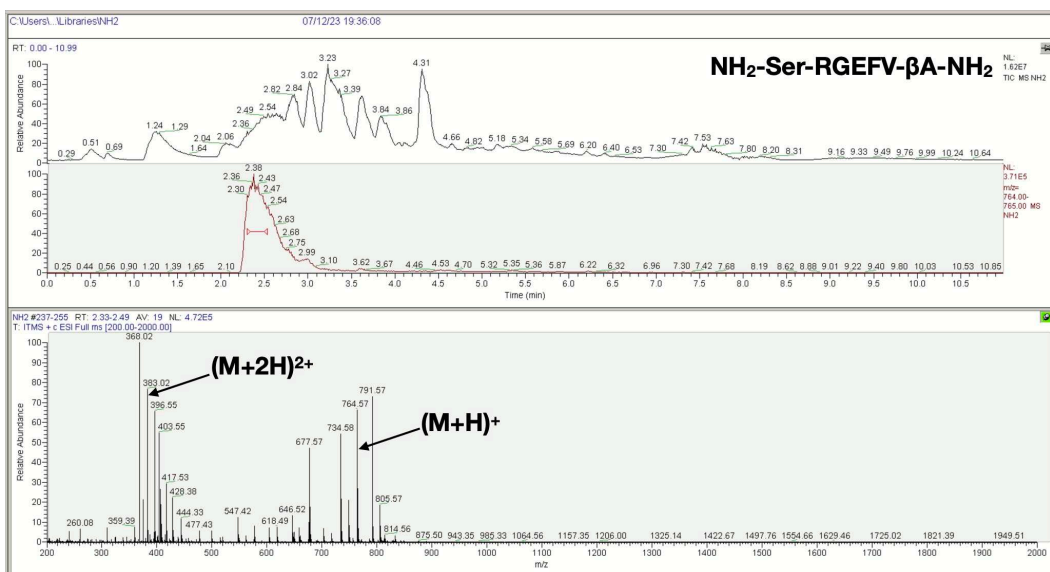
Appendix Figure 119 - LCMS spectra of the NH₂-X-RGEFV-βA-NH₂ libraries, where X = Met.



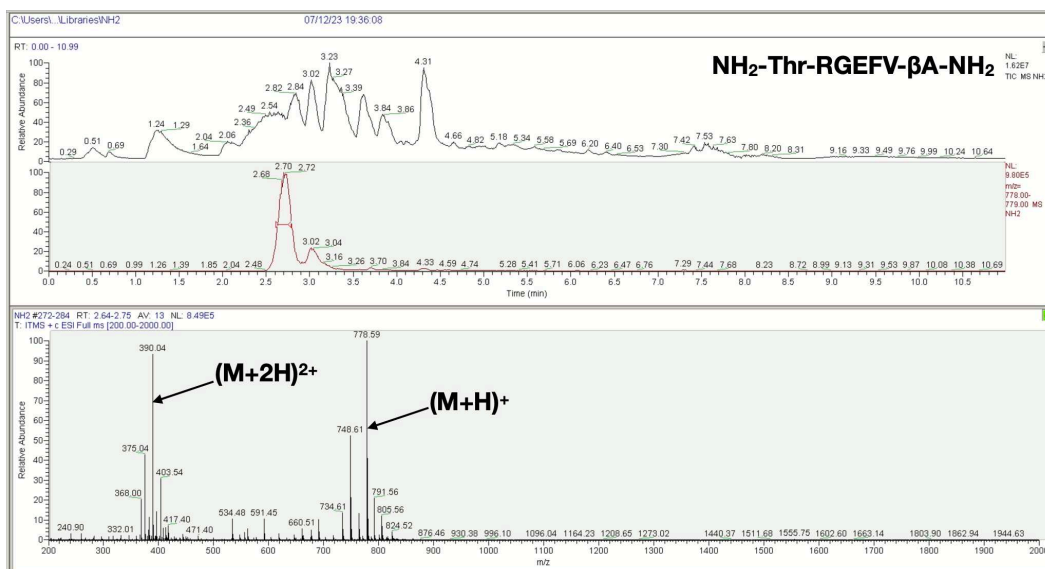
Appendix Figure 120 - LCMS spectra of the NH₂-X-RGEFV-βA-NH₂ libraries, where X = Phe.



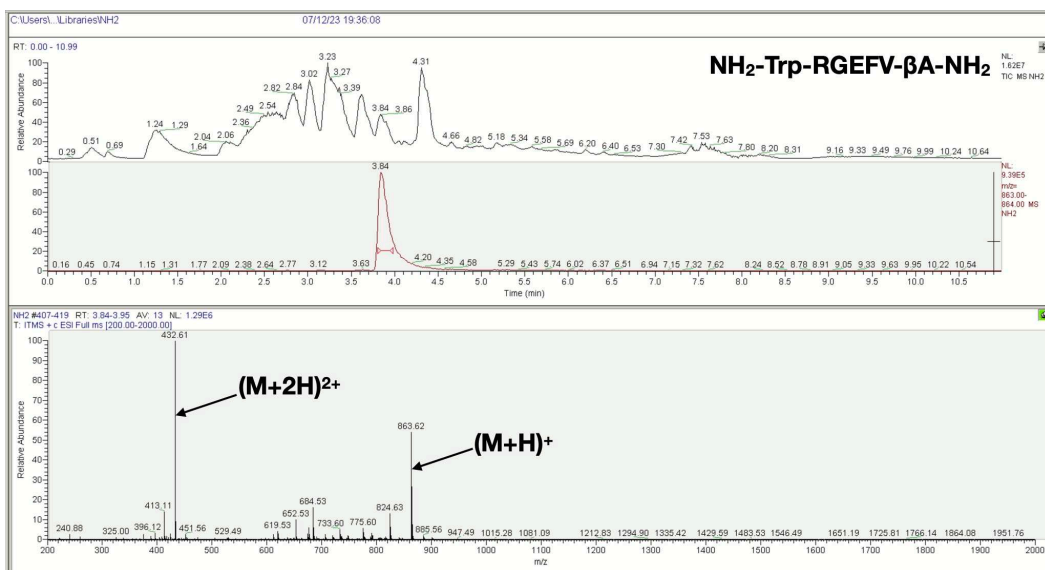
Appendix Figure 121 - LCMS spectra of the NH₂-X-RGEFV-βA-NH₂ libraries, where X = Pro.



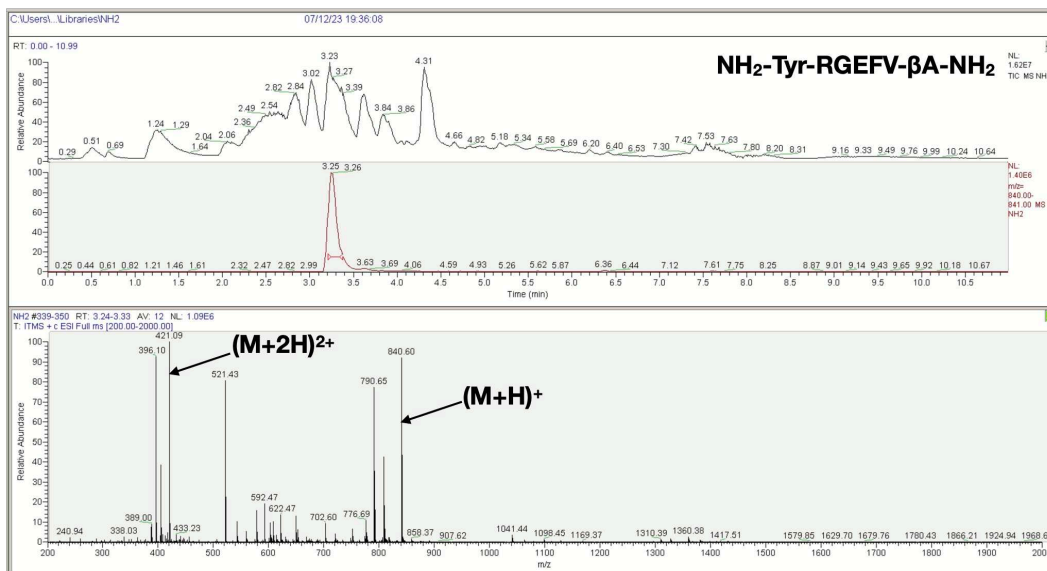
Appendix Figure 122 - LCMS spectra of the NH₂-X-RGEFV-βA-NH₂ libraries, where X = Ser.



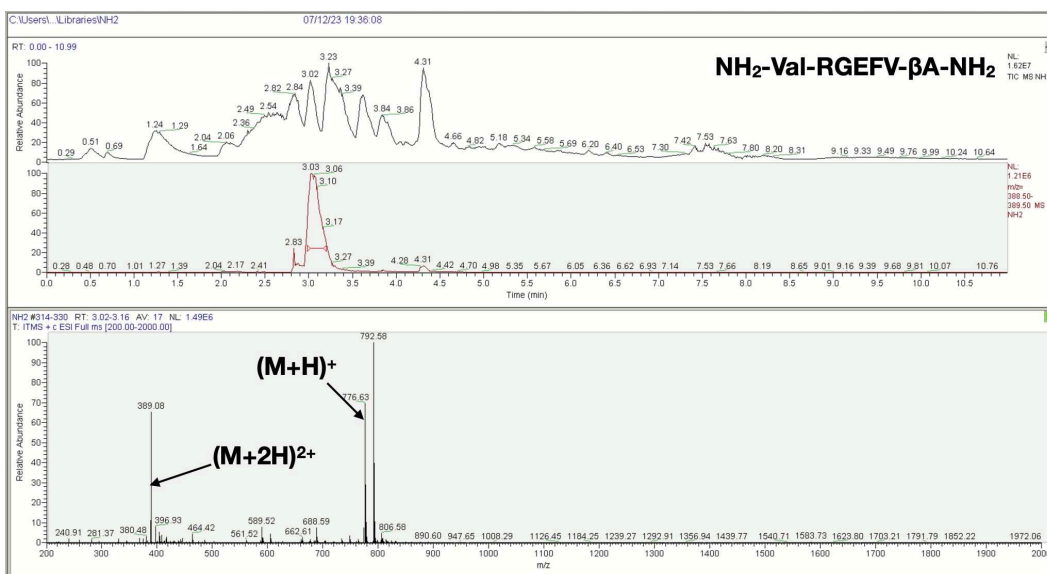
Appendix Figure 123 - LCMS spectra of the NH₂-X-RGEFV-βA-NH₂ libraries, where X = Thr.



Appendix Figure 124 - LCMS spectra of the NH₂-X-RGEFV-βA-NH₂ libraries, where X = Trp.

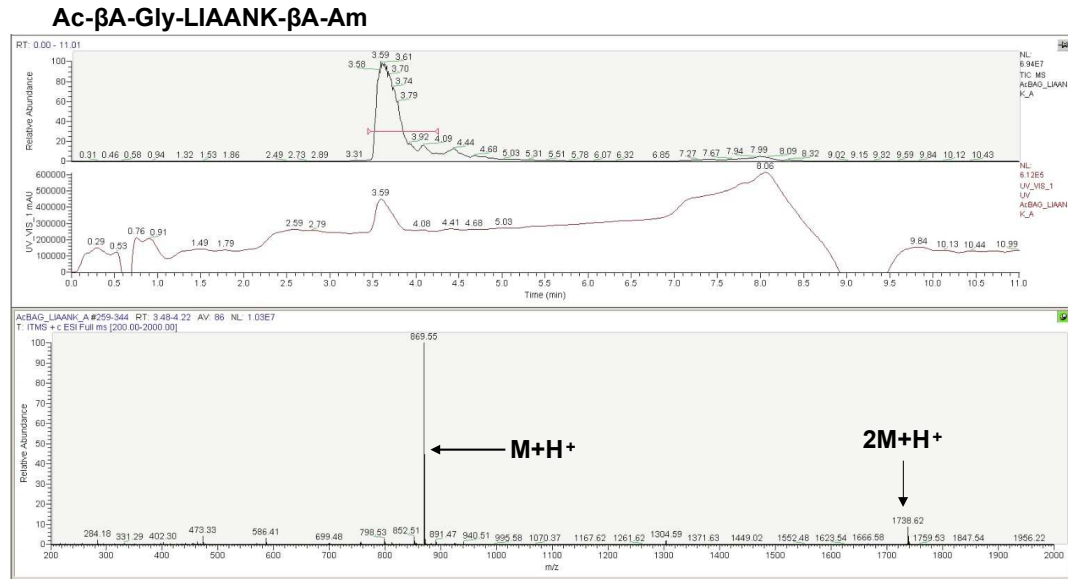


Appendix Figure 125 - LCMS spectra of the NH₂-X-RGEFV-βA-NH₂ libraries, where X = Tyr.

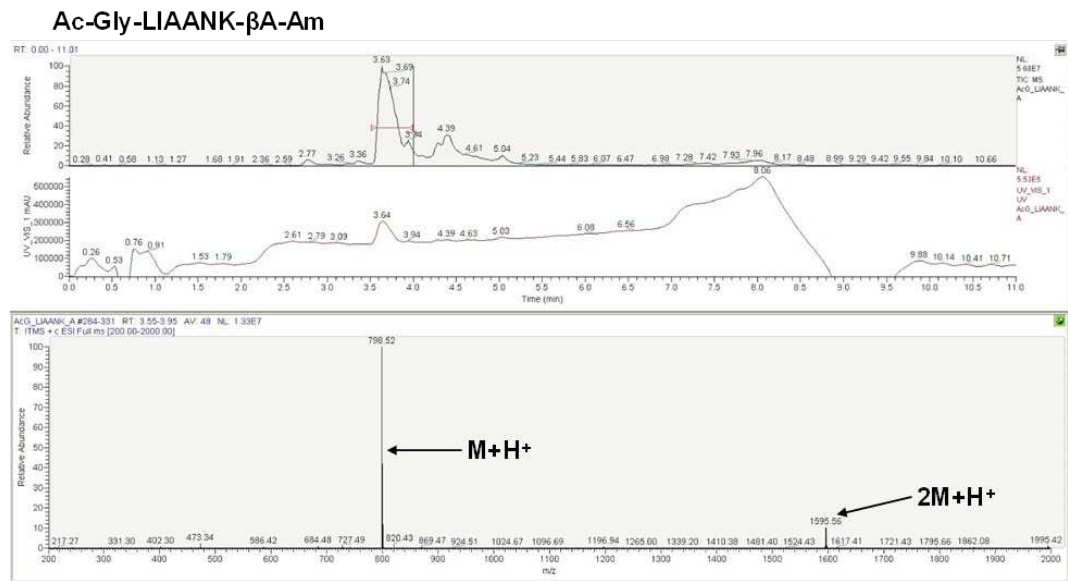


Appendix Figure 126 - LCMS spectra of the NH₂-X-RGEFV-βA-NH₂ libraries, where X = Val.

7.2 LIAANK and IVKVA Peptides

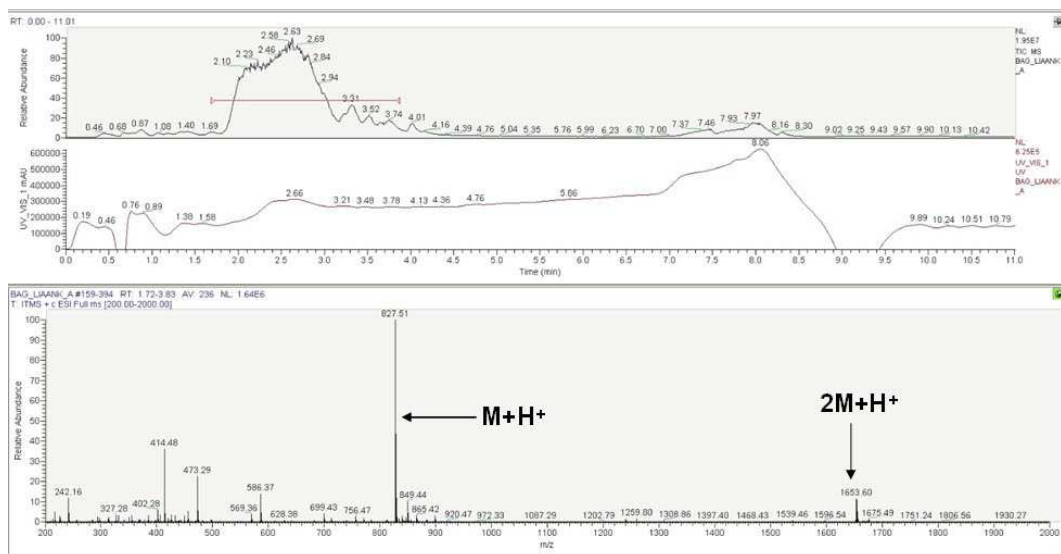


Appendix Figure 127 - LCMS spectra of the LIAANK peptide in which a glycine was placed immediately adjacent to an N-terminal Ac-βA.



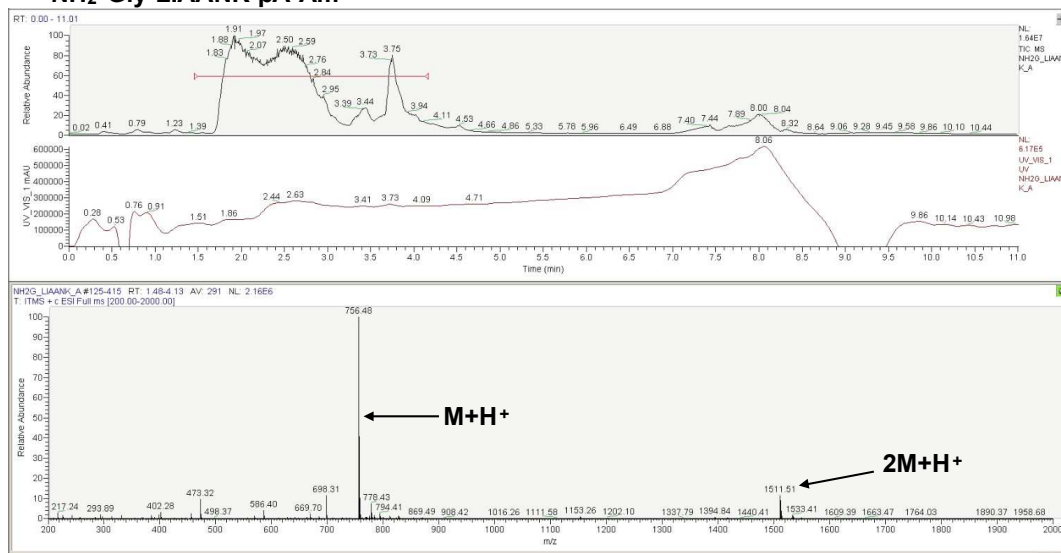
Appendix Figure 128 - LCMS spectra of the LIAANK peptide in which a glycine was placed immediately adjacent to an N-terminal Ac.

NH₂-βA-Gly-LIAANK-βA-Am

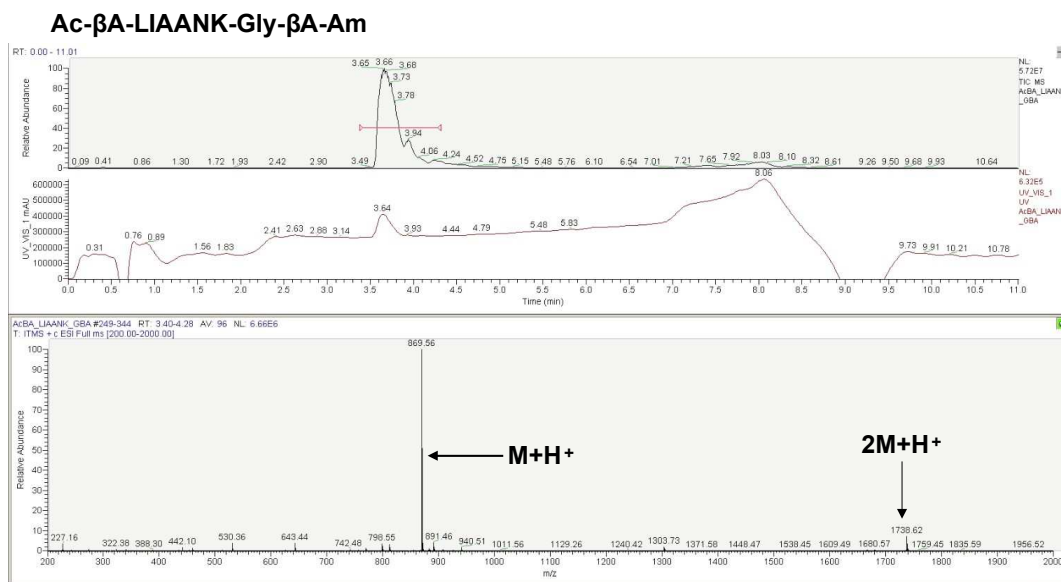


Appendix Figure 129 - LCMS spectra of the LIAANK peptide in which a glycine was placed immediately adjacent to an N-terminal βA.

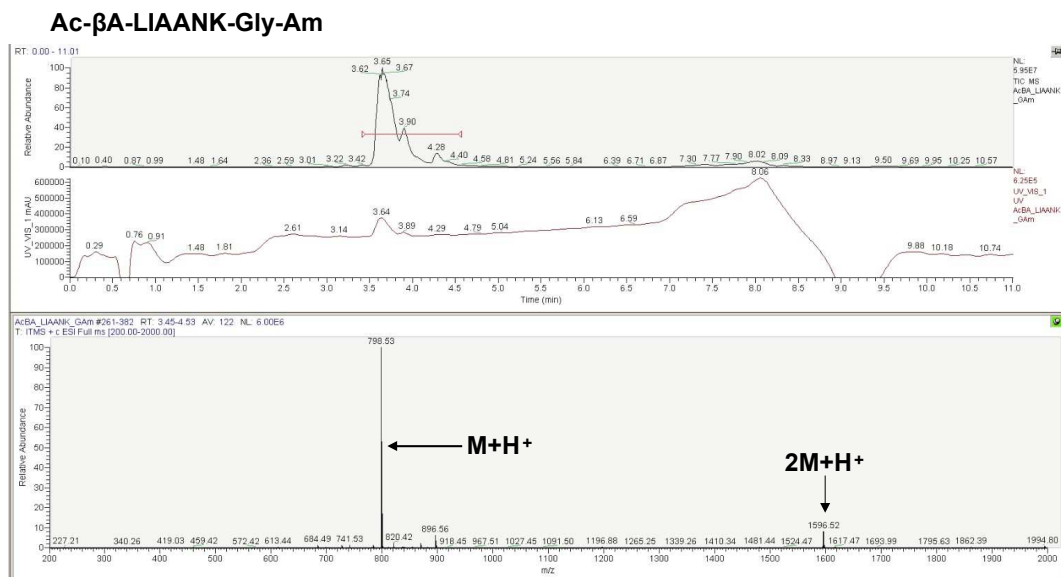
NH₂-Gly-LIAANK-βA-Am



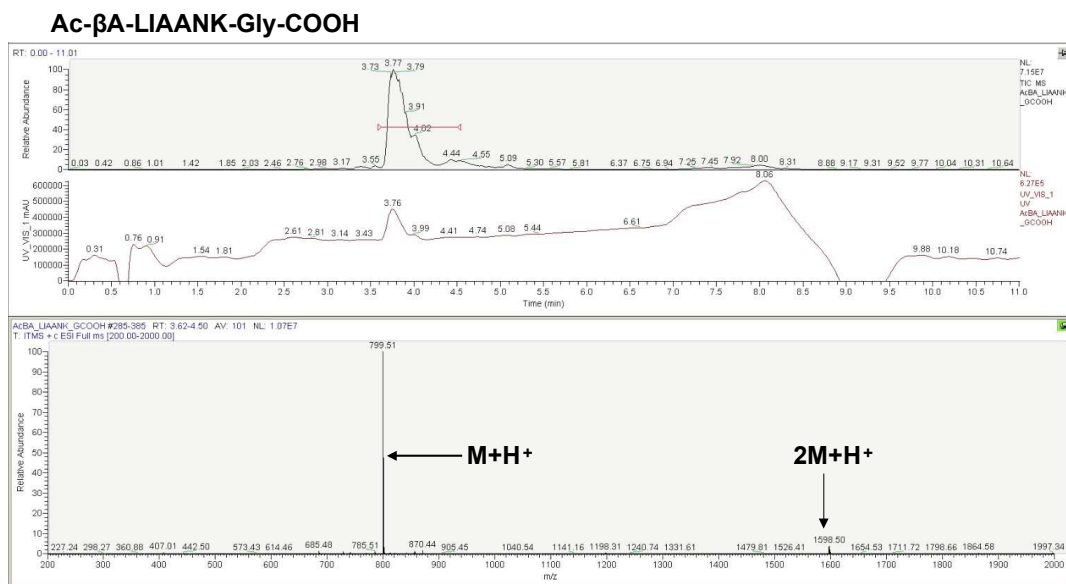
Appendix Figure 130 - LCMS spectra of the LIAANK peptide in which a glycine was placed immediately adjacent to an N-terminal NH₂.



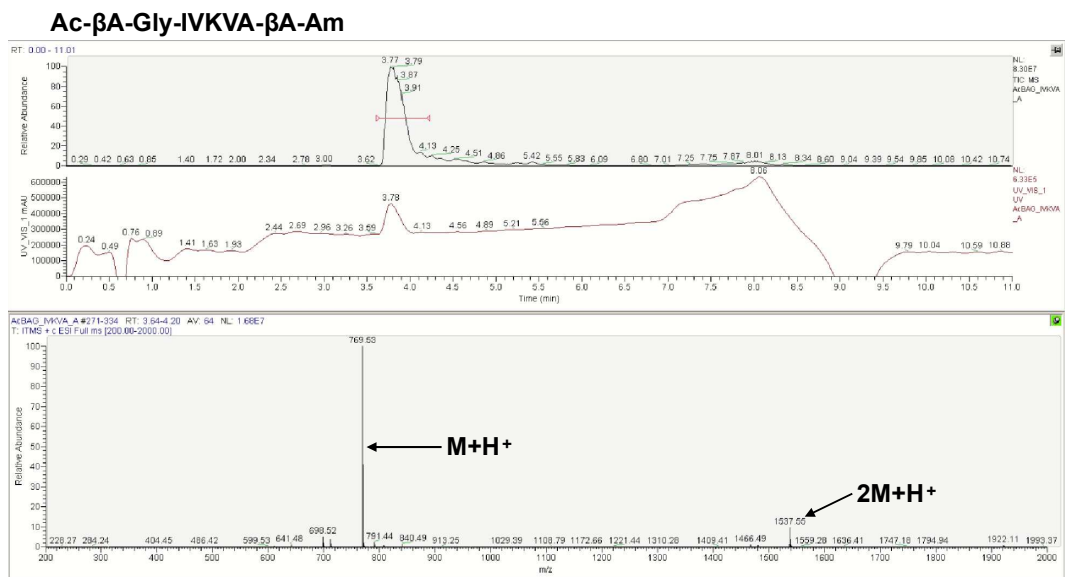
Appendix Figure 131 - LCMS spectra of the LIAANK peptide in which a glycine was placed immediately adjacent to a C-terminal β A.



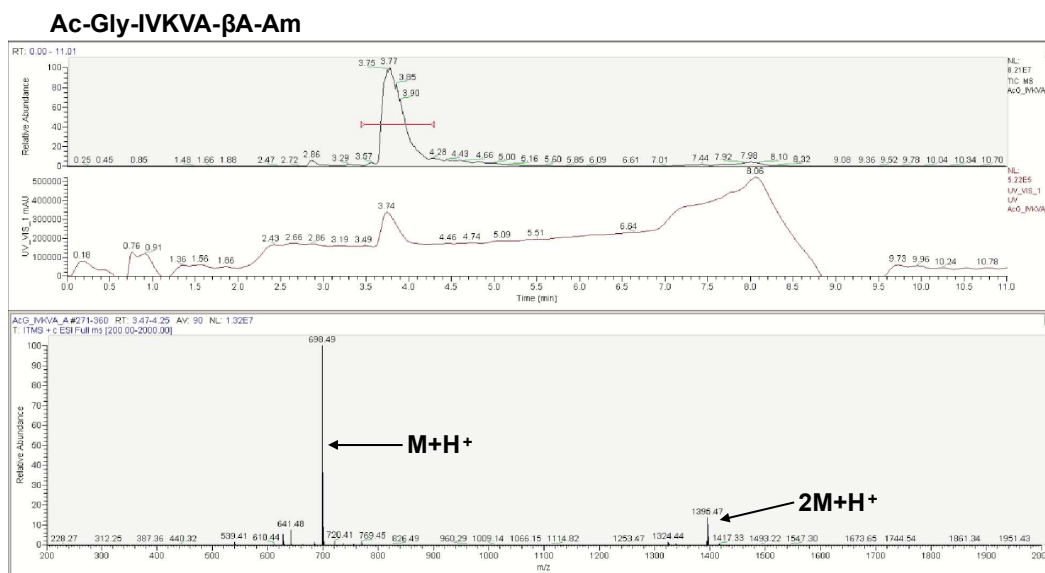
Appendix Figure 132 - LCMS spectra of the LIAANK peptide in which a glycine was placed immediately adjacent to a C-terminal Am.



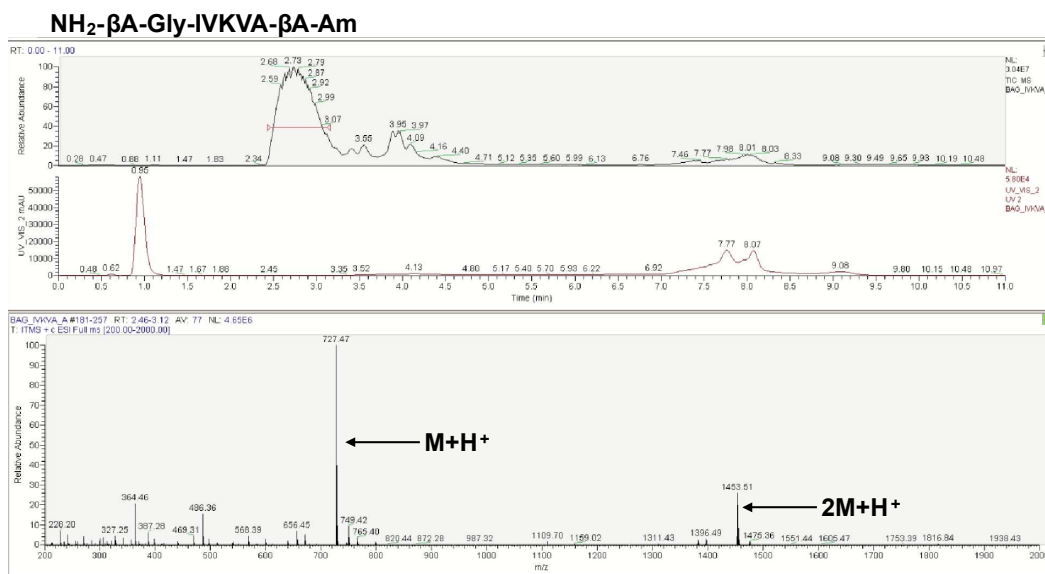
Appendix Figure 133 - LCMS spectra of the LIAANK peptide in which a glycine was placed immediately adjacent to a C-terminal COOH.



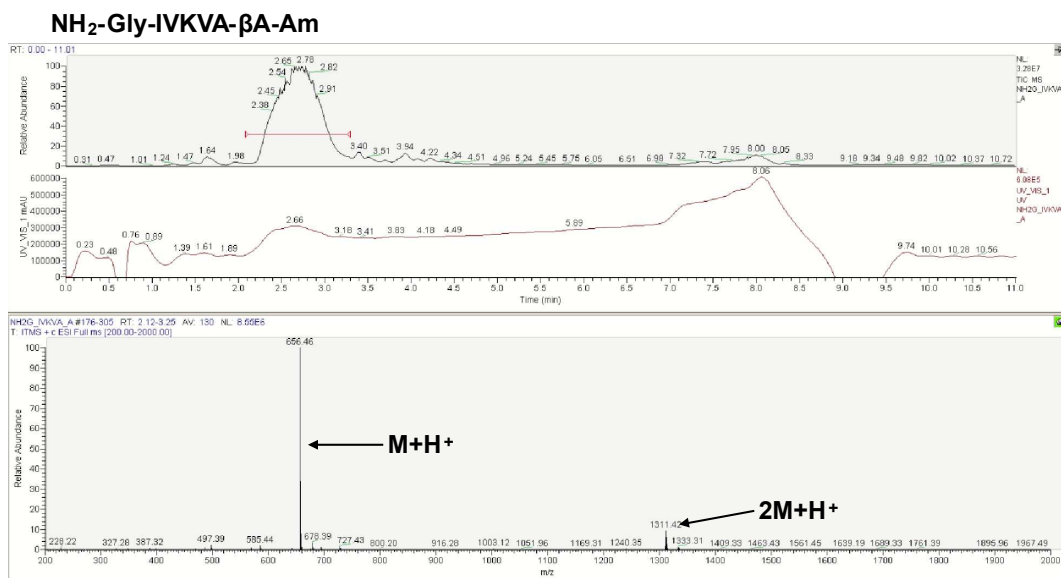
Appendix Figure 134 - LCMS spectra of the IVKVA peptide in which a glycine was placed immediately adjacent to an N-terminal Ac- β A.



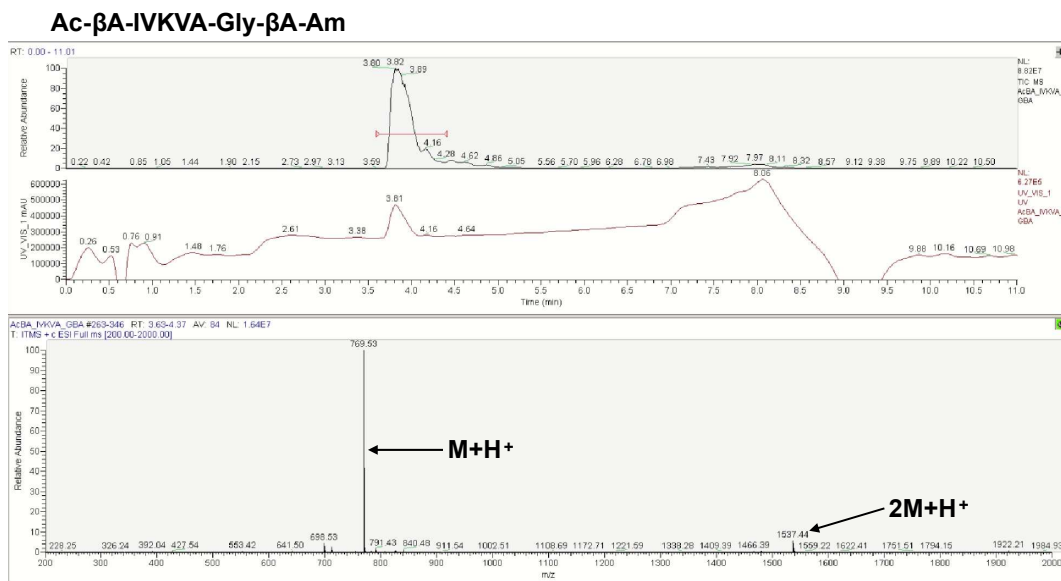
Appendix Figure 135 - LCMS spectra of the IVKVA peptide in which a glycine was placed immediately adjacent to an N-terminal Ac.



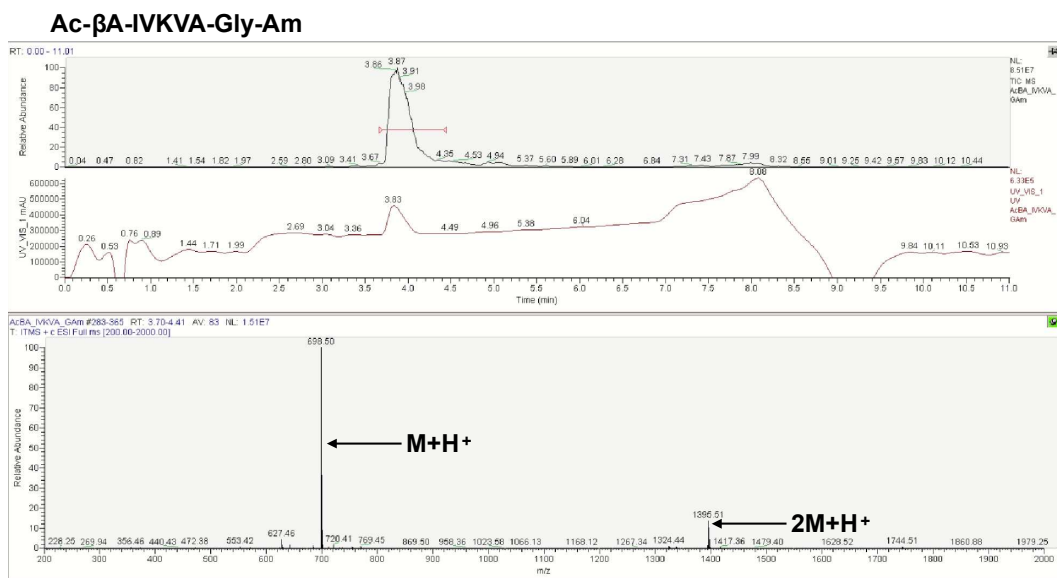
Appendix Figure 136 - LCMS spectra of the IVKVA peptide in which a glycine was placed immediately adjacent to an N-terminal βA.



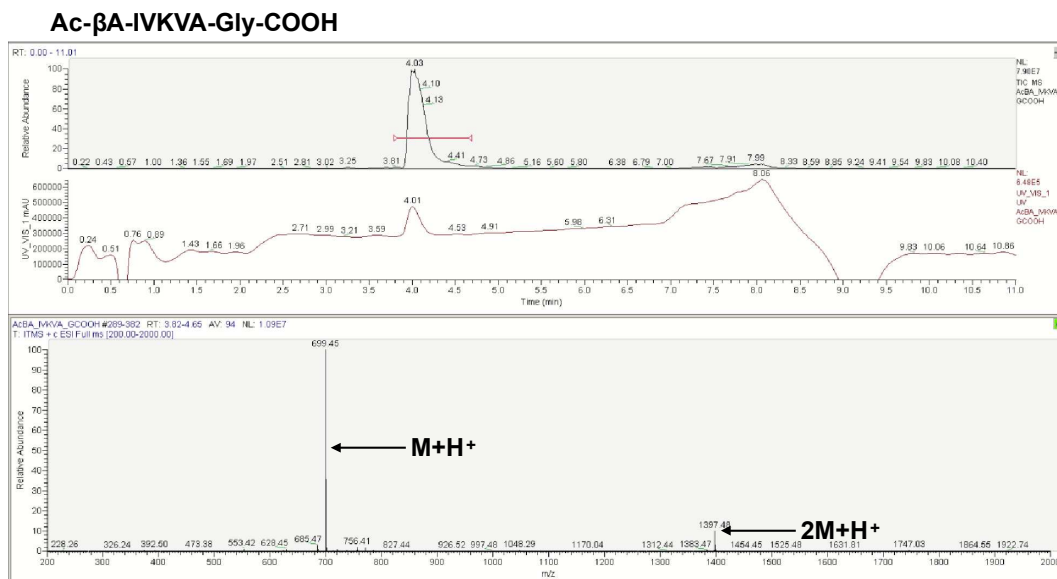
Appendix Figure 137 - LCMS spectra of the IVKVA peptide in which a glycine was placed immediately adjacent to an N-terminal NH₂.



Appendix Figure 138 - LCMS spectra of the IVKVA peptide in which a glycine was placed immediately adjacent to a C-terminal βA.

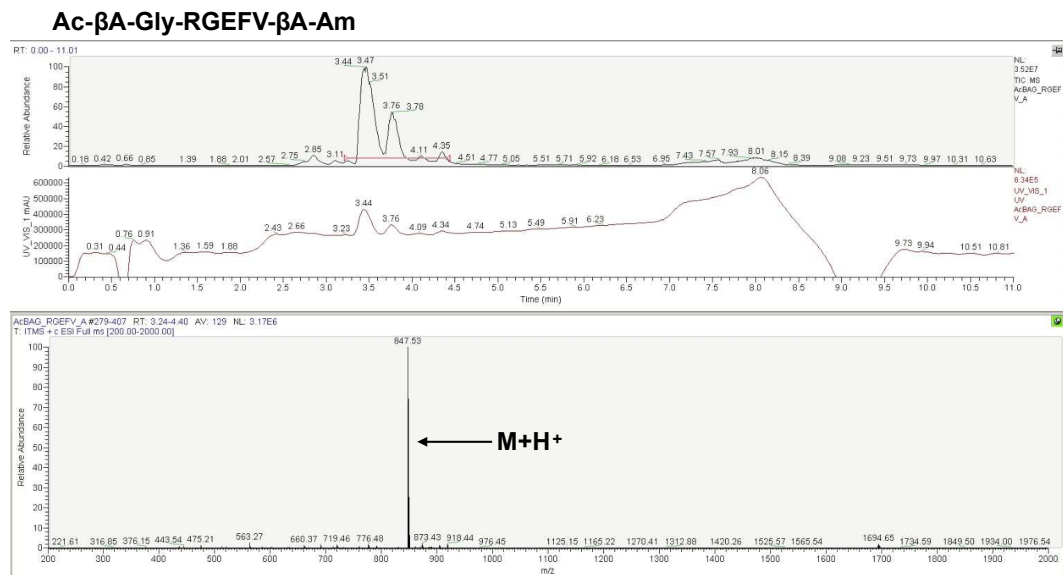


Appendix Figure 139 - LCMS spectra of the IVKVA peptide in which a glycine was placed immediately adjacent to a C-terminal Am.

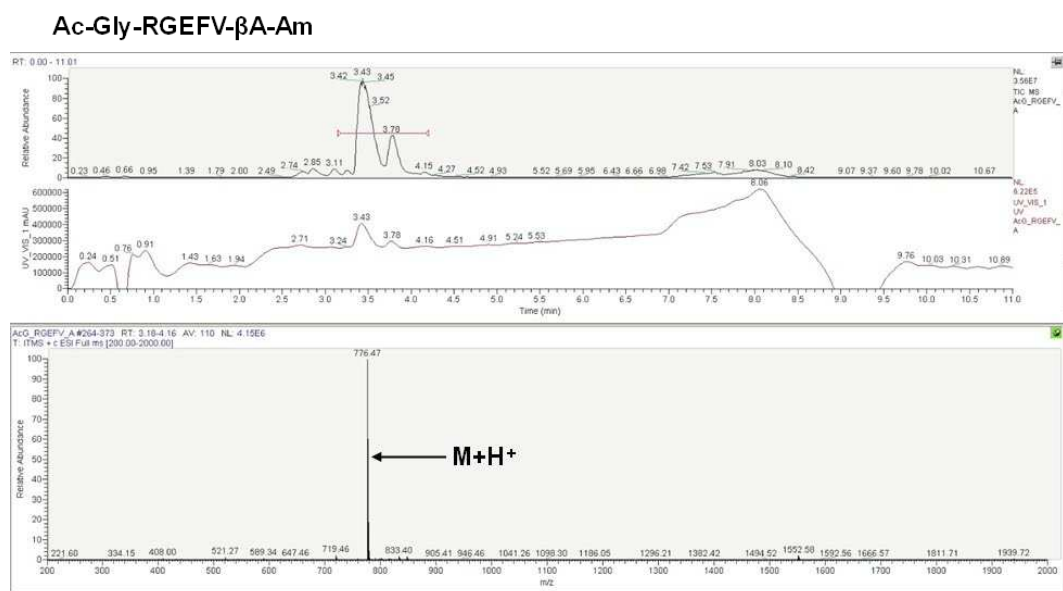


Appendix Figure 140 - LCMS spectra of the IVKVA peptide in which a glycine was placed immediately adjacent to a C-terminal COOH.

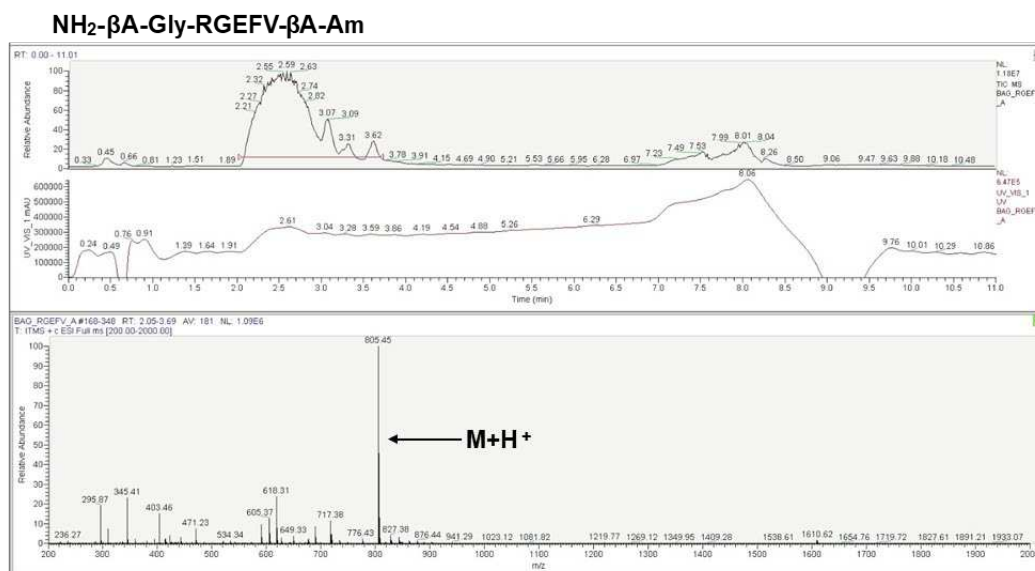
7.3 Glycine, Azide, and PEGylated RGEFV Peptides



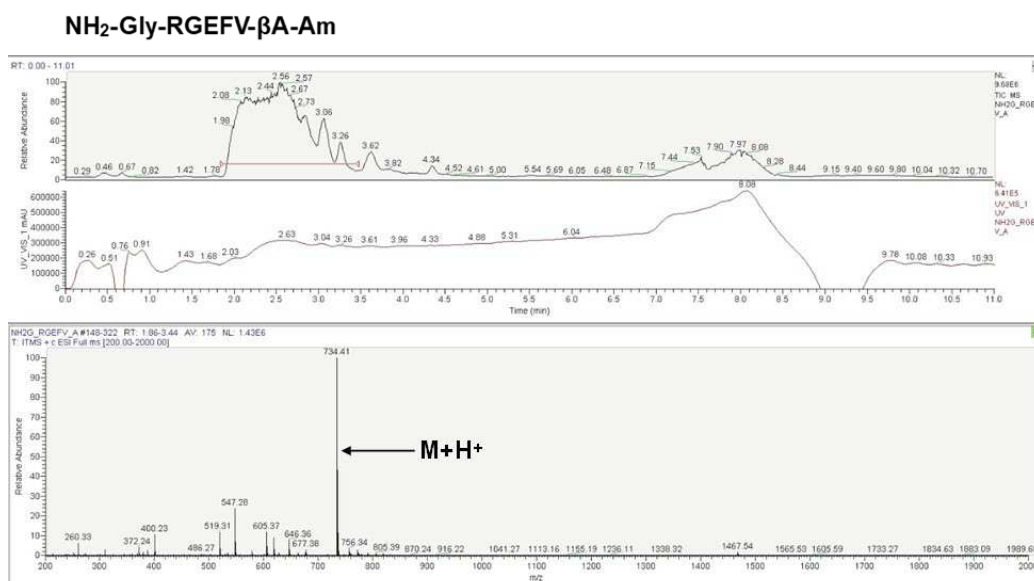
Appendix Figure 141 - LCMS spectra of the peptide used for the concentration studies in which a glycine was placed immediately adjacent to an N-terminal Ac-βA.



Appendix Figure 142 - LCMS spectra of the peptide used for the concentration studies in which a glycine was placed immediately adjacent to an N-terminal Ac.

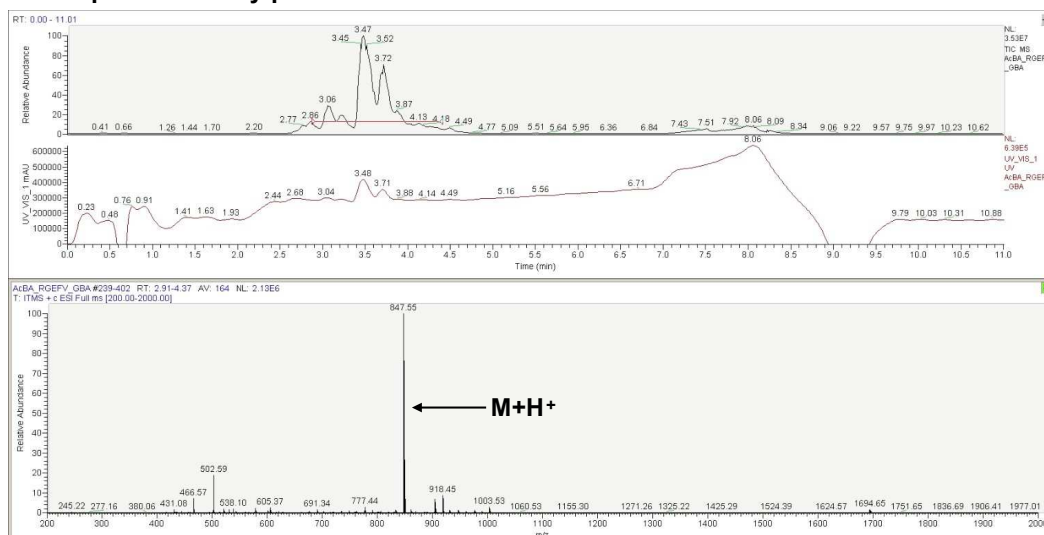


Appendix Figure 143 - LCMS spectra of the peptide used for the concentration studies in which a glycine was placed immediately adjacent to an N-terminal βA.



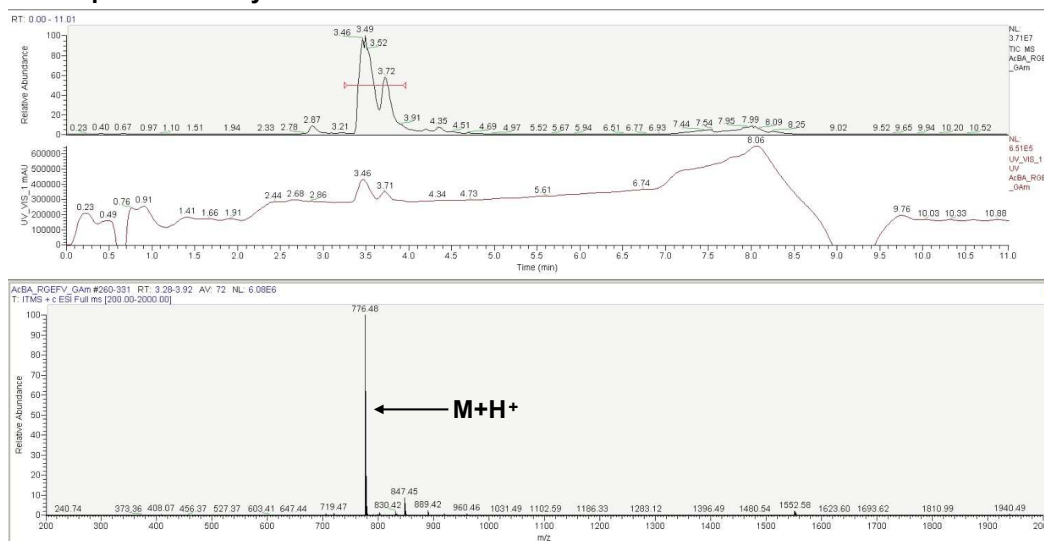
Appendix Figure 144 - LCMS spectra of the peptide used for the concentration studies in which a glycine was placed immediately adjacent to an N-terminal NH₂.

Ac- β A-RGEFV-Gly- β A-Am

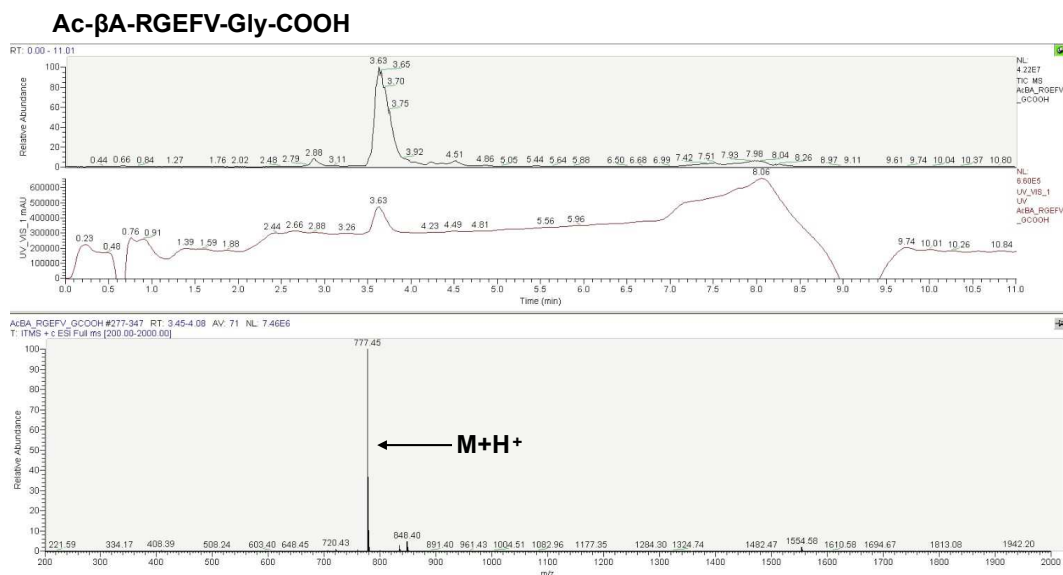


Appendix Figure 145 - LCMS spectra of the peptide used for the concentration studies in which a glycine was placed immediately adjacent to a C-terminal β A.

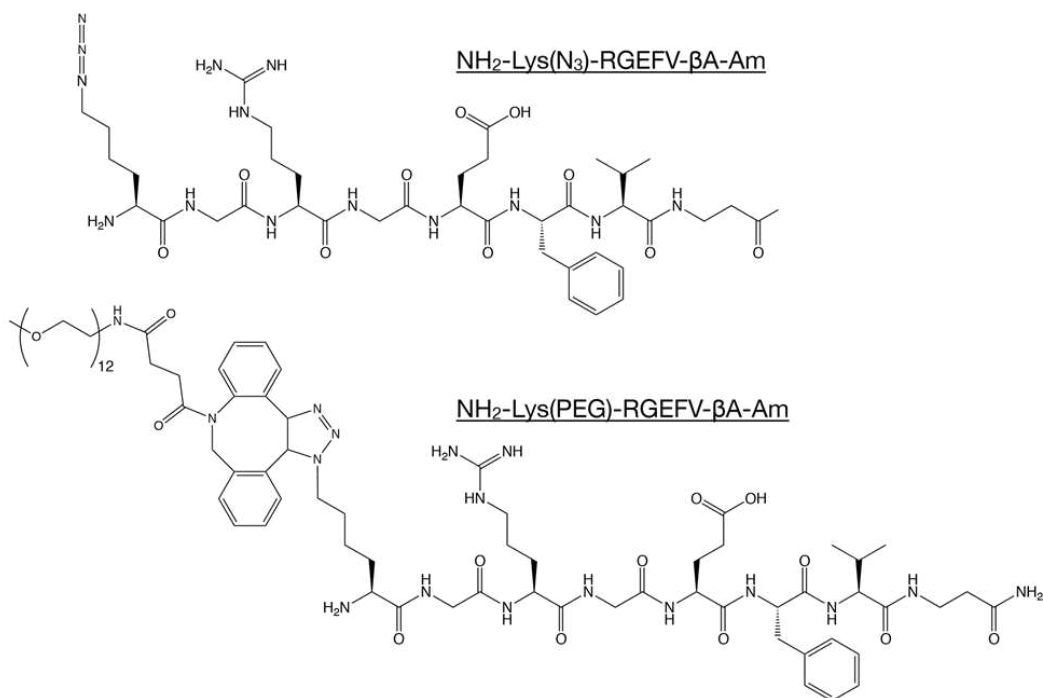
Ac- β A-RGEFV-Gly-Am



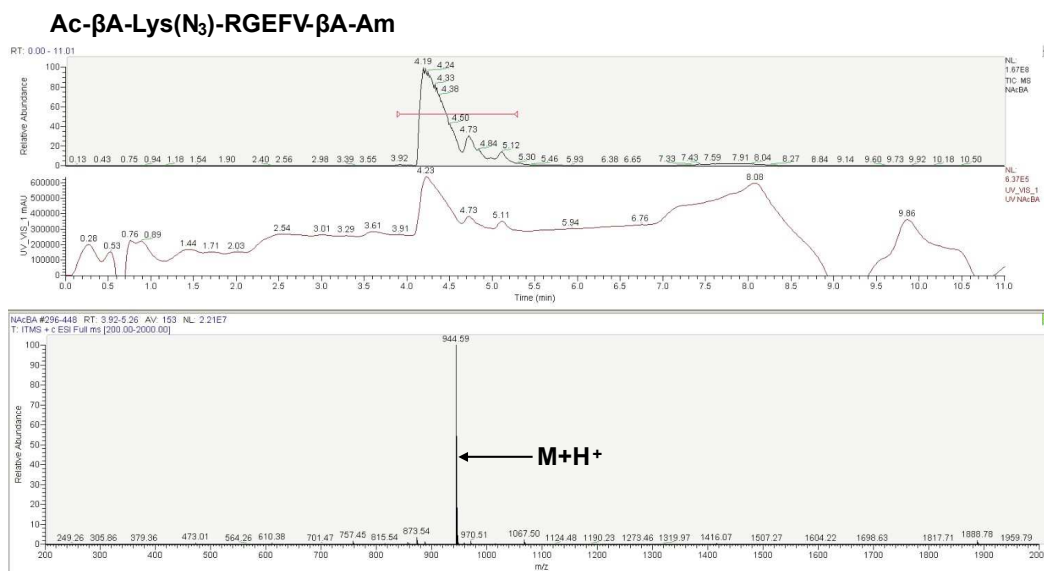
Appendix Figure 146 - LCMS spectra of the peptide used for the concentration studies in which a glycine was placed immediately adjacent to a C-terminal Am.



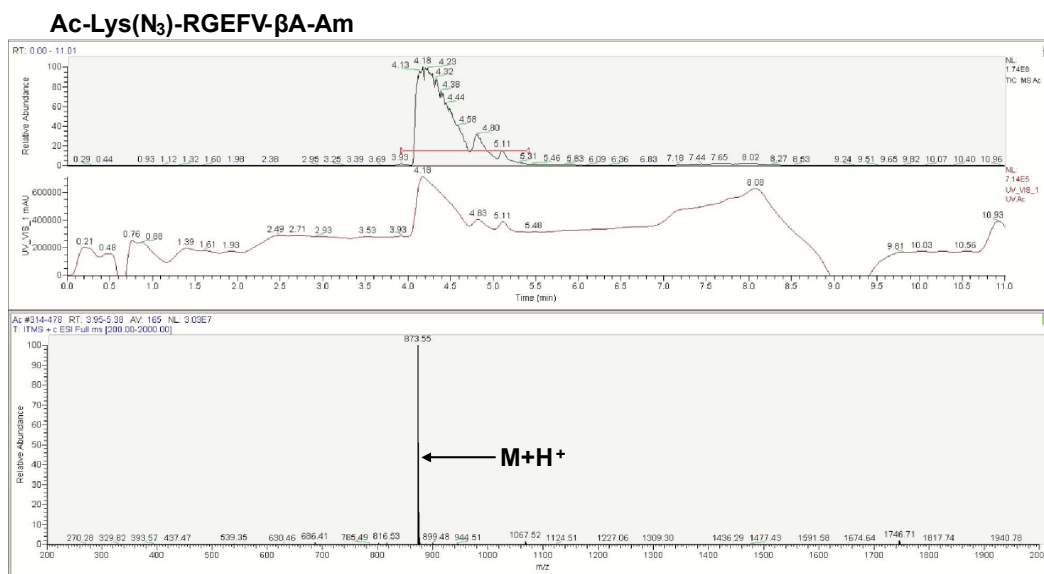
Appendix Figure 147 - LCMS spectra of the peptide used for the concentration studies in which a glycine was placed immediately adjacent to a C-terminal COOH.



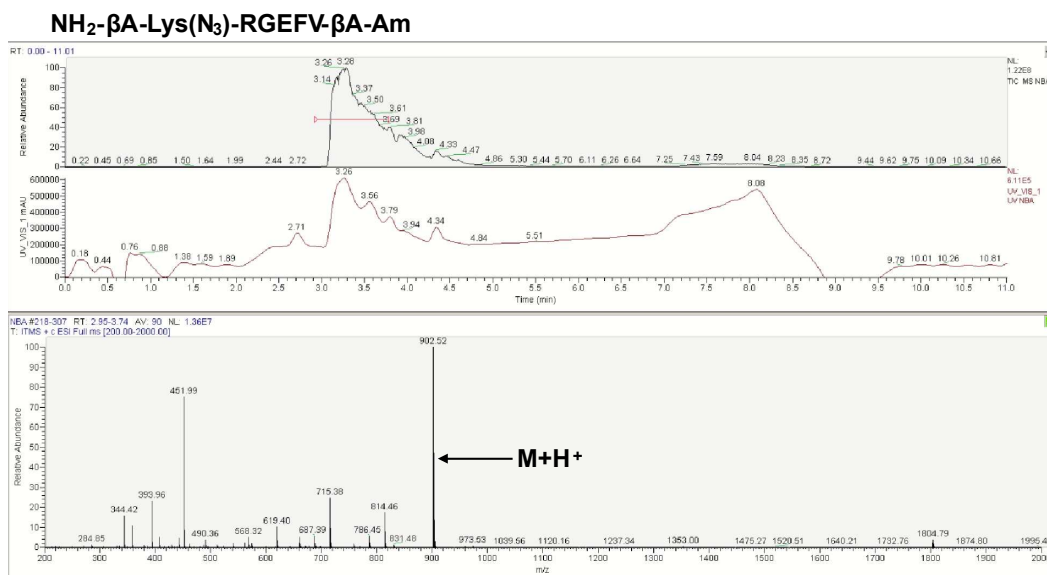
Appendix Figure 148 - The structure of azide and PEG RGEFV peptide. Shown, the structures are immediately adjacent to an amine terminated RGEFV peptide.



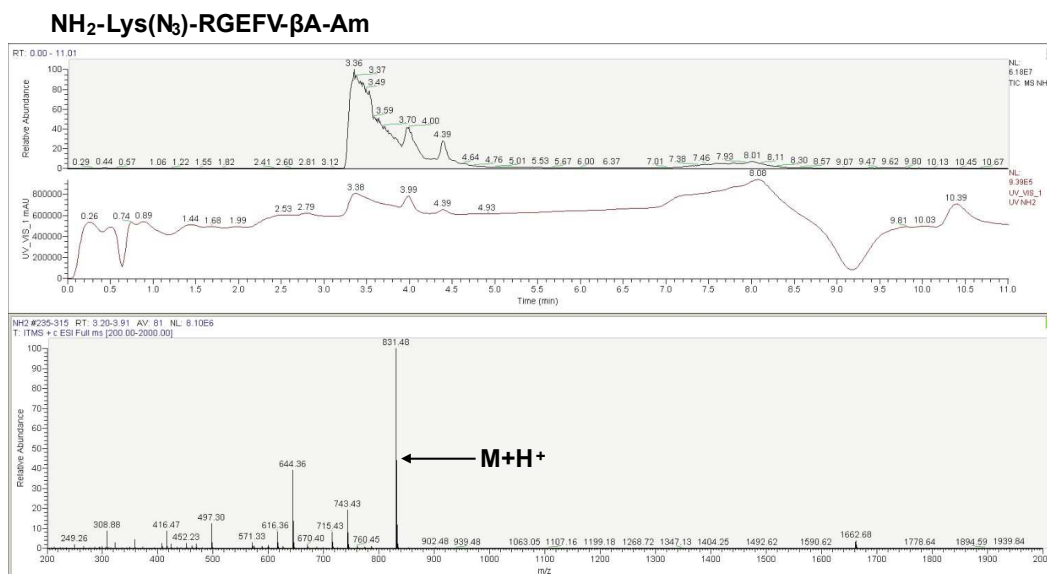
Appendix Figure 149 - LCMS spectra of the Azide modified Ac- β A peptide in which a glycine was placed on the N-terminus.



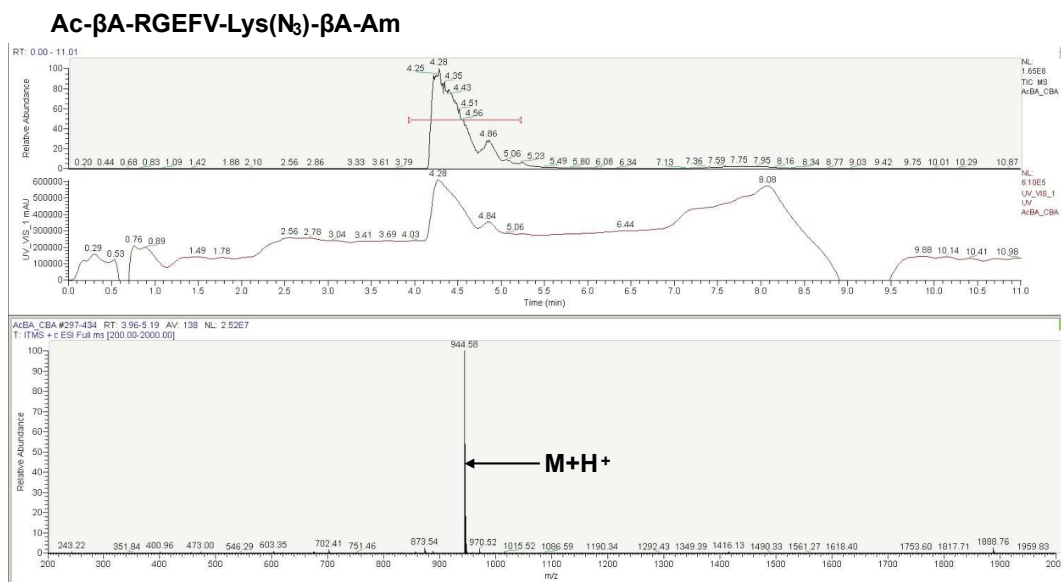
Appendix Figure 150 - LCMS spectra of the Azide modified Ac peptide in which a glycine was placed on the N-terminus.



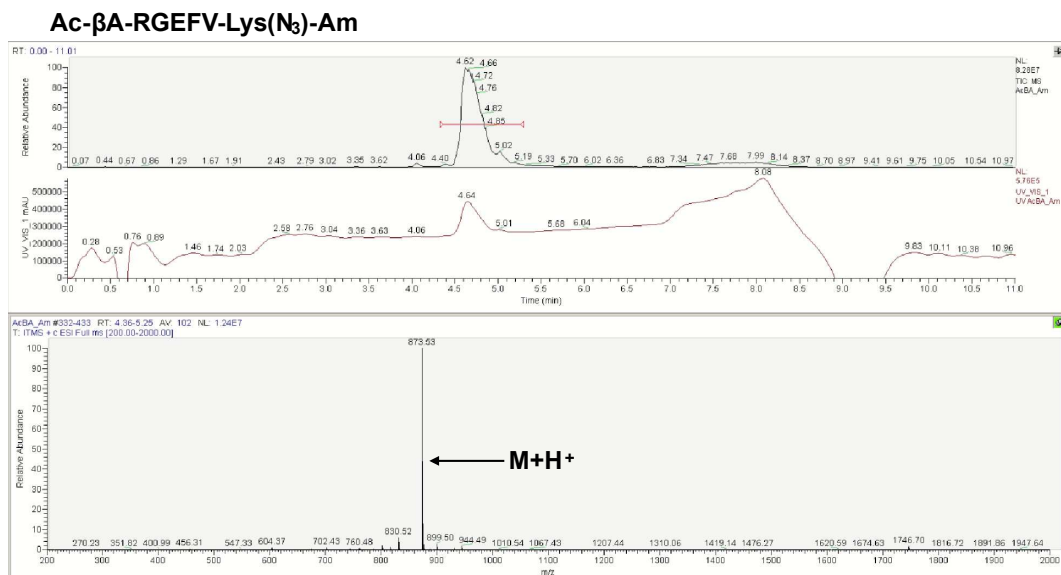
Appendix Figure 151 - LCMS spectra of the Azide modified N-βA peptide in which a glycine was placed on the N-terminus.



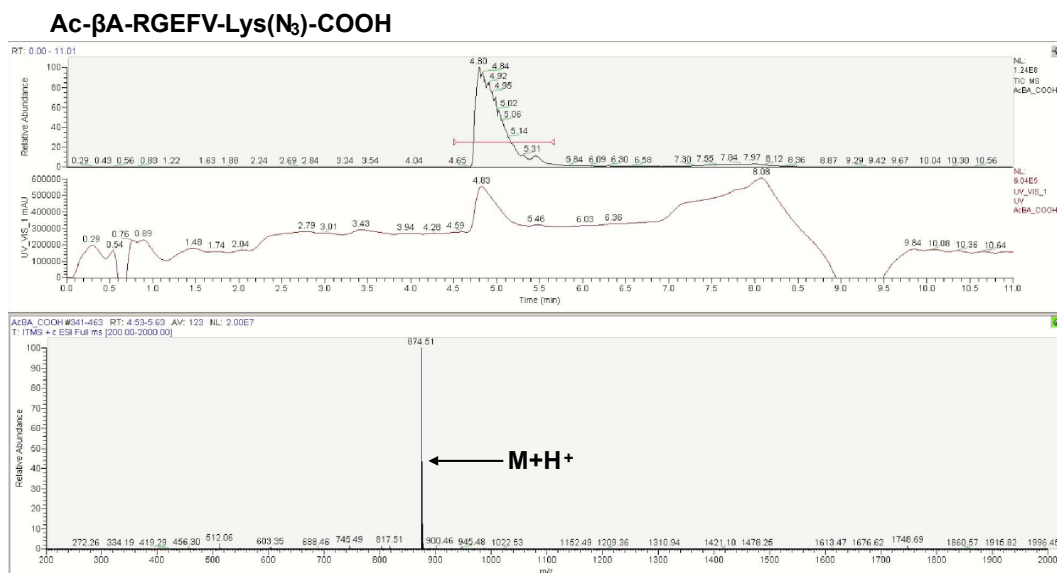
Appendix Figure 152 - LCMS spectra of the Azide modified NH₂ peptide in which a glycine was placed on the N-terminus. f) C-βA, g) Am, h) COOH. The PEG-modified peptides contained the following functionalization's: i) Ac-βA, j) Ac, k) N-βA, l) NH₂, m) C-βA, n) Am, o) COOH.



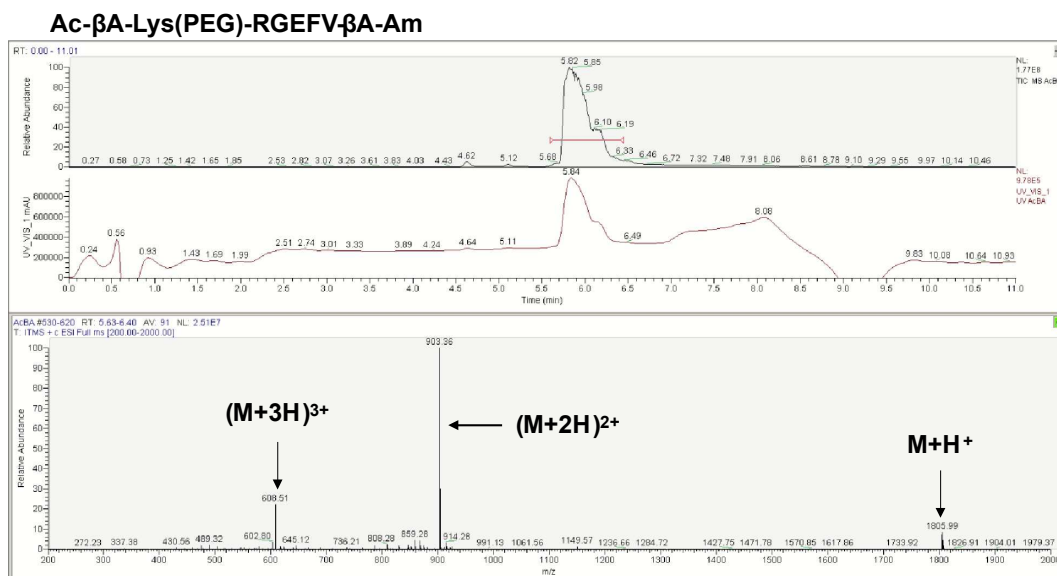
Appendix Figure 153 - LCMS spectra of the Azide modified C- β A peptide in which a glycine was placed on the C-terminus.



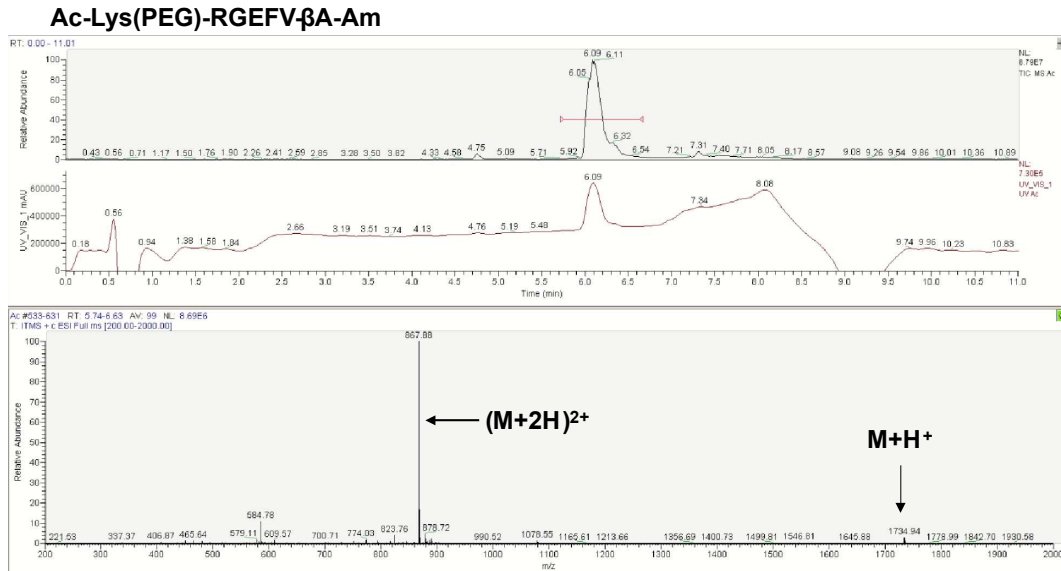
Appendix Figure 154 - LCMS spectra of the Azide modified Am peptide in which a glycine was placed on the C-terminus.



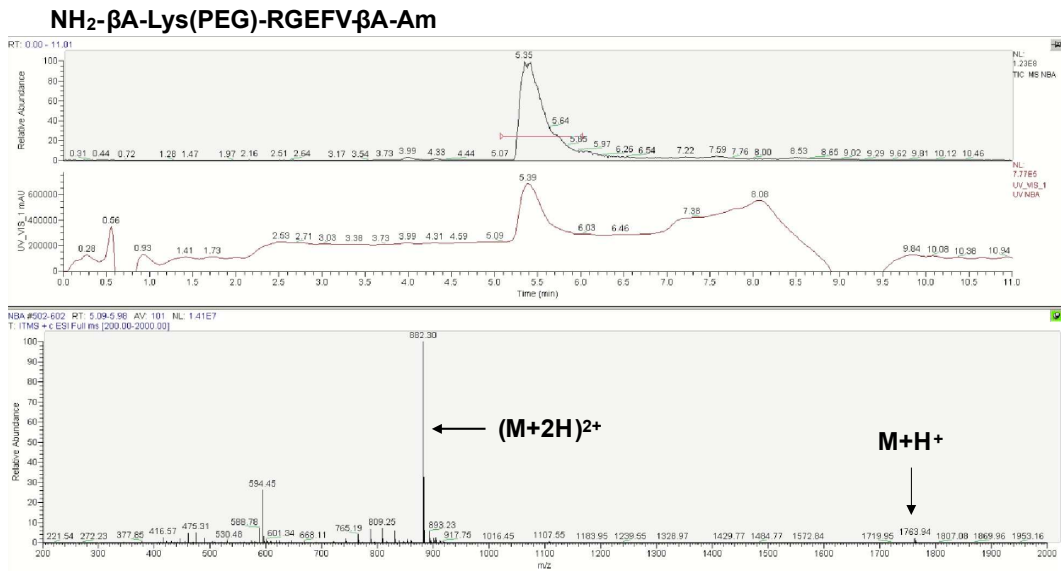
Appendix Figure 155 - LCMS spectra of the Azide modified COOH peptide in which a glycine was placed on the C-terminus.



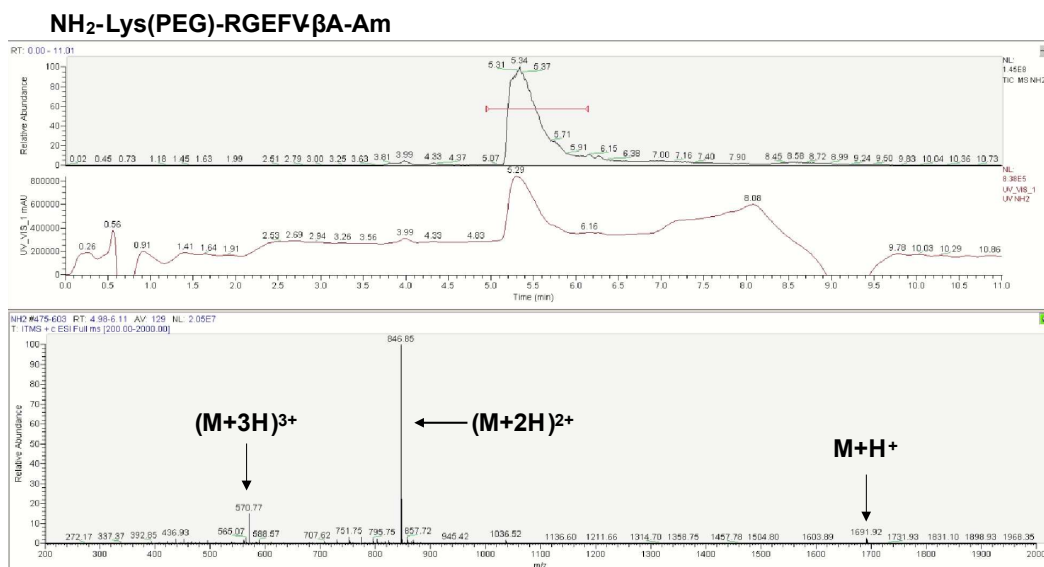
Appendix Figure 156 - LCMS spectra of the PEG modified Ac- β A peptide in which a glycine was placed on the N-terminus.



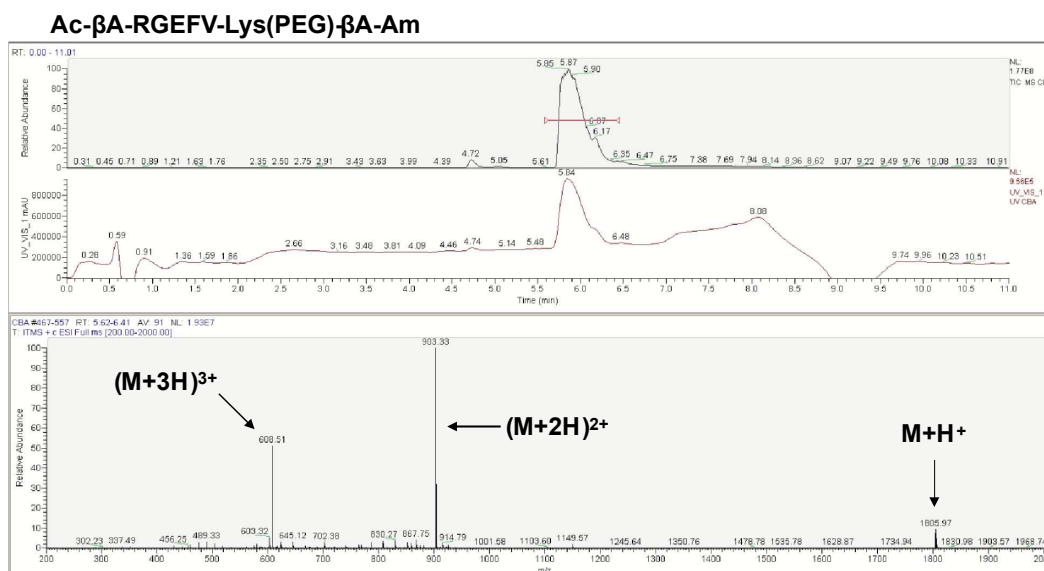
Appendix Figure 157 - LCMS spectra of the PEG modified Ac peptide in which a glycine was placed on the N-terminus.



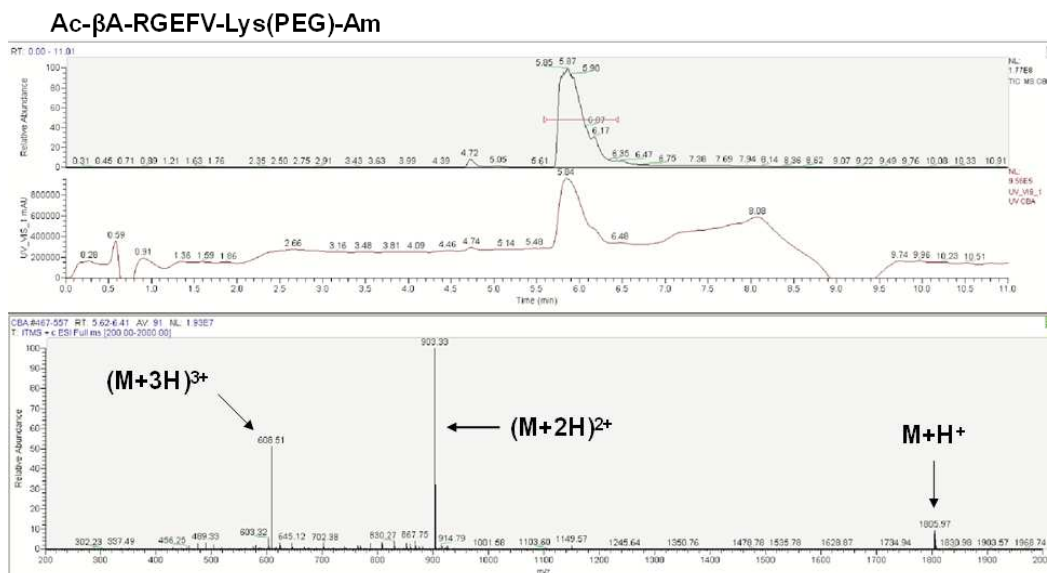
Appendix Figure 158 - LCMS spectra of the PEG modified N-βA peptide in which a glycine was placed on the N-terminus.



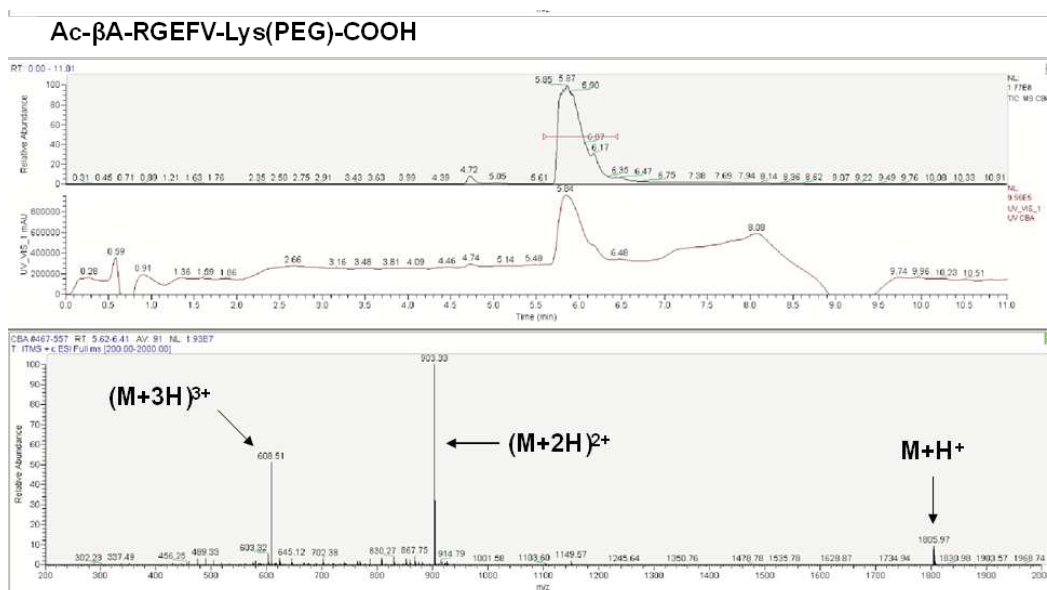
Appendix Figure 159 - LCMS spectra of the PEG modified NH₂ peptide in which a glycine was placed on the N-terminus.



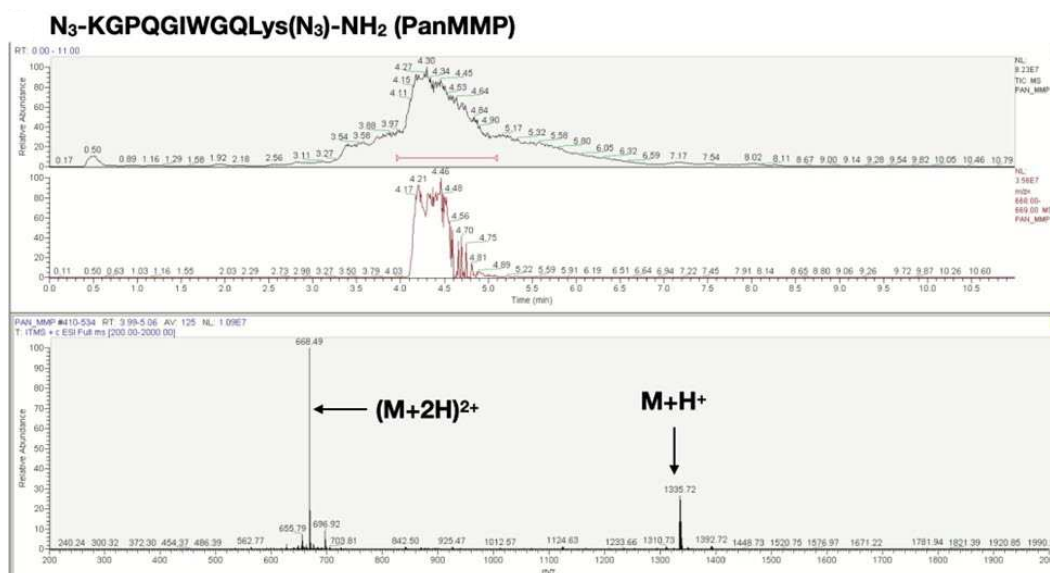
Appendix Figure 160 - LCMS spectra of the PEG modified C-βA peptide in which a glycine was placed on the C-terminus.



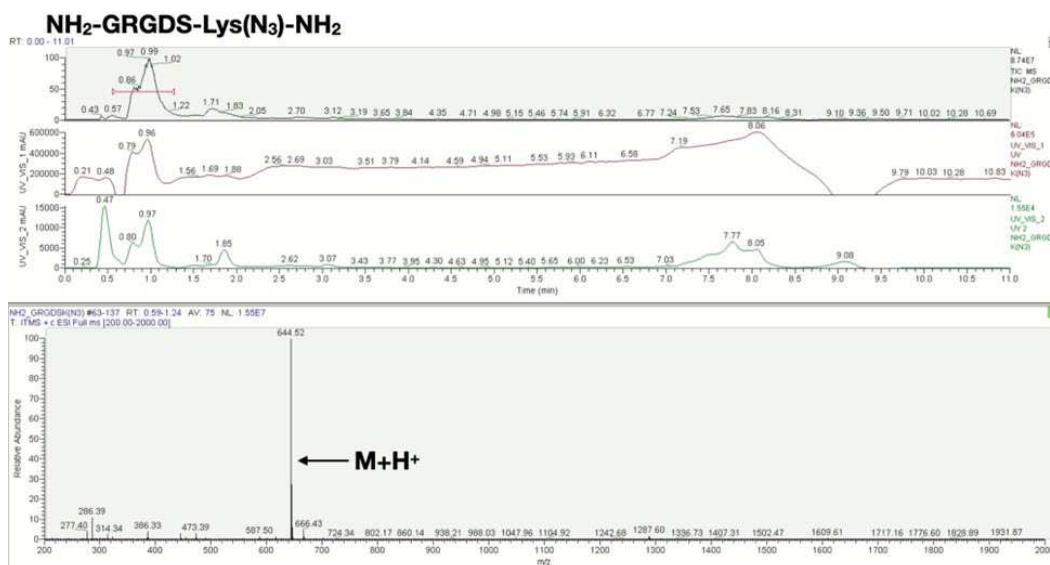
Appendix Figure 161 - LCMS spectra of the PEG modified Am peptide in which a glycine was placed on the C-terminus.



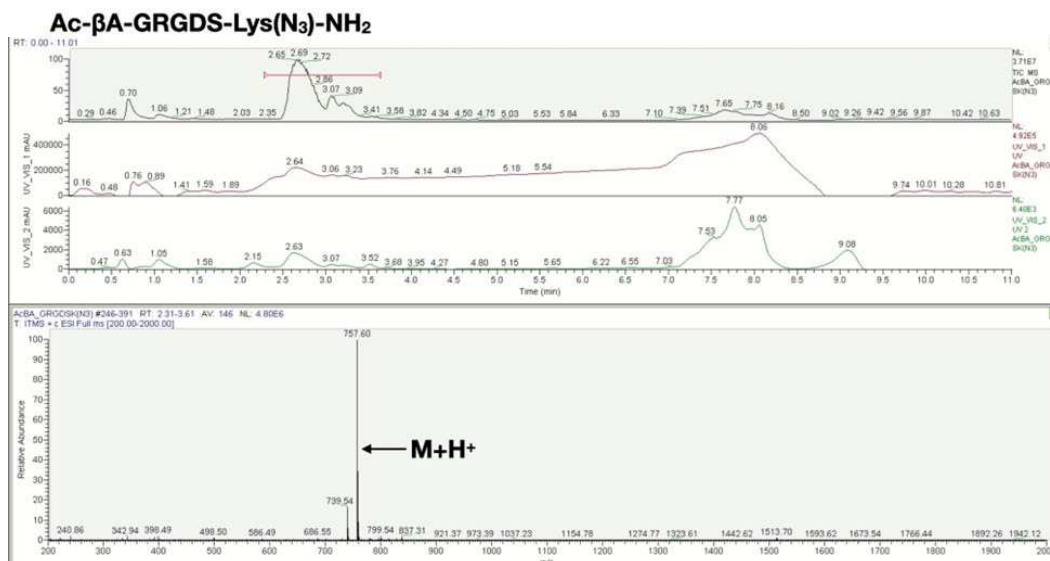
Appendix Figure 162 - LCMS spectra of the PEG modified COOH peptide in which a glycine was placed on the C-terminus.



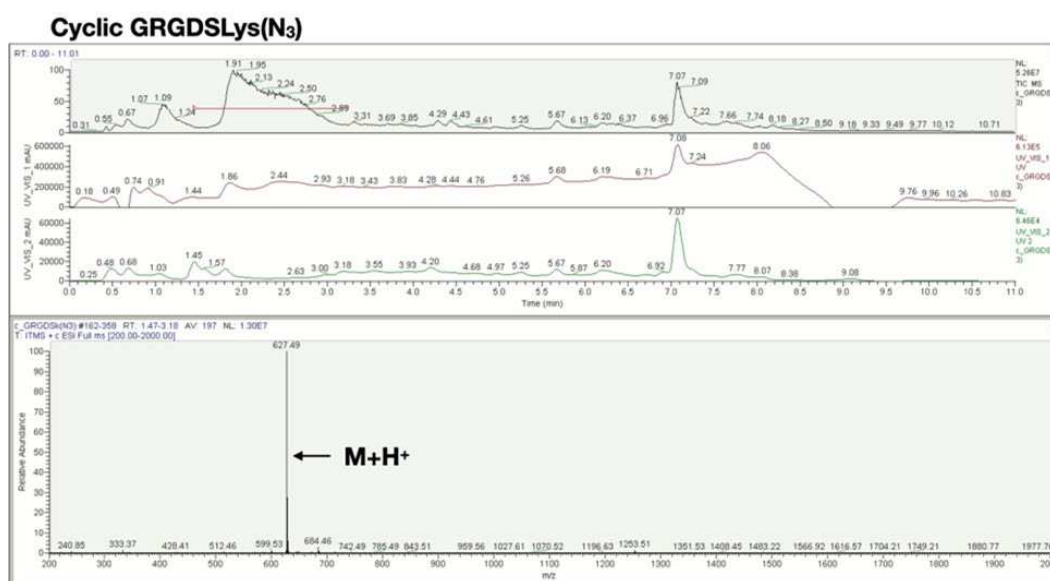
Appendix Figure 163 - LCMS spectra of the peptides used for cell culture: N₃-KGPQGIWGQLys(N₃)-NH₂. Note that the N-terminus of the peptide contained an azide-acetic acid moiety.



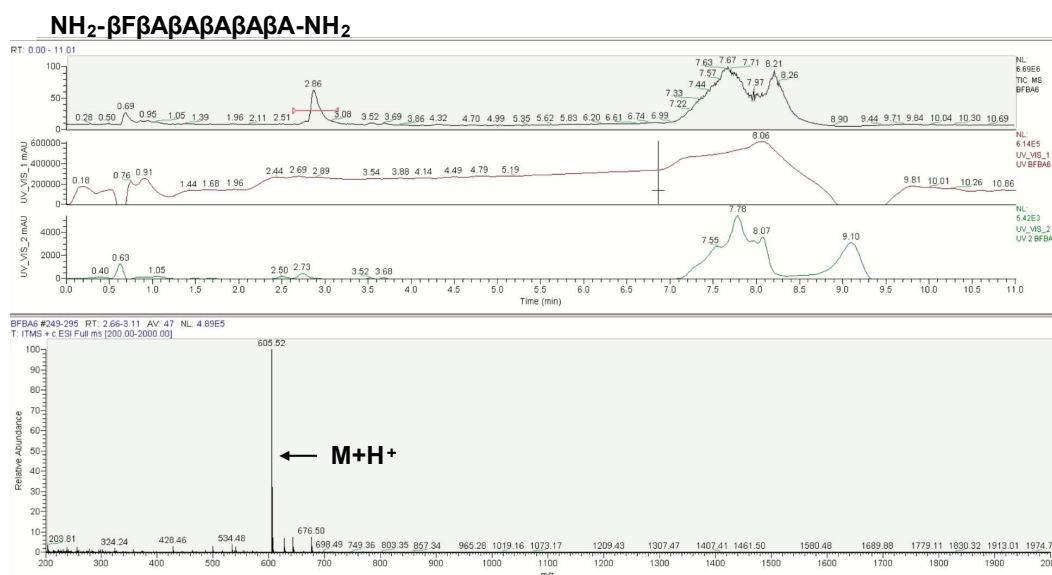
Appendix Figure 164 - LCMS spectra of the peptides used for cell culture: NH₂-GRGDS-Lys(N₃)-NH₂.



Appendix Figure 165 - LCMS spectra of the peptides used for cell culture: Ac- β A-GRGDS-Lys(N₃)-NH₂.

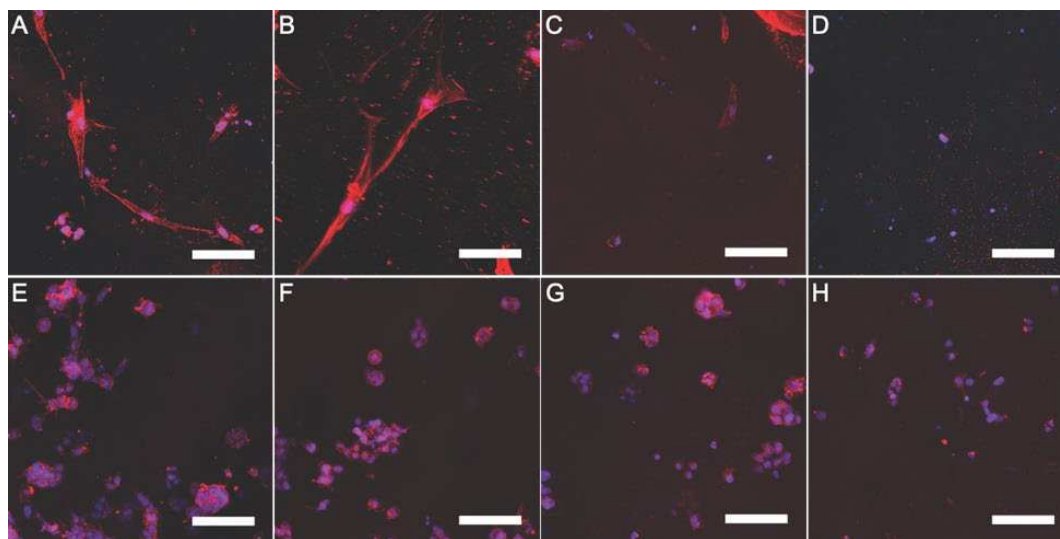


Appendix Figure 166 - LCMS spectra of the peptides used for cell culture: cyclic GRGDS-Lys(N₃).

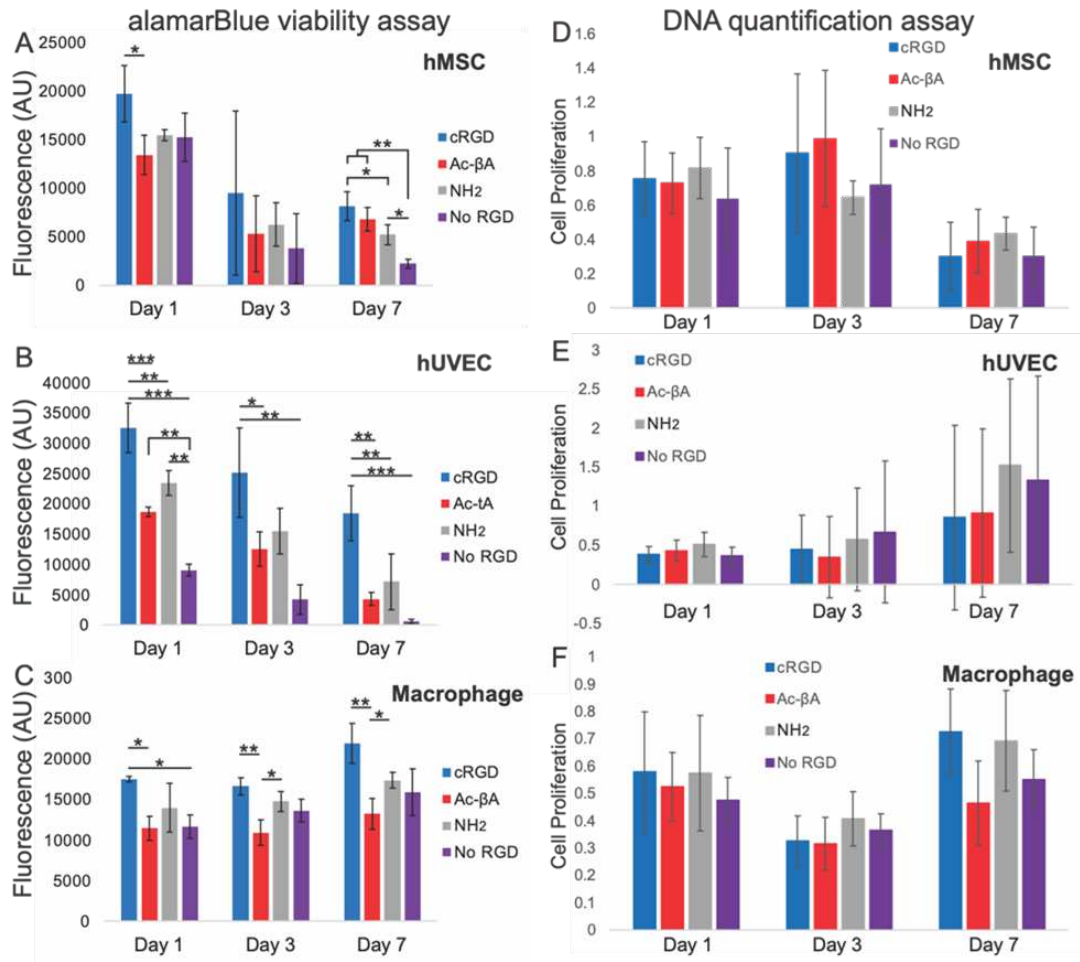


Appendix Figure 167 - LCMS spectra of the peptides used for cell culture: the non-proteolytically degradable NH₂-βFβAβAβAβAβA-NH₂ internal standard.

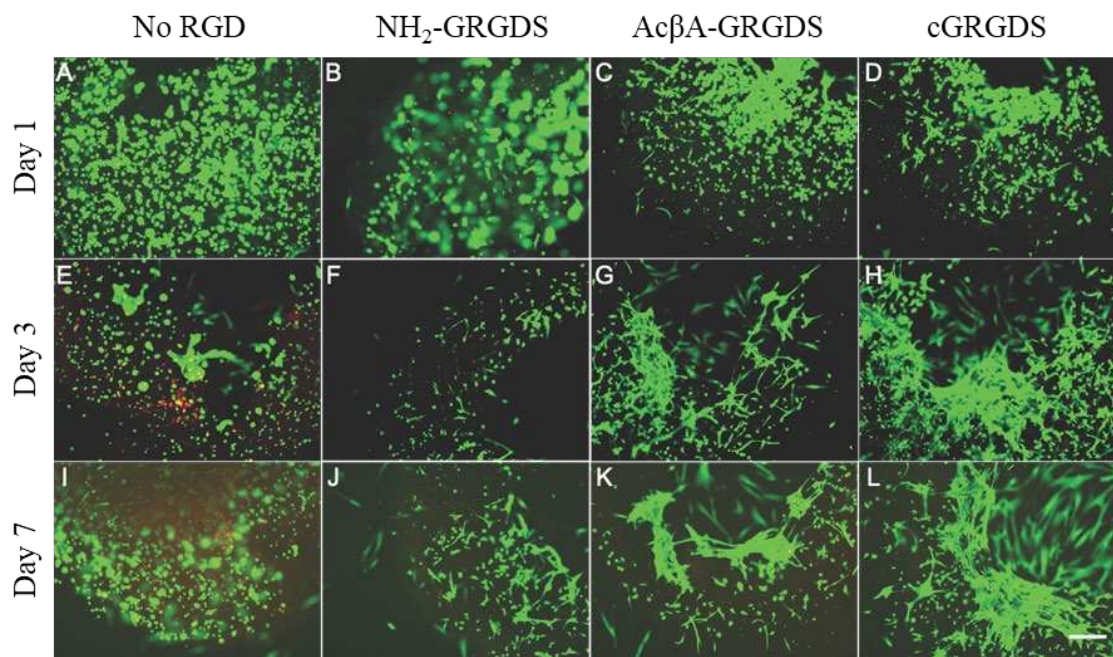
7.3.1 Cells in Gels: Imaging, Viability, DNA, and Live/Dead



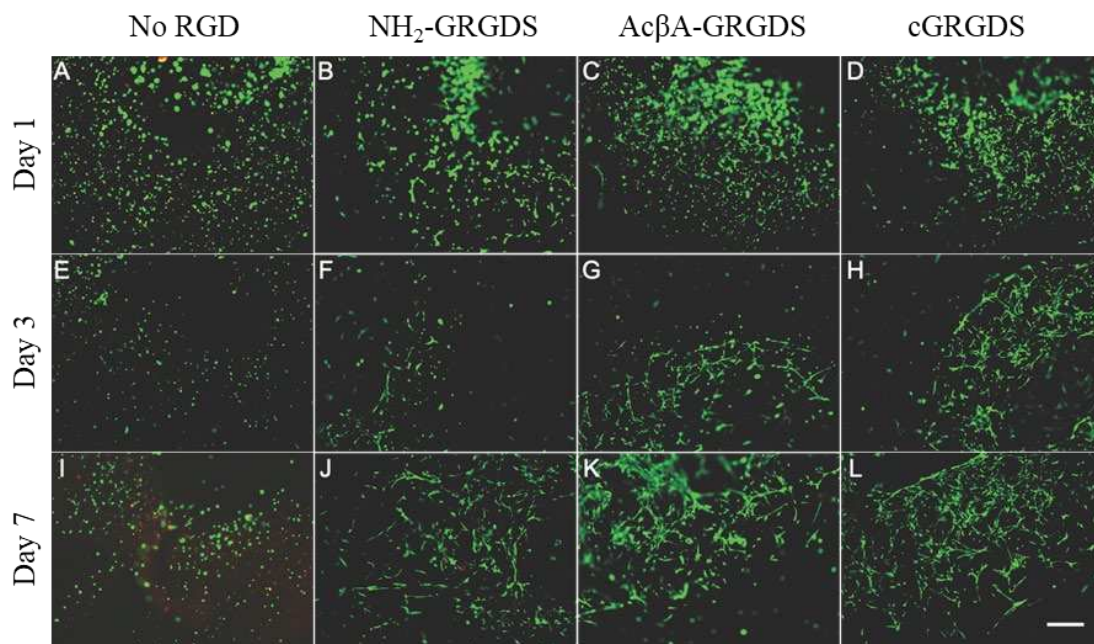
Appendix Figure 168 - Cells growing in gels with different RGD presentations. hUVECs growing in gels with (A) cyclic RGDS, (B) Ac-βA-GRGDS, (C) NH₂-GRGDS, and (D) no added RGDS. Macrophages growing in gels with (E) cyclic RGDS, (F) Ac-βA-GRGDS, (G) NH₂-GRGDS, and (H) no added RGDS. It should be noted that the viability assay (Fig. S9) indicates negligible of metabolic activity within hUVEC gels lacking RGD sequences. Scale bar is 100 μm, and red is actin and blue is the cell nuclei.



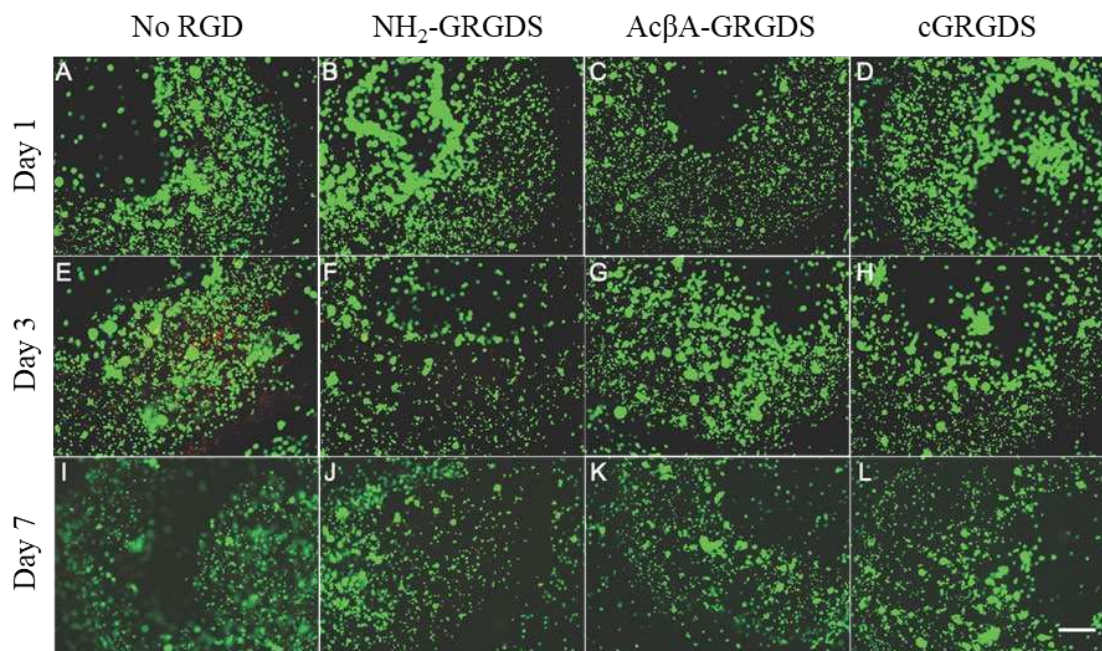
Appendix Figure 169 - Quantification of viability and proliferation in hydrogels containing different RGD sequences. An alamarBlue metabolic activity assays was performed on (A) hMSCs, (B) hUVECs, and (C) macrophages and a DNA quantification assay was performed on (D) hMSCs, (E) hUVECs, and (F) macrophages. * indicates $p < 0.05$, ** indicates $p < 0.01$, *** indicates $p < 0.0001$ by Tukey's post hoc test.



Appendix Figure 170 - Live/dead staining of hMSCs in gels with different RGD conditions. hMSCs were stained at Day 1 in gels with (A) no RGD, (B) NH₂-GRGDS, (C) Ac-βA-GRGDS, and (D) cyclic GRGDS. hMSCs were stained at Day 3 in gels with (E) no RGD, (F) NH₂-GRGDS, (G) Ac-βA-GRGDS, and (H) cyclic GRGDS. hMSCs were stained at Day 7 in gels with (I) no RGD, (J) NH₂-GRGDS, (K) Ac-βA-GRGDS, and (L) cyclic GRGDS. Scale bar is 500 μm.



Appendix Figure 171 - Live/dead staining of hUVECs in gels with different RGD conditions. hUVECs were stained at Day 1 in gels with (A) no RGD, (B) NH₂-GRGDS, (C) Ac-βA-GRGDS, and (D) cyclic GRGDS. hUVECs were stained at Day 3 in gels with (E) no RGD, (F) NH₂-GRGDS, (G) Ac-βA-GRGDS, and (H) cyclic GRGDS. hUVECs were stained at Day 7 in gels with (I) no RGD, (J) NH₂-GRGDS, (K) Ac-βA-GRGDS, and (L) cyclic GRGDS. Scale bar is 500 μm.



Appendix Figure 172 - Live/dead staining of macrophages in gels with different RGD conditions. Macrophages were stained at Day 1 in gels with (A) no RGD, (B) NH₂-GRGDS, (C) Ac-βA-GRGDS, and (D) cyclic GRGDS. Macrophages were stained at Day 3 in gels with (E) no RGD, (F) NH₂-GRGDS, (G) Ac-βA-GRGDS, and (H) cyclic GRGDS. Macrophages were stained at Day 7 in gels with (I) no RGD, (J) NH₂-GRGDS, (K) Ac-βA-GRGDS, and (L) cyclic GRGDS. Scale bar is 500 μm.

7.3.2 Statistical Analysis

A Data for soluble peptides incubated with cells on tissue culture plastic.

	Df	Sum Sq	Mean Sq	F value	Pr(>F)
Celltype	2	279.3	39.65	3125.07	<2e-16 ***
Donor	7	12.4	1.77	39.57	<2e-16 ***
experiment	7	22.7	3.24	72.56	<2e-16 ***
Endgroup	6	376.8	62.79	1405.17	<2e-16 ***
amino_acid	17	36.4	2.14	47.91	<2e-16 ***
timepoint	5	607.1	121.43	2717.35	<2e-16 ***
Residuals	22621	1010.9			

Fit: aov(formula = ave ~ cell + donor + experiment + endgroup + amino_acid + timepoint)

Cell Type

	diff	lwr	upr	p adj
hUVEC-hMSC	0.18174843	0.17324958	0.19024728	0
Macrophage-hMSC	0.26609418	0.25814551	0.27404286	0
Macrophage-hUVEC	0.08434575	0.07639741	0.09229409	0

Endgroup - Averaged over all time points

	diff	lwr	upr	p adj
Am-C β A	-0.035178958	-0.05066638	-0.01969154	0.0000000
COOH-C β A	-0.147212545	-0.16269996	-0.13172512	0.0000000
Ac β A-C β A	-0.004391847	-0.01988046	0.01109677	0.9812038
Ac-C β A	-0.036389911	-0.05188451	-0.02089531	0.0000000
N β A-C β A	-0.093876888	-0.10936431	-0.07838947	0.0000000
NH2-C β A	-0.389396425	-0.40489103	-0.37390182	0.0000000
COOH-Am	-0.112033586	-0.12751981	-0.09654736	0.0000000
Ac β A-Am	0.030787111	0.01529969	0.04627453	0.0000000
Ac-Am	-0.001210953	-0.01670436	0.01428245	0.9999876
N β A-Am	-0.058697929	-0.07418415	-0.04321170	0.0000000
NH2-Am	-0.354217467	-0.36971087	-0.33872406	0.0000000
Ac β A-COOH	0.142820698	0.12733328	0.15830812	0.0000000
Ac-COOH	0.110822633	0.09532923	0.12631604	0.0000000
N β A-COOH	0.053335657	0.03784943	0.06882188	0.0000000
NH2-COOH	-0.242183880	-0.25767729	-0.22669047	0.0000000
Ac-Ac β A	-0.031998064	-0.04749267	-0.01650346	0.0000000
N β A-Ac β A	-0.089485041	-0.10497246	-0.07399762	0.0000000
NH2-Ac β A	-0.385004578	-0.40049918	-0.36950998	0.0000000
N β A-Ac	-0.057486976	-0.07298038	-0.04199357	0.0000000
NH2-Ac	-0.353006513	-0.36850710	-0.33750593	0.0000000
NH2-N β A	-0.295519537	-0.31101294	-0.28002613	0.0000000

Amino Acid

	diff	lwr	upr	p adj
D-A	0.0911418367	0.0617564292	0.1205272442	0.0000000
E-A	0.0674525839	0.0380671764	0.0968379914	0.0000000
F-A	-0.0285623966	-0.0579478041	0.0008230109	0.0680295
G-A	0.0074636879	-0.0219217196	0.0368490954	0.9999903
H-A	-0.0193680806	-0.0487534881	0.0100173269	0.6837704
I_L-A	0.0150238223	-0.0143615852	0.0444092299	0.9485997
K-A	-0.0251598995	-0.0545453070	0.0042255080	0.2061101
M-A	-0.0071542074	-0.0365454494	0.0222370346	0.9999948
N-A	0.0307876787	0.0014022712	0.0601730862	0.0286257
P-A	0.0493901460	0.0200047385	0.0787755535	0.0000005
Q-A	-0.0006024072	-0.0299878147	0.0287830003	1.0000000
R-A	-0.0697643361	-0.0991497436	-0.0403789286	0.0000000
S-A	-0.0104474036	-0.0398328111	0.0189380039	0.9990181
T-A	0.0102079392	-0.0191774683	0.0395933467	0.9992686
V-A	0.0375140807	0.0080876607	0.0669405006	0.0012033
W-A	-0.0644909884	-0.0939115249	-0.0350704518	0.0000000
Y-A	-0.0120895025	-0.0414749100	0.0172959050	0.9943445
E-D	-0.0236892528	-0.0530746603	0.0056961547	0.3045992
F-D	-0.1197042334	-0.1490896409	-0.0903188259	0.0000000
G-D	-0.0836781489	-0.1130635564	-0.0542927414	0.0000000
H-D	-0.1105099174	-0.1398953249	-0.0811245099	0.0000000
I_L-D	-0.0761180144	-0.1055034219	-0.0467326069	0.0000000
K-D	-0.1163017363	-0.1456871438	-0.0869163288	0.0000000
M-D	-0.0982960442	-0.1276872861	-0.0689048022	0.0000000
N-D	-0.0603541581	-0.0897395656	-0.0309687506	0.0000000
P-D	-0.0417516908	-0.0711370983	-0.0123662833	0.0001051
Q-D	-0.0917442439	-0.1211296514	-0.0623588364	0.0000000
R-D	-0.1609061728	-0.1902915803	-0.1315207653	0.0000000
S-D	-0.1015892404	-0.1309746479	-0.0722038329	0.0000000
T-D	-0.0809338976	-0.1103193051	-0.0515484901	0.0000000
V-D	-0.0536277561	-0.0830541760	-0.0242013361	0.0000000
W-D	-0.1556328251	-0.1850533616	-0.1262122886	0.0000000
Y-D	-0.1032313392	-0.1326167467	-0.0738459317	0.0000000
F-E	-0.0960149805	-0.1254003880	-0.0666295730	0.0000000
G-E	-0.0599888960	-0.0893743035	-0.0306034885	0.0000000
H-E	-0.0868206645	-0.1162060720	-0.0574352570	0.0000000
I_L-E	-0.0524287616	-0.0818141691	-0.0230433541	0.0000000
K-E	-0.0926124834	-0.1219978909	-0.0632270759	0.0000000
M-E	-0.0746067913	-0.1039980333	-0.0452155493	0.0000000
N-E	-0.0366649053	-0.0660503128	-0.0072794978	0.0018310
P-E	-0.0180624379	-0.0474478454	0.0113229696	0.7898131
Q-E	-0.0680549911	-0.0974403986	-0.0386695836	0.0000000
R-E	-0.1372169200	-0.1666023275	-0.1078315125	0.0000000
S-E	-0.0778999875	-0.1072853950	-0.0485145800	0.0000000
T-E	-0.0572446447	-0.0866300522	-0.0278592372	0.0000000
V-E	-0.0299385032	-0.0593649232	-0.0005120833	0.0409923

W-E -0.1319435723 -0.1613641088 -0.1025230357 0.0000000
Y-E -0.0795420864 -0.1089274939 -0.0501566789 0.0000000
G-F 0.0360260845 0.0066406770 0.0654114920 0.0025440
H-F 0.0091943160 -0.0201910915 0.0385797235 0.9998155
I_L-F 0.0435862190 0.0142008115 0.0729716265 0.0000338
K-F 0.0034024971 -0.0259829104 0.0327879046 1.0000000
M-F 0.0214081892 -0.0079830528 0.0507994312 0.4981737
N-F 0.0593500753 0.0299646678 0.0887354828 0.0000000
P-F 0.0779525426 0.0485671351 0.1073379501 0.0000000
Q-F 0.0279599894 -0.0014254181 0.0573453970 0.0844257
R-F -0.0412019394 -0.0705873469 -0.0118165319 0.0001460
S-F 0.0181149930 -0.0112704145 0.0475004005 0.7859067
T-F 0.0387703358 0.0093849283 0.0681557433 0.0005903
V-F 0.0660764773 0.0366500574 0.0955028973 0.0000000
W-F -0.0359285917 -0.0653491282 -0.0065080552 0.0027321
Y-F 0.0164728942 -0.0129125133 0.0458583017 0.8898527
H-G -0.0268317685 -0.0562171760 0.0025536390 0.1237204
I_L-G 0.0075601345 -0.0218252730 0.0369455420 0.9999883
K-G -0.0326235874 -0.0620089949 -0.0032381799 0.0129911
M-G -0.0146178953 -0.0440091373 0.0147733467 0.9599599
N-G 0.0233239908 -0.0060614167 0.0527093983 0.3326789
P-G 0.0419264581 0.0125410506 0.0713118656 0.0000946
Q-G -0.0080660950 -0.0374515025 0.0213193125 0.9999702
R-G -0.0772280239 -0.1066134314 -0.0478426164 0.0000000
S-G -0.0179110915 -0.0472964990 0.0114743160 0.8008656
T-G 0.0027442513 -0.0266411562 0.0321296588 1.0000000
V-G 0.0300503928 0.0006239729 0.0594768128 0.0392224
W-G -0.0719546762 -0.1013752127 -0.0425341397 0.0000000
Y-G -0.0195531903 -0.0489385978 0.0098322172 0.6674980
I_L-H 0.0343919030 0.0050064955 0.0637773105 0.0057134
K-H -0.0057918189 -0.0351772264 0.0235935886 0.9999998
M-H 0.0122138732 -0.0171773688 0.0416051152 0.9936667
N-H 0.0501557593 0.0207703518 0.0795411668 0.0000002
P-H 0.0687582266 0.0393728191 0.0981436341 0.0000000
Q-H 0.0187656735 -0.0106197340 0.0481510810 0.7348440
R-H -0.0503962554 -0.0797816629 -0.0210108479 0.0000001
S-H 0.0089206770 -0.0204647305 0.0383060845 0.9998777
T-H 0.0295760198 0.0001906123 0.0589614273 0.0464617
V-H 0.0568821613 0.0274557414 0.0863085813 0.0000000
W-H -0.0451229077 -0.0745434442 -0.0157023712 0.0000130
Y-H 0.0072785782 -0.0221068293 0.0366639857 0.9999933
K-I_L -0.0401837219 -0.0695691294 -0.0107983144 0.0002651
M-I_L -0.0221780298 -0.0515692717 0.0072132122 0.4289220
N-I_L 0.0157638563 -0.0136215512 0.0451492638 0.9223924
P-I_L 0.0343663236 0.0049809161 0.0637517311 0.0057841
Q-I_L -0.0156262295 -0.0450116370 0.0137591780 0.9278480
R-I_L -0.0847881584 -0.1141735659 -0.0554027509 0.0000000
S-I_L -0.0254712260 -0.0548566335 0.0039141815 0.1884060

T-I_L -0.0048158832 -0.0342012907 0.0245695243 1.0000000
V-I_L 0.0224902583 -0.0069361616 0.0519166783 0.4040892
W-I_L -0.0795148107 -0.1089353472 -0.0500942742 0.0000000
Y-I_L -0.0271133248 -0.0564987323 0.0022720827 0.1127786
M-K 0.0180056921 -0.0113855499 0.0473969341 0.7942535
N-K 0.0559475782 0.0265621707 0.0853329857 0.0000000
P-K 0.0745500455 0.0451646380 0.1039354530 0.0000000
Q-K 0.0245574924 -0.0048279151 0.0539428999 0.2435191
R-K -0.0446044365 -0.0739898440 -0.0152190290 0.0000176
S-K 0.0147124959 -0.0146729116 0.0440979034 0.9574387
T-K 0.0353678387 0.0059824312 0.0647532462 0.0035440
V-K 0.0626739802 0.0332475603 0.0921004002 0.0000000
W-K -0.0393310888 -0.0687516253 -0.0099105523 0.0004429
Y-K 0.0130703971 -0.0163150104 0.0424558046 0.9867309
N-M 0.0379418861 0.0085506441 0.0673331280 0.0009334
P-M 0.0565443534 0.0271531114 0.0859355954 0.0000000
Q-M 0.0065518002 -0.0228394418 0.0359430422 0.9999986
R-M -0.0626101287 -0.0920013707 -0.0332188867 0.0000000
S-M -0.0032931962 -0.0326844382 0.0260980458 1.0000000
T-M 0.0173621466 -0.0120290954 0.0467533886 0.8385896
V-M 0.0446682881 0.0152360418 0.0741005344 0.0000177
W-M -0.0573367809 -0.0867631450 -0.0279104169 0.0000000
Y-M -0.0049352951 -0.0343265371 0.0244559469 1.0000000
P-N 0.0186024673 -0.0107829402 0.0479878748 0.7480944
Q-N -0.0313900858 -0.0607754933 -0.0020046783 0.0222507
R-N -0.1005520147 -0.1299374222 -0.0711666072 0.0000000
S-N -0.0412350823 -0.0706204898 -0.0118496748 0.0001432
T-N -0.0205797395 -0.0499651470 0.0088056680 0.5741915
V-N 0.0067264020 -0.0227000179 0.0361528220 0.9999980
W-N -0.0952786670 -0.1246992035 -0.0658581305 0.0000000
Y-N -0.0428771811 -0.0722625886 -0.0134917736 0.0000528
Q-P -0.0499925532 -0.0793779607 -0.0206071457 0.0000002
R-P -0.1191544821 -0.1485398896 -0.0897690746 0.0000000
S-P -0.0598375496 -0.0892229571 -0.0304521421 0.0000000
T-P -0.0391822068 -0.0685676143 -0.0097967993 0.0004690
V-P -0.0118760653 -0.0413024852 0.0175503547 0.9954584
W-P -0.1138811343 -0.1433016708 -0.0844605978 0.0000000
Y-P -0.0614796485 -0.0908650560 -0.0320942410 0.0000000
R-Q -0.0691619289 -0.0985473364 -0.0397765214 0.0000000
S-Q -0.0098449964 -0.0392304039 0.0195404111 0.9995420
T-Q 0.0108103464 -0.0185750611 0.0401957539 0.9984965
V-Q 0.0381164879 0.0086900679 0.0675429078 0.0008703
W-Q -0.0638885812 -0.0933091177 -0.0344680447 0.0000000
Y-Q -0.0114870953 -0.0408725028 0.0178983122 0.9968695
S-R 0.0593169325 0.0299315250 0.0887023400 0.0000000
T-R 0.0799722752 0.0505868677 0.1093576827 0.0000000
V-R 0.1072784168 0.0778519968 0.1367048367 0.0000000
W-R 0.0052733477 -0.0241471888 0.0346938842 1.0000000

Y-R	0.0576748336	0.0282894261	0.0870602411	0.0000000
T-S	0.0206553428	-0.0087300647	0.0500407503	0.5672063
V-S	0.0479614843	0.0185350644	0.0773879043	0.0000017
W-S	-0.0540435847	-0.0834641212	-0.0246230482	0.0000000
Y-S	-0.0016420988	-0.0310275063	0.0277433087	1.0000000
V-T	0.0273061415	-0.0021202784	0.0567325615	0.1070972
W-T	-0.0746989275	-0.1041194640	-0.0452783910	0.0000000
Y-T	-0.0222974416	-0.0516828491	0.0070879659	0.4180775
W-V	-0.1020050690	-0.1314665691	-0.0725435690	0.0000000
Y-V	-0.0496035832	-0.0790300031	-0.0201771632	0.0000004
Y-W	0.0524014859	0.0229809494	0.0818220224	0.0000000

Donor

	diff	lwr	upr	p adj
3088202-3087423	-0.009686784	-0.0295486217	1.017505e-02	0.8747639
3091412-3087423.	-0.040182618	-0.0600444554	-2.032078e-02	0.0000000
310264-3087423	-0.027216718	-0.0470917219	-7.341713e-03	0.0006227
310268-3087423	-0.019910449	-0.0397744766	-4.642087e-05	0.0488963
310280-3087423	-0.055138247	-0.0750000843	-3.527641e-02	0.0000000
4608-3087423	-0.045885753	-0.0657607575	-2.601075e-02	0.0000000
8119-3087423	-0.025544000	-0.0454058378	-5.682163e-03	0.0019297
8478-3087423	-0.030891304	-0.0507531412	-1.102947e-02	0.0000378
THP1-3087423	-0.086540213	-0.1064042410	-6.667619e-02	0.0000000
3091412-3088202.	-0.030495834	-0.0503576714	-1.063400e-02	0.0000520
310264-3088202	-0.017529934	-0.0374049379	2.345071e-03	0.1394945
310268-3088202	-0.010223665	-0.0300876925	9.640363e-03	0.8344493
310280-3088202.	-0.045451463	-0.0653133002	-2.558962e-02	0.0000000
4608-3088202	-0.036198969	-0.0560739735	-1.632396e-02	0.0000001
8119-3088202	-0.015857216	-0.0357190537	4.004622e-03	0.2543606
8478-3088202	-0.021204519	-0.0410663571	-1.342682e-03	0.0254446
THP1-3088202	-0.076853429	-0.0967174569	-5.698940e-02	0.0000000
310264-3091412	0.012965900	-0.0069091041	3.284090e-02	0.5531567
310268-3091412	0.020272169	0.0004081412	4.013620e-02	0.0409855
310280-3091412	-0.014955629	-0.0348174665	4.906209e-03	0.3363452
4608-3091412	-0.005703135	-0.0255781397	1.417187e-02	0.9962700
8119-3091412	0.014638618	-0.0052232200	3.450046e-02	0.3680951
8478-3091412	0.009291314	-0.0105705234	2.915315e-02	0.9003185
	diff	lwr	upr	p adj
THP1-3091412	-0.046357595	-0.0662216232	-2.649357e-02	0.0000000
310268-310264	0.007306269	-0.0125709241	2.718346e-02	0.9777526
310280-310264	-0.027921529	-0.0477965333	-8.046525e-03	0.0003758
4608-310264	-0.018669036	-0.0385571978	1.219127e-03	0.0873723
8119-310264	0.001672718	-0.0182022868	2.154772e-02	0.9999999
8478-310264	-0.003674586	-0.0235495901	1.620042e-02	0.9998916
THP1-310264	-0.059323495	-0.0792006885	-3.944630e-02	0.0000000
310280-310268	-0.035227798	-0.0550918258	-1.536377e-02	0.0000007
4608-310268	-0.025975305	-0.0458524975	-6.098112e-03	0.0014675
8119-310268	-0.005633551	-0.0254975793	1.423048e-02	0.9965883
8478-310268	-0.010980855	-0.0308448827	8.883173e-03	0.7671006
THP1-310268	-0.066629764	-0.0864959822	-4.676355e-02	0.0000000
4608-310280	0.009252493	-0.0106225109	2.912750e-02	0.9029945
8119-310280	0.029594246	0.0097324088	4.945608e-02	0.0001057
8478-310280	0.024246943	0.0043851055	4.410878e-02	0.0044310
THP1-310280	-0.031401966	-0.0512659943	-1.153794e-02	0.0000250
8119-4608	0.020341753	0.0004667488	4.021676e-02	0.0398183
8478-4608	0.014994450	-0.0048805545	3.486945e-02	0.3335221
THP1-4608	-0.040654460	-0.0605316529	-2.077727e-02	0.0000000
8478-8119	-0.005347303	-0.0252091410	1.451453e-02	0.9977135
THP1-8119	-0.060996213	-0.0808602408	-4.113219e-02	0.0000000
THP1-8478	-0.055648910	-0.0755129374	-3.578488e-02	0.0000000

B Soluble peptides with cells on tissue culture plastic, 48 hour time point only

48 hours	Df	Sum Sq	Mean Sq	F value	Pr(>F)
celltype	2	279.3	139.65	1952.84	<2e-16 ***
donor	7	12.4	1.77	24.73	<2e-16 ***
experiment	7	22.7	3.24	45.34	<2e-16 ***
endgroup	6	376.8	62.79	878.08	<2e-16 ***
amino_acid	17	36.4	2.14	29.93	<2e-16 ***
residuals	22626	1618	0.07		

Tukey multiple comparisons of means
95% family-wise confidence level

Fit: aov(formula = ave ~ cell + donor + experiment + endgroup + amino_acid)

<u>Cell type</u>	diff	lwr	upr	p adj
hUVEC-hMSC	0.18174843	0.17099723	0.19249964	0
Mac-hMSC	0.26609418	0.25603896	0.27614940	0
Mac-hUVEC	0.08434575	0.07429095	0.09440055	0

<u>Endgroup</u>	diff	lwr	upr	p adj
Am-CβA	-0.035178958	-0.05477083	-0.01558708	0.0000023
COOH-CβA	-0.147212545	-0.16680442	-0.12762067	0.0000000
AcβA-CβA	-0.004391847	-0.02398523	0.01520154	0.9946058
Ac-CβA	-0.036389911	-0.05599087	-0.01678895	0.0000007
NβA-CβA	-0.093876888	-0.11346876	-0.07428501	0.0000000
NH2-CβA	-0.389396425	-0.40899738	-0.36979547	0.0000000
COOH-Am	-0.112033586	-0.13162395	-0.09244322	0.0000000
AcβA-Am	0.030787111	0.01119524	0.05037899	0.0000737
Ac-Am	-0.001210953	-0.02081040	0.01838849	0.9999969
NβA-Am	-0.058697929	-0.07828829	-0.03910757	0.0000000
NH2-Am	-0.354217467	-0.37381691	-0.33461802	0.0000000
AcβA-COOH	0.142820698	0.12322882	0.16241257	0.0000000
Ac-COOH	0.110822633	0.09122319	0.13042208	0.0000000
NβA-COOH	0.053335657	0.03374529	0.07292602	0.0000000
NH2-COOH	-0.242183880	-0.26178333	-0.22258443	0.0000000
Ac-AcβA	-0.031998064	-0.05159902	-0.01239711	0.0000305
NβA-AcβA	-0.089485041	-0.10907691	-0.06989317	0.0000000
NH2-AcβA	-0.385004578	-0.40460554	-0.36540362	0.0000000
NβA-Ac	-0.057486976	-0.07708642	-0.03788753	0.0000000
NH2-Ac	-0.353006513	-0.37261504	-0.33339799	0.0000000
NH2-NβA	-0.295519537	-0.31511898	-0.27592009	0.0000000

Amino acid

	diff	lwr	upr	p adj
D-A	0.0911418367	0.0539687514	0.1283149221	0.0000000
E-A	0.0674525839	0.0302794985	0.1046256693	0.0000000
F-A	-0.0285623966	-0.0657354820	0.0086106888	0.3938383
G-A	0.0074636879	-0.0297093975	0.0446367732	0.9999997
H-A	-0.0193680806	-0.0565411660	0.0178050047	0.9393452
I_L-A	0.0150238223	-0.0221492630	0.0521969077	0.9953836
K-A	-0.0251598995	-0.0623329849	0.0120131859	0.6374478
M-A	-0.0071542074	-0.0443346735	0.0300262587	0.9999999
N-A	0.0307876787	-0.0063854067	0.0679607640	0.2581939
P-A	0.0493901460	0.0122170606	0.0865632314	0.0005071
Q-A	-0.0006024072	-0.0377754926	0.0365706782	1.0000000
R-A	-0.0697643361	-0.1069374215	-0.0325912507	0.0000000
S-A	-0.0104474036	-0.0476204890	0.0267256818	0.9999583
T-A	0.0102079392	-0.0269651462	0.0473810246	0.9999700
V-A	0.0375140807	0.0002891138	0.0747390476	0.0457894
W-A	-0.0644909884	-0.1017085126	-0.0272734641	0.0000000
Y-A	-0.0120895025	-0.0492625879	0.0250835829	0.9996903
E-D	-0.0236892528	-0.0608623382	0.0134838325	0.7380570
F-D	-0.1197042334	-0.1568773188	-0.0825311480	0.0000000
G-D	-0.0836781489	-0.1208512343	-0.0465050635	0.0000000
H-D	-0.1105099174	-0.1476830028	-0.0733368320	0.0000000
I_L-D	-0.0761180144	-0.1132910998	-0.0389449290	0.0000000
K-D	-0.1163017363	-0.1534748217	-0.0791286509	0.0000000
M-D	-0.0982960442	-0.1354765103	-0.0611155780	0.0000000
N-D	-0.0603541581	-0.0975272435	-0.0231810727	0.0000020
P-D	-0.0417516908	-0.0789247762	-0.0045786054	0.0109361
Q-D	-0.0917442439	-0.1289173293	-0.0545711585	0.0000000
R-D	-0.1609061728	-0.1980792582	-0.1237330874	0.0000000
S-D	-0.1015892404	-0.1387623258	-0.0644161550	0.0000000
T-D	-0.0809338976	-0.1181069830	-0.0437608122	0.0000000
V-D	-0.0536277561	-0.0908527230	-0.0164027892	0.0000738
W-D	-0.1556328251	-0.1928503493	-0.1184153009	0.0000000
Y-D	-0.1032313392	-0.1404044246	-0.0660582538	0.0000000
F-E	-0.0960149805	-0.1331880659	-0.0588418952	0.0000000
G-E	-0.0599888960	-0.0971619814	-0.0228158107	0.0000025
H-E	-0.0868206645	-0.1239937499	-0.0496475792	0.0000000
I_L-E	-0.0524287616	-0.0896018469	-0.0152556762	0.0001263
K-E	-0.0926124834	-0.1297855688	-0.0554393981	0.0000000
M-E	-0.0746067913	-0.1117872574	-0.0374263252	0.0000000
N-E	-0.0366649053	-0.0738379906	0.0005081801	0.0582158
P-E	-0.0180624379	-0.0552355233	0.0191106475	0.9678116
Q-E	-0.0680549911	-0.1052280765	-0.0308819057	0.0000000
R-E	-0.1372169200	-0.1743900054	-0.1000438346	0.0000000
S-E	-0.0778999875	-0.1150730729	-0.0407269021	0.0000000
T-E	-0.0572446447	-0.0944177301	-0.0200715594	0.0000115
V-E	-0.0299385032	-0.0671634701	0.0072864637	0.3088003

W-E -0.1319435723 -0.1691610965 -0.0947260480 0.0000000
Y-E -0.0795420864 -0.1167151718 -0.0423690010 0.0000000
G-F 0.0360260845 -0.0011470009 0.0731991699 0.0701352
H-F 0.0091943160 -0.0279787694 0.0463674014 0.9999934
I_L-F 0.0435862190 0.0064131336 0.0807593044 0.0055425
K-F 0.0034024971 -0.0337705883 0.0405755825 1.0000000
M-F 0.0214081892 -0.0157722769 0.0585886554 0.8654509
N-F 0.0593500753 0.0221769899 0.0965231607 0.0000036
P-F 0.0779525426 0.0407794572 0.1151256280 0.0000000
Q-F 0.0279599894 -0.0092130959 0.0651330748 0.4352011
R-F -0.0412019394 -0.0783750248 -0.0040288541 0.0133051
S-F 0.0181149930 -0.0190580924 0.0552880784 0.9669115
T-F 0.0387703358 0.0015972504 0.0759434212 0.0303156
V-F 0.0660764773 0.0288515104 0.1033014442 0.0000000
W-F -0.0359285917 -0.0731461160 0.0012889325 0.0730109
Y-F 0.0164728942 -0.0207001912 0.0536459796 0.9872413
H-G -0.0268317685 -0.0640048539 0.0103413169 0.5159264
I_L-G 0.0075601345 -0.0296129509 0.0447332199 0.9999997
K-G -0.0326235874 -0.0697966728 0.0045494980 0.1714720
M-G -0.0146178953 -0.0517983614 0.0225625709 0.9966506
N-G 0.0233239908 -0.0138490946 0.0604970762 0.7611846
P-G 0.0419264581 0.0047533727 0.0790995435 0.0102676
Q-G -0.0080660950 -0.0452391804 0.0291069903 0.9999991
R-G -0.0772280239 -0.1144011093 -0.0400549386 0.0000000
S-G -0.0179110915 -0.0550841769 0.0192619939 0.9702995
T-G 0.0027442513 -0.0344288341 0.0399173367 1.0000000
V-G 0.0300503928 -0.0071745741 0.0672753597 0.3021633
W-G -0.0719546762 -0.1091722005 -0.0347371520 0.0000000
Y-G -0.0195531903 -0.0567262757 0.0176198951 0.9341904
I_L-H 0.0343919030 -0.0027811824 0.0715649884 0.1100495
K-H -0.0057918189 -0.0429649043 0.0313812665 1.0000000
M-H 0.0122138732 -0.0249665929 0.0493943394 0.9996463
N-H 0.0501557593 0.0129826739 0.0873288447 0.0003604
P-H 0.0687582266 0.0315851412 0.1059313120 0.0000000
Q-H 0.0187656735 -0.0184074119 0.0559387588 0.9541257
R-H -0.0503962554 -0.0875693408 -0.0132231701 0.0003233
S-H 0.0089206770 -0.0282524084 0.0460937624 0.9999958
T-H 0.0295760198 -0.0075970656 0.0667491052 0.3282941
V-H 0.0568821613 0.0196571944 0.0941071282 0.0000145
W-H -0.0451229077 -0.0823404320 -0.0079053835 0.0031128
Y-H 0.0072785782 -0.0298945072 0.0444516636 0.9999998
K-I_L -0.0401837219 -0.0773568073 -0.0030106365 0.0189500
M-I_L -0.0221780298 -0.0593584959 0.0150024364 0.8274584
N-I_L 0.0157638563 -0.0214092291 0.0529369417 0.9920654
P-I_L 0.0343663236 -0.0028067618 0.0715394090 0.1107945
Q-I_L -0.0156262295 -0.0527993149 0.0215468559 0.9927993
R-I_L -0.0847881584 -0.1219612438 -0.0476150730 0.0000000
S-I_L -0.0254712260 -0.0626443114 0.0117018594 0.6150779

T-I_L -0.0048158832 -0.0419889686 0.0323572022 1.0000000
V-I_L 0.0224902583 -0.0147347086 0.0597152252 0.8120325
W-I_L -0.0795148107 -0.1167323349 -0.0422972865 0.0000000
Y-I_L -0.0271133248 -0.0642864102 0.0100597606 0.4955013
M-K 0.0180056921 -0.0191747740 0.0551861583 0.9688215
N-K 0.0559475782 0.0187744928 0.0931206636 0.0000225
P-K 0.0745500455 0.0373769601 0.1117231309 0.0000000
Q-K 0.0245574924 -0.0126155930 0.0617305777 0.6798651
R-K -0.0446044365 -0.0817775219 -0.0074313512 0.0037393
S-K 0.0147124959 -0.0224605895 0.0518855813 0.9963790
T-K 0.0353678387 -0.0018052467 0.0725409241 0.0844742
V-K 0.0626739802 0.0254490133 0.0998989471 0.0000004
W-K -0.0393310888 -0.0765486131 -0.0021135646 0.0256295
Y-K 0.0130703971 -0.0241026883 0.0502434825 0.9991467
N-M 0.0379418861 0.0007614199 0.0751223522 0.0395549
P-M 0.0565443534 0.0193638873 0.0937248195 0.0000166
Q-M 0.0065518002 -0.0306286659 0.0437322663 1.0000000
R-M -0.0626101287 -0.0997905948 -0.0254296626 0.0000004
S-M -0.0032931962 -0.0404736624 0.0338872699 1.0000000
T-M 0.0173621466 -0.0198183196 0.0545426127 0.9781475
V-M 0.0446682881 0.0074359507 0.0819006254 0.0037499
W-M -0.0573367809 -0.0945616771 -0.0201118848 0.0000114
Y-M -0.0049352951 -0.0421157612 0.0322451711 1.0000000
P-N 0.0186024673 -0.0185706181 0.0557755527 0.9576289
Q-N -0.0313900858 -0.0685631712 0.0057829996 0.2270870
R-N -0.1005520147 -0.1377251001 -0.0633789293 0.0000000
S-N -0.0412350823 -0.0784081677 -0.0040619969 0.0131501
T-N -0.0205797395 -0.0577528249 0.0165933459 0.9000136
V-N 0.0067264020 -0.0304985649 0.0439513689 0.9999999
W-N -0.0952786670 -0.1324961912 -0.0580611428 0.0000000
Y-N -0.0428771811 -0.0800502665 -0.0057040957 0.0072404
Q-P -0.0499925532 -0.0871656386 -0.0128194678 0.0003878
R-P -0.1191544821 -0.1563275675 -0.0819813967 0.0000000
S-P -0.0598375496 -0.0970106350 -0.0226644642 0.0000027
T-P -0.0391822068 -0.0763552922 -0.0020091214 0.0265046
V-P -0.0118760653 -0.0491010322 0.0253489016 0.9997602
W-P -0.1138811343 -0.1510986586 -0.0766636101 0.0000000
Y-P -0.0614796485 -0.0986527338 -0.0243065631 0.0000010
R-Q -0.0691619289 -0.1063350143 -0.0319888435 0.0000000
S-Q -0.0098449964 -0.0470180818 0.0273280889 0.9999822
T-Q 0.0108103464 -0.0263627390 0.0479834317 0.9999325
V-Q 0.0381164879 0.0008915210 0.0753414548 0.0379863
W-Q -0.0638885812 -0.1011061054 -0.0266710569 0.0000001
Y-Q -0.0114870953 -0.0486601807 0.0256859901 0.9998442
S-R 0.0593169325 0.0221438471 0.0964900178 0.0000037
T-R 0.0799722752 0.0427991899 0.1171453606 0.0000000
V-R 0.1072784168 0.0700534499 0.1445033837 0.0000000
W-R 0.0052733477 -0.0319441765 0.0424908720 1.0000000

Y-R	0.0576748336	0.0205017482	0.0948479190	0.0000091
T-S	0.0206553428	-0.0165177426	0.0578284282	0.8971104
V-S	0.0479614843	0.0107365174	0.0851864512	0.0009712
W-S	-0.0540435847	-0.0912611090	-0.0168260605	0.0000600
Y-S	-0.0016420988	-0.0388151842	0.0355309866	1.0000000
V-T	0.0273061415	-0.0099188254	0.0645311084	0.4843365
W-T	-0.0746989275	-0.1119164518	-0.0374814033	0.0000000
Y-T	-0.0222974416	-0.0594705270	0.0148756438	0.8208499
W-V	-0.1020050690	-0.1392744129	-0.0647357252	0.0000000
Y-V	-0.0496035832	-0.0868285501	-0.0123786163	0.0004757
Y-W	0.0524014859	0.0151839616	0.0896190101	0.0001318

<u>Donor</u>	diff	lwr	upr	p adj
3088202-3087423	-0.009686784	-0.0348123771	0.0154388090	0.9694090
3091412-3087423	-0.040182618	-0.0653082108	-0.0150570248	0.0000184
310264-3087423	-0.027216718	-0.0523589667	-0.0020744686	0.0217447
310268-3087423	-0.019910449	-0.0450388124	0.0052179149	0.2644817
310280-3087423	-0.055138247	-0.0802638397	-0.0300126536	0.0000000
4608-3087423	-0.045885753	-0.0710280023	-0.0207435042	0.0000001
8119-3087423	-0.025544000	-0.0506695932	-0.0004184071	0.0425781
8478-3087423	-0.030891304	-0.0560168965	-0.0057657105	0.0039781
THP1-3087423	-0.086540213	-0.1116685768	-0.0614118494	0.0000000
3091412-3088202	-0.030495834	-0.0556214267	-0.0053702407	0.0048322
310264-3088202	-0.017529934	-0.0426721826	0.0076123154	0.4524902
310268-3088202	-0.010223665	-0.0353520283	0.0149046990	0.9567040
310280-3088202	-0.045451463	-0.0705770556	-0.0203258696	0.0000002
4608-3088202	-0.036198969	-0.0613412182	-0.0110567202	0.0002255
8119-3088202	-0.015857216	-0.0409828091	0.0092683769	0.6012720
8478-3088202	-0.021204519	-0.0463301125	0.0039210736	0.1858617
THP1-3088202	-0.076853429	-0.1019817927	-0.0517250654	0.0000000
310264-3091412	0.012965900	-0.0121763489	0.0381081492	0.8328010
310268-3091412	0.020272169	-0.0048561946	0.0454005327	0.2407125
310280-3091412	-0.014955629	-0.0400812219	0.0101699642	0.6805488
4608-3091412	-0.005703135	-0.0308453845	0.0194391136	0.9994131
8119-3091412	0.014638618	-0.0104869754	0.0397642106	0.7073104
8478-3091412	0.009291314	-0.0158342788	0.0344169073	0.9768263
THP1-3091412	-0.046357595	-0.0714859590	-0.0212292317	0.0000000
310268-310264	0.007306269	-0.0178387489	0.0324512868	0.9958988
310280-310264	-0.027921529	-0.0530637780	-0.0027792800	0.0160568
4608-310264	-0.018669036	-0.0438279296	0.0064898584	0.3579557
8119-310264	0.001672718	-0.0234695315	0.0268149665	1.0000000
8478-310264	-0.003674586	-0.0288168349	0.0214676632	0.9999854
THP1-310264	-0.059323495	-0.0844685133	-0.0341784776	0.0000000
310280-310268	-0.035227798	-0.0603561616	-0.0100994343	0.0003921
4608-310268	-0.025975305	-0.0511203224	-0.0008302867	0.0362244
8119-310268	-0.005633551	-0.0307619151	0.0194948122	0.9994664
8478-310268	-0.010980855	-0.0361092185	0.0141475089	0.9327976
THP1-310268	-0.066629764	-0.0917608984	-0.0414986304	0.0000000
4608-310280	0.009252493	-0.0158897556	0.0343947424	0.9775736
8119-310280	0.029594246	0.0044686535	0.0547198395	0.0074457
8478-310280	0.024246943	-0.0008786499	0.0493725361	0.0691966
THP1-310280	-0.031401966	-0.0565303301	-0.0062736028	0.0030867
8119-4608	0.020341753	-0.0048004959	0.0454840021	0.2370098
8478-4608	0.014994450	-0.0101477993	0.0401366988	0.6780747
THP1-4608	-0.040654460	-0.0657994777	-0.0155094420	0.0000137
8478-8119	-0.005347303	-0.0304728964	0.0197782897	0.9996511
THP1-8119	-0.060996213	-0.0861245766	-0.0358678493	0.0000000
THP1-8478	-0.055648910	-0.0807772733	-0.0305205459	0.0000000

C LIAANK peptides at 48 hours

48 hours	Df	Sum Sq	Mean Sq	F value	Pr(>F)
celltype	2	0.082	0.0409	2.13	0.129
endgroup	6	5.773	0.9621	50.11	<2e-16 ***
residuals	54	1.037	0.0192		

Tukey multiple comparisons of means

95% family-wise confidence level

Fit: aov(formula = ave ~ celltype + endgroup)

<u>Cell type</u>	diff	lwr	upr	p adj
Macrophage-hUVEC	-0.072990023	-0.1760419	0.03006182	0.2119027
hMSC-hUVEC.	-0.079463872	-0.1825157	0.02358797	0.1607616
hMSC-Macrophage	-0.006473849	-0.1095257	0.09657800	0.9874458

<u>Endgroup</u>	diff	lwr	upr	p adj
Ac-AcβA	0.07693082	-0.123081655	0.27694329	0.8994233
NβA-AcβA	-0.35614312	-0.556155600	-0.15613065	0.0000252
Am-AcβA	0.13334378	-0.066668695	0.33335625	0.4015930
CβA-AcβAG	0.19615704	-0.003855434	0.39616952	0.0579509
COOH-AcβA	-0.45166561	-0.651678083	-0.25165313	0.0000001
NH2-AcβA	-0.63354877	-0.833561246	-0.43353630	0.0000000
NβA-Ac	-0.43307394	-0.633086420	-0.23306147	0.0000003
Am-Ac	0.05641296	-0.143599515	0.25642543	0.9763913
CβA-Ac	0.11922622	-0.080786254	0.31923870	0.5373659
COOH-Ac	-0.52859643	-0.728608903	-0.32858395	0.0000000
NH2-Ac	-0.71047959	-0.910492066	-0.51046712	0.0000000
Am-NβA	0.48948691	0.289474430	0.68949938	0.0000000
CβA-NβA	0.55230017	0.352287691	0.75231264	0.0000000
COOH-NβA	-0.09552248	-0.295534958	0.10448999	0.7652009
NH2-NβA	-0.27740565	-0.477418121	-0.07739317	0.0015813
CβA-Am	0.06281326	-0.137199214	0.26282574	0.9599996
COOH-Am	-0.58500939	-0.785021863	-0.38499691	0.0000000
NH2G-Am	-0.76689255	-0.966905026	-0.56688008	0.0000000
COOH-CβA	-0.64782265	-0.847835124	-0.44781017	0.0000000
NH2-CβA	-0.82970581	-1.029718287	-0.62969334	0.0000000
NH2-COOH	-0.18188316	-0.381895638	0.01812931	0.0975390

D IVKVA peptides at 48 hours

48 hours	Df	Sum Sq	Mean Sq	F value	Pr(>F)
celltype	2	0.263	0.1314	2.027	0.141577
endgroup	6	1.853	0.3089	4.767	0.000578
residuals	54	3.499	0.0648		

Tukey multiple comparisons of means
95% family-wise confidence level

Fit: aov(formula = ave ~ celltype + endgroup)

<u>Celltype</u>	diff	lwr	upr	p adj
Macrophage-hUVEC	-0.01503481	-0.20436175	0.1742921	0.9800181
hMSC-hUVEC	0.12886108	-0.06046586	0.3181880	0.2377607
hMSC-Macrophage	0.14389589	-0.04543105	0.3332228	0.1690231

<u>Endgroup</u>	diff	lwr	upr	p adj
Ac-AcβA	0.30851472	-0.05894836	0.6759778073	0.1555552
NβA-AcβA	-0.25471927	-0.62218235	0.1127438195	0.3546125
Am-AcβA	-0.02456120	-0.39202429	0.3429018828	0.9999932
CβA-AcβA	0.09053903	-0.27692406	0.4580021099	0.9881916
COOH-AcβA	-0.18941059	-0.55687368	0.1780524904	0.6962825
NH2-AcβA	-0.05986569	-0.42732878	0.3075973939	0.9987708
NβA-Ac	-0.56323399	-0.93069707	-0.1957709032	0.0003595
Am-Ac	-0.33307592	-0.70053901	0.0343871602	0.0995625
CβA-Ac	-0.21797570	-0.58543878	0.1494873873	0.5431482
COOH-Ac	-0.49792532	-0.86538840	-0.1304622322	0.0021639
NH2-Ac	-0.36838041	-0.73584350	-0.0009173288	0.0490434
Am-NβA	0.23015806	-0.13730502	0.5976211480	0.4777630
CβA-NβA	0.34525829	-0.02220479	0.7127213751	0.0786424
COOH-NβA	0.06530867	-0.30215441	0.4327717556	0.9979950
NH2-NβA	0.19485357	-0.17260951	0.5623166590	0.6678880
CβA-Am	0.11510023	-0.25236286	0.4825633118	0.9604966
COOH-Am	-0.16484939	-0.53231248	0.2026136923	0.8130976
NH2-Am	-0.03530449	-0.40276757	0.3321585957	0.9999420
COOH-CβA	-0.27994962	-0.64741270	0.0875134652	0.2477438
NH2-CβA	-0.15040472	-0.51786780	0.2170583686	0.8695873
NH2-COOH	0.12954490	-0.23791818	0.4970079881	0.9314373

E Concentration study peptides at 48 hours

48 hours	Df	Sum Sq	Mean Sq	F value	Pr(>F)
celltype	2	7.184	3.592	97.36	<2e-16 ***
endgroup	6	21.549	3.591	97.34	<2e-16 ***
concentration	4	3.989	0.997	27.03	<2e-16 ***
residuals	302	11.142	0.037		

Tukey multiple comparisons of means

95% family-wise confidence level

Fit: aov(formula = ave ~ Cell + endgroup + concentration, data = concentration_48_stats)

Cell type

	diff	lwr	upr	p adj
hUVEC-hMSC	0.02674739	-0.0356911	0.08918588	0.5717588
macrophage-hMSC	0.33290148	0.2704630	0.39533997	0.0000000
macrophage-hUVEC	0.30615409	0.2437156	0.36859258	0.0000000

Endgroup

	diff	lwr	upr	p adj
Ac_βA-Ac	-0.02869210	-0.14889144	0.09150724	0.9920278
Am-Ac	-0.30279864	-0.42299798	-0.18259929	0.0000000
CβA-Ac	-0.05351273	-0.17371207	0.06668661	0.8415104
COOH-Ac	-0.49469442	-0.61489376	-0.37449508	0.0000000
NβA-Ac	-0.36386417	-0.48406351	-0.24366483	0.0000000
NH2-Ac	-0.76234755	-0.88254689	-0.64214820	0.0000000
Am-Ac_βA	-0.27410654	-0.39430588	-0.15390719	0.0000000
CβA-Ac_βA	-0.02482063	-0.14501997	0.09537871	0.9963800
COOH-Ac_βA	-0.46600232	-0.58620166	-0.34580298	0.0000000
NβA-Ac_βA	-0.33517207	-0.45537141	-0.21497273	0.0000000
NH2-Ac_βA	-0.73365544	-0.85385479	-0.61345610	0.0000000
CβA-Am	0.24928590	0.12908656	0.36948525	0.0000000
COOH-Am	-0.19189578	-0.31209513	-0.07169644	0.0000675
NβA-Am	-0.06106553	-0.18126487	0.05913381	0.7399153
NH2-Am	-0.45954891	-0.57974825	-0.33934957	0.0000000
COOH-CβA	-0.44118169	-0.56138103	-0.32098234	0.0000000
NβA-CβA	-0.31035144	-0.43055078	-0.19015209	0.0000000
NH2-CβA	-0.70883481	-0.82903416	-0.58863547	0.0000000
NβA-COOH	0.13083025	0.01063091	0.25102959	0.0229651
NH2-COOH	-0.26765313	-0.38785247	-0.14745378	0.0000000
NH2-NβA	-0.39848338	-0.51868272	-0.27828403	0.0000000

Concentration

	diff	lwr	upr	p adj
19.5-1250	-0.120196418	-0.21411722	-0.02627562	0.0046316
312-1250	-0.067417531	-0.16133833	0.02650327	0.2832901
5000-1250	0.186144359	0.09222356	0.28006516	0.0000011
78-1250	-0.110330119	-0.20425092	-0.01640932	0.0121507
312-19.5	0.052778887	-0.04114191	0.14669968	0.5358579
5000-19.5	0.306340777	0.21241998	0.40026157	0.0000000
78-19.5	0.009866299	-0.08405450	0.10378710	0.9984852
5000-312	0.253561889	0.15964109	0.34748269	0.0000000
78-312	-0.042912589	-0.13683339	0.05100821	0.7195936
78-5000	-0.296474478	-0.39039527	-0.20255368	0.0000000

F Peptides with either an azide or PEG functionalization at 48 hours

48 hours	Df	Sum Sq	Mean Sq	F value	Pr(>F)
Celltype	2	0.610	0.3050	8.218	0.000459 ***
endgroup	6	4.996	0.8326	22.435	<2e-16 ***
functionalization	1	2.784	2.7837	75.004	3.19e-14 ***
residuals	116	4.305	0.0371		

Tukey multiple comparisons of means

95% family-wise confidence level

Fit: aov(formula = ave ~ cell + endgroup + functionalization)

<u>Cell type</u>	diff	lwr	upr	p adj
hUVEC-hMSC.	0.09160999	-0.008199751	0.1914197	0.0790515
mac-hMSC	0.17027349	0.070463754	0.2700832	0.0002719
mac-hUVEC.	0.07866350	-0.021146233	0.1784732	0.1516898

<u>Endgroup</u>	diff	lwr	upr	p adj
AcβA-Ac	0.003644893	-0.18905250	0.196342286	1.0000000
Am-Ac	-0.147102880	-0.33980027	0.045594513	0.2574162
CβA-Ac	0.069312949	-0.12338444	0.262010342	0.9329731
COOH-Ac	-0.208820203	-0.40151760	-0.016122810	0.0245513
NβA-Ac	-0.193966891	-0.38666428	-0.001269498	0.0473857
NH2-Ac	-0.571832555	-0.76452995	-0.379135162	0.0000000
Am-AcβA	-0.150747773	-0.34344517	0.041949620	0.2308972
CβA-AcβA	0.065668056	-0.12702934	0.258365449	0.9478292
COOH-AcβA	-0.212465097	-0.40516249	-0.019767704	0.0207275
NβA-AcβA.	-0.197611784	-0.39030918	-0.004914391	0.0405243

NH2-AcβA	-0.575477449	-0.76817484	-0.382780056	0.0000000
CβA-Am	0.216415829	0.02371844	0.409113222	0.0171938
COOH-Am	-0.061717323	-0.25441472	0.130980070	0.9612073
NβA-Am	-0.046864011	-0.23956140	0.145833382	0.9904628
NH2-Am	-0.424729675	-0.61742707	-0.232032282	0.0000000
COOH-CβA	-0.278133152	-0.47083055	-0.085435759	0.0006162
NβA-CβA	-0.263279840	-0.45597723	-0.070582447	0.0014642
NH2-CβA	-0.641145504	-0.83384290	-0.448448111	0.0000000
NβA-COOH	0.014853312	-0.17784408	0.207550705	0.9999867
NH2-COOH	-0.363012352	-0.55570975	-0.170314959	0.0000024
NH2-NβA	-0.377865664	-0.57056306	-0.185168271	0.0000008

<u>Functionalization</u>	diff	lwr	upr.	p adj
PEG-azide	0.2972747	0.2292891	0.3652603	0

G Soluble peptides with cells encapsulated in PEG hydrogels at 48 hours

48 hours	Df	Sum Sq	Mean Sq	F value	Pr(>F)
celltype	2	8.19	4.095	125.42	<2e-16 ***
endgroup	6	74.10	12.350	378.28	<2e-16 ***
amino_acid	1081	5.87	0.345	10.58	<2e-16 ***
residuals	22626	35.29	0.033		

Tukey multiple comparisons of means

95% family-wise confidence level

Fit: aov(formula = ave ~ cell + endgroup + amino_acid)

<u>Cell type</u>	diff	lwr	upr	p adj
hUVEC-hMSC.	0.05360174	0.02261208	0.08459139	0.0001559
Macrophage-hMSC	0.20456374	0.17320883	0.23591865	0.0000000
Macrophage-hUVEC	0.15096200	0.11962755	0.18229646	0.0000000

<u>Endgroup</u>	diff	lwr	upr	p adj
AcβA-Ac	0.03708977	-0.02221344	0.09639299	0.5160796
Am-Ac	-0.04452478	-0.10392001	0.01487045	0.2885047
CβA-Ac	0.07091934	0.01161613	0.13022256	0.0078020
COOH-Ac	-0.38434272	-0.44641560	-0.32226984	0.0000000
NβA-Ac	-0.08609557	-0.14539878	-0.02679236	0.0003919
NH2-Ac	-0.68822281	-0.74752602	-0.62891960	0.0000000
Am-AcβA	-0.08161455	-0.14100978	-0.02221933	0.0010355
CβA-AcβA	0.03382957	-0.02547364	0.09313278	0.6262622
COOH-AcβA	-0.42143249	-0.48350537	-0.35935961	0.0000000
NβA-AcβA	-0.12318534	-0.18248856	-0.06388213	0.0000000
NH2-AcβA	-0.72531258	-0.78461579	-0.66600937	0.0000000
CβA-Am	0.11544412	0.05604890	0.17483935	0.0000003
COOH-Am	-0.33981794	-0.40197873	-0.27765714	0.0000000
NβA-Am	-0.04157079	-0.10096602	0.01782444	0.3729682
NH2-Am	-0.64369803	-0.70309326	-0.58430280	0.0000000
COOH-CβA	-0.45526206	-0.51733494	-0.39318918	0.0000000
NβA-CβA	-0.15701491	-0.21631813	-0.09771170	0.0000000
NH2-CβA	-0.75914215	-0.81844536	-0.69983894	0.0000000
NβA-COOH	0.29824715	0.23617427	0.36032003	0.0000000
NH2-COOH	-0.30388009	-0.36595297	-0.24180721	0.0000000
NH2-NβA	-0.60212724	-0.66143045	-0.54282403	0.0000000

Amino acid

	diff	lwr	upr	p adj
D-A	0.1757707421	0.062276920	0.289264564	0.0000112
E-A	0.1257644436	0.012270622	0.239258265	0.0135034
F-A	-0.0196719476	-0.133165769	0.093821874	1.0000000
G-A	0.0399516470	-0.073542175	0.153445469	0.9990828
H-A	-0.0762467186	-0.189740541	0.037247103	0.6465183
I/L-A	0.0768747060	-0.036619116	0.190368528	0.6318774
K-A	-0.0205584614	-0.134052283	0.092935360	0.9999999
M-A	0.0501176495	-0.063376172	0.163611471	0.9871761
N-A	0.0738796244	-0.039614197	0.187373446	0.7003139
P-A	0.1097088102	-0.003785012	0.223202632	0.0718473
Q-A	0.0332618800	-0.080231942	0.146755702	0.9999196
R-A	-0.0392564012	-0.156878612	0.078365810	0.9995371
S-A	0.0100754237	-0.103418398	0.123569246	1.0000000
T-A	0.1035305588	-0.010427452	0.217488570	0.1285330
V-A	0.0913764269	-0.022117395	0.204870249	0.3043976
W-A	-0.0839188068	-0.197412629	0.029575015	0.4650114
Y-A	-0.0678269774	-0.181320799	0.045666845	0.8217720
E-D	-0.0500062985	-0.163500120	0.063487523	0.9874732
F-D	-0.1954426897	-0.308936512	-0.081948868	0.0000004
G-D	-0.1358190951	-0.249312917	-0.022325273	0.0040162
H-D	-0.2520174607	-0.365511283	-0.138523639	0.0000000
I/L-D	-0.0988960361	-0.212389858	0.014597786	0.1798358
K-D	-0.1963292035	-0.309823025	-0.082835382	0.0000003
M-D	-0.1256530926	-0.239146914	-0.012159271	0.0136767
N-D	-0.1018911177	-0.215384940	0.011602704	0.1420506
P-D	-0.0660619319	-0.179555754	0.047431890	0.8513349
Q-D	-0.1425088621	-0.256002684	-0.029015040	0.0016811
R-D	-0.2150271433	-0.332649354	-0.097404933	0.0000000
S-D	-0.1656953184	-0.279189140	-0.052201496	0.0000573
T-D	-0.0722401832	-0.186198194	0.041717828	0.7420538
V-D	-0.0843943152	-0.197888137	0.029099507	0.4539850
W-D	-0.2596895489	-0.373183371	-0.146195727	0.0000000
Y-D	-0.2435977194	-0.357091541	-0.130103898	0.0000000
F-E	-0.1454363912	-0.258930213	-0.031942569	0.0011309
G-E	-0.0858127966	-0.199306618	0.027681025	0.4215805
H-E	-0.2020111622	-0.315504984	-0.088517340	0.0000001
I/L-E	-0.0488897376	-0.162383559	0.064604084	0.9901557
K-E	-0.1463229050	-0.259816727	-0.032829083	0.0010012
M-E	-0.0756467940	-0.189140616	0.037847028	0.6603793
N-E	-0.0518848192	-0.165378641	0.061609003	0.9816517
P-E	-0.0160556334	-0.129549455	0.097438188	1.0000000
Q-E	-0.0925025635	-0.205996385	0.020991258	0.2830723
R-E	-0.1650208448	-0.282643056	-0.047398634	0.0001551
S-E	-0.1156890198	-0.229182842	-0.002195198	0.0401467
T-E	-0.0222338847	-0.136191896	0.091724126	0.9999998
V-E	-0.0343880166	-0.147881839	0.079105805	0.9998728

W-E -0.2096832504 -0.323177072 -0.096189429 0.0000000
Y-E -0.1935914209 -0.307085243 -0.080097599 0.0000005
G-F 0.0596235946 -0.053870227 0.173117416 0.9329647
H-F -0.0565747710 -0.170068593 0.056919051 0.9577398
I/L-F 0.0965466536 -0.016947168 0.210040475 0.2141716
K-F -0.0008865138 -0.114380336 0.112607308 1.0000000
M-F 0.0697895971 -0.043704225 0.183283419 0.7855322
N-F 0.0935515720 -0.019942250 0.207045394 0.2640272
P-F 0.1293807578 0.015886936 0.242874580 0.0088518
Q-F 0.0529338276 -0.060559994 0.166427650 0.9775717
R-F -0.0195844536 -0.137206664 0.098037757 1.0000000
S-F 0.0297473713 -0.083746451 0.143241193 0.9999835
T-F 0.1232025064 0.009244495 0.237160518 0.0190700
V-F 0.1110483745 -0.002445447 0.224542196 0.0633443
W-F -0.0642468592 -0.177740681 0.049246963 0.8785525
Y-F -0.0481550298 -0.161648852 0.065338792 0.9916496
H-G -0.1161983656 -0.229692187 -0.002704544 0.0381172
I/L-G 0.0369230590 -0.076570763 0.150416881 0.9996690
K-G -0.0605101084 -0.174003930 0.052983713 0.9241648
M-G 0.0101660025 -0.103327819 0.123659824 1.0000000
N-G 0.0339279774 -0.079565844 0.147421799 0.9998943
P-G 0.0697571632 -0.043736659 0.183250985 0.7861582
Q-G -0.0066897669 -0.120183589 0.106804055 1.0000000
R-G -0.0792080482 -0.196830259 0.038414163 0.6423060
S-G -0.0298762233 -0.143370045 0.083617599 0.9999824
T-G 0.0635789119 -0.050379099 0.177536923 0.8911749
V-G 0.0514247799 -0.062069042 0.164918602 0.9832443
W-G -0.1238704538 -0.237364276 -0.010376632 0.0167386
Y-G -0.1077786243 -0.221272446 0.005715198 0.0857491
I/L-H 0.1531214246 0.039627603 0.266615246 0.0003828
K-H 0.0556882572 -0.057805565 0.169182079 0.9634656
M-H 0.1263643682 0.012870546 0.239858190 0.0126036
N-H 0.1501263430 0.036632521 0.263620165 0.0005881
P-H 0.1859555288 0.072461707 0.299449351 0.0000020
Q-H 0.1095085987 -0.003985223 0.223002421 0.0731963
R-H 0.0369903174 -0.080631893 0.154612528 0.9997893
S-H 0.0863221424 -0.027171680 0.199815964 0.4101494
T-H 0.1797772775 0.065819266 0.293735289 0.0000065
V-H 0.1676231456 0.054129324 0.281116967 0.0000422
W-H -0.0076720882 -0.121165910 0.105821734 1.0000000
Y-H 0.0084197413 -0.105074081 0.121913563 1.0000000
K-I/L -0.0974331674 -0.210926989 0.016060654 0.2007222
M-I/L -0.0267570565 -0.140250878 0.086736765 0.9999965
N-I/L -0.0029950816 -0.116488903 0.110498740 1.0000000
P-I/L 0.0328341042 -0.080659718 0.146327926 0.9999328
Q-I/L -0.0436128260 -0.157106648 0.069880996 0.9973099
R-I/L -0.1161311072 -0.233753318 0.001491104 0.0575256
S-I/L -0.0667992823 -0.180293104 0.046694540 0.8393481

T-I/L 0.0266558529 -0.087302158 0.140613864 0.9999969
V-I/L 0.0145017209 -0.098992101 0.127995543 1.0000000
W-I/L -0.1607935128 -0.274287335 -0.047299691 0.0001223
Y-I/L -0.1447016834 -0.258195505 -0.031207861 0.0012503
M-K 0.0706761109 -0.042817711 0.184169933 0.7680902
N-K 0.0944380858 -0.019055736 0.207931908 0.2485655
P-K 0.1302672716 0.016773450 0.243761093 0.0079620
Q-K 0.0538203414 -0.059673480 0.167314163 0.9735982
R-K -0.0186979398 -0.136320151 0.098924271 1.0000000
S-K 0.0306338851 -0.082859937 0.144127707 0.9999748
T-K 0.1240890203 0.010131009 0.238047031 0.0172853
V-K 0.1119348883 -0.001558934 0.225428710 0.0581955
W-K -0.0633603454 -0.176854167 0.050133476 0.8906427
Y-K -0.0472685160 -0.160762338 0.066225306 0.9931985
N-M 0.0237619749 -0.089731847 0.137255797 0.9999994
P-M 0.0595911607 -0.053902661 0.173084983 0.9332725
Q-M -0.0168557695 -0.130349591 0.096638052 1.0000000
R-M -0.0893740507 -0.206996261 0.028248160 0.4120489
S-M -0.0400422258 -0.153536048 0.073451596 0.9990562
T-M 0.0534129093 -0.060545102 0.167370921 0.9764516
V-M 0.0412587774 -0.072235044 0.154752599 0.9986283
W-M -0.1340364563 -0.247530278 -0.020542634 0.0050226
Y-M -0.1179446269 -0.231438449 -0.004450805 0.0318220
P-N 0.0358291858 -0.077664636 0.149323008 0.9997782
Q-N -0.0406177444 -0.154111566 0.072876078 0.9988710
R-N -0.1131360256 -0.230758236 0.004486185 0.0755597
S-N -0.0638042007 -0.177298023 0.049689621 0.8846887
T-N 0.0296509344 -0.084307077 0.143608946 0.9999852
V-N 0.0174968025 -0.095997019 0.130990624 1.0000000
W-N -0.1577984312 -0.271292253 -0.044304609 0.0001923
Y-N -0.1417066018 -0.255200424 -0.028212780 0.0018710
Q-P -0.0764469302 -0.189940752 0.037046892 0.6418642
R-P -0.1489652114 -0.266587422 -0.031343001 0.0014252
S-P -0.0996333865 -0.213127208 0.013860435 0.1699198
T-P -0.0061782513 -0.120136263 0.107779760 1.0000000
V-P -0.0183323833 -0.131826205 0.095161439 1.0000000
W-P -0.1936276170 -0.307121439 -0.080133795 0.0000005
Y-P -0.1775357876 -0.291029609 -0.064041966 0.0000083
R-Q -0.0725182812 -0.190140492 0.045103930 0.7819764
S-Q -0.0231864563 -0.136680278 0.090307366 0.9999996
T-Q 0.0702686788 -0.043689332 0.184226690 0.7817920
V-Q 0.0581145469 -0.055379275 0.171608369 0.9462545
W-Q -0.1171806869 -0.230674509 -0.003686865 0.0344542
Y-Q -0.1010888574 -0.214582679 0.012404964 0.1515292
S-R 0.0493318249 -0.068290386 0.166954036 0.9926493
T-R 0.1427869601 0.024716789 0.260857131 0.0033464
V-R 0.1306328281 0.013010617 0.248255039 0.0130714
W-R -0.0446624056 -0.162284616 0.072959805 0.9976678

Y-R	-0.0285705762	-0.146192787	0.089051635	0.9999946
T-S	0.0934551351	-0.020502876	0.207413146	0.2725897
V-S	0.0813010032	-0.032192819	0.194794825	0.5267417
W-S	-0.0939942305	-0.207488052	0.019499591	0.2562335
Y-S	-0.0779024011	-0.191396223	0.035591421	0.6076844
V-T	-0.0121541319	-0.126112143	0.101803879	1.0000000
W-T	-0.1874493657	-0.301407377	-0.073491354	0.0000017
Y-T	-0.1713575362	-0.285315547	-0.057399525	0.0000260
W-V	-0.1752952337	-0.288789056	-0.061801412	0.0000121
Y-V	-0.1592034043	-0.272697226	-0.045709582	0.0001557
Y-W	0.0160918295	-0.097401992	0.129585651	1.0000000

Appendix Figure 173 - Statistical analyses using multi-way ANOVAs with a Turkey post-hoc test. Three technical replicates were averaged to a single values, and statistics were done on experimental/biological replicates. Statistical analysis on a) soluble peptides cultured with cells on tissue culture plastic, all time points b) soluble peptides cultured with cells on tissue culture plastic at 48 hours, c) LIAANK peptides at 48 hours, d) IVKVA peptides at 48 hours E) concentration study peptides at 48 hours F) azide/PEG functionalized peptides cultured with cells at 48 hours G) soluble peptides cultured with cells in PEG hydrogels at 48 hours.

Vita

Samuel Rozans Graduated with his masters in bioengineering from Drexel University, The School of Biomedical Sciences, Engineering, and Technology with a concentration in biomechanics. During his time in Dr. Lin Han's Nanobiomechanics lab he gained expertise in atomic force microscopy based nano-indentation with his name on four abstracts. He joined Dr. Pashuck's research group as a visiting scholar in October of 2019, then officially matriculated into doctoral program at Lehigh University, P.C. Rossin College Engineering, department of Bioengineering in January of 2020, where he ultimately completed his doctoral degree in 2024. In 2021 Sam was a teaching assistant for BIOE343, Integrated Biotechnolgy Laboratory, for two semesters. During his time at Lehigh University gave two talks at BMES (2021) and SFB (2023) and two poster presentations NEBEC (2022) and WBC (2024). In 2023 Sam became co-president of the bioengineering graduate student association where he would help organize the second and third annual Research Day. Sam's contributions to research day include expanding it to a full-day event involving students, faculty, clinicians, and professionals within the biotech space to facilitate meaningful conversation and gain multiple points of view. During the second annual research day he won 1st place for his research poster. On behalf of graduate students Sam successfully advocated for stipend raises. For creating lasting impact in the Lehigh University graduate student community, Sam was awarded the graduate life leadership award in 2024.